Epigenetic regulation of hematopoiesis and acute leukemia

Daria Gianina Valerio

Epigenetic Regulation of Hematopoiesis and Acute Leukemia

Daria Gianina Valerio

Memorial Sloan-Kettering
Cancer Center

ISBN: 978-94-6299-416-4

Author: Daria Giania Valerio

Cover design: Daria Gianina Valerio

Lay-out: Daria Gianina Valerio

Printing: Ridderprint BV

The work described in this thesis was performed at the Cancer Biology and Genetics Department of Memorial Sloan Kettering Cancer Center, New York, USA. The research was financially supported by a research grant from CURE Childhood Cancer; NIH grants PO1 CA66996, R01 CA140575 and P30 CA008748; the Leukemia and Lymphoma Society and Gabrielle's Angel Research Foundation.

We gratefully acknowledge the Erasmus University Rotterdam for providing financial support for the printing of this thesis.

Epigenetic Regulation of Hematopoiesis and Acute Leukemia

Epigenetische Regulatie van Hematopoëse en Acute Leukemie

Proefschrift

ter verkrijging van de graad van doctor aan de
Erasmus Universiteit Rotterdam
op gezag van de rector magnificus
Prof.dr. H.A.P. Pols
en volgens besluit van het College voor Promoties

De openbare verdediging zal plaatsvinden op
6 januari 2017 om 13:30 uur

door

Daria Gianina Valerio

geboren te La Jolla, USA

Erasmus University Rotterdam

Erasmus

Promotiecommissie:

Promotor:

Prof.dr. B. Löwenberg
Prof.dr. H.R. Delwel

Overige leden:

Prof.dr. I.P. Touw
Prof.dr. C.M. Zwaan
Prof.dr. G. de Haan

"I believe the universe wants to be noticed. I think the universe is improbably biased toward the consciousness, that it rewards intelligence, in part because the universe enjoys its elegance being observed. And who am I, living in the middle of history, to tell the universe that it - or my observation of it - is temporary?"

John Green, author

To Chris and my parents

CONTENTS

1

GENERAL INTRODUCTION

THE HEMATOPOIETIC SYSTEM

The hematopoietic system is capable of replenishing all mature blood cell types throughout a complete human lifespan. This is possible due to a strict hierarchical system in which mature blood cells are at the bottom and hematopoietic stem cells (HSCs) are at the very top (Figure 1). HSCs carry the lifelong capacity to self-renew as well as supply the system with progenitors that can differentiate into the various hematopoietic cell lineages.[1,2]

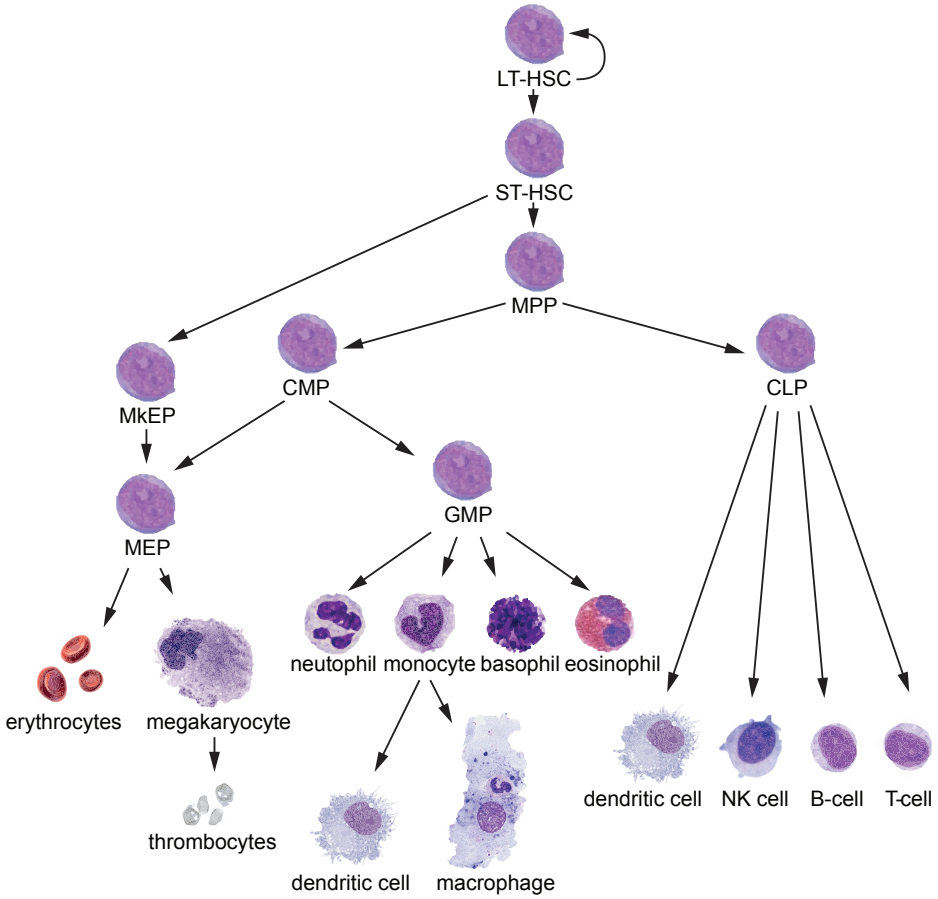

Figure 1. The hierarchy of normal hematopoiesis

The normal hematopoietic system knows a strict hierarchy with hematopoietic stem cells (HSCs) at the very top. HSCs can self-renew as well as supply the system with progenitors that can then differentiate into the various hematopoietic lineages. The scheme shows the different intermediate progenitor cell stages, as well as the fully differentiated cells of the distinct hematopoietic maturation lineages.

LT-HSC: long-term hematopoietic stem cell; ST-HSC: short-term HSC; MPP: multipotent progenitor; MkEP: early megakaryocyte erythrocyte progenitor; CMP: common myeloid progenitor; CLP: common lymphoid progenitor; GMP: granulocyte macrophage progenitor; MEP: megakaryocyte erythrocyte progenitor; NK cell: natural killer cell.

Figure 2. Schematic representation of murine hematopoietic development
The total duration of murine embryogenesis is 19-21 days. Definitive hematopoiesis begins in the Aorta-Gonad-Mesonephros (AGM) system around the embryonic age of 8.5 days (E8.5). At E11.5 the liver has begun to replace the AGM system as the major hematopoietic organ and at E14.5, fetal hematopoiesis is at its peak in the liver, after which it starts to divert to the bone marrow (BM) and spleen. At E18 most hematopoietic progenitors are still located in the liver, where they gradually decrease through postnatal day 14 (P14). While the number of progenitors in liver, spleen and BM is about equal at P2, already at P5 the majority of hematopoietic progenitors are found in the BM compartment.

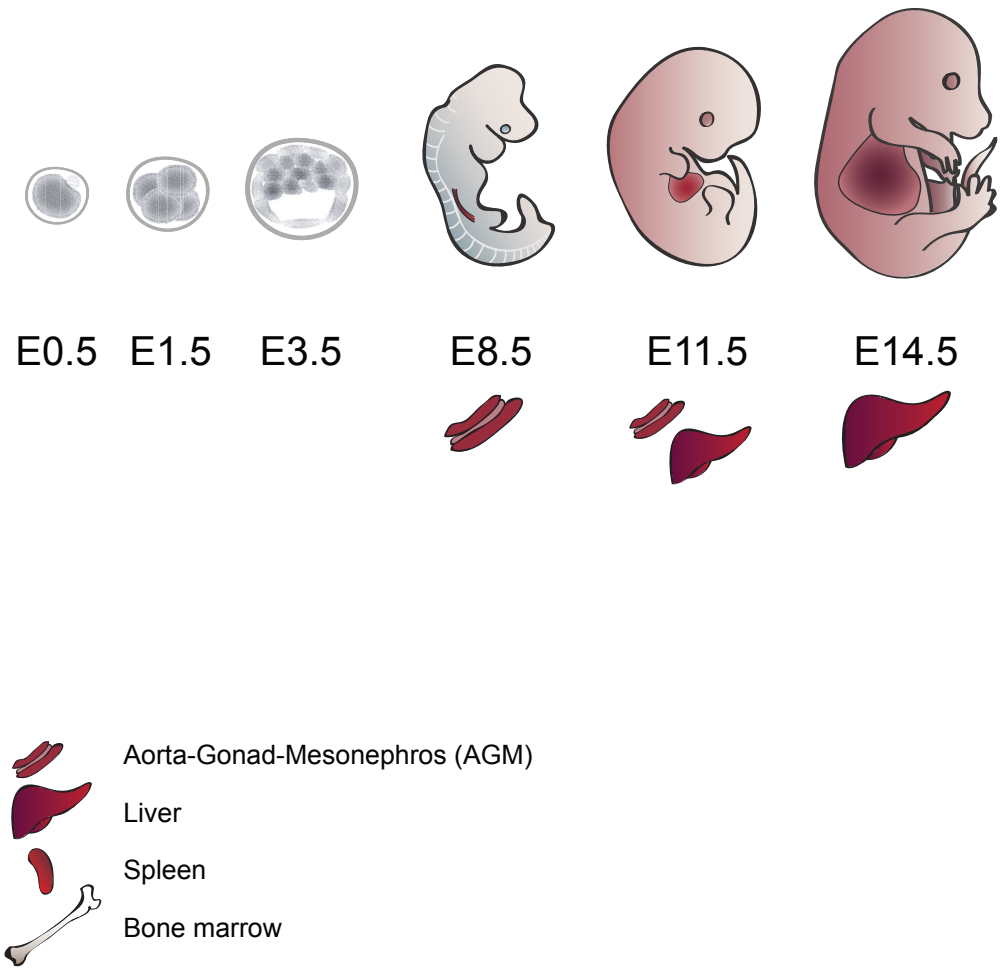

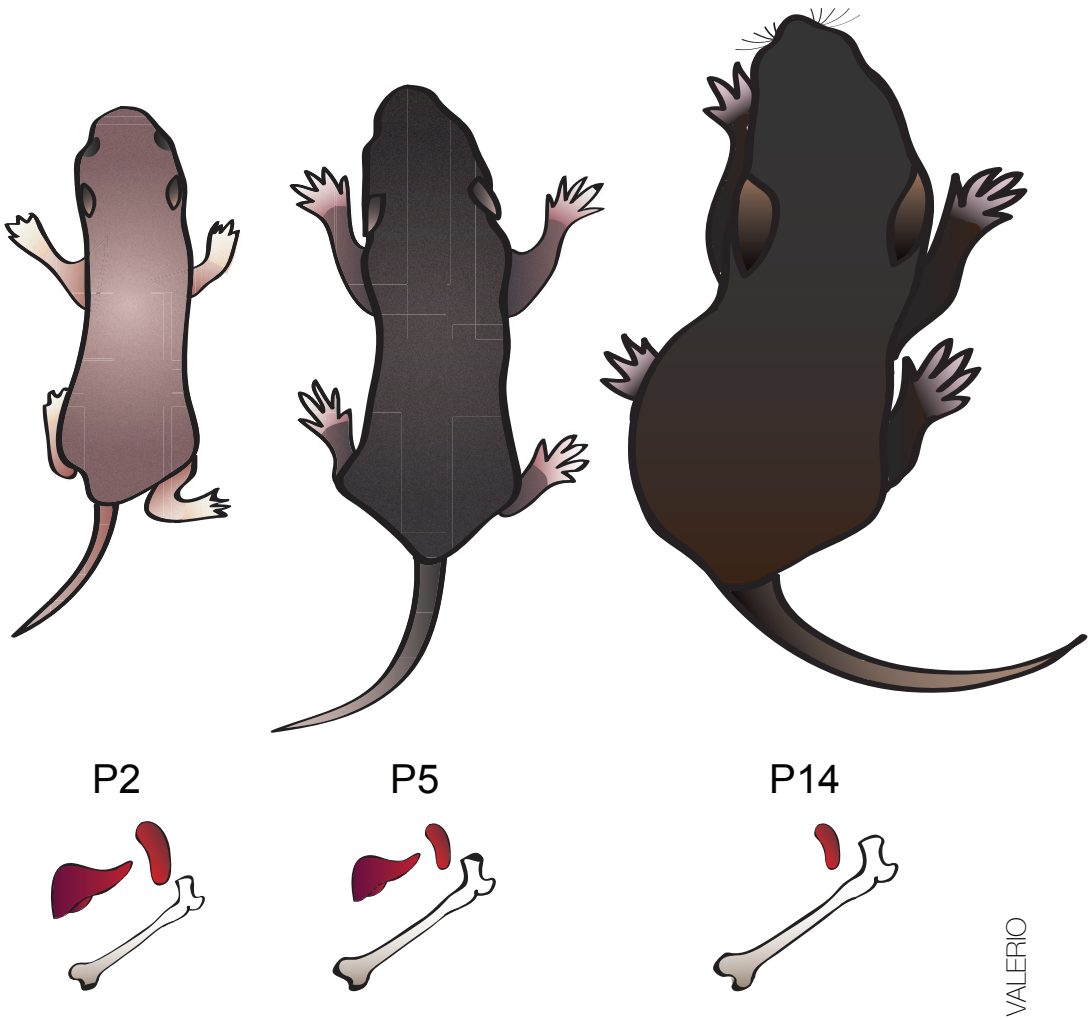

In this thesis we use murine hematopoiesis as a model. Primitive erythropoiesis starts at the embryonic age of 7 days (E7) by formation of blood islands in the visceral yolk-sac. Figure 2 illustrates the development of definitive hematopoiesis, starting around E8.5 in the Aorta-Gonad-Mesonephros (AGM) system.[3] While yolk-sac derived progenitors are limited to mainly erythroid development, AGM derived progenitors are truly multi-potent and contribute to the eventual HSC pool. At E11.5 the liver has begun to replace the AGM system as the major hematopoietic organ and at E14.5, fetal hematopoiesis is at its peak in the liver, after which it starts to divert to the bone marrow (BM) and spleen.[4] At E18 most hematopoietic progenitors are still located in the liver, where they gradually decrease through postnatal day 14 (P14). While the number of progenitors in liver, spleen and BM is about equal at P2, already at P5 the majority of hematopoietic progenitors are found in the BM compartment.[5] The spleen remains a hematopoietic organ throughout the murine life, but its role in adult mice is limited to erythropoiesis and some lymphopoiesis. In adult mice the majority or even all HSCs and progenitors reside in the BM.[5]

While human and murine embryogenesis are clearly distinct, development of definitive hematopoiesis is very similar. Much like in the mouse, in human embryos primitive hematopoiesis is initiated in the yolk sac and definitive hematopoiesis in the AGM system.[6] In contrast to murine hematopoiesis, the human fetal liver seems incapable of producing HSCs; it rather receives hematopoietic progenitors of AGM and yolk-sac origin that then proliferate and differentiate. In week 10-11 of human embryogenesis, hematopoiesis starts its shift to the BM compartment, which, unlike in mice, already operates as a major site of hematopoiesis before birth.[7]

HSCs undergo discrete developmental changes throughout life.[8] The biggest change occurs with the transition from fetal to adult hematopoiesis. Early and mid- gestational hematopoiesis is characterized by a rapid expansion of undifferentiated HSCs[9] and is meanwhile rich in erythroid progenitors, feeding the high demand of erythrocytes and oxygen transport required for embryonic growth and development.[8] In adult hematopoiesis, lifelong production of blood cells depends on the delicate balance between HSC self-renewal and differentiation.[10] In contrast to fetal hematopoiesis, most adult HSCs turn quiescent[11] to ensure maintenance of the HSC pool. This switch sets in at E16.5 and is complete at around 3 weeks after birth.[8] As fetal HSCs markedly differ from adult HSCs with respect to cell cycle status[11], proliferative capacity[9] and differentiation potential[12], it is perceivable that distinct mechanisms control cell homing and self-renewal during fetal and adult life, and indeed, multiple studies have shown that fetal HSCs differ from adult HSCs in gene expression[13,14], marker expression[15,16] and regulation[13,17].

ACUTE LEUKEMIA

Leukemia is characterized by blocked maturation and uncontrolled proliferation of HSCs or hematopoietic progenitors. These immature hematopoietic cells, also known as leukemic blasts, have lost their ability to differentiate and respond to normal cell regulating mechanisms such as signals of cell death. Leukemias are divided in acute and chronic forms and within these categories a myeloid, lymphoid and undifferentiated group are recognized, mainly depending on morphologic features of the malignant cells. Whereas chronic leukemias consist of more mature leukemic blasts and generally develop more slowly, acute leukemia is characterized by a comparatively rapid expansion of blasts that originate from highly immature progenitors. The studies in this thesis focus on acute leukemia. Acute leukemias have an incidence of 4.7 per 100,000 per year in the general population.[18,19] Although acute leukemia accounts for <3% of all cancers, leukemia is the leading cause of cancer death in children and adults aged <39 years; and while acute myeloid leukemia (AML) is most common in adults, acute lymphoid leukemia (ALL) is around 5 times more common than AML in pediatric patients.[20,21] When acute leukemias develop, the infiltration of leukemic blasts in the BM is often so severe that the formation of normal hematopoietic cells becomes highly impaired. This frequently leads to hematopoietic insufficiency with cytopenias (anemia, leukopenia, thrombocytopenia), causing patients to present with symptoms such as fatigue, easy bleeding and recurrent infections. In addition, patients may present with symptoms caused by accumulation of leukemic blasts in various tissues such as liver, spleen, skin, lymph nodes and the central nervous system. Without adequate treatment, acute leukemias progress and are often fatal within months or even weeks after diagnosis.

There is significant heterogeneity in treatment response of patients with AML or ALL. This heterogeneity can in part be correlated to genetic aberrations present in leukemic cells. These genetic aberrations consist of single gene mutations and chromosomal abnormalities. Chromosomal abnormalities include loss or gain of chromosomal material (e.g. trisomies or chromosomal deletions), as well as structural abnormalities due to translocations. Within the wide spectrum of genetic aberrations in cancer, one can distinguish between drivers (genetic events that contribute to tumor progression) and passengers (genetic events that occur at a later stage of cancer development due to general chromosomal instability, but do not significantly contribute to tumor progression). This distinction is critical to the development of new therapies that directly target leukemogenic pathways. In this thesis we discuss two chromosomal translocations that are leukemia drivers. The first translocation concerns a rearrangement of the Mixed-Lineage Leukemia 1 (*MLL1*) gene at chromosome 11q23.[22,23] *MLL* translocations are found in about 10% of all patients with acute leukemia, but this percentage is significantly higher in infant patients where the frequency of *MLL* rearrangements is around 80%.[21,24,25] In *MLL* translocations, the *MLL1* N-terminus is fused to the C-terminus of one of its various fusion gene partners of which *AF9* is one of the most common (*MLL-AF9*).[26] The second group of translocations that will be discussed are those of the Nucleoporin 98 (*NUP98*) gene. NUP98 is part of the nuclear pore complexes

that span the nuclear envelope and mediate exchange of macromolecules between the nucleus and cytoplasm. In *NUP98* translocations, similar to *MLL1*, the *NUP98* N-terminal is fused to the C-terminal of a diverse group of fusion partner genes. Fusion partners include homeobox genes with a conserved DNA-binding domain, such as *HOXA9* and *HOXD13*, and proteins with a histone "writer" or "reader" domain, such as *NSD1*, *JARID1A* and *PHF23*. The frequency of *NUP98* rearrangements in adults with AML is only 1-2%.[27] However, the frequency of *NUP98* rearrangements is significantly greater in childhood AML, i.e. 6-10%.[28-31] Both *NUP98*- and *MLL1*- translocations are associated with an unfavorable prognosis[24,28-31], warranting a research effort into the leukemogenic mechanisms of these fusions to identify novel therapeutic opportunities.

EPIGENETIC DEREGULATION IN LEUKEMIA

The term "epigenetics" was derived from the Greek word "epi" meaning "upon" or "above" and first coined in 1940 by the British geneticist Conrad Waddington.[32] The mechanism of epigenetics refers to heritable changes in gene transcription, caused by external factors that influence accessibility of the DNA or genome without actual changes in the DNA sequence (genetics). Since all cells in a multicellular organism contain essentially the same DNA, it is the cell type specific packaging of this DNA in chromatin that determines transcriptional output. Therefore, epigenetic regulatory mechanisms are instrumental in dictating cell identities and they have been implicated in fundamental biological processes such as development, stem cell differentiation and genome integrity.[33] Epigenetic gene regulation is primarily achieved through DNA methylation and post-translational histone modification (Figure 3). DNA methylation occurs on CpG dinucleotides via the addition of a methyl group to the C5 position of cytosines, and DNA hypermethylation is generally associated with gene silencing.[34] Histone proteins can be modified at specific amino acid residues by the binding of a variety of molecules including methyl, acetyl, phosphoryl or ubiquitin groups. The addition of these histone modifications is catalyzed by a class of enzymes known as chromatin "writers". Chromatin "readers" bind histones that have been marked with specific modifications by writers. They may themselves possess additional chromatin modifying capacities, or alternatively recruit other proteins to modify the local chromatin environment. Finally, chromatin "erasers" catalyze the removal of histone modifications, thereby reversing their biochemical effects on the chromatin fiber. These epigenetic modifications control accessibility of the DNA and thereby control which parts of the genome are being transcribed at a given time.

For several years it has been evident that deregulation of the epigenome is a common feature of various diseases, including cancer. The earliest observations of epigenetic abnormalities in cancer cells were alterations in patterns of DNA methylation and histone acetylation.[35] However, until recently it was unclear whether epigenetic changes play a

causal role in cancer development or whether they merely correlate with the cancerous state. The availability and diminishing cost of whole genome sequencing has instigated a massive amount of cancer sequencing studies. These studies have been crucial in our understanding not only of the cancer genome but also epigenome. We now know that 25-30% of the identified cancer driver mutations affect genes encoding chromatin regulatory proteins.[36,37] Some of the most common epigenetic regulator gene mutations in *de novo* AML are found in *TET2*, *IDH1*, *IDH2*, *DNMT3A* and *ASXL1*.[38] A genome-wide pediatric sequencing study identified different chromatin modifiers such as *EZH2*, *CREBBP*, *SETD2*, *MLL2* and *NSD2* to be mutated in ALL.[39,40] Interestingly it seems that epigenetic regulator gene mutations are enriched in adults and patients of advanced age, compared to children with leukemia.[38,41,42] Together these findings suggest that altered epigenetic states do not just correlate with cancer but likely drive disease pathogenesis. This notion has spurred a significant research effort to understand how altered epigenetic states drive cancer cell phenotypes and how to therapeutically exploit these phenomena.[43]

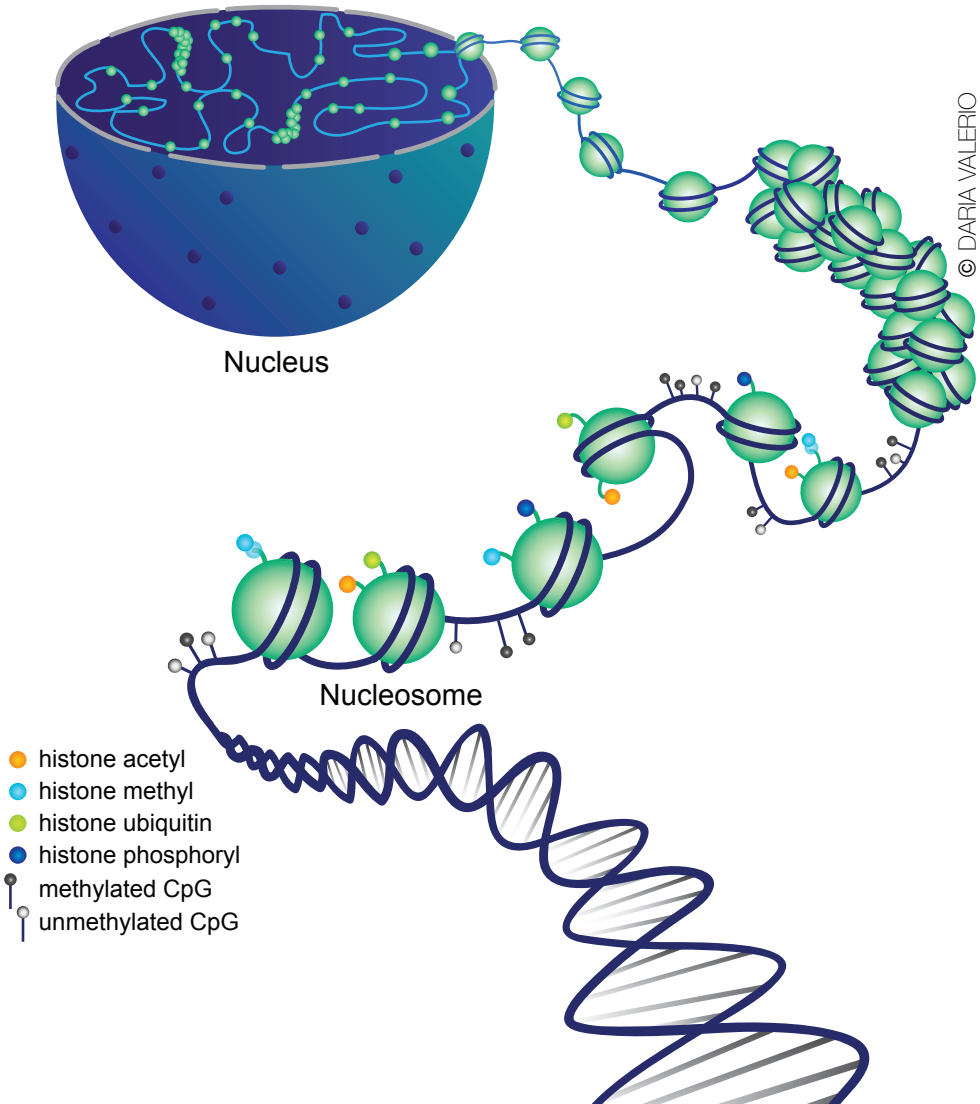

Figure 3. Epigenetic gene regulation is primarily achieved through DNA methylation and post-translational histone modification

In order for all DNA to fit in a cell nucleus, the DNA double helix is wound around a cluster of 8 histone proteins known as nucleosomes. This complex of histones and DNA is referred to as chromatin. When the chromatin is compact, DNA cannot be translated. Various histone modifications contribute to compaction or opening of chromatin.

Leukemic blasts of patients with either an *MLL1* or *NUP98* translocation show elevated expression of *MEIS1* and *HOXA* cluster genes.[28,29,44-47] Studies in *MLL*-rearranged leukemia have shown that *HOXA* and *MEIS1* are direct targets of MLL1 fusion proteins and that the expression of these genes is a crucial part of the leukemogenic program.[47-50] These MLL1 fusion targets are associated with aberrantly high levels of histone 3 lysine 79 dimethylation (H3K79me2), a chromatin mark that was found to be regulated by the histone methyltransferase DOT1L.[50,51] *MLL-r*earranged cells are highly dependent on *Dot1l* for leukemia initiation and maintenance[48,52-54], a discovery that led to the development of small molecule inhibitors targeting DOT1L, one of which is currently undergoing a clinical phase I trial.[55,56] Findings such as these indicate the importance of chromatin regulation in leukemia and beautifully illustrate how our evolving knowledge of epigenetic deregulation in cancer can lead to new therapeutic approaches. The current state of therapeutically targeting the cancer epigenome will be reviewed in Chapter 2.

MOF AND MLL1

In this thesis, we focus on the two chromatin-modifiers MLL1 and MOF, and their respective role in leukemogenesis. MLL1 is a large nuclear protein that contains a SET domain with H3K4 mono- di and tri-methyltransferase activity if bound to the WDR5/RBBP5/ASH2L/DUMPY30 subcomplex.[57-59] *Mll1* loss is embryonically lethal[60] and *Mll1*-deficient fetal and adult hematopoietic cells lack HSC and progenitor activity, illustrating that *Mll1* is crucial for murine definitive hematopoiesis[61,62].

MOF is a histone 4 lysine 16 (H4K16) acetyltransferase[63-65] and is also crucial for murine embryogenesis[65,66]. Murine embryos with homozygous, constitutional loss of *Mof* do not develop beyond the blastocyst stage. MOF is a cell type-dependent regulator of chromatin state and controls various essential cellular processes such as DNA damage response[67-71], cell cycle progression[67,72] and embryonic stem cell self-renewal and pluripotency[73]. The role of MOF in tumorigenesis seems complex. Studies in breast carcinoma[74], medulloblastoma[74] and ovarian cancer[75] indicate that tumor progression is associated with downregulation of *MOF* and H4K16 acetylation (H4K16ac). On the other hand, studies in lung[76,77] and oral[78]

carcinoma have associated high expression of *MOF* with carcinogenesis and suppression of *MOF* with cancer cell death. This suggests that MOF may be involved in tumorigenesis in a cell and tissue dependent manner.

Both MOF and MLL1 function in larger protein complexes. MOF is part of the mammalian non-specific lethal (NSL) complex, containing various other proteins such as WDR5, HCF1, NSL1, NSL2, NSL3, MCRS2, PHF20 and OGT1.[79,80] Three components of the NSL complex, WDR5, HCF1 and PHF20 are shared with the MLL1-core protein complex (Figure 4).[79,80] In addition, human MOF was shown to physically associate with MLL1 in a multi-protein complex that catalyzes both histone acetylation and methylation.[81] These studies demonstrate potential physical and functional association between the NSL and MLL1 complexes.

MOF and MLL1 link back to *NUP98* rearranged leukemia through a couple of studies in *Drosophila*, beginning with a study that has shown that, while wild type, full-length NUP98 is localized at the nuclear envelope in the nuclear pore complex, truncated NUP98 is nucleoplasmic localized and functions as a potential transcriptional activator with a preference for promoters of genes with high H3K4 methylation and H4K16 acetylation.[82] A more recent *Drosophila* study has demonstrated that only nucleoplasm localized NUP98 can physically interact with the NSL and MLL1 complexes.[83] We hypothesized that, since NUP98 fusion proteins contain a truncated NUP98 portion, NUP98 fusions might be localized in the nucleoplasm rather than at the nuclear membrane and therefore may interact with the NSL and MLL1 complex. This hypothesis is the subject of experimental studies presented in Chapter 3.

The functional relation between MLL1 and *MLL-AF9* has previously been studied where it was suggested that MLL1 might be involved in *MLL-AF9* leukemogenesis.[84] However, more recent work has shown that MLL1 H3K4 methyltransferase activity is not required for *MLL-AF9* leukemogenesis.[85] While MLL1 and MOF physically interact[81], we hypothesized that it may be the histone acetyltransferase activity of MOF that is required for *MLL-AF9* leukemogenesis and that MLL1 merely functions as a scaffolding protein, recruiting MOF to the MLL-AF9 fusion complex. This question and our findings are addressed in Chapter 4. Although the function of MLL1 in normal hematopoiesis has been well defined, the role of MOF in general hematopoiesis and hematopoietic development has not previously been studied. In Chapter 5 of this thesis we will depict the important regulatory role of MOF and its histone acetyltransferase activity in mammalian hematopoietic development.

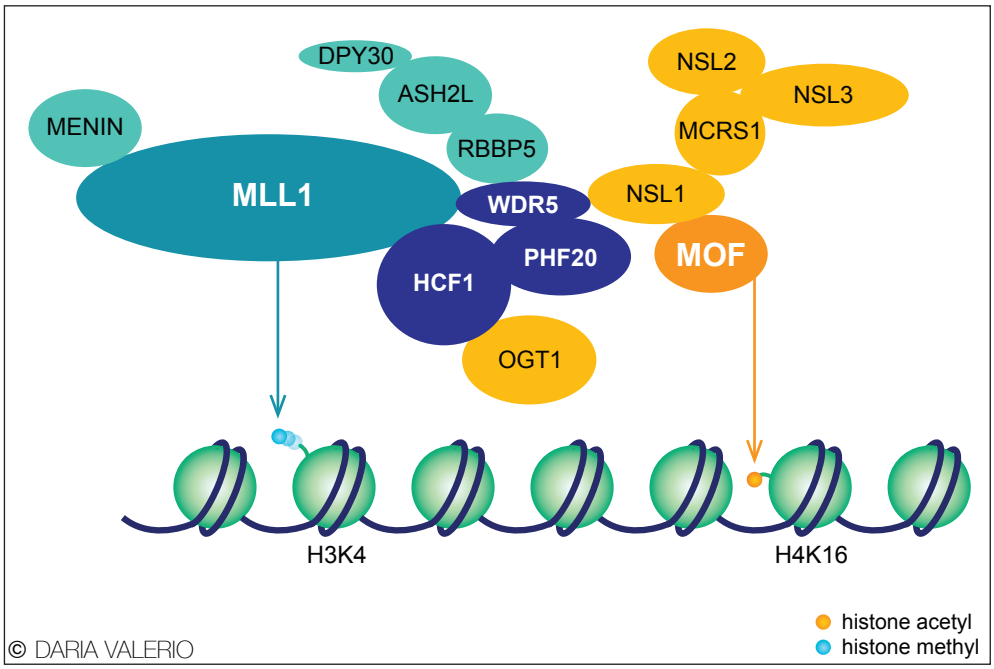

Figure 4. Physical association between the NSL and MLL1-core protein complex
The epigenetic regulators MOF and MLL1 function in larger protein complexes. MOF is part of the mammalian non-specific lethal (NSL) complex. Two components of the NSL complex, WDR5 and HCF1, are shared between the NSL and MLL1-core protein complex.

REFERENCES

1. Weissman IL, Shizuru JA. The origins of the identification and isolation of hematopoietic stem cells, and their capability to induce donor-specific transplantation tolerance and treat autoimmune diseases. *Blood.* 2008;112(9):3543-3553.
2. Reya T, Morrison SJ, Clarke MF, Weissman IL. Stem cells, cancer, and cancer stem cells. *Nature.* 2001;414(6859):105-111.
3. Godin I, Dieterlen-Lievre F, Cumano A. Emergence of multipotent hemopoietic cells in the yolk sac and paraaortic splanchnopleura in mouse embryos, beginning at 8.5 days postcoitus. *Proc Natl Acad Sci U S A.* 1995;92(3):773-777.
4. Dzierzak E, Medvinsky A. Mouse embryonic hematopoiesis. *Trends in genetics.* 1995;11(9):359-366.
5. Wolber FM, Leonard E, Michael S, Orschell-Traycoff CM, Yoder MC, Srour EF. Roles of spleen and liver in development of the murine hematopoietic system. *Exp Hematol.* 2002;30(9):1010-1019.
6. Tavian M, Peault B. Embryonic development of the human hematopoietic system. *Int J Dev Biol.* 2005;49(2-3):243-250.
7. Metcalf D, Moore M. Embryonic aspects of hematopoiesis. *Frontiers of Biology*: North Holland Publishing; 1971:172-271.
8. Mikkola HK, Orkin SH. The journey of developing hematopoietic stem cells. *Development.* 2006;133(19):3733-3744.
9. Lessard J, Faubert A, Sauvageau G. Genetic programs regulating HSC specification, maintenance and expansion. *Oncogene.* 2004;23(43):7199-7209.
10. Cheshier SH, Morrison SJ, Liao X, Weissman IL. In vivo proliferation and cell cycle kinetics of long-term self-renewing hematopoietic stem cells. *Proc Natl Acad Sci U S A.* 1999;96(6):3120-3125.
11. Bowie MB, McKnight KD, Kent DG, McCaffrey L, Hoodless PA, Eaves CJ. Hematopoietic stem cells proliferate until after birth and show a reversible phase-specific engraftment defect. *J Clin Invest.* 2006;116(10):2808-2816.
12. Ikuta K, Kina T, MacNeil I, et al. A developmental switch in thymic lymphocyte maturation potential occurs at the level of hematopoietic stem cells. *Cell.* 1990;62(5):863-874.
13. Kim I, Saunders TL, Morrison SJ. Sox17 dependence distinguishes the transcriptional regulation of fetal from adult hematopoietic stem cells. *Cell.* 2007;130(3):470-483.
14. Ivanova NB, Dimos JT, Schaniel C, Hackney JA, Moore KA, Lemischka IR. A stem cell molecular signature. *Science.* 2002;298(5593):601-604.
15. Kim I, Yilmaz OH, Morrison SJ. CD144 (VE-cadherin) is transiently expressed by fetal liver hematopoietic stem cells. *Blood.* 2005;106(3):903-905.
16. Morrison SJ, Hemmati HD, Wandycz AM, Weissman IL. The purification and characterization of fetal liver hematopoietic stem cells. *Proc Natl Acad Sci U S A.* 1995;92(22):10302-10306.
17. Park IK, Qian D, Kiel M, et al. Bmi-1 is required for maintenance of adult self-renewing haematopoietic stem cells. *Nature.* 2003;423(6937):302-305.
18. Surveillance E, and End Results (SEER) Program (http://www.seer.cancer.gov). SEER*Stat Database: Acute Myeloid Leukemia. *2008-212*: National Institute of Health (NIH).
19. Surveillance E, and End Results (SEER) Program (http://www.seer.cancer.gov). SEER*Stat Database: Acute Lymphocytic Leukemia. *2008-2012*: National Institute of Health (NIH).
20. Deschler B, Lubbert M. Acute myeloid leukemia: epidemiology and etiology. *Cancer.* 2006;107(9):2099-2107.
21. Greaves M. Childhood leukaemia. *BMJ.* 2002;324(7332):283-287.
22. Djabali M, Selleri L, Parry P, Bower M, Young BD, Evans GA. A trithorax-like gene is interrupted by chromosome 11q23 translocations in acute leukaemias. *Nat Genet.* 1992;2(2):113-118.
23. Tkachuk DC, Kohler S, Cleary ML. Involvement of a homolog of Drosophila trithorax by 11q23

chromosomal translocations in acute leukemias. *Cell.* 1992;71(4):691-700.
24. Muntean AG, Hess JL. The pathogenesis of mixed-lineage leukemia. *Annu Rev Pathol.* 2012;7:283-301.
25. Greaves MF. Infant leukaemia biology, aetiology and treatment. *Leukemia.* 1996;10(2):372-377.
26. Meyer C, Hofmann J, Burmeister T, et al. The MLL recombinome of acute leukemias in 2013. *Leukemia.* 2013;27(11):2165-2176.
27. Gough SM, Slape CI, Aplan PD. NUP98 gene fusions and hematopoietic malignancies: common themes and new biologic insights. *Blood.* 2011;118(24):6247-6257.
28. de Rooij JD, Hollink IH, Arentsen-Peters ST, et al. NUP98/JARID1A is a novel recurrent abnormality in pediatric acute megakaryoblastic leukemia with a distinct HOX gene expression pattern. *Leukemia.* 2013;27(12):2280-2288.
29. Hollink IH, van den Heuvel-Eibrink MM, Arentsen-Peters ST, et al. NUP98/NSD1 characterizes a novel poor prognostic group in acute myeloid leukemia with a distinct HOX gene expression pattern. *Blood.* 2011;118(13):3645-3656.
30. Chou WC, Chen CY, Hou HA, et al. Acute myeloid leukemia bearing t(7;11)(p15;p15) is a distinct cytogenetic entity with poor outcome and a distinct mutation profile: comparative analysis of 493 adult patients. *Leukemia.* 2009;23(7):1303-1310.
31. Bisio V PM, Manara E, Masetti R, Togni M, Astolfi A, Mecucci C, Zappavigna V, Salsi V, Merli P, Rizzari C, Fagioli F, Locatelli F and Basso G. NUP98 Fusion Proteins Are Recurrent Aberrancies in Childhood Acute Myeloid Leukemia: A Report from the AIEOP AML-2001-02 Study Group. *56th ASH annual meeting*. December 6-9, 2014, 2014; San Francisco.
32. Holliday R. Epigenetics: a historical overview. *Epigenetics.* 2006;1(2):76-80.
33. Kouzarides T. Chromatin modifications and their function. *Cell.* 2007;128(4):693-705.
34. Galm O, Herman JG, Baylin SB. The fundamental role of epigenetics in hematopoietic malignancies. *Blood Rev.* 2006;20(1):1-13.
35. Feinberg AP, Ohlsson R, Henikoff S. The epigenetic progenitor origin of human cancer. *Nat Rev Genet.* 2006;7(1):21-33.
36. Garraway LA, Lander ES. Lessons from the cancer genome. *Cell.* 2013;153(1):17-37.
37. Welch JS, Ley TJ, Link DC, et al. The origin and evolution of mutations in acute myeloid leukemia. *Cell.* 2012;150(2):264-278.
38. Abdel-Wahab O, Levine RL. Mutations in epigenetic modifiers in the pathogenesis and therapy of acute myeloid leukemia. *Blood.* 2013;121(18):3563-3572.
39. Mullighan CG. The genomic landscape of acute lymphoblastic leukemia in children and young adults. *Hematol Am Soc Hematol Educ Program.* 2014;2014(1):174-180.
40. Mullighan CG, Goorha S, Radtke I, et al. Genome-wide analysis of genetic alterations in acute lymphoblastic leukaemia. *Nature.* 2007;446(7137):758-764.
41. Valerio DG, Katsman-Kuipers JE, Jansen JH, et al. Mapping epigenetic regulator gene mutations in cytogenetically normal pediatric acute myeloid leukemia. *Haematologica.* 2014;99(8):e130-132.
42. Liang DC, Liu HC, Yang CP, et al. Cooperating gene mutations in childhood acute myeloid leukemia with special reference on mutations of ASXL1, TET2, IDH1, IDH2, and DNMT3A. *Blood.* 2013;121(15):2988-2995.
43. Brien Gerard L, Valerio Daria G, Armstrong Scott A. Exploiting the Epigenome to Control Cancer-Promoting Gene-Expression Programs. *Cancer Cell.* 2016;29(4):464-476.
44. Takeda A, Goolsby C, Yaseen NR. NUP98-HOXA9 induces long-term proliferation and blocks differentiation of primary human CD34+ hematopoietic cells. *Cancer Res.* 2006;66(13):6628-6637.
45. Shiba N, Ichikawa H, Taki T, et al. NUP98-NSD1 gene fusion and its related gene expression signature are strongly associated with a poor prognosis in pediatric acute myeloid leukemia. *Genes Chromosomes Cancer.* 2013;52(7):683-693.
46. Armstrong SA, Staunton JE, Silverman LB, et al. MLL translocations specify a distinct gene

expression profile that distinguishes a unique leukemia. *Nat Genet.* 2002;30(1):41-47.
47. Argiropoulos B, Humphries RK. Hox genes in hematopoiesis and leukemogenesis. *Oncogene.* 2007;26(47):6766-6776.
48. Bernt KM, Zhu N, Sinha AU, et al. MLL-rearranged leukemia is dependent on aberrant H3K79 methylation by DOT1L. *Cancer Cell.* 2011;20(1):66-78.
49. Chen CW, Koche RP, Sinha AU, et al. DOT1L inhibits SIRT1-mediated epigenetic silencing to maintain leukemic gene expression in MLL-rearranged leukemia. *Nat Med.* 2015;21(4):335-343.
50. Krivtsov AV, Feng Z, Lemieux ME, et al. H3K79 methylation profiles define murine and human MLL-AF4 leukemias. *Cancer Cell.* 2008;14(5):355-368.
51. Guenther MG, Lawton LN, Rozovskaia T, et al. Aberrant chromatin at genes encoding stem cell regulators in human mixed-lineage leukemia. *Genes Dev.* 2008;22(24):3403-3408.
52. Deshpande AJ, Deshpande A, Sinha AU, et al. AF10 regulates progressive H3K79 methylation and HOX gene expression in diverse AML subtypes. *Cancer Cell.* 2014;26(6):896-908.
53. Chang MJ, Wu H, Achille NJ, et al. Histone H3 lysine 79 methyltransferase Dot1 is required for immortalization by MLL oncogenes. *Cancer Res.* 2010;70(24):10234-10242.
54. Jo SY, Granowicz EM, Maillard I, Thomas D, Hess JL. Requirement for Dot1l in murine postnatal hematopoiesis and leukemogenesis by MLL translocation. *Blood.* 2011;117(18):4759-4768.
55. Daigle SR, Olhava EJ, Therkelsen CA, et al. Potent inhibition of DOT1L as treatment of MLL-fusion leukemia. *Blood.* 2013;122(6):1017-1025.
56. Daigle SR, Olhava EJ, Therkelsen CA, et al. Selective killing of mixed lineage leukemia cells by a potent small-molecule DOT1L inhibitor. *Cancer Cell.* 2011;20(1):53-65.
57. Dou Y, Milne TA, Ruthenburg AJ, et al. Regulation of MLL1 H3K4 methyltransferase activity by its core components. *Nat Struct Mol Biol.* 2006;13(8):713-719.
58. Patel A, Vought VE, Dharmarajan V, Cosgrove MS. A novel non-SET domain multi-subunit methyltransferase required for sequential nucleosomal histone H3 methylation by the mixed lineage leukemia protein-1 (MLL1) core complex. *J Biol Chem.* 2011;286(5):3359-3369.
59. Steward MM, Lee JS, O'Donovan A, Wyatt M, Bernstein BE, Shilatifard A. Molecular regulation of H3K4 trimethylation by ASH2L, a shared subunit of MLL complexes. *Nat Struct Mol Biol.* 2006;13(9):852-854.
60. Yu BD, Hess JL, Horning SE, Brown GA, Korsmeyer SJ. Altered Hox expression and segmental identity in Mll-mutant mice. *Nature.* 1995;378(6556):505-508.
61. Ernst P, Fisher JK, Avery W, Wade S, Foy D, Korsmeyer SJ. Definitive hematopoiesis requires the mixed-lineage leukemia gene. *Dev Cell.* 2004;6(3):437-443.
62. Gan T, Jude CD, Zaffuto K, Ernst P. Developmentally induced Mll1 loss reveals defects in postnatal haematopoiesis. *Leukemia.* 2010;24(10):1732-1741.
63. Smith ER, Cayrou C, Huang R, Lane WS, Cote J, Lucchesi JC. A human protein complex homologous to the Drosophila MSL complex is responsible for the majority of histone H4 acetylation at lysine 16. *Mol Cell Biol.* 2005;25(21):9175-9188.
64. Akhtar A, Becker PB. Activation of transcription through histone H4 acetylation by MOF, an acetyltransferase essential for dosage compensation in Drosophila. *Mol Cell.* 2000;5(2):367-375.
65. Thomas T, Dixon MP, Kueh AJ, Voss AK. Mof (MYST1 or KAT8) is essential for progression of embryonic development past the blastocyst stage and required for normal chromatin architecture. *Mol Cell Biol.* 2008;28(16):5093-5105.
66. Gupta A, Guerin-Peyrou TG, Sharma GG, et al. The mammalian ortholog of Drosophila MOF that acetylates histone H4 lysine 16 is essential for embryogenesis and oncogenesis. *Mol Cell Biol.* 2008;28(1):397-409.
67. Gupta A, Hunt CR, Hegde ML, et al. MOF phosphorylation by ATM regulates 53BP1-mediated double-strand break repair pathway choice. *Cell Rep.* 2014;8(1):177-189.
68. Gupta A, Sharma GG, Young CS, et al. Involvement of human MOF in ATM function. *Mol Cell Biol.*

2005;25(12):5292-5305.
69. Li X, Corsa CA, Pan PW, et al. MOF and H4 K16 acetylation play important roles in DNA damage repair by modulating recruitment of DNA damage repair protein Mdc1. *Mol Cell Biol.* 2010;30(22):5335-5347.
70. Sharma GG, So S, Gupta A, et al. MOF and histone H4 acetylation at lysine 16 are critical for DNA damage response and double-strand break repair. *Mol Cell Biol.* 2010;30(14):3582-3595.
71. Bhadra MP, Horikoshi N, Pushpavallipvalli SN, et al. The role of MOF in the ionizing radiation response is conserved in Drosophila melanogaster. *Chromosoma.* 2012;121(1):79-90.
72. Taipale M, Rea S, Richter K, et al. hMOF histone acetyltransferase is required for histone H4 lysine 16 acetylation in mammalian cells. *Mol Cell Biol.* 2005;25(15):6798-6810.
73. Li X, Li L, Pandey R, et al. The histone acetyltransferase MOF is a key regulator of the embryonic stem cell core transcriptional network. *Cell Stem Cell.* 2012;11(2):163-178.
74. Pfister S, Rea S, Taipale M, et al. The histone acetyltransferase hMOF is frequently downregulated in primary breast carcinoma and medulloblastoma and constitutes a biomarker for clinical outcome in medulloblastoma. *Int J Cancer.* 2008;122(6):1207-1213.
75. Cai M, Hu Z, Liu J, et al. Expression of hMOF in different ovarian tissues and its effects on ovarian cancer prognosis. *Oncol Rep.* 2015;33(2):685-692.
76. Zhang S, Liu X, Zhang Y, Cheng Y, Li Y. RNAi screening identifies KAT8 as a key molecule important for cancer cell survival. *Int J Clin Exp Pathol.* 2013;6(5):870-877.
77. Zhao L, Wang DL, Liu Y, Chen S, Sun FL. Histone acetyltransferase hMOF promotes S phase entry and tumorigenesis in lung cancer. *Cell Signal.* 2013;25(8):1689-1698.
78. Li Q, Sun H, Shu Y, Zou X, Zhao Y, Ge C. hMOF (human males absent on the first), an oncogenic protein of human oral tongue squamous cell carcinoma, targeting EZH2 (enhancer of zeste homolog 2). *Cell Prolif.* 2015;48(4):436-442.
79. Cai Y, Jin J, Swanson SK, et al. Subunit composition and substrate specificity of a MOF-containing histone acetyltransferase distinct from the male-specific lethal (MSL) complex. *J Biol Chem.* 2010;285(7):4268-4272.
80. Raja SJ, Charapitsa I, Conrad T, et al. The nonspecific lethal complex is a transcriptional regulator in Drosophila. *Mol Cell.* 2010;38(6):827-841.
81. Dou Y, Milne TA, Tackett AJ, et al. Physical association and coordinate function of the H3 K4 methyltransferase MLL1 and the H4 K16 acetyltransferase MOF. *Cell.* 2005;121(6):873-885.
82. Kalverda B, Pickersgill H, Shloma VV, Fornerod M. Nucleoporins directly stimulate expression of developmental and cell-cycle genes inside the nucleoplasm. *Cell.* 2010;140(3):360-371.
83. Pascual-Garcia P, Jeong J, Capelson M. Nucleoporin Nup98 associates with Trx/MLL and NSL histone-modifying complexes and regulates Hox gene expression. *Cell Rep.* 2014;9(2):433-442.
84. Thiel AT, Blessington P, Zou T, et al. MLL-AF9-induced leukemogenesis requires coexpression of the wild type Mll allele. *Cancer Cell.* 2010;17(2):148-159.
85. Mishra BP, Zaffuto KM, Artinger EL, et al. The histone methyltransferase activity of MLL1 is dispensable for hematopoiesis and leukemogenesis. *Cell Rep.* 2014;7(4):1239-1247.

Cancer Cell

Volume 29
Number 4

April 11, 2016

www.cell.com

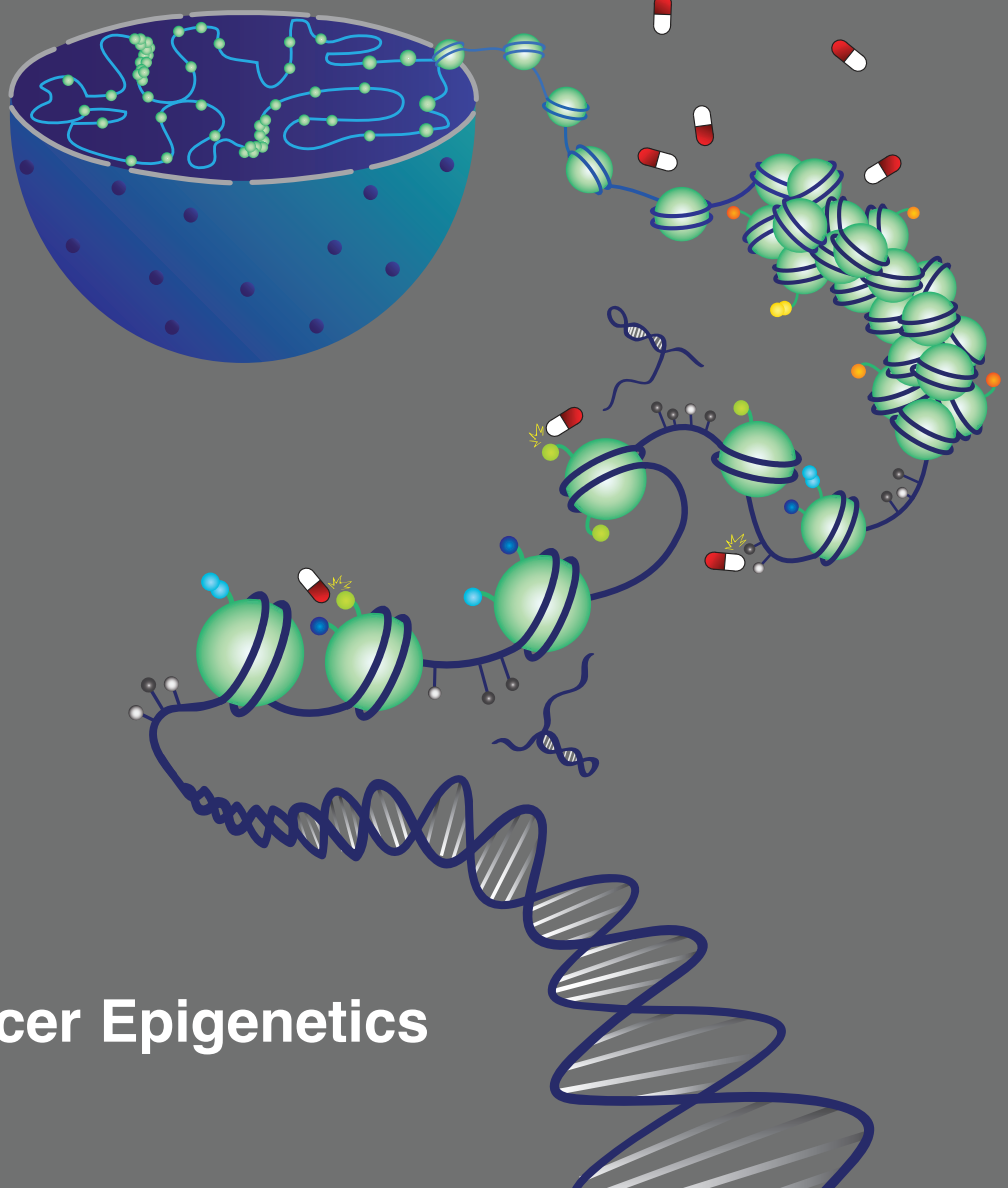

Cancer Epigenetics

2

EXPLOITING THE EPIGENOME TO CONTROL CANCER-PROMOTING GENE-EXPRESSION PROGRAMS

Gerry L. Brien, Daria G. Valerio, Scott A. Armstrong

Cancer Cell. 2016; 29(4): 464-76

ABSTRACT

The epigenome and underlying chromatin biology are key determinants of transcriptional output. Perturbations within the epigenome are thought to be a key feature of many, if not all cancers, and it is now clear that epigenetic changes are instrumental in cancer development. The inherent reversibility of these changes makes them attractive targets for therapeutic manipulation and a number of small molecules targeting chromatin-based mechanisms are currently in clinical trials. In this perspective we discuss how understanding the cancer epigenome is providing insights into disease pathogenesis and informing drug development. We also highlight additional opportunities to further unlock the therapeutic potential within the cancer epigenome.

INTRODUCTION

Epigenetics refers to heritable traits that are not attributable to changes in DNA sequence. In more specific terms, it can be used to describe how chromatin-associated proteins and reversible chemical modifications of DNA and histone proteins maintain transcriptional programs by regulating chromatin structure (Strahl and Allis, 2000). Since all cells in a multicellular organism contain essentially the same DNA, the development of specialized cell types requires a tightly regulated process that leads to the expression of genes critical for a specific cell type; and repression of genes required for alternative cell fates. One important process by which cells regulate cell type specific gene expression is the packaging of DNA into chromatin in a fashion that modulates transcriptional output in a given cell type. Therefore, epigenetic regulatory mechanisms are instrumental in dictating cell identities and have been implicated in fundamental processes such as development, stem cell self-renewal, differentiation, genome integrity and proliferation (Tessarz and Kouzarides, 2014). Epigenetic gene regulation is primarily achieved through the collaboration of multiple regulatory pathways; involving sequence specific DNA binding transcription factors, long non-coding RNAs (lncRNAs), ATP-dependent nucleosome remodeling, DNA methylation, introduction of histone variants, and post-translational modification (PTM) of histone proteins. Histone proteins can be modified at specific amino acid residues by diverse chemical moieties including methylation, acetylation, phosphorylation, ubiquitination and SUMOylation (Kouzarides, 2007). Identification of the chromatin regulatory proteins involved in mediating, removing and binding these modifications has expedited our understanding of the biology of many of these PTMs (Figure 1). Moreover, examining the genome-wide localization of histone PTMs, DNA methylation and chromatin regulatory proteins in a wide spectrum of biological contexts has allowed researchers to begin defining “epigenomic landscapes” and how these relate to cellular phenotypes (Bernstein et al., 2010). Combining these data with gene expression profiles has provided significant insights into the biological significance of many of these entities as they relate to gene expression (Brien and Bracken, 2009).

It has been appreciated for some time that deregulation of the epigenomic landscape is a common feature of a number of diseases, including cancer. Some of the earliest observed epigenetic abnormalities in cancer cells were alterations in the patterns of DNA methylation and histone acetylation (Feinberg and Vogelstein, 1983; Fraga et al., 2005; Greger et al., 1989; Sakai et al., 1991). Localized hypermethylation of gene promoter regions leading to transcriptional repression of tumor suppressor genes such as *CDKN2A* and *RB1* were subsequently found to be a common feature of many cancers (Baylin and Jones, 2011). Moreover, DNA hypermethylation events also occur over broad sub-chromosomal domains encompassing multiple tumor suppressor genes (Coolen et al., 2010; Frigola et al., 2006). The chemotherapeutic agents azacitidine (5-azacytidine) and decitabine (5-aza-2’-deoxycytidine); when used at low doses were shown to irreversibly inhibit the enzymatic activity of the DNA methyltransferase enzyme DNMT1 and induce global hypomethylation. These drugs represent the first targeted epigenetic therapies and were FDA

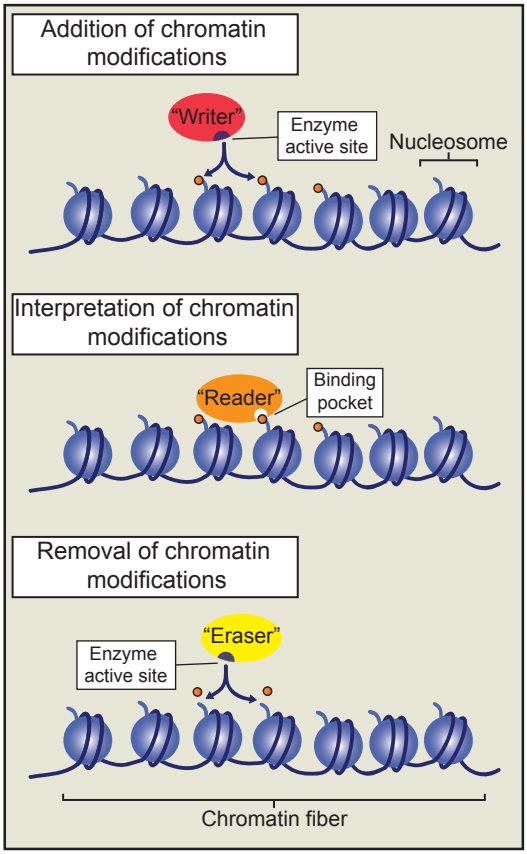

Figure 1. Chromatin writers, readers and erasers in epigenetic gene regulation
The addition of histone post-translational modifications is catalyzed by a class of enzymes known as chromatin "writers". The modifications established by these writers may affect gene transcription by altering electrostatic interactions within or between adjacent nucleosomes. Alternatively they may act as binding substrates for another class of chromatin regulators called chromatin "readers". Chromatin readers employ characteristic binding domains, such as chromo-, bromo-, and PHD-finger domains to bind nucleosomes marked by specific modifications, or a combination of modifications. Chromatin readers may themselves possess additional chromatin modifying activities, or alternatively recruit additional proteins to modify the local chromatin environment. Finally, chromatin "erasers" catalyze the removal of histone modifications, thereby reversing their biochemical effects on the chromatin fiber.

approved in 2005 for the treatment of myelodysplastic syndrome (MDS) and are currently recommended as first line treatments for high-risk MDS patients (Issa and Kantarjian, 2009). Global loss of histone acetylation is also a common feature of many cancers (Fraga et al., 2005), and has been associated with unfavorable patient outcomes in certain cases (Seligson et al., 2005). Vorinostat (Suberoylanilide hydroxamic acid – SAHA) which inhibits the activity of histone deacetylase (HDAC) enzymes, leading to global increases in histone acetylation, was granted FDA approval for the treatment of advanced cutaneous T-cell lymphoma in 2006 (Mann et al., 2007; Wagner et al., 2010). Since this initial success, the HDAC inhibitors romidepsin and panobinostat have been approved for use in cutaneous T-cell lymphoma and multiple myeloma, respectively (Khan and La Thangue, 2012; Laubach et al., 2015). Recently, studies that combine DNA methylation and HDAC inhibitors have been initiated; with several clinical trials currently ongoing examining the utility of these combinations in hematopoietic malignancies and solid tumors (Falkenberg and Johnstone, 2014). Moreover, pre-clinical studies have indicated that combination therapies involving HDAC inhibitors and some of the emerging epigenetic therapies may prove clinically beneficial (Fiskus et al.,

2014; Mazur et al., 2015).

Until recently it was unclear whether epigenetic changes play a causal role in cancer development or whether they merely are a result of the cancerous state. However, recent cancer genome sequencing studies have shown that genes encoding chromatin regulatory proteins are among the most commonly mutated gene sets in cancer (Garraway and Lander, 2013). In fact, 25-30% of the identified cancer driver mutations affect genes encoding chromatin regulatory proteins (Garraway and Lander, 2013; Vogelstein et al., 2013). These findings indicate that altered epigenetic states do not just correlate with cancer but likely drive disease pathogenesis. This has spurred a significant research effort to understand how altered epigenetic states drive cancer cell phenotypes and how to therapeutically exploit these phenomena. We have only begun to scratch the surface with regard to our mechanistic understanding of the cancer epigenome, but this limited knowledge has already delivered tangible successes with regard to our ability to therapeutically manipulate cancer promoting epigenetic states and cancer associated gene expression programs (Table 1) (Cai et al., 2015).

In this perspective we will discuss how our burgeoning understanding of the cancer epigenome and chromatin regulatory mechanisms are yielding significant insights into the mechanisms underlying disease development; and providing a rational means to identify drug targets for the treatment of certain cancers. This is a very exciting time in the field, with

Table 1: Selection of targeted epigenetic therapies in use or under clinical investigation in cancer patients

Protein	Biological function	Cancer type	Small-molecule(s)	Clinical Trial	References
CHROMATIN WRITERS					
DOT1L	H3K79 methylation	AML, ALL	EPZ-5676	NCT01684150 NCT02141828	Daigle et al., 2013
EZH2	H3K27 methylation	Non-Hodgkin lymphoma, SNF5-deficient MRTs	GSK2816126, EPZ-6438, CP1-1205	NCT01897571 NCT02082977 NCT02395601	McCabe et al., 2012; Knutson et al., 2013
DNMT1	DNA Methylation (Hemi-methylated CpGs)	MDS, CMML	Azacitidine, Decitabine	FDA approved	Issa and Kantarjian 2009
CHROMATIN READERS					
BET-family	Acetyl-lysine binding	AML, MDS, lymphoma, glioblastoma, NMC multiple myeloma, Breast cancer, NSCLC, Prostate cancer, Pancreatic cancer	OTX015, CPI-0610,	NCT01713582 NCT01949883 NCT02157636 NCT02158858 NCT02259114 NCT02296476 NCT02303782	Filippakopoulos et al., 2010; Delmore et al., 2011; Zuber et al., 2011
CHROMATIN ERASERS					
LSD1	H3K4/K9 demethylation	AML, MDS, SCLC	GSK2879552, Tranylcypromine	NCT02034123 NCT02177812 NCT02261779 NCT02273102	Harris et al., 2012; Schenk et al.; 2012
HDAC1/2/3	Lysine deacetylation	Cuteanous T cell lymphoma, Multiple myeloma	Vorinstat, Romidepsin, Panobinostat	FDA approved	Mann et al., 2007; Khan and La Thangue 2012

AML - Acute myeloid leukemia, ALL - Acute lymphoid leukemia, MRT - Malignant rhabdoid tumor, MDS - Myelodysplastic syndrome, CMML - Chronic myeloproliferative leukemia, NMC - NUT midline carcinoma, NSCLC - Non-small cell lung cancer, SCLC - Small cell lung cancer

a number of targeted epigenetic therapies in ongoing clinical trials. However, the relatively small number of drug targets identified to date is still a limiting factor and we will also discuss how a more comprehensive approach to studying the cancer epigenome will be necessary in order to truly harness the therapeutic potential therein.

EXPLOITING ONCOGENIC CHROMATIN ACTIVITIES

Oncogenic chromatin writers

The histone methyltransferase (HMT) EZH2 is subject to recurrent gain-of-function mutations in B-cell lymphoma (Morin et al., 2011, 2010). EZH2 is a lysine methyltransferase and the catalytic subunit of the PRC2 complex; as part of this complex, EZH2 mediates the mono-, di- and tri-methylation of lysine 27 of histone H3 (H3K27me1/2/3) (Conway et al., 2015). EZH2 primarily functions as a transcriptional repressor through deposition of H3K27me3 at the promoter regions of PRC2 target genes (Margueron and Reinberg, 2011). In addition, EZH2 mediated H3K27me2 may also be important for transcriptional repression by maintaining the inactive state of intergenic enhancer elements (Ferrari et al., 2014; Lee et al., 2015). Heterozygous point mutations of *EZH2* are found in 22% of patients with diffuse large B-cell lymphoma and 10% with follicular lymphoma. These mutations affect key residues within the active site of the catalytic Su(var)3-9, enhancer of zeste, trithorax (SET) domain (McCabe et al., 2012; Morin et al., 2010). *In vitro* analysis has shown that the preferred enzymatic activity of wild type EZH2 is the conversion of H3K27me0-to-me1 and H3K27me1-to-me2, while the enzyme is relatively inefficient at the final conversion step to H3K27me3. However, owing to alterations in substrate binding modality, the lymphoma associated EZH2 SET domain mutants exhibit enhanced ability to convert H3K27me2-to-me3 (Antonysamy et al., 2013; M. T. McCabe et al., 2012; Sneeringer et al., 2010; Wigle et al., 2011; Yap et al., 2011). This finding suggests that wild type and mutant EZH2 collaborate to push the kinetics of PRC2 activity towards increased H3K27me3 production. Indeed, lymphoma cell lines containing *EZH2* gain-of-function mutations exhibit globally increased levels of H3K27me3, with a concomitant decrease in H3K27me2 (McCabe et al., 2012; Yap et al., 2011). Chromatin immunoprecipitation coupled with next generation sequencing (ChIP-seq) for H3K27me3 in an *in vivo* mouse model of *Ezh2*-mutant lymphoma demonstrated that mutant EZH2 drives aberrant repression of genes required for cell cycle exit and appropriate differentiation of Germinal Center B-cells via accumulation of H3K27me3 at gene promoter regions (Béguelin et al., 2013). Taken together, these data support the idea that mutant EZH2 promotes lymphoma development through alterations in H3K27 methylation levels, leading to a block in Germinal Center B-cell differentiation and enhanced proliferation (Figure 2).

This observation has made EZH2 enzymatic activity an attractive target for treatment of *EZH2*-mutant lymphomas. Several highly selective small molecule EZH2 SET domain inhibitors have been developed (Knutson et al., 2012; McCabe et al., 2012; Qi et al., 2012).

Interestingly, these molecules were shown to reduce H3K27me3 levels to a similar degree in cells, regardless of their *EZH2*-mutational status (McCabe et al., 2012; Qi et al., 2012). However, *EZH2*-mutant cells are acutely sensitive to EZH2 inhibition both *in vitro* and *in vivo*, where EZH2 inhibition leads to up-regulation of repressed H3K27me3 marked genes and apoptotic cell death (Béguelin et al., 2013; McCabe et al., 2012). These data lend further support to the notion that aberrant H3K27me3 accumulation is essential for the survival of *EZH2*-mutant lymphoma cells. Based on these pre-clinical successes, some of these compounds have now entered phase I clinical trials for the treatment of relapsed refractory B-cell lymphoma, and advanced solid tumors (Figure 2, and discussed further below) - NCT02395601, NCT01897571, and NCT02082977 at www.clinicaltrials.gov.

The *NSD2* gene (also known as *MMSET* or *WHSC1*) encodes an HMT, responsible for mediating di-methylation of H3K36 (H3K36me2). NSD2 primarily functions as a transcriptional activator by depositing intragenic H3K36me2 at active genes (Huang et al., 2013; Kuo et al., 2011), although it may also function in transcriptional repression in limited contexts (Marango et al., 2008). *NSD2* was initially discovered because of its involvement in a recurrent chromosomal translocation t(4;14), occurring in 20% of multiple myeloma (MM) cases (Chesi et al., 1998). This translocation places *NSD2*, and its neighboring gene *FGFR3*, under the control of the IgH locus Eμ enhancer, leading to increased expression of both genes, though *NSD2* appears to be the oncogene in this setting (Keats et al., 2003; Santra et al., 2003). *NSD2* is also subject to recurrent gain-of-function mutations in lymphoid malignancies, with the highest prevalence (14%) in pediatric acute lymphoblastic leukemia (ALL) patients carrying an *ETV6-RUNX1* fusion (Jaffe et al., 2013; Oyer et al., 2014). These mutations result in a glutamic acid to lysine switch at position 1099 (E1099K) within the SET domain of NSD2, leading to increased enzymatic activity *in vitro*. Consistent with this, global levels of H3K36me2 are increased in cells harboring either an E1099K activating *NSD2* mutation or a t(4;14) translocation (Huang et al., 2013; Jaffe et al., 2013). Moreover, H3K36me2 ChIP-seq in t(4;14) rearranged MM cells demonstrates that H3K36me2 marked domains undergo a broad expansion into intergenic space as a result of increased *NSD2* expression (Kuo et al., 2011; Popovic et al., 2014). Consistent with the fact that higher order H3K36 methylation directly inhibits the enzymatic activity of the PRC2 complex (Schmitges et al., 2011; Yuan et al., 2011), this expansion of H3K36me2 is accompanied by global losses of H3K27me2/3 (Jaffe et al., 2013). While the exact mechanism by which NSD2 drives malignancy remains unclear, the broad gain of H3K36me2 and loss of repressive H3K27 methylation may lead to an opening of the chromatin landscape, creating a more permissive or “stem cell-like” state which is more amenable to additional reprogramming by transcription factors (Nimura et al., 2009). Consistent with this, expression profiling of t(4;14) MM cells revealed that these cells have increased expression of genes associated with self-renewal, and reduced expression of genes associated with mature B-cell functions (Huang et al., 2013; Kuo et al., 2011; Popovic et al., 2014). Interestingly, despite the global loss of H3K27 methylation, H3K27me3 is focally increased at certain gene promoters, many of which correlate with aberrantly repressed B-cell differentiation genes (Popovic et al., 2014). Together, these findings suggest that

NSD2 activation drives a broad rewiring of the epigenome, which may in turn block terminal differentiation thereby contributing to oncogenesis.

Several studies have demonstrated that the activity of the NSD2 SET domain is essential for the observed chromatin/transcriptional changes and tumorigenicity in MM and lymphoma cells (Jaffe et al., 2013; Kuo et al., 2011). This supports the notion that the changes in H3K36me2 are instrumental for development of these cancers and suggests that targeting the NSD2 SET domain with a specific small-molecule would be an excellent therapeutic approach. However, to date no potent inhibitors of NSD2 have been published (Cain, 2013). In addition to targeting the NSD2 SET domain, recent studies have demonstrated that certain chromatin reading domains in NSD2 are essential for the oncogenic function of the protein (Huang et al., 2013; Popovic et al., 2014). For example, NSD2 protein fragments lacking functionality in the second, third or fourth PHD-finger domain or the second PWWP-domain have reduced transforming activity. These domains potentially mediate the interaction of NSD2 with chromatin, or with ancillary protein co-factors that are important for NSD2 function. It will be important to further elucidate the function of these domains; since they too may be viable drug targets for the treatment of NSD2 activated cancers.

Oncogenic chromatin readers

NUT midline carcinoma (NMC) is an aggressive form of squamous cell cancer that occurs in all age groups and NMC patients have a dismal average overall survival of just 6.7 months (French, 2014). This disease is characterized by translocations of the *NUT* gene to one of two bromodomain and extra terminal (BET) family genes, *BRD4* or *BRD3*. Together these translocations account for approximately 80% of all NMC cases. Alternatively *NUT* may also be indirectly linked to BRD4, through fusion to the BRD4 associated protein NSD3 (French et al., 2014; Shen et al., 2015). This propensity for linkage of NUT to BET family proteins suggests that their collaborative function is important for disease pathogenesis. The function of wild type NUT is unclear, though it has been reported to interact with the lysine acetyltransferases p300/CBP and enhance their activity (Reynoird et al., 2010). BET family proteins are acetyl-lysine readers, that promote transcription by interacting with, and recruiting the positive transcription elongation factor (P-TEFb) and Mediator complexes to chromatin (Jang et al., 2005; Jiang et al., 1998; Lovén et al., 2013; Yang et al., 2005). BRD-NUT fusion proteins bind chromatin in distinctive foci associated with elevated levels of histone acetylation (French et al., 2008). Recent ChIP experiments demonstrate that these foci correspond to broad “megadomains” of BRD-NUT binding, ranging from 100KB-1.4MB in size, typically delimited by topological chromatin domains (Alekseyenko et al., 2015). Moreover, these megadomains are also associated with elevated binding of pTEFb and Mediator components (Wang and You, 2015). Several genes within these megadomains such as *MYC* (Grayson et al., 2014), *TP63* and *MED24* (Alekseyenko et al., 2015) exhibit increased expression in a BRD-NUT dependent manner and are essential for maintaining the undifferentiated and highly proliferative state of NMC cells. Together these data suggest that BRD-NUT megadomains promote the expression of genes that drive NMC pathogenesis.

Interestingly, the formation of these megadomains requires the function of both the BET bromodomains and the acetyltransferase activity of p300/CBP (Reynoird et al., 2010). This suggests a model wherein p300/CBP mediated histone acetylation generates a binding substrate for BET bromodomains, leading to spreading of BRD-NUT into the surrounding chromatin fiber (Alekseyenko et al., 2015; French, 2014). The fact that BET bromodomains are critical for this process has been therapeutically exploited using the small-molecule BET inhibitor JQ1 (Filippakopoulos et al., 2010). Treatment of NMC cell lines with JQ1 induces a rapid differentiation and proliferation arrest. Moreover, JQ1 treatment improves survival in murine xenograft models. Based on these pre-clinical successes, several derivatives of JQ1 with improved pharmacodynamic properties are currently in clinical trials for the treatment of NMC and other cancers (discussed further below) - NCT01587703, NCT01713582, NCT01949883, NCT01987362, and NCT01943851 at www.clinicaltrials.gov.

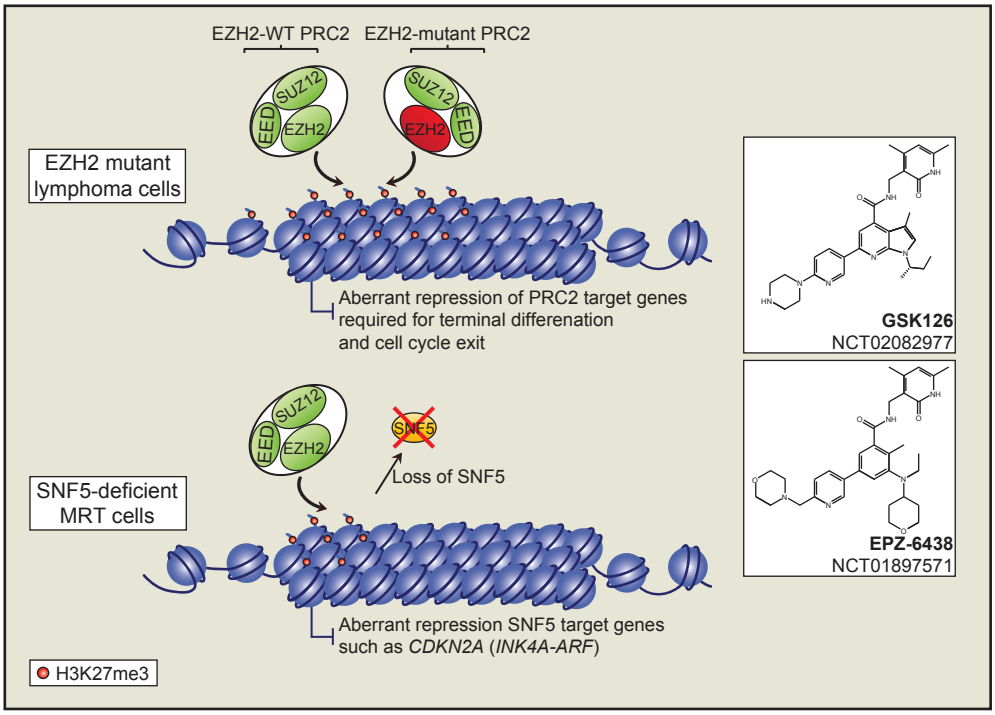

Figure 2. Targeting the oncogenic function of EZH2 in lymphoma and solid tumors

Heterozygous point mutations of the EZH2 SET domain in non-Hodgkin lymphomas leads to an enhanced accumulation of H3K27me3 on the promoters of PRC2 target genes in Germinal Center B-cells (upper panel). This causes aberrant silencing of these genes, many of which are required for terminal B-cell differentiation and cell cycle exit. Small-molecule inhibitors (right panels) of EZH2 enzymatic activity are currently in clinical trials for the treatment of lymphoma patients with activating EZH2 mutations. Moreover, these molecules are also in trials for the treatment of SNF5-deficient malignant rhabdoid tumors (MRTs) where SNF5-loss facilitates aberrant EZH2-mediated silencing of SNF5 target genes, such as the tumor suppressor *CDKN2A* (lower panel).

EXPLOITING NON-ONCOGENE CHROMATIN DEPENDENCIES

Chromosomal rearrangements at 11q23 are associated with acute leukemia which led to the discovery of the *MLL1* gene (Djabali et al., 1992; Gu et al., 1992; Tkachuk et al., 1992; Ziemin-van der Poel et al., 1991). *MLL* translocations are found in ~10% of patients with acute leukemia and are generally associated with an unfavorable prognosis (Krivtsov and Armstrong, 2007; Muntean and Hess, 2012). *MLL* rearrangements are more frequently present in infant and pediatric patients, with the highest frequency of 80% in infant ALL (Greaves, 1996). MLL1 is primarily thought to function as a transcriptional activator at least in part through tri-methylation of H3K4 (H3K4me3) at the promoters of active genes. In *MLL*-rearranged leukemia the N-terminus of *MLL1* is fused to one of over 70 different fusion partners; however, *MLL-AF4* t(4:11), *MLL-AF9* t(9:11), *MLL-ENL* t(11;19), *MLL-AF10* t(10;11) and *MLL-ELL* t(11;19) are the most common translocations, collectively accounting for the vast majority (>80%) of *MLL1*-rearrangements seen in patients (Krivtsov and Armstrong, 2007). *MLL*-rearranged leukemias exhibit a strikingly low rate of somatic mutation (Andersson et al., 2015), supporting the notion that *MLL1* fusions are the primary drivers of these leukemias. Despite the loss of the C-terminal SET domain of MLL1 in *MLL1* fusions, genome-wide levels of H3K4me3 are not reduced in MLL1 fusion leukemia cells; suggesting that alternative H3K4 methyltransferase(s) maintain H3K4 methylation in these cells (Bernt et al., 2011; Mishra et al., 2014). Indeed recent evidence suggests that maintaining H3K4 methylation levels in MLL1 fusion leukemia stem cells may be important for the leukemic potential of these cells (Wong et al., 2015). This highlights the importance of identifying the H3K4 methyltransferase(s) involved in maintaining H3K4 methylation levels in MLL1 fusion leukemia. Some of the first hints toward the mechanisms by which MLL1 fusion proteins mediate leukemogenesis came from the realization that a number of the most common MLL1 fusion partners exist in overlapping protein complexes whose functions are associated with transcriptional elongation (Deshpande et al., 2012). The HMT DOT1L, which mediates mono-, di- and tri-methylation of H3K79 (H3K79me1/2/3), is a component of several of these complexes and perturbations in normal H3K79me2 patterns are a feature of *MLL*-rearranged leukemia (Guenther et al., 2008; Krivtsov et al., 2008). DOT1L-mediated deposition of H3K79me2 downstream of active gene promoters is believed to be important for efficient transcriptional elongation and active gene expression (Nguyen and Zhang, 2011). Subsequent studies demonstrated that the aberrant levels of H3K79me2 in *MLL*-rearranged leukemia accumulate specifically at MLL1 fusion target genes, indicating that this phenomenon is likely driven by MLL1 fusion protein mediated recruitment of DOT1L to these sites (Bernt et al., 2011) (Figure 3). These genes include several key regulators of hematopoietic stem cell identity, such as *Hoxa* cluster genes and *Meis1*. It has recently been shown that a critical function of DOT1L mediated H3K79 methylation is to inhibit repressive mechanisms that would otherwise silence MLL1 fusion driven gene expression (Chen et al., 2015). These data support the hypothesis that MLL1 fusion proteins cause a block in hematopoietic cell differentiation by preventing repression of stem cell regulators.

Genetic inactivation of *Dotl1* in a mouse model of MLL-AF9 driven leukemia led to prolonged survival, demonstrating that DOT1L-mediated H3K79me2 is important for leukemogenesis (Bernt et al., 2011; Jo et al., 2011; Nguyen et al., 2011). Strikingly, *Dot1l* inactivation specifically results in downregulation of MLL-AF9 target genes, suggesting that inhibiting DOT1L may provide a specific means to target these leukemias. Parallel studies demonstrated that pharmacological inhibition of DOT1L enzymatic activity with a small-molecule inhibitor reduced H3K79me2 levels *in vitro* and *in vivo*, leading to reduced expression of MLL-AF9 target genes (Daigle et al., 2011) (Figure 3). These early successes lead to the development of an improved DOT1L inhibitor (Daigle et al., 2013), which is currently in ongoing clinical trials for the treatment of patients with *MLL*-rearranged leukemia - NCT02141828 and NCT01684150 at https://clinicaltrials.gov.

Until the discovery of the first histone demethylase LSD1 (also known as KDM1A) histone demethylation was thought to be a passive process, accomplished through dilution of methylated histones during cell division. LSD1 is a member of the FAD-dependent monooxidase family of enzymes and is primarily responsible for mediating the demethylation of the mono- and di-methylated forms of H3K4 and H3K9 (H3K4me1/me2 and H3K9me1/me2) (Metzger et al., 2005; Shi et al., 2004). Interest in LSD1 as a potential therapeutic target in cancer was spurred by observations of increased LSD1 expression in several cancers including neuroblastoma (Schulte et al., 2009), prostate cancer (Kahl et al., 2006), bladder cancer (Kauffman et al., 2011), colorectal and lung cancer (Hayami et al., 2011; Mohammad et al., 2015) and certain hematopoietic cancers (Harris et al., 2012). Significantly, recent studies using both genetic inactivation and pharmacologic inhibition of LSD1 in the context of AML have provided evidence for a functional link between LSD1 and leukemia (Harris et al., 2012; Schenk et al., 2012). Moreover, LSD1 inhibition can sensitize AML cells to all-*trans*-retinoic acid (ATRA) induced differentiation, and combining LSD1 inhibition with ATRA treatment reduces engraftment of primary AML patient samples in xenograft models (Schenk et al., 2012). Interestingly, LSD1 inhibition is not associated with global increases in either H3K4me1/2 or H3K9me1/2 levels across the genome; and the underlying epigenetic mechanism(s) of how LSD1 inhibition affects leukemia cell phenotypes is still unclear. This is confounded by the fact that focal decreases, as well as increases in H3K4me2 are apparent in LSD1 inhibitor treated leukemia cells (Harris et al., 2012; Schenk et al., 2012). LSD1 inhibition has also recently been shown to have clinical efficacy in small cell lung cancer (SCLC) (Mohammad et al., 2015). As with AML, LSD1 inhibition in the setting of SCLC does not have a global effect on H3K4me1/2 levels. Moreover, LSD1 inhibition results in generally non-overlapping transcriptional changes in sensitive cell lines. As such, a clear mechanistic understanding of the role of LSD1 in sustaining leukemia and lung cancer cells is currently lacking. However, despite the lack of a clear mechanistic understanding of the role of LSD1 in leukemia and SCLC these pre-clinical successes have lead to LSD1 inhibitors entering clinical trials for the treatment of these diseases – NCT02273102, NCT02177812, NCT02261779 and NCT02034123 at https://clinicaltrials.gov.

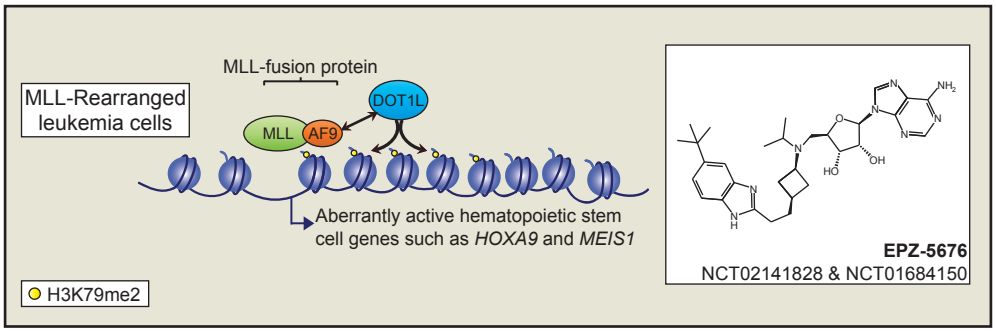

Figure 3. Targeting *MLL*-rearranged leukemia through co-opted DOT1L activity
Studies have demonstrated that MLL1 fusion proteins, such as MLL-AF9, recruit aberrant chromatin activity in the form of DOT1L mediated H3K79me2 to the promoter of MLL1 fusion target genes in primitive hematopoietic cells. DOT1L activity is essntial for the expression of MLL1 fusion target genes such as *HOXA9* and *MEIS1*, and this requirement has been exploited through the development of small-molecule inhibitors of DOT1L enzymatic activity (right panel). DOT1L inhibitors are currently in clinical trials for the treatment of *MLL*-rearranged leukemia.

EXPLOITING TRANSCRIPTIONAL ADDICTIONS

A number of recent studies have demonstrated that several chromatin regulatory proteins, namely BRD4, CDK7 and CDK9, all of which play general roles in transcriptional activation, are specifically required for cancer cell survival in certain contexts (ChIPumuro et al., 2014; Christensen et al., 2014; Dawson et al., 2011; Delmore et al., 2011; Kwiatkowski et al., 2014; Wang et al., 2015; Zuber et al., 2011). As mentioned above, BRD4 binds acetylated histones and modulates the localization and function of transcriptional complexes such as pTEFb and Mediator. CDK7 and CDK9 are cyclin-dependent kinases and components of the TFIIH and pTEFb complexes, respectively. Within these complexes CDK7 and CDK9 promote transcription by phosphorylating RNA polymerase II (RNAPII), thereby enabling active transcriptional initiation and elongation (Larochelle et al., 2012; Zhou et al., 2012). Given the general role of BRD4, CDK7 and CDK9 in facilitating transcription, the fact that cancer cells show a greater dependency on these proteins is somewhat surprising, but there is growing evidence that cancer cells may be significantly addicted to high rates of transcription (Lin et al., 2012). Interestingly, an overarching theme emerging from these studies is that inhibiting these proteins leads to preferential downregulation of super-enhancer associated genes (ChIPumuro et al., 2014; Kwiatkowski et al., 2014; Lovén et al., 2013; Shi and Vakoc, 2014; Wang et al., 2015). Super-enhancers are clusters of enhancer elements that activate the expression of genes required for cell identity; and in cancer cells, super-enhancers also drive the expression of key oncogenes (Lovén et al., 2013). ChIP-seq studies have demonstrated that BRD4 and CDK7 are preferentially bound at super-enhancers (ChIPumuro et al., 2014;

Lovén et al., 2013), and recent work indicates that mutations in enhancer elements, or oncogenic transcription factors may drive the formation of super-enhancers in tumor cells (Mansour et al., 2014; Oldridge et al., 2015). Taken together, these findings suggest that inhibiting certain components of the general transcriptional machinery provides a means to target transcriptional addictions to oncogenic transcription factors such as MYC (Shi and Vakoc, 2014), MYCN (ChIPumuro et al., 2014), TAL1 (Kwiatkowski et al., 2014) and others (Christensen et al., 2014). A critical next step will be to understand how these addictions develop and to determine which specific components of the transcriptional machinery are required in which cancer types.

EXPLOITING CHROMATIN BASED MECHANISMS OF ACQUIRED DRUG RESISTANCE

A significant clinical challenge in cancer treatment is the emergence of therapeutic resistance. Rewiring of signaling programs and epigenomic changes are increasingly being recognized as mechanisms of acquired drug resistance (Brown et al., 2014; Holohan et al., 2013; Sharma et al., 2010). For example, breast cancers with activated PI3K and ERBB2 signaling are typically treated with kinase inhibitors targeting these pathways. However, resistance often emerges owing to upregulation of alternative receptor tyrosine kinase (RTK) genes which compensate for the inhibited enzyme (Azuma et al., 2011; Britschgi et al., 2012; Chandarlapaty et al., 2011; Rexer et al., 2011). Combination therapies targeting multiple RTKs can in some instances circumvent resistance, but the multitude of upregulated RTKs limits the effectiveness of this approach. Recent work has demonstrated that combining PI3K or ERBB2 inhibitors with BET bromodomain inhibition re-sensitizes previously resistant breast cancer cells to kinase inhibition (Stratikopoulos et al., 2015; Stuhlmiller et al., 2015). The effectiveness of adding BET inhibitors in this context can be explained by increased BRD4 binding at the promoter/enhancer regions of transcriptionally activated RTKs in response to PI3K inhibition, suggesting that BRD4 facilitates the upregulation of alternative RTKs (Stratikopoulos et al., 2015). Moreover, BRD4 also appears to be important for transcriptional activation of the downstream target genes of these RTKs (Stuhlmiller et al., 2015), further explaining the utility of BET inhibitors in this setting. BRD4 inhibition may also have utility in prostate cancers resistant to androgen receptor (AR) inhibition. Sustained AR signaling is a primary driver of castration-resistant prostate cancer, and inhibition of AR signaling is used as a therapeutic approach in this subset of patients. Unfortunately, these patients often develop resistance to AR inhibitors and invariably succumb to disease (Watson et al., 2015). BRD4 directly interacts with the N-terminus of the AR in a bromodomain dependent manner, and AR signaling-positive prostate cancer cells are exquisitely sensitive to BET inhibition (Asangani et al., 2014). BRD4 and AR colocalize on chromatin and BET inhibition leads to a robust downregulation of AR target genes, suggesting that BET inhibition might be an

approach to circumvent acquired resistance to AR inhibitors. Another example of resistance mediated by epigenetic changes concerns patients with T-cell acute lymphoblastic leukemia (T-ALL) driven by activating mutations in *NOTCH1*. Small molecule y-secretase inhibitors (GSI) block NOTCH1 signaling in T-ALL lymphoblasts, but response to these inhibitors is only transient, suggesting that resistance limits their clinical efficacy (Palomero and Ferrando, 2009). GSI-resistant cells exhibit increased BRD4 binding on chromatin compared to GSI-naive cells, and maintain MYC expression via alternative enhancer usage at the MYC locus, independent of NOTCH1 (Knoechel et al., 2014; Yashiro-Ohtani et al., 2014). This renders GSI resistant cells markedly more sensitive to JQ1 treatment, and *in vivo* GSI-JQ1 combination therapy is significantly more effective against primary human T-ALL than treatment with either single agent (Knoechel et al., 2014). These findings demonstrate that acquired drug resistance may in fact be commonly driven by epigenetic changes, which may be addressed by incorporating epigenetic modulators in combination therapies.

A number of recent studies have identified mechanisms of acquired resistance to novel epigenetic therapies. For example, resistance to the BET bromodomain inhibitors JQ1 and I-BET in MLL-AF9 AML cells is mediated in part by alternative enhancer usage at the MYC locus; which maintains expression levels of MYC in resistant cell lines (Fong et al., 2015; Rathert et al., 2015). Interestingly, this appears to be downstream of the WNT signaling pathway and inhibition of WNT signaling may provide a means to circumvent resistance in this setting (Fong et al., 2015). Significantly, a distinct mechanism of BET inhibitor resistance has been described in triple-negative breast cancer cells (Shu et al., 2016). In this setting, resistant cells accumulate increased levels of phosphorylated BRD4, which appears to be crucial for the acquisition of resistance. Despite being bound by JQ1 phosphorylated BRD4 remains on chromatin indicating that the association of BRD4 with chromatin in this context is bromodomain independent. It will be important to further characterize the underlying mechanism(s) involved in this resistance phenotype; particularly in the context of the signaling pathway(s) driving BRD4 phosphorylation since modulation of these pathways may re-sensitize cells to BET inhibition. Taken together, these studies demonstrate that non-overlapping, and perhaps context dependent mechanisms can contribute to acquired resistance to a single epigenetic therapy; illustrating the need to study resistance mechanisms in multiple cancer models. Resistance to EZH2 inhibitors has also recently been described in *EZH2* gain-of-function lymphoma cells (Gibaja et al., 2015). This resistance was shown to be mediated by the acquisition of distinct mutations in the mutant (Y661D) and wildtype (Y111L) EZH2 alleles, respectively. These mutations render the PRC2 complex insensitive to treatment with EZH2 inhibitors, potentially by reducing the ability of these compounds to bind EZH2 (Gibaja et al., 2015). Studying the underlying mechanisms of acquired resistance to epigenetic therapies is of the utmost importance as it will be essential for our ability to circumvent these clinical barriers. Moreover, understanding these mechanisms may also provide a means of predicting therapeutic responses based on the identification of biomarkers of resistance or sensitivity.

IDENTIFYING ADDITIONAL THERAPEUTIC OPPORTUNITIES WITHIN THE CANCER EPIGENOME

The majority of somatic mutations affecting chromatin regulatory proteins in cancer are loss-of-function mutations leading to a reduction, or complete loss of chromatin modifying activities (Garraway and Lander, 2013). However, our ability to intervene therapeutically in this context is currently limited since it is often unclear what mechanisms are driving oncogenesis. The demonstration of "epigenetic antagonism" between the SWI/SNF and PRC2 complexes in cancer cells provides an interesting concept to consider in this context (Knutson et al., 2013; Wilson et al., 2010). The SWI/SNF complex is an ATP-dependent chromatin-remodeling complex that primarily functions in transcriptional activation. SWI/SNF activity plays important tumor suppressive roles *in vivo* and many SWI/SNF components are inactivated in cancer (Kadoch and Crabtree, 2015; Kadoch et al., 2013). In *Drosophila melanogaster* SWI/SNF genes were discovered as antagonists of PRC2 mediated gene repression (Kennison and Tamkun, 1988; Tamkun et al., 1992). This antagonism is conserved in mammals where SWI/SNF components directly oppose PRC2 mediated gene repression (Kia et al., 2008). In cancer, loss of the SWI/SNF component *SNF5* (also known as *SMARCB1* or *BAF47*) leads to elevated levels of H3K27me3 genome-wide, suggesting that *SNF5*-deficient cancers may rely on EZH2-mediated H3K27me3 to drive tumorigenesis. Roberts and colleagues demonstrated that this is indeed the case as concurrent loss of *Ezh2* and *Snf5* is not compatible with cancer development (Wilson et al., 2010). This finding has been exploited therapeutically using EZH2 SET domain inhibitors to treat *SNF5*-deficient rhabdoid tumors, which are markedly more sensitive to this treatment than *SNF5* wild type cancers (Knutson et al., 2013) (Figure 2). Moreover, EZH2 inhibitor treatment of non-small cell lung cancer cells with mutations in the SWI/SNF component *BRG1* (also known as *SMARCA4*) sensitizes these cells to chemotherapy, an effect that was not apparent in *BRG1* wild type cells (Fillmore et al., 2015). These are significant observations given the fact that approximately 20% of all cancers contain inactivating mutations in SWI/SNF components (Kadoch et al., 2013); and suggest that EZH2 inhibitors may have broad clinical utility outside of merely an EZH2 gain-of-function context. Following these observations, EZH2 inhibitors are now entering clinical trials for the treatment of *SNF5*-deficient tumors - NCT02601937 and NCT02601937 https://clinicaltrials.gov.

The central tenet that has emerged here is how loss of a single chromatin modifying activity may facilitate an increase in another, or perhaps multiple, functionally antagonistic activities which themselves promote oncogenesis (Figure 4). This highlights the need to expand our understanding of the interconnectedness of the epigenome, and how loss (and gain) of a single activity in cancer cells impacts the epigenome at large. This knowledge will shed light on mechanisms of disease pathogenesis and allow us to identify additional therapeutic opportunities. Recent advancements in sensitivity and accuracy of mass spectrometry and the introduction of quantitative labeling techniques such as SILAC and iTRAQ is now allowing

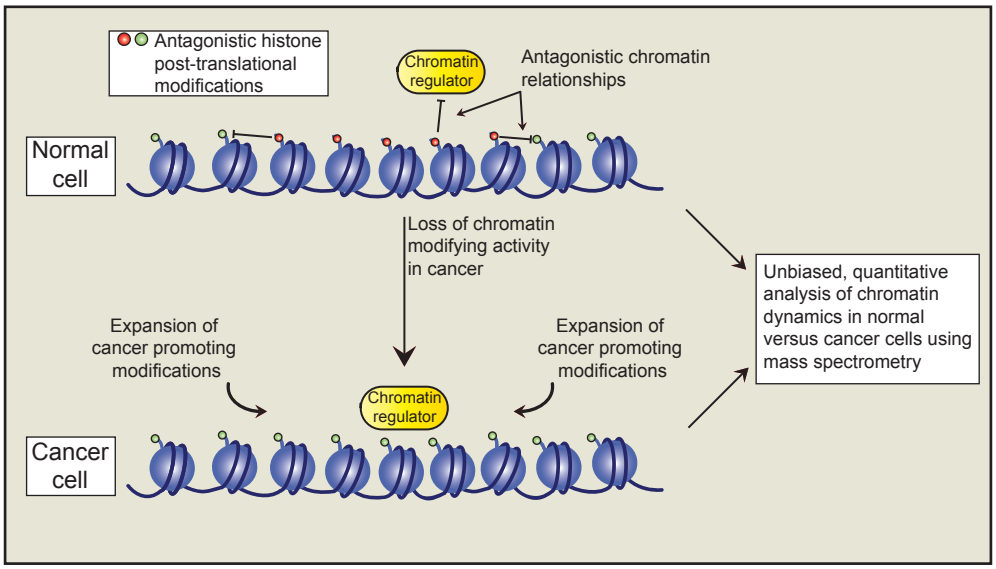

Figure 4. Defining the epigenomic changes in cancer

The alteration of a single chromatin modifying activity in cancer cells is known to have profound effects on the landscape of additional related chromatin modifications and other chromatin regulators. These alterations are likely instrumental in disease pathogenesis; however until recently our ability to systematically annotate such changes has been limited. The use of unbiased quantitative mass spectrometry techniques holds great promise for the annotation of chromatin dynamics in response to cancer promoting alterations in epigenetic pathways. This may facilitate the identification of additional therapeutic targets within the cancer epigenome.

for the molecular characterization of global epigenetic signatures (Britton et al., 2011). The use of these quantitative techniques has already identified antagonistic relationships involving cancer relevant histone methylation at H3K27 and H3K36 (Jaffe et al., 2013; Pasini et al., 2010; Yuan et al., 2011). For example, loss of PRC2 mediated H3K27 methylation due to mutation or deletion of PRC2 components in certain hematopoietic malignancies, malignant peripheral nerve sheath tumors (MPNSTs), melanomas and glioblastomas; leads to global increases in H3K27 acetylation (H3K27ac) and H3K36me1/2/3 (De Raedt et al., 2014; Ernst et al., 2010; Jaffe et al., 2013; Lee et al., 2014; Nikoloski et al., 2010; Ntziachristos et al., 2012; Zhang et al., 2012, 2014). The functional role of increased H3K36 methylation in a PRC2-deficient context has yet to be addressed; however, ChIP-seq studies have demonstrated that the increases in H3K27ac typically occur at previously silenced gene enhancer elements, potentially leading to inappropriate enhancer activity and transcriptional activation of associated genes (Ferrari et al., 2014). Consistent with this, transcriptional profiling of PRC2-deficient MPNST and T-ALL cells demonstrates that these cancers have characteristic expression signatures involving aberrant activation of PRC2 target genes with associated increases in H3K27ac and H3K9ac (Lee et al., 2014; Ntziachristos et al., 2012).

Re-introduction of PRC2 activity into PRC2-deficient MPNST cells leads to silencing of these aberrantly active genes, which is associated with loss of H3K27ac and cell growth arrest. Taken together, these findings suggest that increases in H3K27ac in response to PRC2-loss may be instrumental in driving oncogenic gene expression programs. This implicates H3K27ac as a potential therapeutic target for the treatment of PRC2-deficient cancers. The use of quantitative mass spectrometry to define global epigenomic changes in cancer cells will yield significant mechanistic insights into the role of altered epigenomic states in cancer development (Creech et al., 2014; Stunnenberg and Vermeulen, 2011) (Figure 4). Moreover, this will provide a rationale for therapeutically targeting such modifications.

PERSPECTIVES

The manipulation of cancer-promoting epigenetic states holds significant potential for the development of new cancer therapies. However, our understanding of the epigenomic alterations that promote oncogenesis and their influences on chromatin-based mechanisms are still limited. Additional effort is needed to deliver on this therapeutic promise. Unbiased analyses of the epigenomic changes in cancer cells will provide significant insights into the chromatin alterations that are instrumental in disease pathogenesis. Additionally, the use of chromatin-focused genomic screening techniques, particularly those utilizing the CRISPR/Cas9-mediated genome editing technology, are already facilitating the identification of epigenetic dependencies in cancer cells (Shi et al., 2015; Zuber et al., 2011). Application of these approaches will be important for the identification of additional therapeutic targets within the cancer epigenome. Moreover, their use in the context of drug resistance will facilitate the annotation of mechanisms related to drug sensitivity (Chen et al., 2015) and thereby aid the rational design of treatment regimens to circumvent the emergence of drug resistant cells. Structure based drug design towards the development of small-molecule therapeutics is often hampered by difficulties producing high-resolution structures for target molecules using traditional methods such as X-ray crystallography. However, recent advancements in cryogenic-electron microscopy (cryo-EM) techniques are revolutionizing the structural biology field and may well soon help alleviate this bottleneck (Nogales, 2016). Moreover, novel approaches to drug design such as the use of phthalimide conjugates to mediate proteosomal degradation of target proteins may overcome several limitations of conventional small-molecules (Winter et al., 2015). The mechanistic dissection of altered epigenomic states in cancer cells will undoubtedly accelerate the development of clinical strategies to manipulate these phenomena. In the next 10 years we will surely see the identification of new context-specific drug targets, complimented by the development of novel small-molecule therapeutics. As the field matures, this interface of basic and clinical research will hopefully allow us to thoroughly exploit the therapeutic potential of the cancer epigenome and provide curative options for cancer patients.

ACKNOWLEDGMENTS

We thank members of the Armstrong laboratory for helpful discussions during the preparation of this manuscript. Work in the Armstrong lab is supported by NIH grants PO1 CA66996 and R01 CA140575; the Leukemia and Lymphoma Society; and Gabrielle's Angel Research Foundation. G.L.B. is supported by an EMBO Long-Term Fellowship (ALTF 1235-2015) with additional support from Marie Curie Actions. D.G.V. is supported by a CURE Childhood Cancer Research Grant.

REFERENCES

Alekseyenko, A. a, Walsh, E.M., Wang, X., Grayson, A.R., Hsi, P.T., Kharchenko, P. V, Kuroda, M.I., French, C. a, 2015. The oncogenic BRD4-NUT chromatin regulator drives aberrant transcription within large topological domains 1507–1523. doi:10.1101/gad.267583.115.7

Andersson, A.K., Ma, J., Wang, J., Chen, X., Gedman, A.L., Dang, J., Nakitandwe, J., Holmfeldt, L., Parker, M., Easton, J., Huether, R., Kriwacki, R., Rusch, M., Wu, G., Li, Y., Mulder, H., Raimondi, S., Pounds, S., Kang, G., Shi, L., Becksfort, J., Gupta, P., Payne-Turner, D., Vadodaria, B., Boggs, K., Yergeau, D., Manne, J., Song, G., Edmonson, M., Nagahawatte, P., Wei, L., Cheng, C., Pei, D., Sutton, R., Venn, N.C., Chetcuti, A., Rush, A., Catchpoole, D., Heldrup, J., Fioretos, T., Lu, C., Ding, L., Pui, C.-H., Shurtleff, S., Mullighan, C.G., Mardis, E.R., Wilson, R.K., Gruber, T. a, Zhang, J., Downing, J.R., 2015. The landscape of somatic mutations in infant MLL-rearranged acute lymphoblastic leukemias. Nat Genet. 47, 1–147. doi:10.1038/ng.3230

Antonysamy, S., Condon, B., Druzina, Z., Bonanno, J.B., Gheyi, T., Zhang, F., MacEwan, I., Zhang, A., Ashok, S., Rodgers, L., Russell, M., Luz, J.G., 2013. Structural context of disease-associated mutations and putative mechanism of autoinhibition revealed by X-Ray crystallographic analysis of the EZH2-SET domain. PLoS One. 8, 1–15. doi:10.1371/journal.pone.0084147

Asangani, I. a, Dommeti, V.L., Wang, X., Malik, R., Cieslik, M., Yang, R., Escara-Wilke, J., Wilder-Romans, K., Dhanireddy, S., Engelke, C., Iyer, M.K., Jing, X., Wu, Y.-M., Cao, X., Qin, Z.S., Wang, S., Feng, F.Y., Chinnaiyan, A.M., 2014. Therapeutic targeting of BET bromodomain proteins in castration-resistant prostate cancer. Nature. 510, 278–82. doi:10.1038/nature13229

Azuma, K., Tsurutani, J., Sakai, K., Kaneda, H., Fujisaka, Y., Takeda, M., Watatani, M., Arao, T., Satoh, T., Okamoto, I., Kurata, T., Nishio, K., Nakagawa, K., 2011. Switching addictions between HER2 and FGFR2 in HER2-positive breast tumor cells: FGFR2 as a potential target for salvage after lapatinib failure. Biochem Biophys Res Commun. 407, 219–24. doi:10.1016/j.bbrc.2011.03.002

Baylin, S.B., Jones, P.A., 2011. A decade of exploring the cancer epigenome — biological and translational implications. Nucleus. doi:10.1038/nrc3130

Béguelin, W., Popovic, R., Teater, M., Jiang, Y., Bunting, K.L., Rosen, M., Shen, H., Yang, S.N., Wang, L., Ezponda, T., Martinez-Garcia, E., Zhang, H., Zheng, Y., Verma, S.K., McCabe, M.T., Ott, H.M., Van Aller, G.S., Kruger, R.G., Liu, Y., McHugh, C.F., Scott, D.W., Chung, Y.R., Kelleher, N., Shaknovich, R., Creasy, C.L., Gascoyne, R.D., Wong, K.-K., Cerchietti, L., Levine, R.L., Abdel-Wahab, O., Licht, J.D., Elemento, O., Melnick, A.M., 2013. EZH2 is required for germinal center formation and somatic EZH2 mutations promote lymphoid transformation. Cancer Cell. 23, 677–92. doi:10.1016/j.ccr.2013.04.011

Bernstein, B.E., Stamatoyannopoulos, J.A., Costello, J.F., Ren, B., Milosavljevic, A., Meissner, A., Kellis, M., Marra, M.A., Beaudet, A.L., Ecker, J.R., Farnham, P.J., Hirst, M., Lander, E.S., Mikkelsen, T.S., Thomson, J.A., 2010. The NIH Roadmap Epigenomics Mapping Consortium. Nat Biotechnol. 28, 1045–1048. doi:10.1038/nbt1010-1045

Bernt, K.M., Zhu, N., Sinha, A.U., Vempati, S., Faber, J., Krivtsov, A. V, Feng, Z., Punt, N., Daigle, A., Bullinger, L., Pollock, R.M., Richon, V.M., Kung, A.L., Armstrong, S.A., 2011. MLL-rearranged leukemia is dependent on aberrant H3K79 methylation by DOT1L. Cancer Cell. 20, 66–78. doi:10.1016/j.ccr.2011.06.010

Brien, G.L., Bracken, A.P., 2009. Transcriptomics: unravelling the biology of transcription factors and chromatin remodelers during development and differentiation. Semin Cell Dev Biol. 20, 835–841.

doi:S1084-9521(09)00162-1 [pii]10.1016/j.semcdb.2009.07.010

Britschgi, A., Andraos, R., Brinkhaus, H., Klebba, I., Romanet, V., Müller, U., Murakami, M., Radimerski, T., Bentires-Alj, M., 2012. JAK2/STAT5 Inhibition Circumvents Resistance to PI3K/mTOR Blockade: A Rationale for Cotargeting These Pathways in Metastatic Breast Cancer. Cancer Cell. 22, 796–811. doi:10.1016/j.ccr.2012.10.023

Britton, L.-M.P., Gonzales-Cope, M., Zee, B.M., Garcia, B.A., 2011. Breaking the histone code with quantitative mass spectrometry. Expert Rev Proteomics. 8, 631–43. doi:10.1586/epr.11.47

Brown, R., Curry, E., Magnani, L., Wilhelm-Benartzi, C.S., Borley, J., 2014. Poised epigenetic states and acquired drug resistance in cancer. Nat Rev Cancer. 14, 747–53. doi:10.1038/nrc3819

Cai, S.F., Chen, C.-W., Armstrong, S.A., 2015. Drugging Chromatin in Cancer: Recent Advances and Novel Approaches. Mol Cell. 60, 561–570. doi:10.1016/j.molcel.2015.10.042

Cain, C., 2013. NSD2 momentum. Sci Exch. 6, doi:10.1038/scibx.2013.1083. doi:10.1038/ng.2777

Chandarlapaty, S., Sawai, A., Scaltriti, M., Rodrik-Outmezguine, V., Grbovic-Huezo, O., Serra, V., Majumder, P.K., Baselga, J., Rosen, N., 2011. AKT Inhibition Relieves Feedback Suppression of Receptor Tyrosine Kinase Expression and Activity. Cancer Cell 19, 58–71. doi:10.1016/j.ccr.2010.10.031

Chen, C.-W., Koche, R.P., Sinha, A.U., Deshpande, A.J., Zhu, N., Eng, R., Doench, J.G., Xu, H., Chu, S.H., Qi, J., Wang, X., Delaney, C., Bernt, K.M., Root, D.E., Hahn, W.C., Bradner, J.E., Armstrong, S. a, 2015. DOT1L inhibits SIRT1-mediated epigenetic silencing to maintain leukemic gene expression in MLL-rearranged leukemia. Nat Med. 1–10. doi:10.1038/nm.3832

Chesi, M., Nardini, E., Lim, R.S., Smith, K.D., Kuehl, W.M., Bergsagel, P.L., 1998. The t(4;14) translocation in myeloma dysregulates both FGFR3 and a novel gene, MMSET, resulting in IgH/MMSET hybrid transcripts. Blood. 92, 3025–3034.

ChIPumuro, E., Marco, E., Christensen, C.L., Kwiatkowski, N., Zhang, T., Hatheway, C.M., Abraham, B.J., Sharma, B., Yeung, C., Altabef, A., Perez-Atayde, A., Wong, K.-K., Yuan, G.-C., Gray, N.S., Young, R.A., George, R.E., 2014. CDK7 Inhibition Suppresses Super-Enhancer-Linked Oncogenic Transcription in MYCN-Driven Cancer. Cell. 159, 1126–1139. doi:10.1016/j.cell.2014.10.024

Christensen, C.L., Kwiatkowski, N., Abraham, B.J., Carretero, J., Al-Shahrour, F., Zhang, T., ChIPumuro, E., Herter-Sprie, G.S., Akbay, E.A., Altabef, A., Zhang, J., Shimamura, T., Capelletti, M., Reibel, J.B., Cavanaugh, J.D., Gao, P., Liu, Y., Michaelsen, S.R., Poulsen, H.S., Aref, A.R., Barbie, D.A., Bradner, J.E., George, R.E., Gray, N.S., Young, R.A., Wong, K.-K., 2014. Targeting Transcriptional Addictions in Small Cell Lung Cancer with a Covalent CDK7 Inhibitor. Cancer Cell. 26, 909–922. doi:10.1016/j.ccell.2014.10.019

Conway, E., Healy, E., Bracken, A.P., 2015. PRC2 mediated H3K27 methylations in cellular identity and cancer. Curr Opin Cell Biol. 37, 42–48. doi:10.1016/j.ceb.2015.10.003

Coolen, M.W., Stirzaker, C., Song, J.Z., Statham, A.L., Kassir, Z., Moreno, C.S., Young, A.N., Varma, V., Speed, T.P., Cowley, M., Lacaze, P., Kaplan, W., Robinson, M.D., Clark, S.J., 2010. Consolidation of the cancer genome into domains of repressive chromatin by long-range epigenetic silencing (LRES) reduces transcriptional plasticity. Nat Cell Biol. 12, 235–246. doi:10.1038/ncb2023

Creech, A.L., Taylor, J.E., Maier, V.K., Wu, X., Feeney, C.M., Udeshi, N.D., Peach, S.E., Boehm, J.S., Lee, J.T., Carr, S. a, Jaffe, J.D., 2014. Building the Connectivity Map of epigenetics: Chromatin profiling by quantitative targeted mass spectrometry. Methods. 72, 57–64. doi:10.1016/j.ymeth.2014.10.033

Daigle, S.R., Olhava, E.J., Therkelsen, C. a., Basavapathruni, A., Jin, L., Boriack-Sjodin, P.A., Allain, C.J., Klaus, C.R., Raimondi, A., Scott, M.P., Waters, N.J., Chesworth, R., Moyer, M.P., Copeland, R. a., Richon, V.M., Pollock, R.M., 2013. Potent inhibition of DOT1L as treatment of MLL-fusion leukemia. Blood. 122, 1017–1025. doi:10.1182/blood-2013-04-497644

Daigle, S.R., Olhava, E.J., Therkelsen, C. a., Majer, C.R., Sneeringer, C.J., Song, J., Johnston, L.D., Scott, M.P., Smith, J.J., Xiao, Y., Jin, L., Kuntz, K.W., Chesworth, R., Moyer, M.P., Bernt, K.M., Tseng, J.C., Kung, A.L., Armstrong, S. a., Copeland, R. a., Richon, V.M., Pollock, R.M., 2011. Selective Killing of Mixed Lineage Leukemia Cells by a Potent Small-Molecule DOT1L Inhibitor. Cancer Cell. 20, 53–65. doi:10.1016/j.ccr.2011.06.009

Dawson, M.A., Prinjha, R.K., Dittmann, A., Giotopoulos, G., Bantscheff, M., Chan, W.-I., Robson, S.C., Chung, C., Hopf, C., Savitski, M.M., Huthmacher, C., Gudgin, E., Lugo, D., Beinke, S., Chapman, T.D., Roberts, E.J., Soden, P.E., Auger, K.R., Mirguet, O., Doehner, K., Delwel, R., Burnett, A.K., Jeffrey, P., Drewes, G., Lee, K., Huntly, B.J.P., Kouzarides, T., 2011. Inhibition of BET recruitment to chromatin as an effective treatment for MLL-fusion leukaemia. Nature. 478, 529–33. doi:10.1038/nature10509

De Raedt, T., Beert, E., Pasmant, E., Luscan, A., Brems, H., Ortonne, N., Helin, K., Hornick, J.L., Mautner, V., Kehrer-Sawatzki, H., Clapp, W., Bradner, J., Vidaud, M., Upadhyaya, M., Legius, E., Cichowski, K., 2014. PRC2 loss amplifies Ras-driven transcription and confers sensitivity to BRD4-based therapies. Nature. 514, 247–251. doi:10.1038/nature13561

Delmore, J.E., Issa, G.C., Lemieux, M.E., Rahl, P.B., Shi, J., Jacobs, H.M., Kastritis, E., Gilpatrick, T., Paranal, R.M., Qi, J., Chesi, M., Schinzel, A.C., McKeown, M.R., Heffernan, T.P., Vakoc, C.R., Bergsagel, P.L., Ghobrial, I.M., Richardson, P.G., Young, R.A., Hahn, W.C., Anderson, K.C., Kung, A.L., Bradner, J.E., Mitsiades, C.S., 2011. BET Bromodomain Inhibition as a Therapeutic Strategy to Target c-Myc. Cell. 146, 904–917. doi:10.1016/j.cell.2011.08.017

Deshpande, A.J., Bradner, J., Armstrong, S. a., 2012. Chromatin modifications as therapeutic targets in MLL-rearranged leukemia. Trends Immunol. 33, 563–570. doi:10.1016/j.it.2012.06.002

Djabali, M., Selleri, L., Parry, P., Bower, M., Young, B.D., Evans, G. a, 1992. A trithorax-like gene is interrupted by chromosome 11q23 translocations in acute leukaemias. Nat Genet. 2, 113–118. doi:10.1038/ng1092-113

Ernst, T., Chase, A.J., Score, J., Hidalgo-Curtis, C.E., Bryant, C., Jones, A. V, Waghorn, K., Zoi, K., Ross, F.M., Reiter, A., Hochhaus, A., Drexler, H.G., Duncombe, A., Cervantes, F., Oscier, D., Boultwood, J., Grand, F.H., Cross, N.C.P., 2010. Inactivating mutations of the histone methyltransferase gene EZH2 in myeloid disorders. Nat Genet. 42, 722–726. doi:10.1038/ng.621

Falkenberg, K.J., Johnstone, R.W., 2014. Histone deacetylases and their inhibitors in cancer, neurological diseases and immune disorders. Nat Rev Drug Discov. 13, 673–91. doi:10.1038/nrd4360

Feinberg, A.P., Vogelstein, B., 1983. Hypomethylation of ras oncogenes in primary human cancers. Biochem Biophys Res Commun. 111, 47–54.

Ferrari, K.J., Scelfo, A., Jammula, S., Cuomo, A., Barozzi, I., Stützer, A., Fischle, W., Bonaldi, T., Pasini, D., 2014. Polycomb-Dependent H3K27me1 and H3K27me2 Regulate Active Transcription and Enhancer Fidelity. Mol Cell. 53, 49–62. doi:10.1016/j.molcel.2013.10.030

Filippakopoulos, P., Qi, J., Picaud, S., Shen, Y., Smith, W.B., Fedorov, O., Morse, E.M., Keates, T., Hickman, T.T., Felletar, I., Philpott, M., Munro, S., McKeown, M.R., Wang, Y., Christie, A.L., West, N., Cameron, M.J., Schwartz, B., Heightman, T.D., La Thangue, N., French, C.A., Wiest, O., Kung, A.L.,

Knapp, S., Bradner, J.E., 2010. Selective inhibition of BET bromodomains. Nature. 468, 1067–73. doi:10.1038/nature09504

Fillmore, C.M., Xu, C., Desai, P.T., Berry, J.M., Rowbotham, S.P., Lin, Y.-J., Zhang, H., Marquez, V.E., Hammerman, P.S., Wong, K.-K., Kim, C.F., 2015. EZH2 inhibition sensitizes BRG1 and EGFR mutant lung tumours to TopoII inhibitors. Nature. 520, 239–42. doi:10.1038/nature14122

Fiskus, W., Sharma, S., Shah, B., Portier, B.P., Devaraj, S.G.T., Liu, K., Iyer, S.P., Bearss, D., Bhalla, K.N., 2014. Highly effective combination of LSD1 (KDM1A) antagonist and pan-histone deacetylase inhibitor against human AML cells. Leukemia. 28, 2155–64. doi:10.1038/leu.2014.119

Fong, C.Y., Gilan, O., Lam, E.Y.N., Rubin, A.F., Ftouni, S., Tyler, D., Stanley, K., Sinha, D., Yeh, P., Morison, J., Giotopoulos, G., Lugo, D., Jeffrey, P., Lee, S.C.W., Carpenter, C., Gregory, R., Ramsay, R.G., Lane, S.W., Abdel-Wahab, O., Kouzarides, T., Johnstone, R.W., Dawson, S.J., Huntly, B.J.P., Prinjha, R.K., Papenfuss, A.T., Dawson, M.A., 2015. BET inhibitor resistance emerges from leukaemia stem cells. Nature. 525, 538–+. doi:10.1038/nature14888

Fraga, M.F., Ballestar, E., Villar-Garea, A., Boix-Chornet, M., Espada, J., Schotta, G., Bonaldi, T., Haydon, C., Ropero, S., Petrie, K., Iyer, N.G., Pérez-Rosado, A., Calvo, E., Lopez, J.A., Cano, A., Calasanz, M.J., Colomer, D., Piris, M.Á., Ahn, N., Imhof, A., Caldas, C., Jenuwein, T., Esteller, M., 2005. Loss of acetylation at Lys16 and trimethylation at Lys20 of histone H4 is a common hallmark of human cancer. Nat Genet. 37, 391–400. doi:10.1038/ng1531

French, C.A, Ramirez, C.L., Kolmakova, J., Hickman, T.T., Cameron, M.J., Thyne, M.E., Kutok, J.L., Toretsky, J.A Tadavarthy, A.K., Kees, U.R., Fletcher, J.A, Aster, J.C., 2008. BRD-NUT oncoproteins: a family of closely related nuclear proteins that block epithelial differentiation and maintain the growth of carcinoma cells. Oncogene. 27, 2237–2242. doi:10.1038/sj.onc.1210852

French, C.A., Rahman, S., Walsh, E.M., Kühnle, S., Grayson, A.R., Lemieux, M.E., Grunfeld, N., Rubin, B.P., Antonescu, C.R., Zhang, S., Venkatramani, R., Dal Cin, P., Howley, P.M., 2014. NSD3-NUT fusion oncoprotein in NUT midline carcinoma: Implications for a novel oncogenic mechanism. Cancer Discov. 4, 929–941. doi:10.1158/2159-8290.CD-14-0014

French, C.A., 2014. NUT midline carcinoma. Nat Rev Cancer. 14, 149–50. doi:10.1016/j.cancergencyto.2010.06.007

Frigola, J., Song, J., Stirzaker, C., Hinshelwood, R.A., Peinado, M.A., Clark, S.J., 2006. Epigenetic remodeling in colorectal cancer results in coordinate gene suppression across an entire chromosome band. Nat Genet. 38, 540–549. doi:10.1038/ng1781

Garraway, L.A., Lander, E.S., 2013. Lessons from the Cancer Genome. Cell. 153, 17–37. doi:10.1016/j.cell.2013.03.002

Gibaja, V., Shen, F., Harari, J., Korn, J., Ruddy, D., Saenz-Vash, V., Zhai, H., Rejtar, T., Paris, C.G., Yu, Z., Lira, M., King, D., Qi, W., Keen, N., Hassan, A.Q., Chan, H.M., 2015. Development of secondary mutations in wild type and mutant EZH2 alleles cooperates to confer resistance to EZH2 inhibitors. Oncogene. 1–9. doi:10.1038/onc.2015.114

Grayson, A.R., Walsh, E.M., Cameron, M.J., Godec, J., Ashworth, T., Ambrose, J.M., Aserlind, A.B., Wang, H., Evan, G.I., Kluk, M.J., Bradner, J.E., Aster, J.C., French, C.A., 2014. MYC, a downstream target of BRD-NUT, is necessary and sufficient for the blockade of differentiation in NUT midline carcinoma. Oncogene. 33, 1736–1742. doi:10.1038/onc.2013.126

Greaves, M., 1996. Infant leukaemia biology, aetiology and treatment. Leukemia. 10, 372–377.

Greger, V., Passarge, E., Höpping, W., Messmer, E., Horsthemke, B., 1989. Epigenetic changes may contribute to the formation and spontaneous regression of retinoblastoma. Hum Genet. 83, 155–158. doi:10.1007/BF00286709

Gu, Y., Nakamura, T., Alder, H., Prasad, R., Canaani, O., Cimino, G., Croce, C.M., Canaani, E., 1992. The t(4;11) chromosome translocation of human acute leukemias fuses the ALL-1 gene, related to Drosophila trithorax, to the AF-4 gene. Cell. 71, 701–708. doi:10.1016/0092-8674(92)90603-A

Guenther, M.G., Lawton, L.N., Rozovskaia, T., Frampton, G.M., Levine, S.S., Volkert, T.L., Croce, C.M., Nakamura, T., Canaani, E., Young, R. a., 2008. Aberrant chromatin at genes encoding stem cell regulators in human mixed-lineage leukemia. Genes Dev. 22, 3403–3408. doi:10.1101/gad.1741408

Harris, W.J., Huang, X., Lynch, J.T., Spencer, G.J., Hitchin, J.R., Li, Y., Ciceri, F., Blaser, J.G., Greystoke, B.F., Jordan, A.M., Miller, C.J., Ogilvie, D.J., Somervaille, T.C.P., 2012. The Histone Demethylase KDM1A Sustains the Oncogenic Potential of MLL-AF9 Leukemia Stem Cells. Cancer Cell. 21, 473–487. doi:10.1016/j.ccr.2012.03.014

Hayami, S., Kelly, J.D., Cho, H.S., Yoshimatsu, M., Unoki, M., Tsunoda, T., Field, H.I., Neal, D.E., Yamaue, H., Ponder, B.A.J., Nakamura, Y., Hamamoto, R., 2011. Overexpression of LSD1 contributes to human carcinogenesis through chromatin regulation in various cancers. Int J Cancer. 128, 574–586. doi:10.1002/ijc.25349

Holohan, C., Van Schaeybroeck, S., Longley, D.B., Johnston, P.G., 2013. Cancer drug resistance: an evolving paradigm. Nat Rev Cancer 13, 714–726. doi:10.1038/nrc3599

Huang, Z., Wu, H., Chuai, S., Xu, F., Yan, F., Englund, N., Wang, Z., Zhang, H., Fang, M., Wang, Y., Gu, J., Zhang, M., Yang, T., Zhao, K., Yu, Y., Dai, J., Yi, W., Zhou, S., Li, Q., Wu, J., Liu, J., Wu, X., Chan, H., Lu, C., Atadja, P., Li, E., Wang, Y., Hu, M., 2013. NSD2 Is Recruited through Its PHD Domain to Oncogenic Gene Loci to Drive Multiple Myeloma. Cancer Res. 73, 6277–6288. doi:10.1158/0008-5472.CAN-13-1000

Issa, J.-P.J., Kantarjian, H.M., 2009. Targeting DNA Methylation. Clin Cancer Res. 15, 3938–3946. doi:10.1158/1078-0432.CCR-08-2783

Jaffe, J.D., Wang, Y., Chan, H.M., Zhang, J., Huether, R., Kryukov, G. V, Bhang, H.C., Taylor, J.E., Hu, M., Englund, N.P., Yan, F., Wang, Z., Robert McDonald, E., Wei, L., Ma, J., Easton, J., Yu, Z., deBeaumount, R., Gibaja, V., Venkatesan, K., Schlegel, R., Sellers, W.R., Keen, N., Liu, J., Caponigro, G., Barretina, J., Cooke, V.G., Mullighan, C., Carr, S.A., Downing, J.R., Garraway, L.A., Stegmeier, F., 2013. Global chromatin profiling reveals NSD2 mutations in pediatric acute lymphoblastic leukemia. Nat Genet. 45, 1386–91. doi:10.1038/ng.2777

Jang, M.K., Mochizuki, K., Zhou, M., Jeong, H.-S., Brady, J.N., Ozato, K., 2005. The bromodomain protein Brd4 is a positive regulatory component of P-TEFb and stimulates RNA polymerase II-dependent transcription. Mol Cell. 19, 523–34. doi:10.1016/j.molcel.2005.06.027

Jiang, Y.W., Veschambre, P., Erdjument-Bromage, H., Tempst, P., Conaway, J.W., Conaway, R.C., Kornberg, R.D., 1998. Mammalian mediator of transcriptional regulation and its possible role as an end-point of signal transduction pathways. Proc Natl Acad Sci U S A. 95, 8538–8543. doi:10.1073/pnas.95.15.8538

Jo, S.Y., Granowicz, E.M., Maillard, I., Thomas, D., Hess, J.L., 2011. Requirement for Dot1l in murine

postnatal hematopoiesis and leukemogenesis by MLL translocation. Blood. 117, 4759–4768. doi:10.1182/blood-2010-12-327668

Kadoch, C., Crabtree, G.R., 2015. Mammalian SWI/SNF chromatin remodeling complexes and cancer: Mechanistic insights gained from human genomics. Sci Adv. 1, e1500447–e1500447. doi:10.1126/sciadv.1500447

Kadoch, C., Hargreaves, D.C., Hodges, C., Elias, L., Ho, L., Ranish, J., Crabtree, G.R., 2013. Proteomic and bioinformatic analysis of mammalian SWI/SNF complexes identifies extensive roles in human malignancy. Nat Genet. 45, 592–601. doi:10.1038/ng.2628

Kahl, P., Gullotti, L., Heukamp, L.C., Wolf, S., Friedrichs, N., Vorreuther, R., Solleder, G., Bastian, P.J., Ellinger, J., Metzger, E., Schüle, R., Buettner, R., 2006. Androgen receptor coactivators lysine-specific histone demethylase 1 and four and a half LIM domain protein 2 predict risk of prostate cancer recurrence. Cancer Res. 66, 11341–11347. doi:10.1158/0008-5472.CAN-06-1570

Kauffman, E.C., Robinson, B.D., Downes, M.J., Powell, L.G., Lee, M.M., Scherr, D.S., Gudas, L.J., Mongan, N.P., 2011. Role of androgen receptor and associated lysine-demethylase coregulators, LSD1 and JMJD2A, in localized and advanced human bladder cancer. Mol Carcinog. 50, 931–944. doi:10.1002/mc.20758

Keats, J.J., Reiman, T., Maxwell, C. a, Taylor, B.J., Larratt, L.M., Mant, M.J., Belch, A.R., Pilarski, L.M., 2003. In multiple myeloma, t(4;14)(p16;q32) is an adverse prognostic factor irrespective of FGFR3 expression. Blood. 101, 1520–1529. doi:10.1182/blood-2002-06-1675

Kennison, J. a, Tamkun, J.W., 1988. Dosage-dependent modifiers of polycomb and antennapedia mutations in Drosophila. Proc Natl Acad Sci U S A. 85, 8136–8140. doi:10.1073/pnas.85.21.8136

Khan, O., La Thangue, N.B., 2012. HDAC inhibitors in cancer biology: emerging mechanisms and clinical applications. Immunol Cell Biol. 90, 85–94. doi:10.1038/icb.2011.100

Kia, S.K., Gorski, M.M., Giannakopoulos, S., Verrijzer, C.P., 2008. SWI/SNF mediates polycomb eviction and epigenetic reprogramming of the INK4b-ARF-INK4a locus. Mol Cell Biol. 28, 3457–3464. doi:MCB.02019-07 [pii]10.1128/MCB.02019-07

Knoechel, B., Roderick, J.E., Williamson, K.E., Zhu, J., Lohr, J.G., Cotton, M.J., Gillespie, S.M., Fernandez, D., Ku, M., Wang, H., Piccioni, F., Silver, S.J., Jain, M., Pearson, D., Kluk, M.J., Ott, C.J., Shultz, L.D., Brehm, M.A., Greiner, D.L., Gutierrez, A., Stegmaier, K., Kung, A.L., Root, D.E., Bradner, J.E., Aster, J.C., Kelliher, M.A., Bernstein, B.E., 2014. An epigenetic mechanism of resistance to targeted therapy in T cell acute lymphoblastic leukemia. Nat Genet. 46, 364–370. doi:10.1038/ng.2913

Knutson, S.K., Warholic, N.M., Wigle, T.J., Klaus, C.R., Allain, C.J., Raimondi, A., Porter Scott, M., Chesworth, R., Moyer, M.P., Copeland, R.A., Richon, V.M., Pollock, R.M., Kuntz, K.W., Keilhack, H., 2013. Durable tumor regression in genetically altered malignant rhabdoid tumors by inhibition of methyltransferase EZH2. Proc Natl Acad Sci. 110, 7922–7927. doi:10.1073/pnas.1303800110

Knutson, S.K., Wigle, T.J., Warholic, N.M., Sneeringer, C.J., Allain, C.J., Klaus, C.R., Sacks, J.D., Raimondi, A., Majer, C.R., Song, J., Scott, M.P., Jin, L., Smith, J.J., Olhava, E.J., Chesworth, R., Moyer, M.P., Richon, V.M., Copeland, R. a, Keilhack, H., Pollock, R.M., Kuntz, K.W., 2012. A selective inhibitor of EZH2 blocks H3K27 methylation and kills mutant lymphoma cells. Nat Chem Biol. 8, 890–896. doi:10.1038/nchembio.1084

Kouzarides, T., 2007. Chromatin Modifications and Their Function. Cell. doi:10.1016/j.cell.2007.02.005

Krivtsov, A. V, Armstrong, S.A., 2007. MLL translocations, histone modifications and leukaemia stem-cell development. Nat Rev Cancer. 7, 823–833. doi:nrc2253 [pii]10.1038/nrc2253

Krivtsov, A. V, Feng, Z., Lemieux, M.E., Faber, J., Vempati, S., Sinha, A.U., Xia, X., Jesneck, J., Bracken, A.P., Silverman, L.B., Kutok, J.L., Kung, A.L., Armstrong, S.A., 2008. H3K79 methylation profiles define murine and human MLL-AF4 leukemias. Cancer Cell. 14, 355–68. doi:10.1016/j.ccr.2008.10.001

Kuo, A.J., Cheung, P., Chen, K., Zee, B.M., Kioi, M., Lauring, J., Xi, Y., Park, B.H., Shi, X., Garcia, B.A., Li, W., Gozani, O., 2011. NSD2 links dimethylation of histone H3 at lysine 36 to oncogenic programming. Mol Cell. 44, 609–20. doi:10.1016/j.molcel.2011.08.042

Kwiatkowski, N., Zhang, T., Rahl, P.B., Abraham, B.J., Reddy, J., Ficarro, S.B., Dastur, A., Amzallag, A., Ramaswamy, S., Tesar, B., Jenkins, C.E., Hannett, N.M., McMillin, D., Sanda, T., Sim, T., Kim, N.D., Look, T., Mitsiades, C.S., Weng, A.P., Brown, J.R., Benes, C.H., Marto, J.A., Young, R.A., Gray, N.S., 2014. Targeting transcription regulation in cancer with a covalent CDK7 inhibitor. Nature. 511, 616–620. doi:10.1038/nature13393

Larochelle, S., Amat, R., Glover-Cutter, K., Sansó, M., Zhang, C., Allen, J.J., Shokat, K.M., Bentley, D.L., Fisher, R.P., 2012. Cyclin-dependent kinase control of the initiation-to-elongation switch of RNA polymerase II. Nat Struct Mol Biol. 19, 1108–1115. doi:10.1038/nsmb.2399

Laubach, J.P., Moreau, P., San-Miguel, J.F., Richardson, P.G., 2015. Panobinostat for the Treatment of Multiple Myeloma. Clin Cancer Res. 4767–4774. doi:10.1158/1078-0432.CCR-15-0530

Lee, H., Kahn, T.G., Simcox, A., Schwartz, Y.B., Pirrotta, V., 2015. Genome-wide activities of Polycomb complexes control pervasive transcription. Genome Res. 25, 1170–1181. doi:10.1101/gr.188920.114.

Lee, W., Teckie, S., Wiesner, T., Ran, L., Prieto Granada, C.N., Lin, M., Zhu, S., Cao, Z., Liang, Y., Sboner, A., Tap, W.D., Fletcher, J. a, Huberman, K.H., Qin, L.-X., Viale, A., Singer, S., Zheng, D., Berger, M.F., Chen, Y., Antonescu, C.R., Chi, P., 2014. PRC2 is recurrently inactivated through EED or SUZ12 loss in malignant peripheral nerve sheath tumors. Nat Genet. 46, 1227–32. doi:10.1038/ng.3095

Lin, C.Y., Lovén, J., Rahl, P.B., Paranal, R.M., Burge, C.B., Bradner, J.E., Lee, T.I., Young, R.A., 2012. Transcriptional amplification in tumor cells with elevated c-Myc. Cell. 151, 56–67. doi:10.1016/j.cell.2012.08.026

Lovén, J., Hoke, H. a., Lin, C.Y., Lau, A., Orlando, D. a., Vakoc, C.R., Bradner, J.E., Lee, T.I., Young, R. a., 2013. Selective inhibition of tumor oncogenes by disruption of super-enhancers. Cell. 153, 320–334. doi:10.1016/j.cell.2013.03.036

Mann, B.S., Johnson, J.R., Cohen, M.H., Justice, R., Pazdur, R., 2007. FDA approval summary: vorinostat for treatment of advanced primary cutaneous T-cell lymphoma. Oncologist. 12, 1247–52. doi:10.1634/theoncologist.12-10-1247

Mansour, M.R., Abraham, B.J., Anders, L., Gutierrez, A., Durbin, A.D., Lawton, L., Sallan, S.E., Silverman, L.B., Loh, M.L., Hunger, S.P., Sanda, T., Richard, A., Berezovskaya, A., Gutierrez, A., Durbin, A.D., Etchin, J., Lawton, L., Sallan, S.E., Silverman, L.B., Loh, M.L., Hunger, S.P., Sanda, T., Young, R.A., Look, A.T., 2014. An oncogenic super-enhancer formed through somatic mutation of a noncoding intergenic element. Science. 346, 1373–1377. doi:10.1126/science.1259037

Marango, J., Shimoyama, M., Nishio, H., Meyer, J.A., Min, D.-J., Sirulnik, A., Martinez-Martinez, Y., Chesi, M., Bergsagel, P.L., Zhou, M.-M., Waxman, S., Leibovitch, B.A., Walsh, M.J., Licht, J.D., 2008. The MMSET protein is a histone methyltransferase with characteristics of a transcriptional corepressor.

Blood. 111, 3145–54. doi:10.1182/blood-2007-06-092122

Margueron, R., Reinberg, D., 2011. The Polycomb complex PRC2 and its mark in life. Nature. 469, 343–349. doi:nature09784 [pii]10.1038/nature09784

Mazur, P.K., Herner, A., Mello, S.S., Wirth, M., Hausmann, S., Sánchez-Rivera, F.J., Lofgren, S.M., Kuschma, T., Hahn, S.A., Vangala, D., Trajkovic-Arsic, M., Gupta, A., Heid, I., Noël, P.B., Braren, R., Erkan, M., Kleeff, J., Sipos, B., Sayles, L.C., Heikenwalder, M., Heßmann, E., Ellenrieder, V., Esposito, I., Jacks, T., Bradner, J.E., Khatri, P., Sweet-Cordero, E.A., Attardi, L.D., Schmid, R.M., Schneider, G., Sage, J., Siveke, J.T., 2015. Combined inhibition of BET family proteins and histone deacetylases as a potential epigenetics-based therapy for pancreatic ductal adenocarcinoma. Nat Med. 21, 1163–71. doi:10.1038/nm.3952

McCabe, M.T., Graves, A.P., Ganji, G., Diaz, E., Halsey, W.S., Jiang, Y., Smitheman, K.N., Ott, H.M., Pappalardi, M.B., Allen, K.E., Chen, S.B., Della Pietra, A., Dul, E., Hughes, A.M., Gilbert, S. a., Thrall, S.H., Tummino, P.J., Kruger, R.G., Brandt, M., Schwartz, B., Creasy, C.L., 2012. Mutation of A677 in histone methyltransferase EZH2 in human B-cell lymphoma promotes hypertrimethylation of histone H3 on lysine 27 (H3K27). Proc Natl Acad Sci. 109, 2989–2994. doi:10.1073/pnas.1116418109

McCabe, M.T., Ott, H.M., Ganji, G., Korenchuk, S., Thompson, C., Van Aller, G.S., Liu, Y., Graves, A.P., Della Pietra, A., Diaz, E., LaFrance, L. V, Mellinger, M., Duquenne, C., Tian, X., Kruger, R.G., McHugh, C.F., Brandt, M., Miller, W.H., Dhanak, D., Verma, S.K., Tummino, P.J., Creasy, C.L., 2012. EZH2 inhibition as a therapeutic strategy for lymphoma with EZH2-activating mutations. Nature. 492, 108–12. doi:10.1038/nature11606

Metzger, E., Wissmann, M., Yin, N., Müller, J.M., Schneider, R., Peters, A.H.F.M., Günther, T., Buettner, R., Schüle, R., 2005. LSD1 demethylates repressive histone marks to promote androgen-receptor-dependent transcription. Nature. 437, 436–439. doi:10.1038/nature04020

Mishra, B.P., Zaffuto, K.M., Artinger, E.L., Org, T., Mikkola, H.K. a, Cheng, C., Djabali, M., Ernst, P., 2014. (with supp.) The histone methyltransferase activity of MLL1 is dispensable for hematopoiesis and leukemogenesis. Cell Rep. 7, 1239–1247. doi:10.1016/j.celrep.2014.04.015

Mohammad, H., Smitheman, K., Kamat, C., Soong, D., Federowicz, K., VanAller, G., Schneck, J., Carson, J., Liu, Y., Butticello, M., Bonnette, W., Gorman, S., Degenhardt, Y., Bai, Y., McCabe, M., Pappalardi, M., Kasparec, J., Tian, X., McNulty, K., Rouse, M., McDevitt, P., Ho, T., Crouthamel, M., Hart, T., Concha, N., McHugh, C., Miller, W., Dhanak, D., Tummino, P., Carpenter, C., Johnson, N., Hann, C., Kruger, R., 2015. A DNA Hypomethylation Signature Predicts Antitumor Activity of LSD1 Inhibitors in SCLC. Cancer Cell. 28, 57–69. doi:10.1016/j.ccell.2015.06.002

Morin, R.D., Johnson, N.A., Severson, T.M., Mungall, A.J., An, J., Goya, R., Paul, J.E., Boyle, M., Woolcock, B.W., Kuchenbauer, F., Yap, D., Humphries, R.K., Griffith, O.L., Shah, S., Zhu, H., Kimbara, M., Shashkin, P., Charlot, J.F., Tcherpakov, M., Corbett, R., Tam, A., Varhol, R., Smailus, D., Moksa, M., Zhao, Y., Delaney, A., Qian, H., Birol, I., Schein, J., Moore, R., Holt, R., Horsman, D.E., Connors, J.M., Jones, S., Aparicio, S., Hirst, M., Gascoyne, R.D., Marra, M.A., 2010. Somatic mutations altering EZH2 (Tyr641) in follicular and diffuse large B-cell lymphomas of germinal-center origin. Nat Genet. 42, 181–185. doi:ng.518 [pii]10.1038/ng.518

Morin, R.D., Mendez-Lago, M., Mungall, A.J., Goya, R., Mungall, K.L., Corbett, R.D., Johnson, N. a, Severson, T.M., Chiu, R., Field, M., Jackman, S., Krzywinski, M., Scott, D.W., Trinh, D.L., Tamura-Wells, J., Li, S., Firme, M.R., Rogic, S., Griffith, M., Chan, S., Yakovenko, O., Meyer, I.M., Zhao, E.Y., Smailus, D., Moksa, M., Chittaranjan, S., Rimsza, L., Brooks-Wilson, A., Spinelli, J.J., Ben-Neriah, S., Meissner, B.,

Woolcock, B., Boyle, M., McDonald, H., Tam, A., Zhao, Y., Delaney, A., Zeng, T., Tse, K., Butterfield, Y., Birol, I., Holt, R., Schein, J., Horsman, D.E., Moore, R., Jones, S.J.M., Connors, J.M., Hirst, M., Gascoyne, R.D., Marra, M. a, 2011. Frequent mutation of histone-modifying genes in non-Hodgkin lymphoma. Nature. 476, 298–303. doi:10.1038/nature10351

Muntean, A.G., Hess, J.L., 2012. The Pathogenesis of Mixed-Lineage Leukemia. Annu Rev Pathol Mech Dis. 7, 283–301. doi:10.1146/annurev-pathol-011811-132434

Nguyen, A.T., Taranova, O., He, J., Zhang, Y., 2011. DOT1L, the H3K79 methyltransferase, is required for MLL-AF9 - Mediated leukemogenesis. Blood. 117, 6912–6922. doi:10.1182/blood-2011-02-334359

Nguyen, A.T., Zhang, Y., 2011. The diverse functions of Dot1 and H3K79 methylation. Genes Dev. 25, 1345–58. doi:10.1101/gad.2057811

Nikoloski, G., Langemeijer, S.M.C., Kuiper, R.P., Knops, R., Massop, M., Tönnissen, E.R.L.T.M., van der Heijden, A., Scheele, T.N., Vandenberghe, P., de Witte, T., van der Reijden, B.A., Jansen, J.H., 2010. Somatic mutations of the histone methyltransferase gene EZH2 in myelodysplastic syndromes. Nat Genet. 42, 665–667. doi:10.1038/ng.620

Nimura, K., Ura, K., Shiratori, H., Ikawa, M., Okabe, M., Schwartz, R.J., Kaneda, Y., 2009. A histone H3 lysine 36 trimethyltransferase links Nkx2-5 to Wolf-Hirschhorn syndrome. Nature. 460, 287–291. doi:10.1038/nature08086

Nogales, E., 2016. The development of cryo-EM into a mainstream structural biology technique 13, 24–27. doi:10.1038/nmeth.3694

Ntziachristos, P., Tsirigos, A., Vlierberghe, P. Van, Nedjic, J., Trimarchi, T., Flaherty, M.S., Ferres-Marco, D., da Ros, V., Tang, Z., Siegle, J., Asp, P., Hadler, M., Rigo, I., Keersmaecker, K. De, Patel, J., Huynh, T., Utro, F., Poglio, S., Samon, J.B., Paietta, E., Racevskis, J., Rowe, J.M., Rabadan, R., Levine, R.L., Brown, S., Pflumio, F., Dominguez, M., Ferrando, A., Aifantis, I., 2012. Genetic inactivation of the polycomb repressive complex 2 in T cell acute lymphoblastic leukemia. Nat Med. 18, 298–303. doi:10.1038/nm.2651

Oldridge, D.A., Wood, A.C., Weichert-Leahey, N., Crimmins, I., Sussman, R., Winter, C., McDaniel, L.D., Diamond, M., Hart, L.S., Zhu, S., Durbin, A.D., Abraham, B.J., Anders, L., Tian, L., Zhang, S., Wei, J.S., Khan, J., Bramlett, K., Rahman, N., Capasso, M., Iolascon, A., Gerhard, D.S., Guidry Auvil, J.M., Young, R.A., Hakonarson, H., Diskin, S.J., Thomas Look, A., Maris, J.M., 2015. Genetic predisposition to neuroblastoma mediated by a LMO1 super-enhancer polymorphism. Nature. 528, 418–421. doi:10.1038/nature15540

Oyer, J. a, Huang, X., Zheng, Y., Shim, J., Ezponda, T., Carpenter, Z., Allegretta, M., Okot-Kotber, C.I., Patel, J.P., Melnick, A, Levine, R.L., Ferrando, A, Mackerell, A.D., Kelleher, N.L., Licht, J.D., Popovic, R., 2014. Point mutation E1099K in MMSET/NSD2 enhances its methyltranferase activity and leads to altered global chromatin methylation in lymphoid malignancies. Leukemia. 28, 198–201. doi:10.1038/leu.2013.204

Palomero, T., Ferrando, A., 2009. Therapeutic targeting of NOTCH1 signaling in T-cell acute lymphoblastic leukemia. Clin. Lymphoma Myeloma 9 Suppl 3, S205–S210. doi:10.3816/CLM.2009.s.013

Pasini, D., Malatesta, M., Jung, H.R., Walfridsson, J., Willer, A., Olsson, L., Skotte, J., Wutz, A., Porse, B., Jensen, O.N., Helin, K., 2010. Characterization of an antagonistic switch between histone H3 lysine 27 methylation and acetylation in the transcriptional regulation of Polycomb group target genes. Nucleic Acids Res.. 38, 4958–4969. doi:10.1093/nar/gkq244

Popovic, R., Martinez-Garcia, E., Giannopoulou, E.G., Zhang, Q., Zhang, Q., Ezponda, T., Shah, M.Y., Zheng, Y., Will, C.M., Small, E.C., Hua, Y., Bulic, M., Jiang, Y., Carrara, M., Calogero, R.A., Kath, W.L., Kelleher, N.L., Wang, J.-P., Elemento, O., Licht, J.D., 2014. Histone methyltransferase MMSET/NSD2 alters EZH2 binding and reprograms the myeloma epigenome through global and focal changes in H3K36 and H3K27 methylation. PLoS Genet. 10, e1004566. doi:10.1371/journal.pgen.1004566

Qi, W., Chan, H., Teng, L., Li, L., Chuai, S., Zhang, R., Zeng, J., Li, M., Fan, H., 2012. Selective inhibition of Ezh2 by a small molecule inhibitor blocks tumor cells proliferation. Proc Natl Acad Sci U S A. 109, 21360–21365.

Rathert, P., Roth, M., Neumann, T., Muerdter, F., Roe, J.-S., Muhar, M., Deswal, S., Cerny-Reiterer, S., Peter, B., Jude, J., Hoffmann, T., Boryń, Ł.M., Axelsson, E., Schweifer, N., Tontsch-Grunt, U., Dow, L.E., Gianni, D., Pearson, M., Valent, P., Stark, A., Kraut, N., Vakoc, C.R., Zuber, J., 2015. Transcriptional plasticity promotes primary and acquired resistance to BET inhibition. Nature. 525, 543–547. doi:10.1038/nature14898

Rexer, B.N., Ham, A.J.L., Rinehart, C., Hill, S., Granja-Ingram, N.D.M., González-Angulo, A.M., Mills, G.B., Dave, B., Chang, J.C., Liebler, D.C., Arteaga, C.L., 2011. Phosphoproteomic mass spectrometry profiling links Src family kinases to escape from HER2 tyrosine kinase inhibition. Oncogene. 30, 4163–74. doi:10.1038/onc.2011.130

Reynoird, N., Schwartz, B.E., Delvecchio, M., Sadoul, K., Meyers, D., Mukherjee, C., Caron, C., Kimura, H., Rousseaux, S., Cole, P.A., Panne, D., French, C.A., Khochbin, S., 2010. Oncogenesis by sequestration of CBP/p300 in transcriptionally inactive hyperacetylated chromatin domains. EMBO J. 29, 2943–52. doi:10.1038/emboj.2010.176

Sakai, T., Toguchida, J., Ohtani, N., Yandell, D.W., Rapaport, J.M., Dryja, T.P., 1991. Allele-specific hypermethylation of the retinoblastoma tumor-suppressor gene. Am J Hum Genet. 48, 880–8. doi:10.1007/BF02890404

Santra, M., Zhan, F., Tian, E., Barlogie, B., Jr, J.S., 2003. Brief report A subset of multiple myeloma harboring the t(4;14)(p16;q32) translocation lacks FGFR3 expression but maintains an IGH / MMSET fusion transcript. 101, 2374–2376. doi:10.1182/blood-2002-09-2801.

Schenk, T., Chen, W.C., Göllner, S., Howell, L., Jin, L., Hebestreit, K., Klein, H.-U., Popescu, A.C., Burnett, A., Mills, K., Casero, R. a, Marton, L., Woster, P., Minden, M.D., Dugas, M., Wang, J.C.Y., Dick, J.E., Müller-Tidow, C., Petrie, K., Zelent, A., 2012. Inhibition of the LSD1 (KDM1A) demethylase reactivates the all-trans-retinoic acid differentiation pathway in acute myeloid leukemia. Nat Med. 18, 605–11. doi:10.1038/nm.2661

Schmitges, F.W., Prusty, A.B., Faty, M., Stutzer, A., Lingaraju, G.M., Aiwazian, J., Sack, R., Hess, D., Li, L., Zhou, S., Bunker, R.D., Wirth, U., Bouwmeester, T., Bauer, A., Ly-Hartig, N., Zhao, K., Chan, H., Gu, J., Gut, H., Fischle, W., Muller, J., Thoma, N.H., 2011. Histone methylation by PRC2 is inhibited by active chromatin marks. Mol Cell. 42, 330–341. doi:S1097-2765(11)00287-5 [pii]10.1016/j.molcel.2011.03.025

Schulte, J.H., Lim, S., Schramm, A., Friedrichs, N., Koster, J., Versteeg, R., Ora, I., Pajtler, K., Klein-Hitpass, L., Kuhfittig-Kulle, S., Metzger, E., Sch??le, R., Eggert, A., Buettner, R., Kirfel, J., 2009. Lysine-specific demethylase 1 is strongly expressed in poorly differentiated neuroblastoma: Implications for therapy. Cancer Res. 69, 2065–2071. doi:10.1158/0008-5472.CAN-08-1735

Seligson, D.B., Horvath, S., Shi, T., Yu, H., Tze, S., Grunstein, M., Kurdistani, S.K., 2005. Global histone modification patterns predict risk of prostate cancer recurrence. Nature. 435, 1262–1266. doi:10.1038/nature03672

Sharma, S. V., Lee, D.Y., Li, B., Quinlan, M.P., Takahashi, F., Maheswaran, S., McDermott, U., Azizian, N., Zou, L., Fischbach, M.A., Wong, K.K., Brandstetter, K., Wittner, B., Ramaswamy, S., Classon, M., Settleman, J., 2010. A Chromatin-Mediated Reversible Drug-Tolerant State in Cancer Cell Subpopulations. Cell. 141, 69–80. doi:10.1016/j.cell.2010.02.027

Shen, C., Ipsaro, J.J., Shi, J., Milazzo, J.P., Wang, E., Roe, J.-S., Suzuki, Y., Pappin, D.J., Joshua-Tor, L., Vakoc, C.R., 2015. NSD3-Short Is an Adaptor Protein that Couples BRD4 to the CHD8 Chromatin Remodeler. Mol Cell. 60, 847–859. doi:10.1016/j.molcel.2015.10.033

Shi, J., Vakoc, C.R., 2014. The Mechanisms behind the Therapeutic Activity of BET Bromodomain Inhibition. Mol Cell. 54, 72–736. doi:10.1016/j.molcel.2014.05.016

Shi, J., Wang, E., Milazzo, J.P., Wang, Z., Kinney, J.B., Vakoc, C.R., 2015. Discovery of cancer drug targets by CRISPR-Cas9 screening of protein domains. Nat Biotechnol. 1–10. doi:10.1038/nbt.3235

Shi, Y., Lan, F., Matson, C., Mulligan, P., Whetstine, J.R., Cole, P. a., Casero, R. a., Shi, Y., 2004. Histone demethylation mediated by the nuclear amine oxidase homolog LSD1. Cell. 119, 941–953. doi:10.1016/j.cell.2004.12.012

Shu, S., Lin, C.Y., He, H.H., Witwicki, R.M., Tabassum, D.P., Roberts, J.M., Janiszewska, M., Jin Huh, S., Liang, Y., Ryan, J., Doherty, E., Mohammed, H., Guo, H., Stover, D.G., Ekram, M.B., Peluffo, G., Brown, J., D'Santos, C., Krop, I.E., Dillon, D., McKeown, M., Ott, C., Qi, J., Ni, M., Rao, P.K., Duarte, M., Wu, S.-Y., Chiang, C.-M., Anders, L., Young, R.A., Winer, E.P., Letai, A., Barry, W.T., Carroll, J.S., Long, H.W., Brown, M., Shirley Liu, X., Meyer, C.A., Bradner, J.E., Polyak, K., 2016. Response and resistance to BET bromodomain inhibitors in triple-negative breast cancer. Nature. 1–24. doi:10.1038/nature16508

Sneeringer, C.J., Scott, M.P., Kuntz, K.W., Knutson, S.K., Pollock, R.M., Richon, V.M., Copeland, R.A., 2010. Coordinated activities of wild type plus mutant EZH2 drive tumor-associated hypertrimethylation of lysine 27 on histone H3 (H3K27) in human B-cell lymphomas. Proc Natl Acad Sci U S A. 107, 20980–5. doi:10.1073/pnas.1012525107

Strahl, B.D., Allis, C.D., 2000. The language of covalent histone modifications. Nature. 403, 41–45. doi:10.1038/47412

Stratikopoulos, E.E., Dendy, M., Szabolcs, M., Khaykin, A.J., Lefebvre, C., Zhou, M.-M., Parsons, R., 2015. Kinase and BET Inhibitors Together Clamp Inhibition of PI3K Signaling and Overcome Resistance to Therapy. Cancer Cell. 27, 837–851. doi:10.1016/j.ccell.2015.05.006

Stuhlmiller, T.J., Miller, S.M., Zawistowski, J.S., Nakamura, K., Beltran, A.S., Duncan, J.S., Angus, S.P., Collins, K.A.L., Granger, D.A., Reuther, R.A., Graves, L.M., Gomez, S.M., Kuan, P.-F., Parker, J.S., Chen, X., Sciaky, N., Carey, L.A., Earp, H.S., Jin, J., Johnson, G.L., 2015. Inhibition of Lapatinib-Induced Kinome Reprogramming in ERBB2-Positive Breast Cancer by Targeting BET Family Bromodomains. Cell Rep. 11, 390–404. doi:10.1016/j.celrep.2015.03.037

Stunnenberg, H.G., Vermeulen, M., 2011. Towards cracking the epigenetic code using a combination of high-throughput epigenomics and quantitative mass spectrometry-based proteomics. BioEssays. 33, 547–551. doi:10.1002/bies.201100044

Tamkun, J.W., Deuring, R., Scott, M.P., Kissinger, M., Pattatucci, A.M., Kaufman, T.C., Kennison, J. a, 1992. brahma: a regulator of Drosophila homeotic genes structurally related to the yeast transcriptional activator SNF2/SWI2. Cell. 68, 561–572. doi:10.1016/0092-8674(92)90191-E

Tessarz, P., Kouzarides, T., 2014. Histone core modifications regulating nucleosome structure and

dynamics. Nat Rev Mol Cell Biol. 15, 703–708. doi:10.1038/nrm3890

Tkachuk, D.C., Kohler, S., Cleary, M.L., 1992. Involvement of a homolog of Drosophila trithorax by 11q23 chromosomal translocations in acute leukemias. Cell. 71, 691–700. doi:10.1016/0092-8674(92)90602-9

Vogelstein, B., Papadopoulos, N., Velculescu, V.E., Zhou, S., Diaz Jr., L.A., Kinzler, K.W., 2013. Cancer Genome Landscapes. Science. 339, 1546–1558. doi:10.1126/science.1235122

Wagner, J.M., Hackanson, B., Lübbert, M., Jung, M., 2010. Histone deacetylase (HDAC) inhibitors in recent clinical trials for cancer therapy. Clin Epigenetics. 1, 117–136. doi:10.1007/s13148-010-0012-4

Wang, R., You, J., 2015. Mechanistic analysis of the role of bromodomain-containing protein 4 (BRD4) in BRD4-NUT oncoprotein-induced transcriptional activation. J Biol Chem. 290, 2744–58. doi:10.1074/jbc.M114.600759

Wang, Y., Zhang, T., Kwiatkowski, N., Young, R.A., Gray, N.S., Zhao, J.J., Wang, Y., Zhang, T., Kwiatkowski, N., Abraham, B.J., Lee, T.I., Xie, S., 2015. CDK7-Dependent Transcriptional Addiction in Triple-Negative Breast Cancer Article CDK7-Dependent Transcriptional Addiction in Triple-Negative Breast Cancer. Cell. 163, 174–186. doi:10.1016/j.cell.2015.08.063

Watson, P.A., Arora, V.K., Sawyers, C.L., 2015. Emerging mechanisms of resistance to androgen receptor inhibitors in prostate cancer. Nat Rev Cancer. 15, 701–711. doi:10.1038/nrc4016

Wigle, T.J., Knutson, S.K., Jin, L., Kuntz, K.W., Pollock, R.M., Richon, V.M., Copeland, R.A., Scott, M.P., 2011. The Y641C mutation of EZH2 alters substrate specificity for histone H3 lysine 27 methylation states. FEBS Lett. 585, 3011–4. doi:10.1016/j.febslet.2011.08.018

Wilson, B.G., Wang, X., Shen, X., McKenna, E.S., Lemieux, M.E., Cho, Y.-J., Koellhoffer, E.C., Pomeroy, S.L., Orkin, S.H., Roberts, C.W.M., 2010. Epigenetic Antagonism between Polycomb and SWI/SNF Complexes during Oncogenic Transformation. Cancer Cell. 18, 316–328. doi:10.1016/j.ccr.2010.09.006

Winter, G.E., Buckley, D.L., Paulk, J., Roberts, J.M., Souza, A., Dhe-Paganon, S., Bradner, J.E., 2015. Phthalimide conjugation as a strategy for in vivo target protein degradation. Science. 348, 1376–1381. doi:10.1126/science.aab1433

Wong, S.H.K., Goode, D.L., Iwasaki, M., Wei, M.C., Kuo, H.P., Zhu, L., Schneidawind, D., Duque-Afonso, J., Weng, Z., Cleary, M.L., 2015. The H3K4-Methyl Epigenome Regulates Leukemia Stem Cell Oncogenic Potential. Cancer Cell. 28, 198–209. doi:10.1016/j.ccell.2015.06.003

Yang, Z., Yik, J.H.N., Chen, R., He, N., Jang, M.K., Ozato, K., Zhou, Q., 2005. Recruitment of P-TEFb for stimulation of transcriptional elongation by the bromodomain protein Brd4. Mol Cell. 19, 535–45. doi:10.1016/j.molcel.2005.06.029

Yap, D.B., Chu, J., Berg, T., Schapira, M., Cheng, S.W., Moradian, A., Morin, R.D., Mungall, A.J., Meissner, B., Boyle, M., Marquez, V.E., Marra, M.A., Gascoyne, R.D., Humphries, R.K., Arrowsmith, C.H., Morin, G.B., Aparicio, S.A., 2011. Somatic mutations at EZH2 Y641 act dominantly through a mechanism of selectively altered PRC2 catalytic activity, to increase H3K27 trimethylation. Blood. 117, 2451–2459. doi:blood-2010-11-321208 [pii]10.1182/blood-2010-11-321208

Yashiro-Ohtani, Y., Wang, H., Zang, C., Arnett, K.L., Bailis, W., Ho, Y., Knoechel, B., Lanauze, C., Louis, L., Forsyth, K.S., Chen, S., Chung, Y., Schug, J., Blobel, G. a, Liebhaber, S. a, Bernstein, B.E., Blacklow, S.C., Liu, X.S., Aster, J.C., Pear, W.S., 2014. Long-range enhancer activity determines Myc sensitivity to Notch inhibitors in T cell leukemia. Proc Natl Acad Sci U S A. 111, E4946–53. doi:10.1073/pnas.1407079111

Yuan, W., Xu, M., Huang, C., Liu, N., Chen, S., Zhu, B., 2011. H3K36 methylation antagonizes PRC2-mediated H3K27 methylation. J Biol Chem. 286, 7983–7989. doi:M110.194027 [pii]10.1074/jbc.M110.194027

Zhang, J., Ding, L., Holmfeldt, L., Wu, G., Heatley, S.L., Payne-Turner, D., Easton, J., Chen, X., Wang, J., Rusch, M., Lu, C., Chen, S.-C., Wei, L., Collins-Underwood, J.R., Ma, J., Roberts, K.G., Pounds, S.B., Ulyanov, A., Becksfort, J., Gupta, P., Huether, R., Kriwacki, R.W., Parker, M., McGoldrick, D.J., Zhao, D., Alford, D., Espy, S., Bobba, K.C., Song, G., Pei, D., Cheng, C., Roberts, S., Barbato, M.I., Campana, D., Coustan-Smith, E., Shurtleff, S.A., Raimondi, S.C., Kleppe, M., Cools, J., Shimano, K.A., Hermiston, M.L., Doulatov, S., Eppert, K., Laurenti, E., Notta, F., Dick, J.E., Basso, G., Hunger, S.P., Loh, M.L., Devidas, M., Wood, B., Winter, S., Dunsmore, K.P., Fulton, R.S., Fulton, L.L., Hong, X., Harris, C.C., Dooling, D.J., Ochoa, K., Johnson, K.J., Obenauer, J.C., Evans, W.E., Pui, C.-H., Naeve, C.W., Ley, T.J., Mardis, E.R., Wilson, R.K., Downing, J.R., Mullighan, C.G., 2012. The genetic basis of early T-cell precursor acute lymphoblastic leukaemia. Nature. 481, 157–163. doi:10.1038/nature10725

Zhang, M., Wang, Y., Jones, S., Sausen, M., McMahon, K., Sharma, R., Wang, Q., Belzberg, A.J., Chaichana, K., Gallia, G.L., Gokaslan, Z.L., Riggins, G.J., Wolinksy, J.-P., Wood, L.D., Montgomery, E.A., Hruban, R.H., Kinzler, K.W., Papadopoulos, N., Vogelstein, B., Bettegowda, C., 2014. Somatic mutations of SUZ12 in malignant peripheral nerve sheath tumors. Nat Genet. 46, 1170–2. doi:10.1038/ng.3116

Zhou, Q., Li, T., Price, D.H., 2012. RNA Polymerase II Elongation Control. Annu Rev Biochem. 81, 119–143. doi:10.1146/annurev-biochem-052610-095910

Ziemin-van der Poel, S., McCabe, N.R., Gill, H.J., Espinosa, R., Patel, Y., Harden, A, Rubinelli, P., Smith, S.D., LeBeau, M.M., Rowley, J.D., 1991. Identification of a gene, MLL, that spans the breakpoint in 11q23 translocations associated with human leukemias. Proc Natl Acad Sci U S A. 88, 10735–10739. doi:10.1073/pnas.89.9.4220f

Zuber, J., Shi, J., Wang, E., Rappaport, A.R., Herrmann, H., Sison, E.A., Magoon, D., Qi, J., Blatt, K., Wunderlich, M., Taylor, M.J., Johns, C., Chicas, A., Mulloy, J.C., Kogan, S.C., Brown, P., Valent, P., Bradner, J.E., Lowe, S.W., Vakoc, C.R., 2011. RNAi screen identifies Brd4 as a therapeutic target in acute myeloid leukaemia. Nature. 478, 524–8. doi:10.1038/nature10334

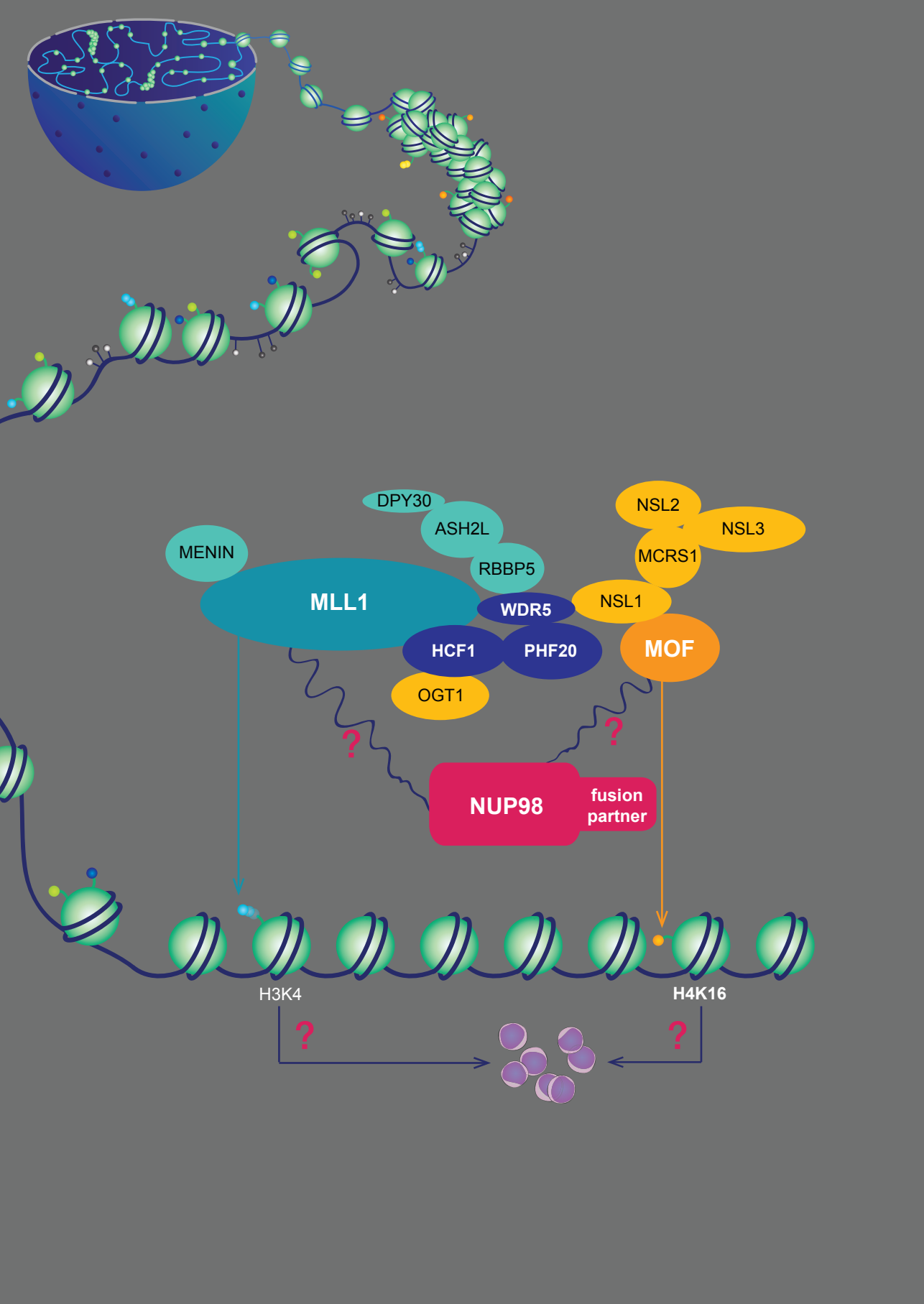
DPY30
ASH2L
RBBP5
MENIN
MLL1
WDR5
HCF1
PHF20
OGT1
NSL2
NSL3
MCRS1
NSL1
MOF
?
?
NUP98
fusion
partner
H3K4
H4K16
?
?

3

NUP98 FUSION PROTEINS INTERACT WITH THE NSL AND MLL1 COMPLEXES TO DRIVE LEUKEMOGENESIS

Haiming Xu & Daria G. Valerio, Meghan E. Eisold, Amit Sinha, Richard P. Koche, Wenhuo Hu, Chun-Wei Chen, S. Haihua Chu, Gerard L. Brien, James J. Shieh, Patricia Ernst, Scott A. Armstrong

Cancer Cell. 2016; in press

HIGHLIGHTS

- NUP98 fusions interact with MLL1 and NSL histone-modifying complexes.
- NUP98 fusions and MLL1 colocalize at *Hoxa* and *Hoxb* cluster gene loci.
- *Mll1* is required for *NUP98-HOXA9*-induced leukemogenesis *in vitro* and *in vivo.*
- *Mll1*-dependent gene expression signatures resemble human *NUP98-NSD1* AML.

ABSTRACT

The Nucleoporin 98 gene (*NUP98*) is fused to a variety of partner genes in an array of hematopoietic malignancies via chromosomal translocations involving 11p15. Here we demonstrate that NUP98 fusion proteins encoded by these translocations, including NUP98-HOXA9 (NHA9), NUP98-HOXD13 (NHD13), NUP98-NSD1, NUP98-PHF23, and NUP98-TOP1 physically interact with mixed lineage leukemia 1 (MLL1) and the non-specific lethal (NSL) histone-modifying complexes. We identified the target genes to which NHA9 and MLL1 bind in *NHA9* transformed cells, and found significant colocalization of these proteins. Furthermore, *Mll1* is required for the colony formation of *NHA9* cells *in vitro* and the maintenance of *NHA9* leukemia *in vivo*. Inactivation of *Mll1* led to decreased expression of genes where NHA9 and MLL1 were colocalized and reversed a gene expression signature found in *NUP98*-rearranged human leukemias. Our data reveal a molecular mechanism for *Mll1* function in *NUP98*-fusion driven leukemogenesis and suggest that targeting the MLL1/NSL complexes might be a novel approach to target this disease.

INTRODUCTION

The nuclear pore complexes (NPCs) span the nuclear envelope and mediate the exchange of macromolecules between the nucleus and cytoplasm, including the movement of small molecules and the selective, facilitated transport of large proteins and RNAs (Tran et al., 2006; D'Anfelo et al., 2008). The proteins that make up the nuclear pore complex are known as nucleoporins. The 98 kD nucleoporin (NUP98), a component of NPCs, is generated through a biogenesis pathway that involves synthesis and proteolytic cleavage of a 186 kD precursor protein (Fontoura et al., 1999). NUP98 was initially identified as a docking protein for cytosol-mediated docking of transport substrates (Radu et al., 1995). The NH_3-terminus of the NUP98 protein contains 38 nontandem repeats that possess the amino acids phenylalanine (F), leucine (L) and glycine (G) in various orders including FG, FXFG, or GLFG (where X is any amino acid). This repeat region provides docking sites for a family of nuclear transport signal receptor proteins known as importins, exportins and transportins (Griffis et al., 2002). The Gle2-binding sequence (GLEBS) at the amino terminal of NUP98 is responsible for the binding of Ribonucleic Acid Export 1 (REA1, the mammalian homologue of the mRNA export protein Gle2p) (Fontoura et al., 1999; Radu et al., 1995). The C-terminal part of NUP98 encodes the RNA binding domain (RBD) and nuclear localization signal (NLS). NUP98 is mainly localized to the nuclear envelope within the NPC (Radu et al., 1995), however a small fraction of NUP98 has been detected within the nucleus in cells from *Xenopus Laevis* (Radu et al., 1995) or human (Iwamoto et al., 2013), indicating potential dynamic movement of NUP98 between the nuclear interior and the nuclear pore complex (Griffis et al., 2002). The GLFG domain of NUP98 is required for the nucleoplasmic localization of NUP98 (Enninga et al., 2002; Powers et al., 1997). Recent studies (Kalverda et al., 2010) in *Drosophila* show that nucleoplasmic localized Nup98 functions as a potential transcriptional activator with a preference for promoters of genes with high H3K4 methylation and H4K16 acetylation involved in development, cell signaling, and cell cycle regulation. Another study in *Drosophila* demonstrated that nucleoplasm localized Nup98, but not nuclear envelop localized, NPC-associated full-length Nup98, physically interact with the non-specific lethal (NSL) and trithorax (Trx)/mixed lineage leukemia (MLL) complexes (Pascual-Garcia et al., 2014).

Similar to the *Drosophila* NSL complex, the human NSL complex contains the histone acetyltransferase (HAT) males absent on the first (MOF), and multiple other components including NSL1, NSL2, NSL3, MCRS2, plant homeodomain-linked finger-containing proteins PHF20, O-linked N-acetylglucosamine transferase isoform 1 (OGT1), host cell factor 1 (HCF1), and the tryptophan-aspartate (WD) repeat domain 5 (WDR5) (Prestel et al., 2010; Raja et al., 2010; Cai et al., 2010). Two components of the human NSL complex WDR5 and HCF1 are shared among members of the mixed-lineage leukemia/set-domain containing (MLL/SET) family of histone 3 lysine 4 (H3K4) methyltransferase complexes (Raja et al., 2010; Cai et al., 2010). MLL1 (also known as KMT2A) is a histone methyltransferase (Milne at al., 2002). Human MOF has been shown to physically associate with MLL1 in a multi-protein complex that catalyzes both histone acetylation and methylation (Dou et al., 2005). These

previous studies demonstrate potential physical association and functional links between the NSL and MLL1 complexes, but the extent to which the MLL1 and NSL complexes represent one large regulatory complex or multiple complexes composed of various components remains unclear.

NUP98 translocations have been detected in patients with various hematopoietic disorders, such as myelodysplastic syndrome (MDS), chronic myeloid leukemia (CML) in blast crisis, acute myeloid leukemia (AML), and acute lymphoblastic leukemia (ALL). Although the frequency of *NUP98* rearrangements in unselected adult patients with AML is rare (around1% to 2%), the frequency of *NUP98* rearrangements in patients with an 11p15 abnormality is 35% (Gough et al., 2011). However, the frequency of *NUP98*-rearrangements is greater in childhood AML with between 6-10% of cases harboring this translocation (Bisio et al., 2014). Adults and children with AMLs carrying a *NUP98* translocation have a relatively poor prognosis (Hollink et al., 2011; de Rooij et al., 2013; Chou et al, 2009). All the *NUP98* translocations produce gene rearrangements that encode fusion proteins which possess a common NH_3-terminus which invariably contains the nucleoporin FG/GLFG repeat motifs and GLEBS domain fused in-frame with various COOH-terminal fusion partners. Therefore, the RBD and NLS at the C-terminal portion of NUP98 are replaced by the C-terminus of the fusion partner. The various *NUP98* fusion partners, include homeobox genes with the conserved DNA-binding domain, such as *HOXA9* and *HOXD13*, and proteins with a histone "writer" or "reader" domain, such as nuclear receptor binding SET domain protein 1 (*NSD1*), jumonji/ARID domain-containing protein 1A (*JARID1A*) and PHD finger protein 23 (*PHF23*). Studies using mouse models expressing *NUP98* fusions including *NUP98-HOXA9*, *NUP98-HOXD13*, *NUP98-Topoisomerase I (NUP98-TOP1), NUP98-NSD1*, *NUP98-JARID1A* and *NUP98-PHF23* confirmed their leukemogenic potential (Kroon et al., 2001; Pinearlt et al., 2003; Gurevich et al., 2004, Wang et al., 2007, Wang et al., 2009; Gough et al., 2014). *NUP98*-rearranged leukemias show elevated *HOXA* and *HOXB* cluster genes and mouse model systems have recapitulated this high-level expression independent of whether the leukemias are derived from mouse or human bone marrow (BM) (Kroon et al., 2001; Pinearlt et al., 2003; Wang et al., 2007, Wang et al., 2009; Gough et al., 2014; Takeda et al., 2006; Chung et al., 2006; Hollink et al., 2011; de Rooij et al., 2013 and Shiba et al., 2013). However, the molecular mechanisms of *NUP98*-fusion mediated leukemogenesis and elevated *HOX* gene expression in this leukemia are unclear.

In this study, we demonstrate that the NUP98 fusions NUP98-HOXA9 (NHA9), NUP98-HOXD13 (NHD13), NUP98-NSD1, NUP98-PHF23 and NUP98-TOP1 physically interact with the MLL1 and NSL complexes. Genome-wide chromatin immunoprecipitation followed by next generation sequencing (ChIP-seq) illustrated that NUP98-HOXA9 and MLL1 colocalize on chromatin and are found associated with *Hox* gene promoter regions. We further demonstrate the dependence of the *NUP98*-fusion driven gene expression signature and leukemia maintenance on *Mll1 in vitro* and *in vivo* and that inactivation of *Mll1* reverses a gene expression program found in *NUP98*-rearranged human leukemia. Together, our data show a functional interaction between NUP98 fusions and the NSL/MLL1 complexes that reveals

a crucial role for *Mll1* in the epigenetic regulation of *HOX* gene expression in *NUP98*-fusion driven leukemia.

RESULTS

NUP98 fusions and the N-terminus of NUP98 localize to the nucleus

A schematic of wild type (WT) NUP98 is shown in Figure 1A. The first GLFG domain (GLFG-1) contains a total of 17 FG/GLFG repeats; while the second GLFG domain (GLFG-2) contains 21 FG/GLFG repeats. For NHA9 and NHD13 fusions, the HOXA9 or the HOXD13 portion of the fusion protein still processes the helix-turn-helix (homeobox) DNA-binding domain. To assess the subcellular localization of NUP98 and NUP98 fusions, we overexpressed Human influenza hemagglutinin (HA)-tagged WT full-length NUP98, HA-tagged NHA9 and NHD13 fusion proteins, and HA-tagged NH_3-terminal portion of WT NUP98 (N-NUP98, 1-469 amino acids of the N-terminal NUP98 preserved in NUP98 fusions) in 293T cells by transient transfection. To confirm the expression of NUP98 proteins, Western blot analysis was performed using whole cell lysates from transiently transfected 293T cells. Indeed, we detected expression of the appropriately sized N-NUP98, full-length NUP98, NHA9, and NHD13 fusion proteins (Figure 1B). To determine whether HA-tagged NUP98 or NUP98 fusions associate with NPCs, cells were double stained for HA and NUP214, a component of NPCs, mainly localized at the nuclear envelop. Immunofluorescence showed that the full-length NUP98 protein is primarily localized to the nuclear envelope with a distinct staining around the rim of the nucleus, and displayed highly overlapping immunolabeling patterns to NUP214 at the nuclear rim (Figure 1C). However, the NUP98 fusion proteins (NHA9 and NHD13) do not colocalize with NUP214 signal at the nuclear envelope, and are predominantly located in the nucleoplasm with multiple punctate foci (Figure 1C). In contrast to full-length NUP98, the N-NUP98 protein, which contains all 38 FG/GLFG repeats, failed to form the typical rim structure at the nuclear envelope and showed more defined FG/GLFG body staining throughout the nucleus (Figure 1C). These data suggest that the C-terminal sequence of full-length NUP98 is required for its subcellular localization at the nuclear envelope within the NPCs as previously demonstrated (Griffis et al., 2002). Our data further demonstrate that N-NUP98 exhibits a similar intranuclear localization as the NUP98 fusions NHA9 and NHD13, which is distinct from full-length NUP98. This suggests that the NH_3-terminus of NUP98 is necessary for the intranuclear localization of NUP98 fusions, and loss of the COOH-terminus of NUP98 frees NUP98 and NUP98 fusions from the nuclear envelope.

To define how individual domains of the retained NH_3-terminal NUP98 affect the nuclear localization pattern of NUP98 fusion proteins, we generated a series of Flag-Avi-tagged NHA9 mutants. Figure 1D shows the various NHA9 mutants with either deletion of the GLFG-1 domain (2-156, NHA9-GLFG-1 del), deletion of the GLEBS domain (157-213, NHA9-GLEBS del), deletion of the GLFG-2 domain (214-469, NHA9-GLFG-2 del) or deletion of both the GLFG-1 and GLFG-2 domain (all 38 FG/GLFG repeats deleted, NHA9-(GLFG-1+2) del).

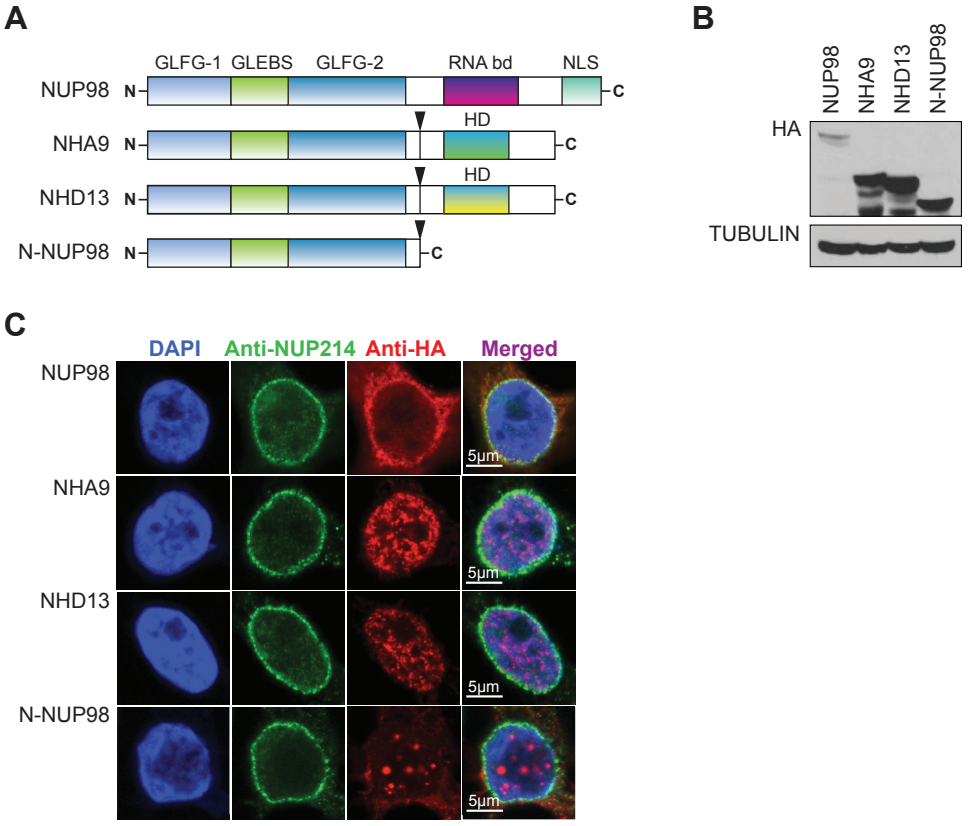

Figure 1. The subcellular localization and expression of NUP98 and NUP98 fusions

(A) Schematic representation of WT full-length NUP98, NUP98-HOXA9 (NHA9), NUP98-HOXD13 (NHD13) and N-NUP98. Fusion break points are indicated with arrows. GLFG, glycine-leucine-phenylalanine-glycine; GLEBS, GLE2-binding sequence; bd, binding domain; NLS, nuclear localization signal.

(B) Western blot analysis of whole cell lysates from transfected 293T cells detected by anti-HA and anti-beta Tubulin antibodies. One representative experiment of three is shown.

(C) Immunofluorescence staining of 293T cells transfected with the HA-tagged full-length NUP98, NHA9, NHD13 and N-NUP98 vectors. Cells were fixed, permeabilized and stained with an anti-HA and an anti-NUP214 antibody for double-immunofluorescence analysis by confocal microscopy. HA was labeled with Alexa Fluor 568-conjugated secondary antibody (red), and the NUP214 was labeled with Alexa Fluor 488-conjugated secondary antibody (green). Nuclei were counterstained with (DAPI, blue).

(D) Schematic of the various NHA9 mutant constructs used in this study. Arrow indicates break point.

(E) Western blot analysis of whole cell lysates from transfected 293T cells detected by anti-Flag and anti-beta Tubulin antibodies. One representative experiment of three is shown.

(F) Immunofluorescence staining of 293T cells transfected with Flag-Avi-tagged NHA9 and NHA9 mutant vectors. Cells were fixed, permeabilized and stained with an anti-Flag and an anti-NUP214 antibody for double-immunofluorescence analysis by confocal microscopy. Flag was labeled with Alexa Fluor 568-conjugated secondary antibody (red), and the NUP214 was labeled with Alexa Fluor 488-conjugated secondary antibody (green). Nuclei were counterstained with DAPI (blue).

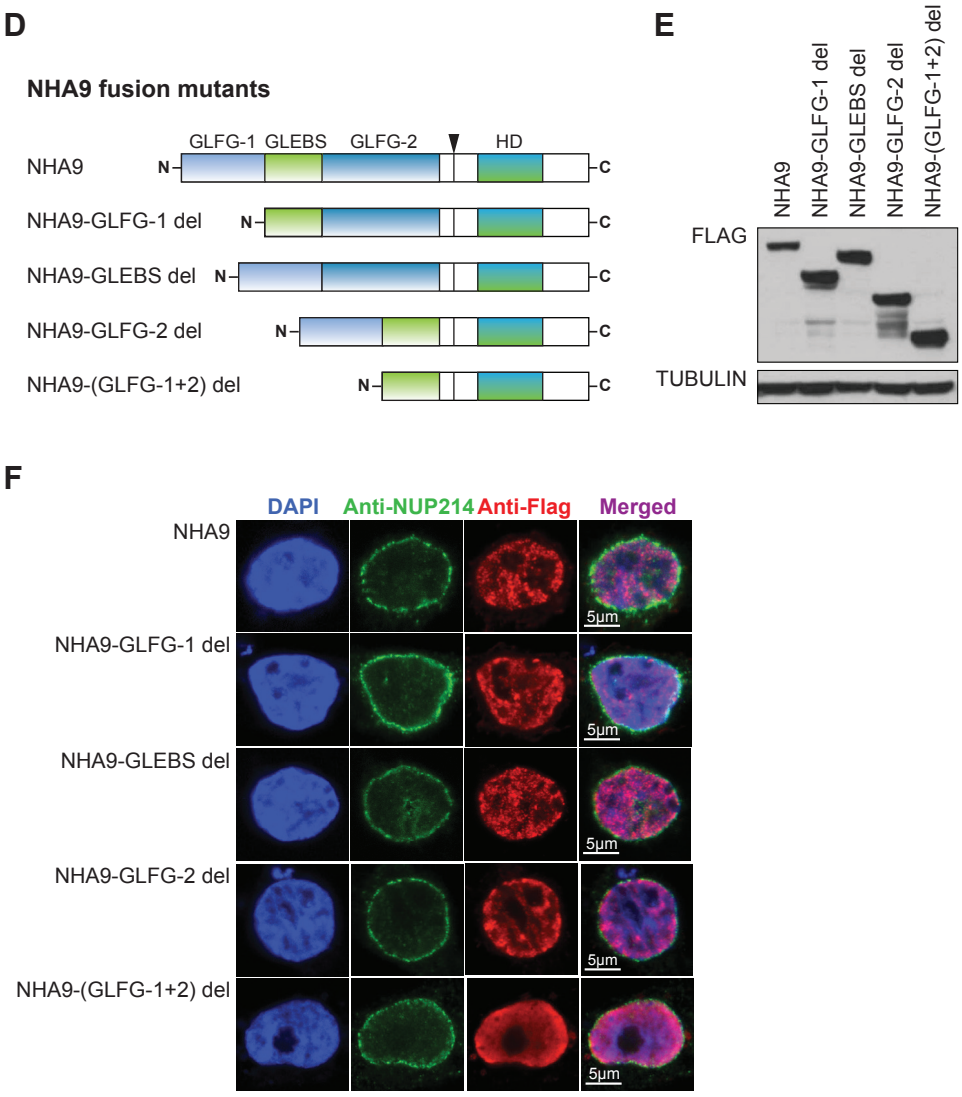

The expression of these mutant NHA9 proteins in transiently transfected 293Ts was detected by Western blot (Figure 1E) and the subcellular distribution of the proteins was examined by immunofluorescence staining using anti-Flag and anti-NUP214 antibodies (Figure 1F). The NHA9-GLEBS del mutant showed similar intranuclear localization to intact NHA9 with multiple punctate foci, whereas the NHA9-(GLFG1+2) del mutant with no FG/GLFG repeats localized diffusely throughout the nucleus. The NHA9-GLFG-1 del and the NHA9-GLFG-2 del displayed fewer punctated nuclear foci compared to WT NHA9 overexpressing cells. These data confirm that the FG/GLFG repeats, and not the GLEBS domain, are required for NUP98 fusion proteins to form punctated, intranuclear localized foci.

NUP98 fusions interact with MLL1 and NSL histone-modifying complexes

The physical and functional interaction between Nup98 and histone-modifying complexes NSL and Trx, found in *Drosophila* (Pascual-Garcia et al., 2014), suggests that the intranuclear localized and FG/GLFG repeats containing NUP98 leukemic fusion proteins might also interact with the NSL and MLL1 complex. To test this hypothesis, we generated 293T cell lines that stably express bacterial BirA biotin ligase and a COOH-terminal Flag-Avi-tagged NUP98 fusion protein consisting of the NHA9 fusion protein, the NHD13 fusion protein or N-NUP98. Whole cell lysates were prepared from each cell line and subjected to biotin-mediated affinity purification with streptavidin magnetic beads. The eluted proteins from the streptavidin beads were fractionated by SDS-PAGE and analyzed by Western blotting for the presence of NSL/MLL1 protein complex members. As shown in Figure 2A, the known NSL/MLL1 complex components were detected by anti-MOF, anti-PHF20, anti-OGT1, anti-HCF1, anti-WDR5 and anti-MLL1 antibodies in streptavidin bead eluates from Flag-Avi-tagged NHA9, NHD13 and N-NUP98 expressing cells, but not from control cells with BirA expression only. Moreover, proteins such as CXXC1 (a unique component of the SETD1 complex) and EZH2 (the catalytic subunit of the Polycomb repressive complex 2), which are not found in the NSL/MLL1 complexes, were not detected in the eluted protein from streptavidin beads after biotin-mediated affinity purification. To test the interaction in a different system, we generated U937 cell lines that stably express bacterial BirA biotin ligase and a COOH-terminal Flag-Avi-tagged NHA9 or NHD13 fusion protein (Figure S1A). As shown in Figure S1B, the interaction between NUP98 fusion proteins and the NSL/MLL1 complex was also detected in U937 cells, a human leukemic monocyte cell line.

Considering that most NUP98 fusion proteins possess a similar NH_3-terminal portion of NUP98, we explored whether other NUP98 fusion proteins also interact with the NSL/MLL1 complex. Consistent with our data above, three other NUP98 fusions, NUP98-NSD1, NUP98-PHF23 and NUP98-TOP1 also interacted with NSL/MLL1 complex proteins including MOF, PHF20, OGT1, HCF1, WDR5 and MLL1n (Figure 2B). Our results demonstrate that NUP98 fusions, such as NHA9, NHD13, NUP98-NSD1, NUP98-PHF23 and NUP98-TOP1, physically interact with the NSL/MLL1 complex. These data suggest that the common NH_3-terminus of NUP98 mediates binding of NUP98 fusions to the NSL/MLL1 complex, and further implicate a potential role for the NSL/MLL1 complex in *NUP98*-fusion driven leukemia.

To further assess the specificity of these interactions, we determined whether full-length NUP98 interacts with the NSL/MLL1 complex. 293T cells were transfected with vectors expressing Flag-tagged full-length NUP98 and NHD13, and proteins were immunoprecipitated using an anti-Flag antibody. The NHD13 fusion again showed interaction with NSL/MLL1 complex members such as MOF, PHF20, HCF1 and WDR5 (Figure 2B). However, none of these NSL/MLL1 complex proteins were detected in immunoprecipitates from the cells expressing WT full-length NUP98 (Figure 2C). These data indicate that nuclear envelope associated full-length NUP98 is not available for the interaction with the NSL/MLL1 complex, which occurs inside the nuclear interior, suggesting that the intranuclear localized GLFG repeat-rich portion of NUP98 fusions may be essential for their interaction with the complex.

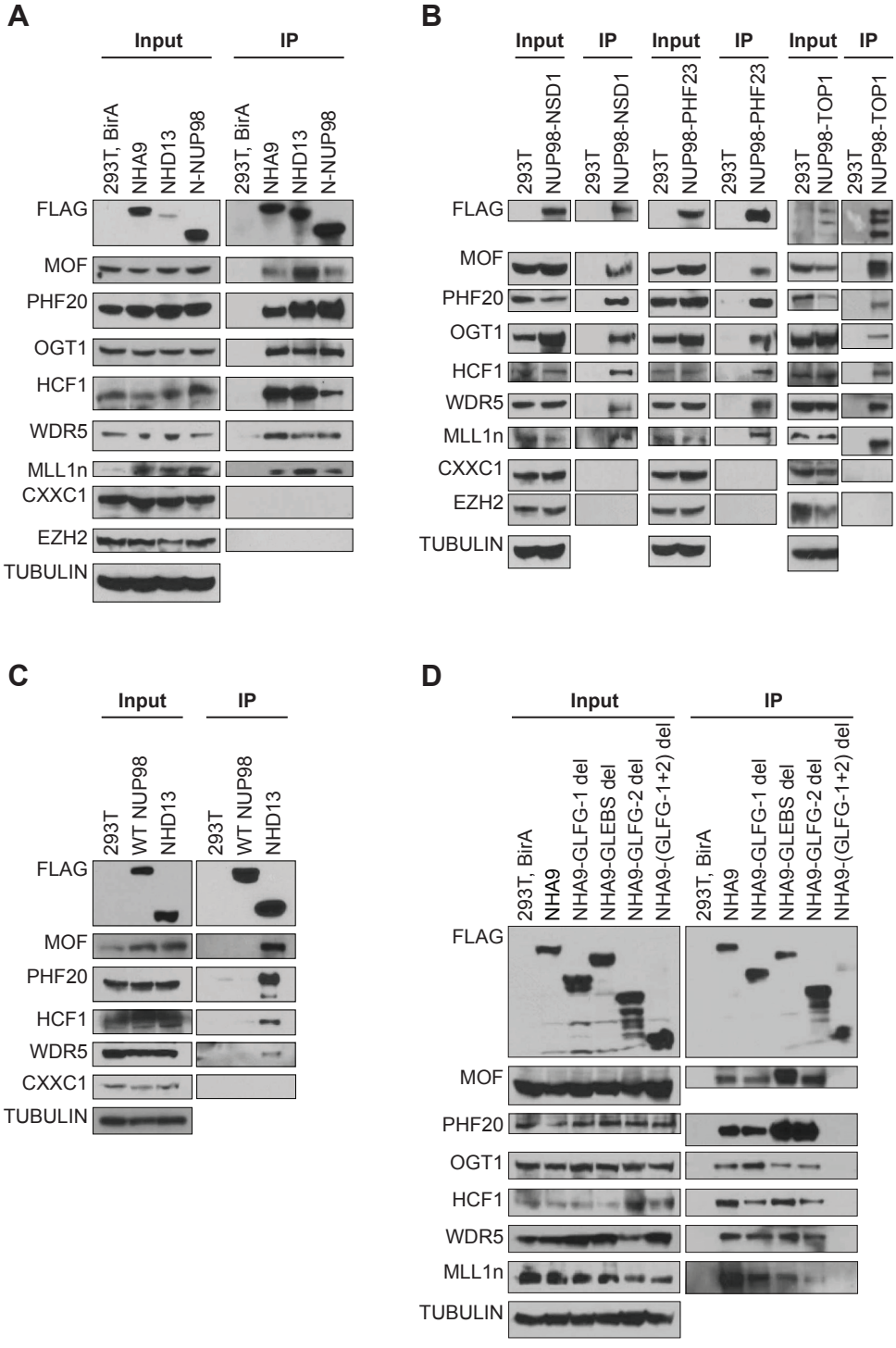
A
Input
IP
293T, BirA
NHA9
NHD13
N-NUP98
FLAG
MOF
PHF20
OGT1
HCF1
WDR5
MLL1n
CXXC1
EZH2
TUBULIN
B
Input
IP
293T
NUP98-NSD1
NUP98-PHF23
NUP98-TOP1
C
WT NUP98
D
NHA9-GLFG-1 del
NHA9-GLEBS del
NHA9-GLFG-2 del
NHA9-(GLFG-1+2) del

Figure 2. NUP98 fusions interact with MLL1 and the NSL histone-modifying complex
(A) Immunoprecipitation (IP) with streptavidin magnetic beads for NHA9, NHD13, N-NUP98 and the various NSL/MLL1 complex members. The Flag-Avi-tagged NHA9, NHD13 and N-NUP98 were stably expressed in 293T cells with co-expression of the BirA biotin ligase. Whole cell lysates were prepared and subjected to IP using streptavidin magnetic beads. Cell lysates (Input) and proteins eluted from the streptavidin beads (IP) were separated by SDS–PAGE and analyzed by Western blotting with anti-Flag, anti-MOF, anti-PHF20, anti-OGT1, anti-HCF1, anti-WDR5, anti-MLL1n, anti-CXXC1, anti-EZH2 and anti-beta Tubulin antibodies.
(B) Co-IP was performed on lysates from Flag-tagged NUP98-NSD1 (left), NUP98-PHF23 (middle) and NUP98-TOP1 (right) transfected 293T cells with an anti-Flag antibody, and analyzed by Western blotting.
(C) Immunoblots of Co-IP on lysates from Flag-tagged full-length *NUP98* (WT NUP98) or *NHD13* transfected 293T cells with an anti-Flag antibody.
(D) Co-IP was performed on lysates from Flag-Avi-tagged NHA9 or NHA9-mutant transfected 293T cells with co-expression of the BirA biotin ligase, and analyzed by Western blotting. Data are representative of three individual experiments.

To further elucidate the NUP98 fusion domains responsible for the interaction with the NSL/MLL1 complex, we performed biotin-mediated affinity purification on 293T cell lysates expressing BirA biotin ligase and Flag-Avi-tagged NHA9 or one of the NHA9 mutant proteins. Removal of the first 17 FG/GLFG repeats (NHA9-GLFG-1 del) or the GLEBS domain (NHA9-GLEBS del) of the NUP98 moiety did not affect binding of NHA9 to NSL/MLL1 complex members (Figure 2D). However, upon deletion of the 21 FG/GLFG repeats (NHA9-GLFG-2 del), the interaction with MLL1 was significantly reduced (Figure 2D). The interaction of NHA9 with NSL/MLL1 complex was completely abolished by deletion of both GLFG domains with 38 FG/GLFG repeats (NHA9-(GLFG1+2) del) (Figure 2D). These data demonstrate that the FG/GLFG repeat motifs rather than the GLEBS domain of NHA9 are required for the interaction between NHA9 and the NSL/MLL1 complex.

NUP98 fusion proteins bind to chromatin to drive gene expression
The importance of the NSL and MLL1 complexes in chromatin regulation and transcriptional activation raises the question of how recruitment of the NSL/MLL1 complexes by NUP98 fusions might affect the expression of NUP98 fusion target genes in leukemia. However, direct binding targets of NUP98 fusion proteins have not been identified. To define these targets, we immortalized mouse BM lineage-negative (Lin^-), $SCA1^+$, $cKIT^+$ (LSK) cells by enforced expression of *NHA9* or *NHD13* through retroviral transduction with vectors carrying C-terminally Flag-Avi-tagged *NHA9* or *NHD13*, and *BirA* ligase (Figure S2A). These immortalized cells form dense, round, blast-like colonies in a colony-forming unit (CFU) assay *in vitro* (Figure S2B) and can be maintained in liquid medium for long-term culture (data not shown). Using these immortalized cells with the expression of Flag-Avi-tagged *NUP98* fusions and *BirA*, the genome-wide direct binding targets of NHA9 and NHD13 were

identified through the metabolic labeling of NHA9 or NHD13 with biotin, followed by biotin-mediated chromatin affinity purification coupled with high throughput sequencing using streptavidin beads.

After calling peaks genome wide, 6514 NHD13-bound and 2872 NHA9-bound regions were defined. Interestingly, 10% of the NHA9 peaks (274 genes) and 15% of the NHD13 peaks (995 genes) were detected at promoter regions; similar percentage (29%) of the NHA9 peaks (833 genes) and NHD13 peaks (1896 genes) map to the gene body region (containing introns, exons, untranslated regions and transcription termination sites); while the majority of identified NHA9 peaks (61%, 1745) and NHD13 peaks (56%, 3623) present at intergenic regions (Figure 3A). Relative to the background distribution of all such annotated sites in the mouse genome, NUP98 fusion bound regions showed a marked enrichment for promoters (enriched 9.61 fold and 15.27 fold over background for NHA9 and NHD13, respectively) compared to that at gene body and intergenetic regions (~1 for both NHA9 and NHD13) (Figure S2C). Next, we asked whether the two NUP98 fusions (NHA9 and NHD13) bind to any loci in common. A pairwise comparison between the NHA9 and NHD13 enrichment at all binding loci revealed 191 overlapping binding sites at promoter regions (p=1.24e-207, hypergeometric test), 599 overlapping genes in the gene body regions (p=0) and 1129 overlapping targets at intergenic regions (p=0) (Figure 3A). This significant overlap in binding targets between NHA9 and NHD13 (hereafter simply referred to as NUP98-HOX) suggests that NUP98-HOX fusions likely use the same transcriptional program to drive leukemia development. Given that *HOX* genes are activated in both *MLL-AF9* and *NUP98* fusion leukemia, we then compared the NHA9 and NHD13 ChIP-seq data with previously reported MLL-AF9 ChIP-seq data (Bernt et al., 2011). As MLL-AF9 has been shown to act on promoters and NUP98-HOX fusion binding sites are enriched at such regions (Figure S2C), we focused our further analyses on the NUP98 fusion targets at the promoter region. 17 NUP98-HOX fusion binding targets overlapped with MLL-AF9 target genes at their promoter regions (Figure 3B, 3C), including genes with a known important function in *MLL-AF9* leukemia, such as *Hoxa3, Hoxa7, Hoxa9, Meis1, Jmjd1c, Mir196b* and less well-defined targets, such as *Baz2b* and *Cdk17* (Figure 3B), suggesting that *Hoxa* cluster genes and *Meis1* may also be important to the *NUP98*-fusion driven leukemogenic gene expression program. Interestingly, at promoters, NHA9 and NHD13 have unique binding targets such as *Hoxb* cluster genes, which are not bound by MLL-AF9 (Figure 3C). To further examine whether the NUP98-HOX direct binding targets defined here are functionally important in murine and human cells expressing these fusion proteins, we compared the ChIP-seq results to published gene expression profiling datasets. Gene set enrichment analysis (GSEA) revealed a highly significant enrichment of the NHD13 promoter region binding targets in the upregulated gene sets from murine $Lin^{-}SCA1^{+}$(LS) BM cells transduced with *NHD13* (Palmqvist et al., 2007) (Figure 3D, NES 1.60; FDR-q=0.08%). Moreover, 10 of the 182 genes whose expression increased ≥2 fold in human cord blood $CD34^{+}$ cells within 3 days of *NHA9* expression (Takeda et al. 2007) were also direct targets in our system thus showing significant enrichment (p=5.74e-06, hypergeometric test) (Figure 3E). Among these

10 genes, *Hoxa7*, *Hoxa9* and *Pbx3* were significantly upregulated in the before mentioned *NHD13* transduced murine LS BM cells (Palmqvist et al., 2007). There was no overlap between the 30 downregulated genes in human cord blood *NHA9* transduced cells (Takeda et al., 2006) and the 274 NHA9 promoter targets as defined in Figure 3A. These results show that NUP98-HOX binding is associated with elevated expression of target genes in mouse and human cells, and *Hoxa7, Hoxa9* and *Pbx3* are among the common activated targets of NUP98-HOX fusions. Given the essential role of *Hoxa7, Hoxa9* and *Meis1* genes in *MLL-AF9* leukemia (Ayton et al., 2003; Martin et al., 2003; Kumar et al., 2009), our results suggest that the binding of NUP98-HOX fusions to the *Hox* gene locus to activate *Hox* gene expression may contribute to *NUP98-HOX* fusion leukemia transformation.

To determine whether our findings for NUP98-HOX fusions hold true for other NUP98 fusions with fusion partners other than homeobox genes, we immortalized mouse BM LSKs by retroviral transduction with vectors carrying Flag-Avi-tagged *NUP98-TOP1* and *BirA* ligase (Figure S2A and B). Biotin-mediated ChIP-seq was performed to define the direct binding targets of NUP98-TOP1. Genome-wide analysis revealed NUP98-TOP1 occupation at 833 promoter regions, 1588 gene body regions and 3476 intergenic regions (Figure S2D). ChIP-qPCR confirmed the significant enrichment of NUP98-TOP1 at promoter regions of *Hoxa7, Hoxa9, Hoxb5, Evi1 and Meis1* (Figure S2E), though the enrichment of NUP98-TOP1 at the *Hoxb5* promoter region was less than that of NHA9 (Figure S2F). NUP98-TOP1 binding sites largely overlap with the common NUP98-HOX targets at promoter regions (183 overlapping genes including *Hoxa* cluster genes, *Hoxb* cluster genes, *Eya1*, *Pbx3* and *Meis1,* p=1.27e-269, hypergeometric test), gene body regions (571 overlapping targets, p=0) and intergenic regions (1067 overlapping sites, p=0) (Figure S2G), indicating that NUP98 fusion proteins with distinct fusion partners share common target genes.

To further dissect the contribution of the NUP98 portion to the DNA binding properties of NUP98 fusion proteins, we retrovirally overexpressed Flag-Avi-tagged *N-NUP98*, and *BirA* ligase in mouse BM LSKs (S2A) to perform a Biotin-mediated ChIP-seq. Genome-wide peak detection analysis identified a total of 1296 N-NUP98 binding targets, significantly fewer than for all NUP98 fusions (NHD13, NHA9 and NUP98-TOP1). Among the N-NUP98 target loci, 227 sites were located at promoter regions, 343 sites at gene body regions and 726 binding sites at intergenic regions (Figure S2H). Interestingly, the 227 N-NUP98 targets at promoter regions included *Hoxa7, Hoxa9, Hoxb5, Pbx3*, *Evi1* and *Meis1*. ChIP-qPCR validated the significant enrichment of N-NUP98 at these promoter regions (Figure S2I). We then compared the annotated N-NUP98 targets to the common targets between NUP98-TOP1 and NUP98-HOX fusions defined in Figure S2G (NUP98 fusions) and found an overlap at 67 promoter regions (p=1.69e-93, hypergeometric test), 226 gene body regions (p=2.34e-302) and 310 intergenic regions (p=1.33E-239)(Figure S2J). The significant overlap in binding targets between N-NUP98 and NUP98 fusions, and the colocalization of N-NUP98 and NUP98 fusions at *Hoxa, Hoxb* and *Meis1* loci, as illustrated by genome browser tracks (Figure S2K), suggests that the NUP98 moiety of NUP98 fusion proteins contributes to the binding of NUP98 fusions at these target genes.

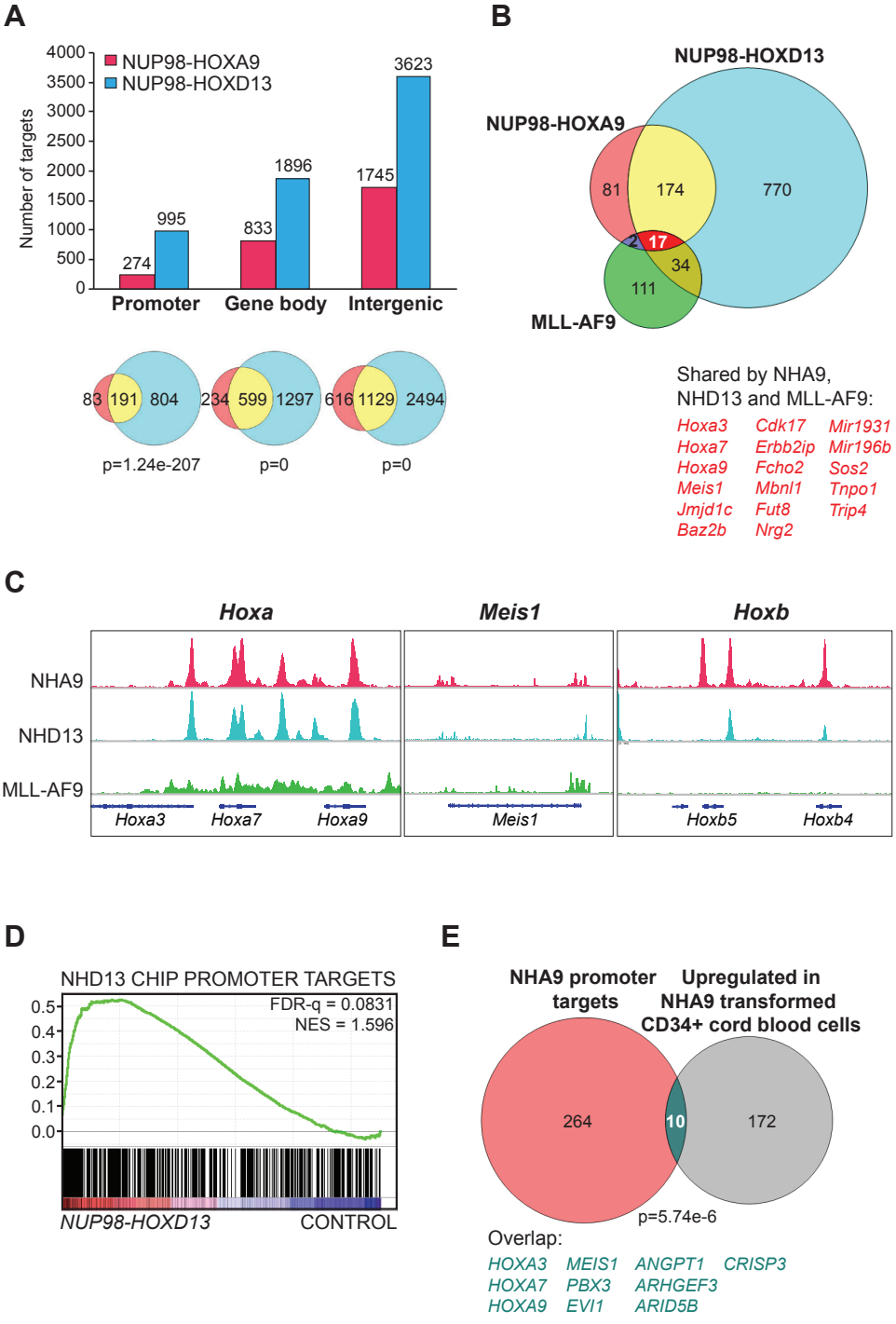
A
NUP98-HOXA9
NUP98-HOXD13
Number of targets
4000
3500
3000
2500
2000
1500
1000
500
0
274
995
833
1896
1745
3623
Promoter
Gene body
Intergenic
83 191 804
234 599 1297
616 1129 2494
p=1.24e-207
p=0
p=0
B
NUP98-HOXD13
NUP98-HOXA9
MLL-AF9
81
174
770
2
17
34
111
Shared by NHA9, NHD13 and MLL-AF9:
Hoxa3 Cdk17 Mir1931
Hoxa7 Erbb2ip Mir196b
Hoxa9 Fcho2 Sos2
Meis1 Mbnl1 Tnpo1
Jmjd1c Fut8 Trip4
Baz2b Nrg2
C
Hoxa
Meis1
Hoxb
NHA9
NHD13
MLL-AF9
Hoxa3
Hoxa7
Hoxa9
Meis1
Hoxb5
Hoxb4
D
NHD13 CHIP PROMOTER TARGETS
FDR-q = 0.0831
NES = 1.596
0.5
0.4
0.3
0.2
0.1
0.0
NUP98-HOXD13
CONTROL
E
NHA9 promoter targets
Upregulated in NHA9 transformed CD34+ cord blood cells
264
10
172
p=5.74e-6
Overlap:
HOXA3 MEIS1 ANGPT1 CRISP3
HOXA7 PBX3 ARHGEF3
HOXA9 EVI1 ARID5B

Figure 3. Genome-wide binding of NUP98 fusions in immortalized mouse bone marrow cells and functional correlation of their target genes in mouse and human cells

(A) ChIP-seq experiments were performed using immortalized mouse BM cells by enforced expression of *NHA9* or *NHD13* through retroviral transduction of LSKs with vectors carrying C-terminal Flag-Avi-tagged *NHA9* or *NHD13*, and *BirA* ligase. Mapping of NHA9 and NHD13 ChIP-seq data identified binding sites to different genomic regions (promoter, gene body or intergenic) as shown in the bar graph. The Venn diagrams illustrate overlapped targets (yellow) between NHA9 (blue) and NHD13 (red) among different genomic regions with a p-value calculated by hypergeometric test.

(B) Venn diagram for overlap of NHA9 (red), NHD13 (blue) and previously published MLL-AF9 (green) binding sites at promoter regions.

(C) Genome browser tracks representing the shared binding sites of NHA9, NHD13 and MLL-AF9 at the *Hoxa* cluster loci, the *Meis1* locus, and the unique binding of NHA9 and NHD13 at the *Hoxb* cluster loci.

(D) Gene set enrichment analysis (GSEA) illustrates enrichment of NHD13 promoter region binding targets in a previously published gene expression microarray dataset from murine LS BM cells transduced with *NHD13*. NES, normalized enrichment score; FDR, false discovery rate.

(E) Venn diagram showing the overlap between NHA9 promoter targets (red) and the upregulated genes in a previously published gene expression microarray dataset from *NHA9* transduced human $CD34^+$ cord blood cells (gray).

Colocalization of NHA9 and MLL1 at *Hoxa* and *Hoxb* cluster gene loci

Our data show an interaction between NUP98 fusions and the NSL/MLL1 complexes, as well as the association of NUP98 fusions (NHA9, NHD13, and NUP98-TOP1) with the *Hoxa* and *Hoxb* cluster gene loci. MLL1 has been shown to directly regulate *HOX* gene expression (Yu et al., 1995; Milne et al., 2002; Ayton et al., 2003; Hsieh et al., 2003; Ernst et al., 2004; Hess et al., 2004; Milne et al., 2005). To test whether NUP98 fusions and MLL1 were recruited to the same regions of *Hox* gene clusters, MLL1 ChIP-seq analysis was carried out on murine *NHA9* cells using an antibody that recognizes the NH_3-terminus of MLL1. ChIP-seq results revealed MLL1 binding sites distributed across all chromosomes. Analysis of all bound genomic loci indicated that 937 MLL1 binding sites mapped to promoter regions, while 4132 MLL1 peaks were bound to the gene bodies (Figure 4A). We then compared MLL1 and NHA9 binding regions and found a significant overlap at promoters (37 genes, p=3.7e-14, hypergeometric test) and gene bodies (520 genes, p=1.45e-204) (Figure 4B). The 37 overlapping promoter region targets include *Hoxa3*, *Hoxa7, Hoxa9, Hoxb4, Hoxb5, Meis1, Eya1* and *Pbx3* loci. To further confirm the co-occupancy of NHA9 and MLL1 at *Hoxa* gene loci, we performed sequential ChIP for NHA9 followed by MLL1 (data not shown), and found that the *Hoxa9* locus is bound by both NHA9 and MLL1. The overlap in binding sites between MLL1 and NHA9 shows that NHA9 and MLL1 colocalize on chromatin and supports our earlier finding that NHA9 interacts with MLL1 and the extended NSL/MLL1 complexes.

Given that that MOF and MLL1 are both part of the NSL/MLL1 complexes and work in concert to modify H4K16ac and H3K4me3 at promoters (Dou et al., 2005), we further tested whether H3K4me3 and H4K16ac modifications are associated with NHA9-bound regions in murine *NHA9* cells by anti-H3K4me3 and anti-H4K16ac ChIP-seq. The distribution patterns of H3K4me3 (Figure 4C) and H4K16ac (Figure 4D), shown as the average profile around TSSs (±1.5Kb), indicate high enrichment of H3K4me3 and H4K16ac in regions of chromatin where NHA9 and MLL1 are found (Figure 4C and 4D). Among a total of ~34,000 transcripts, most of the NHA9-bound promoter targets (blue dots) and co-bound promoter targets of NHA9 and MLL1 (red dots) showed a positive correlation between H3K4me3 and H4K16ac level by scatter plot analysis (Figure 4E). The presence of both H3K4me3 and H4K16ac marks at NHA9 promoter region binding targets is in line with the coordinated roles of MOF-mediated H4K16 acetylation and MLL1/SET-mediated H3K4 methylation. Importantly, specific individual peaks of H3K4me3 and H4K16ac overlapped with NHA9 and MLL1 binding targets, such as *Hoxa* cluster genes, *Hoxb* cluster genes, *Pbx3* and *Meis1*, suggesting a tight association between NHA9 and these modifications (Figure 4F). We repeated the MLL1 ChIP-seq experiment using an anti-NH_3-terminus MLL1 antibody (MO435) (Liu et al., 2014). This additional experiment confirmed the colocalization of MLL1 with NHA9, H3K4me3 and H4K16ac at NHA9 target gene loci (Figure S2L). Together our findings demonstrate that NHA9 and MLL1 are recruited to the same *Hox* loci, and this recruitment is associated with chromatin modifications of active gene expression, supporting the notion that the association between NUP98 fusions and the NSL/MLL1 complexes is important for *NUP98*-fusion driven leukemogenic gene expression.

Figure 4. Colocalization of NHA9 and MLL1 at *Hoxa* and *Hoxb* cluster gene loci

(A) MLL1 ChIP-seq was performed using an anti-MLL1n antibody in murine transformed *NHA9* LSKs. The bar graph indicates the number of MLL1-bound targets defined to promoter and gene body regions.

(B) Venn diagram shows the overlap between NHA9 (red) and MLL1 (purple) binding targets at promoter (left) and gene body regions (right) with a p-value calculated using the hypergeometric test.

(C) ChIP-seq experiments for H3K4me3 were performed in murine *NHA9* transformed cells. Shown are the average binding profiles of H3K4me3 at a region of ±1.5 kb around the annotated TSSs of NHA9-bound (red), MLL1-bound (purple) and NHA9/MLL1 co-bound targets (turquoise). Tag densities were normalized to the input (gray).

(D) ChIP-seq experiments for H4K16ac were performed in murine *NHA9* transformed cells. Average binding profiles of H4K16ac are shown.

(E) Genome-wide representation of the relation between H3K4me3 and H4K16ac in *NHA9* cells at NHA9 promoter targets (blue) and NHA9/MLL1 co-bound promoter targets (dark red) compared to all ~34000 transcripts (gray). The x and y-axis represent binding read numbers per Kb.

(F) Genome browser tracks of genomic regions showing colocalization of NHA9, MLL1, H3K4me3 and H4K16ac at four representative, well-known MLL1 targets; *Hoxa* cluster genes, *Hoxb* cluster genes, *Pbx3* and *Meis1*.

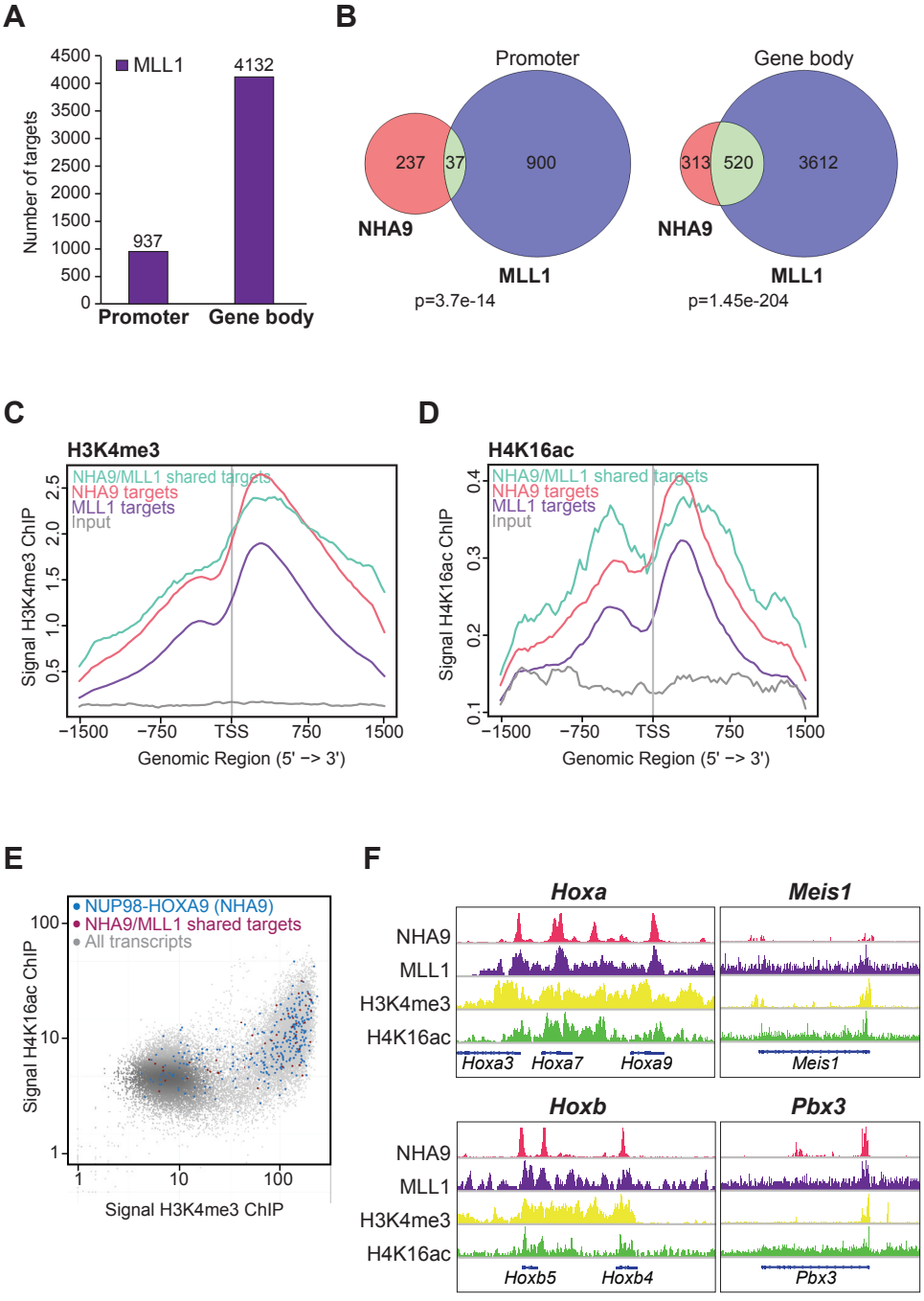
A
MLL1
Number of targets
4500
4000
3500
3000
2500
2000
1500
1000
500
0
937
4132
Promoter
Gene body
B
Promoter
Gene body
237
37
900
313
520
3612
NHA9
MLL1
NHA9
MLL1
p=3.7e-14
p=1.45e-204
C
H3K4me3
NHA9/MLL1 shared targets
NHA9 targets
MLL1 targets
Input
Signal H3K4me3 ChIP
0.5
1.0
1.5
2.0
2.5
−1500
−750
TSS
750
1500
Genomic Region (5' –> 3')
D
H4K16ac
NHA9/MLL1 shared targets
NHA9 targets
MLL1 targets
Input
Signal H4K16ac ChIP
0.1
0.2
0.3
0.4
−1500
−750
TSS
750
1500
Genomic Region (5' –> 3')
E
NUP98-HOXA9 (NHA9)
NHA9/MLL1 shared targets
All transcripts
Signal H4K16ac ChIP
100
10
1
1
10
100
Signal H3K4me3 ChIP
F
Hoxa
Meis1
NHA9
MLL1
H3K4me3
H4K16ac
Hoxa3
Hoxa7
Hoxa9
Meis1
Hoxb
Pbx3
NHA9
MLL1
H3K4me3
H4K16ac
Hoxb5
Hoxb4
Pbx3

Mll1* is required for *NHA9* driven leukemogenesis *in vitro* and *in vivo

To test the function of *Mll1* in *NHA9* driven leukemia, we first assessed the impact of *Mll1* deletion on colony formation from *NHA9* transduced mouse BM cells. LSKs were purified from the BM of a well described *Mll1* conditional knockout model where *Cre*-recombinase is driven by the estrogen receptor (*ER^{T2}-cre;$Mll1^{f/f}$, ER^{T2}-cre;$Mll1^{f/+}$ and $Mll1^{f/f}$)* (Jude et al., 2007; Artinger et al., 2013*),* and cells were transduced with *NHA9* retrovirus (Figure 5A). After immortalization with *NHA9*, cells were treated with 4-hydroxyl tamoxifen (4-OHT) for 48 hours to induce excision of the *Mll1* gene and either plated in a semi-solid medium or kept in liquid culture. The induced excision of floxed *Mll1* was confirmed by genomic PCR (Figure S3A). Loss of *Mll1* dramatically reduced the number of colonies formed by *NHA9* transformed *ER^{T2}-cre;$Mll1^{f/f}$ ($Mll1^{-/-}$NHA9)* BM cells compared to those from the *NHA9* transformed *$Mll1^{f/f}$ ($Mll1^{+/+}$NHA9*) control (Figure 5B, 5C) and reduced cell growth in liquid culture (Figure S3B). The heterozygous loss of one *Mll1* allele in *NHA9* transformed *ER^{T2}-cre;$Mll1^{f/+}$ ($Mll1^{+/-}$NHA9)* cells also showed a modest reduction of colony number in CFU assay (Figure 5B, 5C) and cell growth in liquid culture (Figure S3B), suggesting a potential gene dosage effect of *Mll1* on the clonogenic capacity and cell growth of *NHA9* cells. Moreover, the *$Mll1^{-/-}$NHA9* cells failed to form compact and hypercellular blast colonies, which were seen in about 50% of colonies formed in *$Mll1^{+/-}$NHA9* and *$Mll1^{+/+}$NHA9* cells (Figure 5D, 5E). Finally, *$Mll1^{-/-}$NHA9* cells displayed a significant degree of granulocytic differentiation on Wright-Giemsa–stained cytospin preparations compared to the characteristic blast-like morphology with a high nucleus to cytoplasmic ratio and the absence of granular cytosolic structures observed in *$Mll1^{+/-}$NHA9* and *$Mll1^{+/+}$NHA9* cells (Figure 5F). These results indicate that *Mll1* is required for maintenance of *NHA9* transformed cells *in vitro*.

Mice transplanted with BM cells expressing *NHA9* through retroviral transduction develop AML with a long latency (Kroon et al., 2001). To determine the effect of *Mll1* loss on *NHA9* driven leukemogenesis *in vivo*, we decided to use a mouse model where co-expression of *NHA9* and *Meis1a* induces rapid AML development based on the rationale that *NHA9* function should still be required in this model since *Meis1* cannot transform mouse BM by itself (Kroon et al., 2001). *NHA9* transformed *ER^{T2}-cre;$Mll1^{f/f}$, ER^{T2}-cre* and *$Mll1^{f/f}$* BM LSKs were transduced with a retrovirus encoding *Meis1a*-YFP, and sorted based on the expression of GFP (*NHA9*) and YFP (*Meis1a*) by flow cytometry (FACS) (Figure S3C). The transduced GFP^+YFP^+ BM cells of individual genotypes were transplanted into lethally irradiated C57BL/6 mice with $0.2x10^6$ helper cells (Figure 5A). Peripheral white blood cell (WBC) count and GFP^+YFP^+ percentage in peripheral blood (PB) were monitored. 15 days after transplantation, the primary mice transplanted with *NHA9-Meis1a* cells showed comparable GFP^+YFP^+ percentage in PB by FACS analysis (79.7% in mice with *ER^{T2}-cre;$Mll1^{f/f}$* cells, 80.6% in mice with *ER^{T2}-cre* cells, and 86.2% in mice with *$Mll1^{f/f}$* cells, Figure 5G). Next, 4-OHT was administered by oral gavage to examine the impact of *Mll1* excision on the initiation of *NHA9-Meis1a*-induced AML. Homozygous deletion of *Mll1* resulted in significant reduction of the GFP^+YFP^+ percentage in the PB, 7 and 14 days post induction of *Cre*-recombinase (39.6% and 30.7% respectively, Figure 5G, $p < 0.01$). This significant

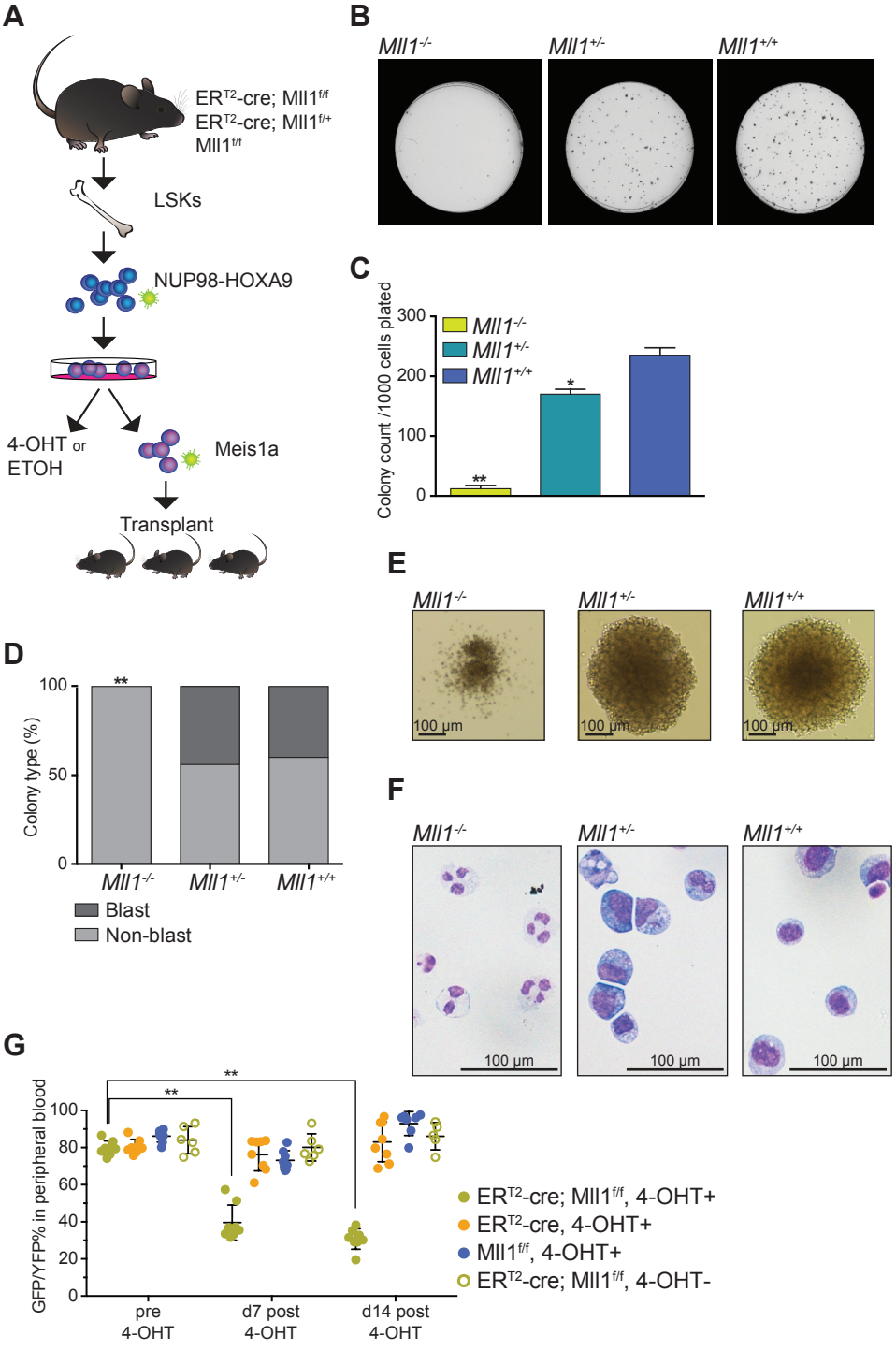
A
ERT2-cre; Mll1f/f
ERT2-cre; Mll1f/+
Mll1f/f
LSKs
NUP98-HOXA9
4-OHT or ETOH
Meis1a
Transplant
B
Mll1-/-
Mll1+/-
Mll1+/+
C
Colony count /1000 cells plated
300
200
100
0
Mll1-/-
Mll1+/-
Mll1+/+
**
*
D
Colony type (%)
100
50
0
**
Mll1-/-
Mll1+/-
Mll1+/+
Blast
Non-blast
E
Mll1-/-
Mll1+/-
Mll1+/+
100 µm
F
Mll1-/-
Mll1+/-
Mll1+/+
100 µm
G
GFP/YFP% in peripheral blood
100
80
60
40
20
0
**
**
pre 4-OHT
d7 post 4-OHT
d14 post 4-OHT
ERT2-cre; Mll1f/f, 4-OHT+
ERT2-cre, 4-OHT+
Mll1f/f, 4-OHT+
ERT2-cre; Mll1f/f, 4-OHT-

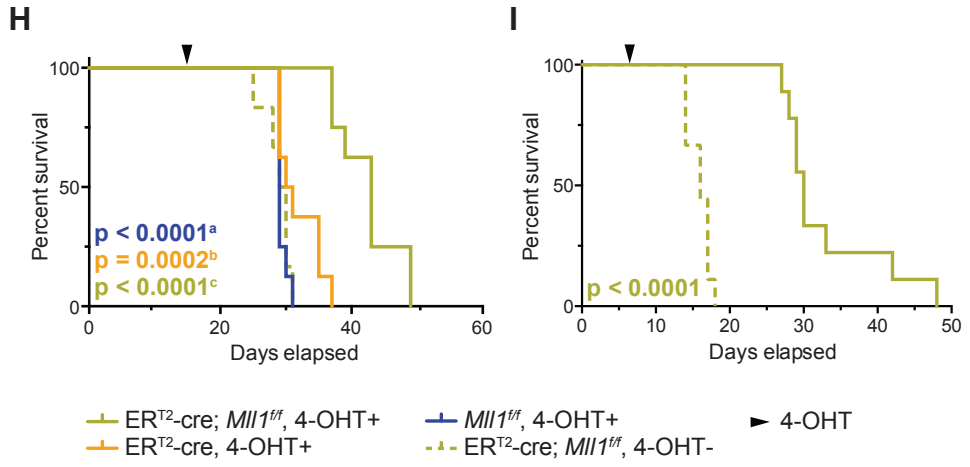

Figure 5. *Mll1* loss in a murine *NHA9* driven leukemia model leads to differentiation, decrease in tumor load and prolonged survival

(A) Schematic for *in vitro* and *in vivo Mll1* knockout experiments.

(B) Day 7 of methylcellulose colony-forming (CFU) assay of *NHA9 in vitro* transformed *ER^{T2}-cre;Mll1$^{f/f}$*, *ER^{T2}-cre;Mll1$^{f/+}$* or wild type (*Mll1$^{+/+}$*) LSKs plated after 48 hours of tamoxifen (4-OHT) treatment. Representative petri dishes are shown.

(C) Bar graph indicates mean number of colonies per 35mm dish after 7 days. 1000 cells were plated per dish. Data are representative of four individual experiments.

(D) Shown is the mean percentage of blast versus non-blast colonies relative to all colonies counted per dish, per genotype.

(E) Representative images of colonies at day 7 of CFU assay.

(F) Representative images of Wright-Giemsa–stained cytospin preparations of cells harvested at day 7 of CFU assay.

(G) *ER^{T2}-cre;Mll1$^{f/f}$*, *ER^{T2}-cre* or *Mll1$^{f/f}$* LSKs were retrovirally transduced with *GFP-NUP98-HOXA9* and *YFP-Meis1a,* sorted for double positive cells and injected into lethally irradiated C57Bl/6 mice (n=8 per group). Mice were treated with 4-OHT at day 15 post transplant to excise *Mll1*. Plotted is the GFP$^+$YFP$^+$% of live cells in PB of mice before 4-OHT treatment and at two different time-points post treatment. A dot represents a single mouse in the experiment.

(H) Survival curve of mice in primary leukemia experiment. Mice were treated with 4-OHT at day 15 after transplant. Data are representative of three individual experiments.

(I) Primary *ER^{T2}-cre;Mll1$^{f/f}$ NHA9-Meis1a* mouse leukemia BM cells were injected into sub-lethally irradiated C57Bl/6 mice. Half of the mice (n=10) were treated with 4-OHT at day 7 after transplant to excise *Mll1* (p-value calculated by log-rank test).

* p < 0.05, ** p < 0.01. Error bars represent SD of mean.

a. Log-rank test p-value comparing survival for *ERT2-cre;Mll1f/f* to *Mll1f/f*

b. Log-rank test p-value comparing survival for *ERT2-cre;Mll1f/f* to *ERT2-cre*

c. Log-rank test p-value comparing survival for *ERT2-cre;Mll1f/f* to *ERT2-cre;Mll1f/f* without 4OHT treatment

reduction was not observed in mice transplanted with either *ER^{T2}-cre* or *Mll1$^{f/f}$ NHA9-Meis1a* cells. The primary recipient mice were followed until they succumbed to leukemia. Consistent with a previous report (Kroon et al., 2001), the mice transplanted with *NHA9* and *Meis1a* co-transduced BM cells rapidly developed AML. Diseased mice were characterized by extremely elevated peripheral nucleated cell counts, anemia (data not shown), and splenomegaly (Figure S3D). At time of death, FACS analysis demonstrated more than 90% GFP$^+$YFP$^+$ cells in the PB (Figure S3E), BM and spleen (data not shown) of leukemic mice. The majority of GFP$^+$YFP$^+$ cells in BM, spleen and PB expressed the myeloid cell markers CD11b (MAC1) or GR1, indicating a myeloid leukemia phenotype (Figure S3F). Mice transplanted with *ER^{T2}-cre;Mll1$^{f/f}$ NHA9-Meis1a* cells and treated with 4-OHT, developed AML with a median survival of 43 days, compared to the mice transplanted with *ER^{T2}-cre NHA9-Meis1a* cells, *Mll1$^{f/f}$ NHA9-Meis1a* cells, or *ER^{T2}-cre;Mll1$^{f/f}$ NHA9-Meis1a* cells without 4-OHT treatment, developing AML with a median survival of 30.5 days, 29 days and 29.5 days respectively (Figure 5H). These data demonstrate that homozygous loss of *Mll1* leads to prolonged survival in an *NHA9-Meis1a* primary leukemia model. At time of death, GFP$^+$YFP$^+$ BM cells of *ER^{T2}-cre;Mll1$^{f/f}$ NHA9-Meis1a*, 4-OHT+ mice were no longer completely excised (Figure S3G), indicating that the leukemias that eventually form are caused by cells that have escaped *Mll1* deletion. Together, these results show that *Mll1* is essential for the initiation of *NHA9* driven leukemia.

NHA9-Meis1a–induced acute leukemia was also transplantable into secondary recipient mice. To test whether *Mll1* is required for the maintenance of *NHA9* driven AML, 10,000 primary leukemia cells harvested from the BM of unexcised *ER^{T2}-cre;Mll1$^{f/f}$ NHA9/Meis1a* leukemic mice were injected into sub-lethally irradiated C57BL/6 recipients. The excision of *Mll1* was induced by treatment with 4-OHT after 7 days of transplantation. Loss of *Mll1* revealed a significant increase in survival compared to the secondary AML that developed in untreated mice, with a median latency of 30 versus 16 days respectively (Figure 5I, $p < 0.0001$). Similar to the primary leukemia experiment, the leukemias that formed in the *ER^{T2}-cre;Mll1$^{f/f}$ NHA9-Meis1a* 4-OHT+ mice were no longer fully excised (data not shown). These data show that *Mll1* is essential for the maintenance of *NHA9* driven AML.

To further evaluate the role of *Mll1* in other *NUP98* fusion leukemias, we carried out analogous *in vitro* experiments for a diverse set of *NUP98* fusions. Consistent with our observations for *NHA9*, 4-OHT–induced homozygous deletion of *Mll1* in *NHD13* (Figure S4A-D), *NUP98-JARID1A* (Figure S4E-H) or *NUP98-TOP1* (Figure S4I-L) transformed cells, led to a significant reduction in CFU assay colony number and increased granulocytic differentiation. These results demonstrate that *Mll1* is indispensable for the maintenance of *NUP98* fusion transformed cells *in vitro*, suggesting that the requirement of *Mll1* may be a shared feature for most, if not all, *NUP98*-fusion driven leukemia.

We next compared the *Mll1* dependence of *NUP98* fusions to the previously reported *Mll1* dependence of *MLL-AF9* (Thiel et al., 2010). We found that the deletion of *Mll1* had a much more dramatic effect on colony formation in *NUP98*-fusion transformed cells than in cells transformed with *MLL-AF9,* both in CFU assays and liquid culture (Figure S5A-G). The

overexpression of *Hoxa9* and *Meis1* has been shown to transform mouse BM cells *in vitro* and induce AML *in vivo* (Kroon et al., 1998). We confirmed that the loss of *Mll1* does not inhibit colony formation of BM LSKs transfomed by *Hoxa9/Meis1*, as described before (Thiel et al., 2010) (Figure S5H-L). In addition, loss of *Mll1* did not affect *Hoxa9/Meis1* induced *in vivo* leukemogenesis (Figure S5M-N). These results demonstrate that the deletion of *Mll1* in *NUP98*-fusion transformed cells had a much more profound effect than did *Mll1* deletion in cells transformed with *MLL-AF9,* and had no effect on cells transformed with *Hoxa9/Meis1*, indicating the specificity of *Mll1* dependence in *NUP98* fusion leukemia.

Mll1-dependent gene expression signatures resemble human _NUP98-NSD1_ AML

To identify *Mll1*-dependent genes involved in the maintenance of *NHA9* transformed BM cells, we performed gene expression analysis after *Mll1* deletion by RNA sequencing (RNA-seq). *ER^{T2}-cre;Mll1$^{f/f}$ NHA9* cells were treated with 4-OHT for 48 hours to induce *Mll1* excision, and harvested for RNA extraction another 3 days later. *Mll1$^{f/f}$ NHA9* vehicle treated BM cells were used as a control. Assessment of normalized gene expression differences between control and *Mll1*-deficient *NHA9* cells revealed an *Mll1*-dependent gene expression signature. GSEA showed positive enrichment for gene signatures associated with hematopoietic cell differentiation (Figure 6A, left panel, NES 1.749, FDR-q 0.002), and negative enrichment for hematopoietic stem cell and progenitor gene signatures in *Mll1*-deficient *NHA9* cells (Figure 6A, right panel, NES -1.938, FDR-q <0.001). These data fit with the increased myeloid differentiation phenotype observed in *Mll1$^{-/-}$NHA9* cells. Interestingly, GSEA also demonstrated a significant negative enrichment of genes directly co-bound by NHA9 and MLL1 (Figure 6B, NES -1.493, FDR-q 0.026) in the *Mll1* knockout cells. Changes in expression of NHA9 and MLL1 co-bound targets were assessed in more detail by checking the log2 fold change between *Mll1$^{-/-}$NHA9* and *Mll1$^{+/+}$NHA9* cells, confirming that these co-bound targets, such as *Hoxa* cluster, *Hoxb* cluster, *Eya1* and *Meis1*, were among the most strongly decreased genes upon *Mll1* deletion in *NHA9* BM cells (Figure 6C, $p < 0.001$). We validated the decreased expression of *Hoxa* genes, *Hoxb* genes and *Meis1* by qRT-PCR at various time-points after *Mll1* deletion (Figure 6D and Figure S6A). These data indicate that *Mll1* is required to sustain expression of oncogenic programs targeted by NHA9. Of note, reduction of *Hoxa9, Hoxa10, Hoxb6* and *Meis1* gene expression was also detected in *NHD13* (Figure S6B) and *NUP98-JARID1A* (Figure S6C) cells upon homozygous *Mll1* deletion. The *Mll1* dependent transcriptome in *MLL-AF9* cells has previously been characterized (Cao et al., 2014). However, in our hands, *MLL-AF9* transformed cells only show minimal to no changes of *Hoxa7, Hoxa9, Hoxa10* and *Meis1* gene expression upon *Mll1* loss (Figure S5G), once more suggesting a unique dependency of *NUP98* fusions on *Mll1*.

To examine the potential clinical relevance of the *Mll1*-dependent gene expression signature found in *NHA9* cells, we first compared this gene signature to the microarray dataset of human cord blood CD34$^+$ cells retrovirally infected with *NHA9* or t(8;21) (*AML1-ETO*) (Abdul-Nabi et al., 2010). GSEA exhibits enrichment of NHA9/MLL1 co-bound promoter targets (Figure 6E, left panel, NES 1.302, FDR-q 0.169), and enrichment of the *Mll1*-

dependent gene expression signature (Figure 6E, right panel, NES1.214, FDR-q 0.166) in the upregulated genes from human CD34+ *NHA9* vs *AML1-ETO* cells. We further compared our RNA-seq data to published human microarray data from pediatric *de novo* AML patients with a *NUP98-NSD1* translocation versus a t(8;21) rearrangement, which showed high expression of *HOXA* and *B* cluster genes in AML with *NUP98-NSD1* translocations (Hollink et al., 2011). GSEA analysis on this dataset illustrates significant enrichment of NHA9/MLL1 co-bound promoter targets (Figure 6F left panel, NES 1.771, FDR-q 0.004), and enrichment of the *Mll1*-dependent gene expression signature (Figure 6F right panel, NES 1.413, FDR-q 0.091) in *NUP98-NSD1* vs *AML1-ETO* AML patient gene expression data. These findings demonstrate a strong similarity between the *Mll1*-dependent gene expression signature in our murine *NHA9* AML model and the expression profile of human *NUP98* fusion AML, indicating that our findings in murine AML models can be extended to human leukemia, and suggesting that *Mll1* is likely an important determinant of human *NUP98*-fusion driven AML.

→

Figure 6. *Mll1*-dependent gene expression signature in *NHA9* transformed mouse LSKs resembles human *NUP98-NSD1* leukemia

(A) GSEA with a differential expression analysis ranked list comparing RNA-seq data from *ER^{T2}-cre;Mll1$^{f/f}$ NHA9* cells at day 3 post tamoxifen (4-OHT) treatment (*Mll1$^{-/-}$)* to *ER^{T2}-cre;Mll1$^{f/f}$* treated with vehicle control (*Mll1$^{f/f}$*). Enrichment was assessed for genes that are either upregulated in mature hematopoietic populations (left) or in hematopoietic progenitors and stem cells (right) derived from mouse BM and fetal liver compartments.

(B) A gene set was created using the list of NHA9/MLL1 co-bound promoter targets from the ChIP-seq analysis using *NHA9 in vitro* transformed LSKs. GSEA was generated using the RNA-seq differential expression analysis comparing *Mll1$^{-/-}$* to *Mll1$^{f/f}$ NHA9* cells.

(C) Bar graphs indicate log2 fold change in gene expression as measured by RNA-seq when comparing *Mll1$^{-/-}$* to *Mll1$^{f/f}$ NHA9* cells.

(D) *NHA9 in vitro* transformed *ER^{T2}-cre;Mll1$^{f/f}$* LSKs were plated in liquid culture following 48 hours of 4-OHT or vehicle (ETOH) treatment. Cells were replated and harvested every 3 days. Bar graphs illustrate relative expression levels (RT-qPCR) as mean log fold change compared to vehicle control treated cells. The x-axis indicates cells harvested at various time-points post treatment. Data are representative of three individual experiments.

(E) A gene set was created using the NHA9/MLL1 co-bound promoter targets (left). Another *Mll1*-dependent gene set was created using the list of significantly downregulated genes when comparing *ER^{T2}-cre;Mll1$^{f/f}$* cells at day 3 post 4-OHT (*Mll1$^{-/-}$*) treatment to *ER^{T2}-cre;Mll1$^{f/f}$* treated with vehicle control (*Mll1$^{f/f}$*) with LFC < -1 and adjusted $p < 0.05$ (right). Enrichment of these *Mll1*-dependent gene sets in previously published human gene expression microarray data from *NHA9* versus *AML1-ETO* transfected human CD34+ cord blood cells (GSE57194) was assessed.

(F) Same *Mll1*-dependent gene sets as in Figure 6E were used to assess enrichment in previously published human gene expression microarray data from pediatric *de novo* AML patients with a *NUP98-NSD1* translocation versus patients with an *AML1-ETO* rearrangement (GSE17855).

NES, normalized enrichment score; FDR, false discovery rate.

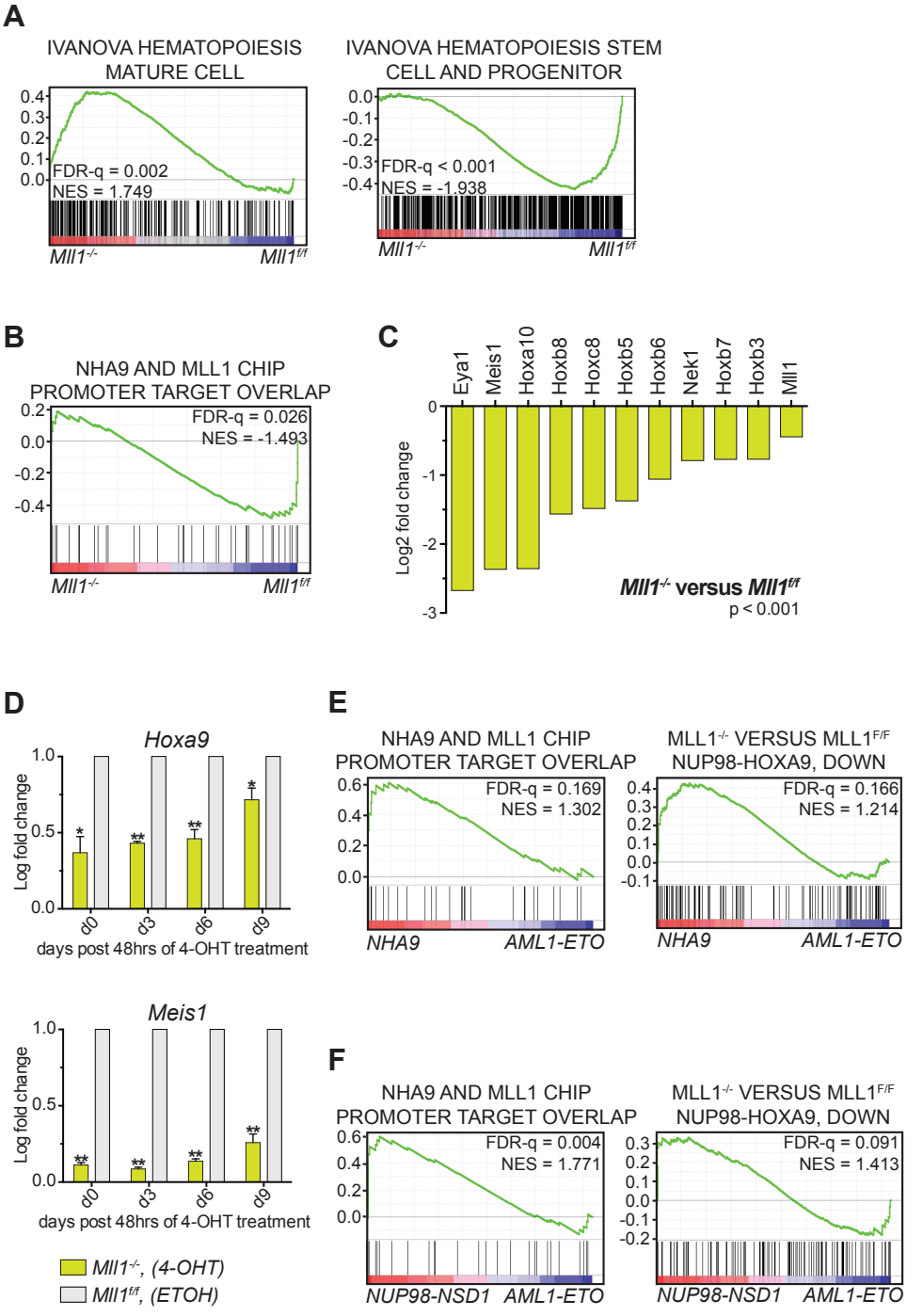
A
IVANOVA HEMATOPOIESIS MATURE CELL
FDR-q = 0.002
NES = 1.749
Mll1-/-
Mll1f/f
IVANOVA HEMATOPOIESIS STEM CELL AND PROGENITOR
FDR-q < 0.001
NES = -1.938
Mll1-/-
Mll1f/f
B
NHA9 AND MLL1 CHIP PROMOTER TARGET OVERLAP
FDR-q = 0.026
NES = -1.493
Mll1-/-
Mll1f/f
C
Eya1
Meis1
Hoxa10
Hoxb8
Hoxc8
Hoxb5
Hoxb6
Nek1
Hoxb7
Hoxb3
Mll1
Log2 fold change
Mll1-/- versus Mll1f/f
p < 0.001
D
Hoxa9
Log fold change
days post 48hrs of 4-OHT treatment
Meis1
Log fold change
days post 48hrs of 4-OHT treatment
Mll1-/-, (4-OHT)
Mll1f/f, (ETOH)
E
NHA9 AND MLL1 CHIP PROMOTER TARGET OVERLAP
FDR-q = 0.169
NES = 1.302
NHA9
AML1-ETO
MLL1-/- VERSUS MLL1F/F NUP98-HOXA9, DOWN
FDR-q = 0.166
NES = 1.214
NHA9
AML1-ETO
F
NHA9 AND MLL1 CHIP PROMOTER TARGET OVERLAP
FDR-q = 0.004
NES = 1.771
NUP98-NSD1
AML1-ETO
MLL1-/- VERSUS MLL1F/F NUP98-HOXA9, DOWN
FDR-q = 0.091
NES = 1.413
NUP98-NSD1
AML1-ETO

***Hoxa9* and *Meis1* overexpression rescues *NHA9* driven leukemia from *Mll1* dependence**

The significant downregulation of *Hoxa9* and *Meis1* in *Mll1*$^{-/-}$*NHA9* BM cells (Figure 6D) suggests an important role of *Hoxa9* and *Meis1* in *NHA9* induced leukemia. To test whether the overexpression of *Hoxa9/Meis1* can rescue *NHA9* cells from their dependence on *Mll1*, *NHA9* transduced *ER*^{T2}*-cre;Mll1*$^{f/f}$, *ER*^{T2}*-cre;Mll1*$^{f/+}$ and *Mll1*$^{f/f}$ BM cells were transduced with a *Hoxa9/Meis1*-expressing retrovirus and selected by hygromycin (Figure 7A). Following deletion of *Mll1*, cells were plated in methylcellulose for a CFU assay. Consistent with the prior results, deletion of *Mll1* in *NHA9* cells reduced the colony number compared to those of *Mll1*$^{+/+}$*NHA9* BM cells (Figure 7B). The overexpression of *Hoxa9/Meis1* had no effect on the colony formation of *Mll1*$^{-/-}$*NHA9* cells in the first plating assay (Figure 7B), but restored the clonogenic capacity of *Mll1*$^{-/-}$*NHA9* cells in the second round of the replating assay (Figure 7B). Strikingly, at the 1st and 2nd plating, more than 80% of the colonies formed in *Hoxa9/Meis1* overexpressed *Mll1*$^{-/-}$*NHA9* cells exhibited a typical dense, round blast colony shape (Figure 7C, 7D) and displayed blast morphology in Wright-Giemsa–stained cytospins (Figure 7E). This is significantly different from the differentiation seen in *Mll1*$^{-/-}$*NHA9* cells (Figure 7C, $p < 0.01$). As a control, effective *Mll1* excision was observed by PCR in 4-OHT treated cells (Figure 7F). These data show that upregulation of *Hoxa9* and *Meis1* by *Mll1* in *NHA9* cells contributes to the maintenance of *NHA9* transformed cell proliferation *in vitro*. To further examine whether *Hoxa9*/*Meis1* overexpression rescues the leukemogenicity of *NHA9* cells from *Mll1* dependence, *NHA9* transformed *ER*^{T2}*-cre;Mll1*$^{f/f}$ BM LSKs overexpressing *Hoxa9* and *Meis1*, were transplanted into lethally irradiated C57BL/6 mice (Figure 7A). After 4-OHT induced *Mll1* deletion, mice transplanted with *Mll1*$^{-/-}$*NHA9* + *Hoxa9/Meis1* cells displayed a significant increase in leukemia burden as measured by percentage of GFP^{+}YFP^{+} cells in PB (Figure 7G), compared to the non-rescue *Mll1*$^{-/-}$*NHA9* control. In addition *Mll1*$^{-/-}$*NHA9* + *Hoxa9/Meis1* mice had a significantly shortened overall survival (Figure 7H). PCR analysis confirmed that both floxed *Mll1* alleles were excised at time of death in the 4-OHT treated *ER*^{T2}*-cre;Mll1*$^{f/f}$ *NHA9* + *Hoxa9/Meis1* mice (Figure 7I). These results illustrate that the upregulation of *Hoxa9* and *Meis1* by *Mll1* contributes to *NHA9* driven leukemia. The overexpression of *Hoxa9* or *Meis1* alone did not rescue the impaired clonogenic capacity of *Mll1*$^{-/-}$*NHA9* cells (data not shown), suggesting that the interplay between *Hoxa9* and *Meis1* is required for *NHA9* induced leukemia.

Gene expression analysis demonstrated the downregulation of *Hoxb* cluster genes in *NHA9* cells upon *Mll1* loss. To determine whether the *Mll1* dependence in *NHA9* is not only *Hoxa*, but also *Hoxb* gene reliant, analogous *in vitro* rescue experiments were performed using *NHA9* transformed *ER*^{T2}*-cre;Mll1*$^{f/f}$ cells. The overexpression of *Hoxb6* alone or in combination with *Meis1*, could rescue the clonogenic defect of *Mll1*$^{-/-}$*NHA9* cells in a serial CFU replating assay (Figure S7A-B), and inhibited *Mll1*-loss induced differentiation (Figure S7C-D). Together these data provide strong evidence that *NUP98* fusion proteins drive leukemogenesis, at least in part through dysregulation of both *Hoxa* and *Hoxb* gene expression by *Mll1*.

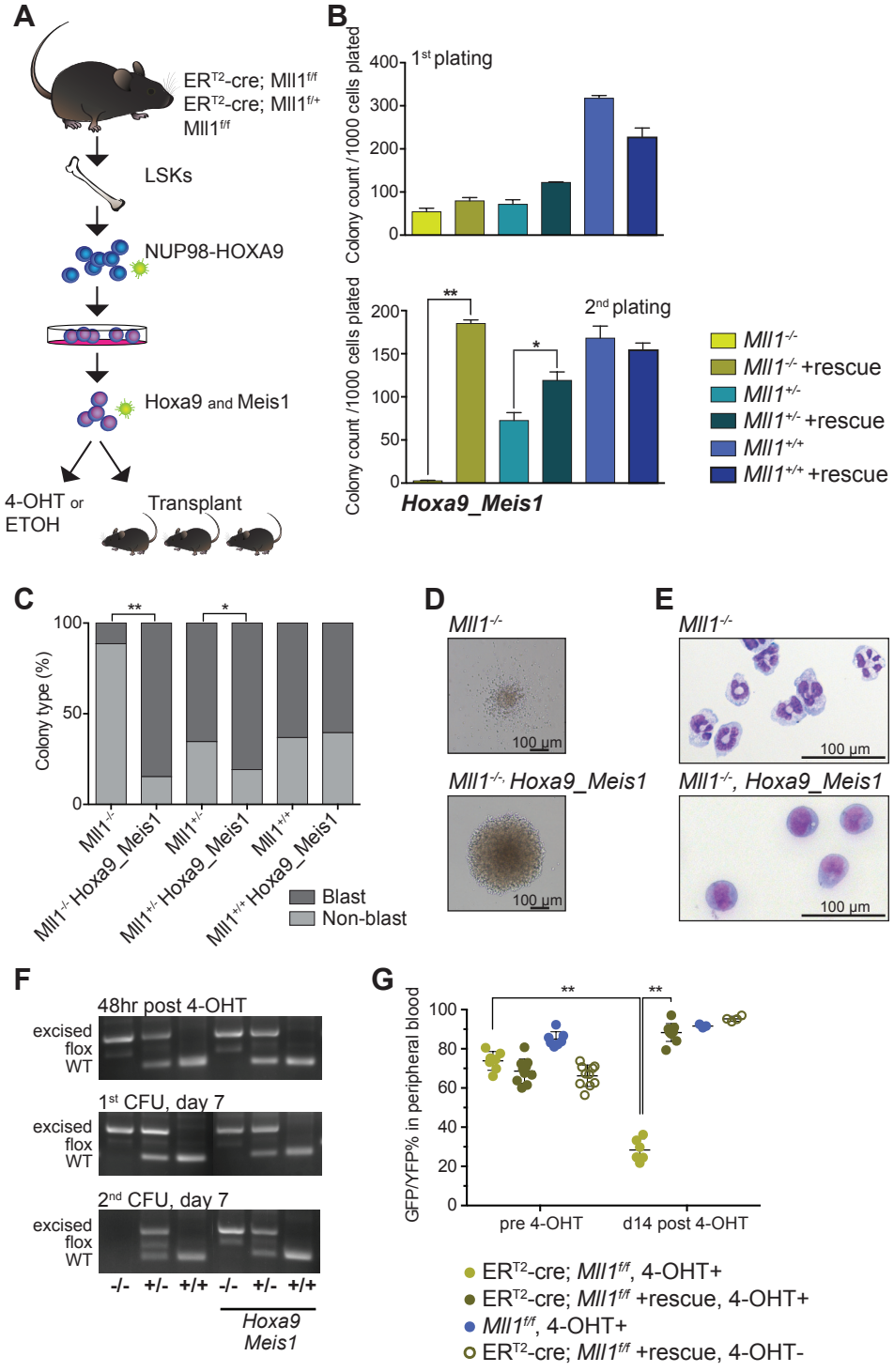
A
ERT2-cre; Mll1f/f
ERT2-cre; Mll1f/+
Mll1f/f
LSKs
NUP98-HOXA9
Hoxa9 and Meis1
4-OHT or ETOH
Transplant
B
1st plating
Colony count /1000 cells plated
2nd plating
Hoxa9_Meis1
Mll1-/-
Mll1-/- +rescue
Mll1+/-
Mll1+/- +rescue
Mll1+/+
Mll1+/+ +rescue
C
Colony type (%)
Mll1-/-
Mll1-/- Hoxa9_Meis1
Mll1+/-
Mll1+/- Hoxa9_Meis1
Mll1+/+
Mll1+/+ Hoxa9_Meis1
Blast
Non-blast
D
Mll1-/-
Mll1-/- Hoxa9_Meis1
100 µm
E
Mll1-/-
Mll1-/-, Hoxa9_Meis1
100 µm
F
48hr post 4-OHT
1st CFU, day 7
2nd CFU, day 7
excised
flox
WT
-/- +/- +/+ -/- +/- +/+
Hoxa9
Meis1
G
GFP/YFP% in peripheral blood
pre 4-OHT
d14 post 4-OHT
ERT2-cre; Mll1f/f, 4-OHT+
ERT2-cre; Mll1f/f +rescue, 4-OHT+
Mll1f/f, 4-OHT+
ERT2-cre; Mll1f/f +rescue, 4-OHT-

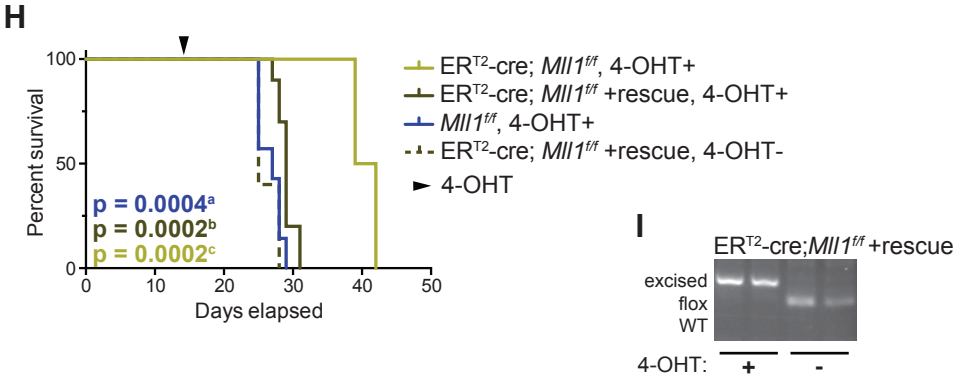

Figure 7. *Hoxa9* and *Meis1* overexpression rescues murine *NHA9* driven leukemia from *Mll1* dependence

(A) Schematic for *in vitro* and *in vivo Mll1* knockout rescue experiments.

(B) Day 7 of CFU assay of *NHA9 in vitro* transformed *ER^{T2}-cre;Mll1$^{f/f}$*, *ER^{T2}-cre;Mll1$^{f/+}$* or *Mll1$^{+/+}$* LSKs, plated after 48 hours of tamoxifen (4-OHT) treatment. Samples stating "+rescue" were infected with virus containing *Hoxa9* and *Meis1* and selected by hygromycine treatment, prior to excision. Bar graphs display mean number of colonies per 35mm dish. 1000 cells were plated per dish. Day 7 of the 1st plating (left) and 2nd plating (right). Data are representative of three individual experiments.

(C) Shown is the mean percentage of blast versus non-blast colonies relative to all colonies counted per dish, per sample after the 1st plating.

(D) Representative images of colonies formed at day 7 of the 1st plating.

(E) Representative images of Wright-Giemsa–stained cytospin preparations of cells harvested at day 7 of the 1st plating.

(F) PCR analysis illustrates excision throughout the duration of a colony-forming experiment. Representative gel images are shown.

(G) *ER^{T2}-cre;Mll1$^{f/f}$*, *ER^{T2}-cre* or *Mll1$^{f/f}$* LSKs were retrovirally transduced with *NHA9* and *Meis1a* or both *Meis1a* and *Hoxa9* ("+rescue"). Cells were then sorted and injected into lethally irradiated C57Bl/6 mice. Mice were treated with 4-OHT at day 15 post transplant to excise *Mll1*. Plotted is the GFP$^+$YFP$^+$% of live cells in PB of mice before 4-OHT treatment and 14 days post treatment. A dot represents a single mouse in the experiment.

(H) Survival curve. Mice were treated with 4-OHT at day 15 after transplant.

(I) PCR analysis illustrates *Mll1* excision in the murine BM of *ER^{T2}-cre;Mll1$^{f/f}$* + *Hoxa9/Meis1* recipient mice at time of death. Representative gel images are shown.

* $p < 0.05$, ** $p < 0.01$. Error bars represent SD of mean.

a. Log-rank test p-value comparing survival for *ERT2-cre;Mll1f/f* to *Mll1f/f*

b. Log-rank test p-value comparing survival for *ERT2-cre;Mll1f/f* to *ERT2-cre;Mll1f/f + Hoxa9/Meis1*

c. Log-rank test p-value comparing survival for *ERT2-cre;Mll1f/f* to non 4OHT-treated

DISCUSSION

NUP98 fusion proteins are generated by the fusion of the NH_3-terminus of NUP98 to the COOH-terminus of various proteins, some of which possess DNA or chromatin binding domains, and many of which are proteins of unknown function (Gough et al., 2011). These findings raise the question how NUP98 fusion proteins with such drastically different fusion partners drive leukemogenesis. We identified a novel interaction between NUP98 fusions and the NSL and MLL1 complexes, both of which contain histone-modifying enzymes. We show that a portion of the NH_3-terminus of NUP98 with GLFG repeats, which is preserved in all NUP98 fusion proteins, interacts with the NSL/MLL1 complexes. In addition, we demonstrate that *Mll1* is critical for the ability of *NUP98* fusions to drive leukemogenic gene expression and maintain leukemogenic transformation. Of note, we found that the HOXA9 portion of the NHA9 protein or the HOXD13 portion of the NHD13 protein alone, do not interact with the NSL/MLL1 complexes (data not shown), providing further support for the NH_3-terminus of NUP98 as the critical interaction site for NSL/MLL1. The intranuclear localization of NUP98 fusion proteins and N-NUP98 indicates that this interaction occurs in the nuclear interior and away from the nuclear pores. The FG/GLFG repeats containing domains, but not the GLEBS domain, are required for the NUP98 fusion proteins to form punctated nuclear foci and interact with the NSL/MLL1 complexes, suggesting that the FG/GLFG repeats in the NUP98-moiety may be involved in the binding to the NSL/MLL1 complexes. A study in *Drosophila* demonstrates a component of the NSL complex, MBD-R2, is required for the recruitment of Nup98 to chromatin (Pascual-Garcia et al., 2014). These data suggest that the association of NUP98 fusions with NSL/MLL1 complexes may be through the direct binding of the NUP98 fusion FG/GLFG repeats to PHF20 (the human homologue of *Drosophila* MBD-R2). However the specific site of FG/GLFG repeats mediating the binding with PHF20 remains to be determined.

NUP98 fusion proteins with distinct fusion partners share common target genes, suggesting that the shared NUP98 moiety of these fusion proteins may contribute to the DNA binding properties of NUP98 fusions. The significant overlap in binding targets between N-NUP98 and NUP98 fusions further support this hypothesis. Since N-NUP98 does not contain any recognizable DNA-binding or chromatin-binding motif itself, the recruitment of N-NUP98 to these specific gene loci is likely due to the interaction between N-NUP98 and other proteins or protein complexes with DNA or chromatin binding capacity, including the NSL/MLL1 complex. Our results suggest that this NUP98 moiety-mediated recruitment of NUP98 fusions to certain regions of the chromatin by the interaction with NSL/MLL1 complexes may be a shared general pathogenic mechanism of *NUP98* fusions in AML. This would help to explain how NUP98 fusions bind to *Hox* gene loci. As an example, HOXA9 itself does not bind to *Hox* genes (Huang et al., 2012), but NHA9 does, suggesting that the recruitment of NHA9 to *Hox* gene loci is not via the homeobox domain of the HOXA9 protein retained in NHA9 fusion protein.

The colocalization of NHA9 and MLL1 at *Hox* cluster gene loci, as revealed by ChIP-

seq, not only supports the identified interaction between NHA9 and NSL/MLL1 complexes, but also indicates that NHA9 utilizes this interaction to be recruited to chromatin, at least to part of the NHA9 binding targets, including *Hox* gene loci. A recent publication showed chromatin-prebound CRM1 influences localization of the NHA9 fusion to induce expression of *Hox* cluster genes (Oka et al., 2015). However, CRM1 targets are generally associated with H3K27me3 repressive modifications, thus the mechanisms of CRM1 activity are unclear. Of note, this study was performed in murine embryonic stem (ES) cells, in which the chromatin modifications associated with *HOX* loci are quite different from those in other cell types. For example, in ES cells, *HOX* cluster genes are bivalent for both H3K4me3 and H3K27me3, a phenomenon that is not seen in hematopoietic stem cells. Therefore, these findings in ES cells need to be interpreted with the cellular context in mind.

The colocalization of MLL1 and NHA9 at *Hoxa* and *Hoxb* gene promoters demonstrated here, and the direct regulation of *Hox* genes by *Mll1* (Yu et al., 1995; Milne et al., 2002; Ayton et al., 2003; Hsieh et al., 2003; Ernst et al., 2004; Hess et al., 2004; Milne et al., 2005), prompted us to explore whether NUP98 fusions co-opt mechanisms used during normal development in order to drive leukemogenesis. *In vitro* and *in vivo* functional assays showed that *Mll1* is crucial for the growth and block in differentiation of *NHA9* transformed cells, and for the initiation and maintenance of *NHA9* driven AML. Therefore, both growth and differentiation may represent mechanisms by which *Mll1* influences *NHA9* leukemogenesis. These findings were further supported by transcriptome analyses which show a significant enrichment of MLL1 and NHA9 co-bound targets among the genes downregulated in the absence of *Mll1*, and rescue experiments which show the overexpression of *Hoxa9*/*Meis1* restored the *in vitro* transformation defects and *in vivo* leukemogenicity of *NHA9 Mll1* deficient cells. Together these results demonstrate that *Mll1* controls *NHA9* induced leukemogenesis by maintaining the expression of *Hox* genes and other stem cell associated genes to support the maintenance of leukemic cells. Furthermore, we have established the *in vitro* dependence on *Mll1* for other *NUP98* fusions such as *NHD13, NUP98-JARID1A* and *NUP98-TOP1*, suggesting a more general role for *Mll1* in *NUP98*-fusion driven leukemia. Previous studies show that *NUP98-HOX* fusions promote self-renewal and aberrant gene expression to a significantly greater extent than *NUP98* fusions with non-homeobox partners (Saw et al., 2013), suggesting that the COOH-terminal fusion partner may influence the oncogenic potency of *NUP98* fusions. Whether and how *Mll1* differentially affects this aspect of *NUP98* fusions remains to be explored.

The role of endogenous *Mll1* in other AML subtypes, such as *MLL1*-fusion driven leukemia has previously been reported (Milne et al., 2010; Thiel et al., 2010), but the *NUP98*-fusion dependence on *Mll1* appears to be even more absolute than for *MLL-AF9*. These data are of particular interest given the recent publication showing that the histone methyltransferase activity of MLL1 is dispensable for *MLL-AF9* leukemogenesis (Mishra et al., 2014). Therefore our findings indicate a specific, and more dramatic requirement for MLL1 in *NUP98*-fusion driven leukemia. It is noteworthy that the NHA9 and MLL1 co-bound *Hoxb* gene targets, which play a critical role in hematopoietic stem cell self-renewal (Sauvageau et al., 1995;

Bijl et al., 2006), are not bound by MLL-AF9. The deletion of *Mll1* in *NHA9* cells resulted in significant downregulation of not only *Hoxa*, but also *Hoxb* cluster genes, including *Hoxb5, Hoxb6*, *Hoxb7* and *Hoxb8.* However, the *Hoxb* cluster genes are not activated in *MLL-AF9* leukemia cells, and as expected, *Mll1* deficient *MLL-AF9* cells did not show any change in *Hoxb* gene expression (Cao et al., 2014). This differential *Hox* gene expression pattern between *NHA9* and *MLL-AF9* leukemia might explain part of the more dramatic dependency of *NUP98* fusion leukemia on *Mll1*. The capability of *Hoxb6* alone to rescue the clonogenic capacity of *Mll1*$^{-/-}$*NHA9* cells further supports the idea that this unique *Hoxb* gene expression pattern is dependent on *Mll1* and functionally important for *NUP98*-fusion driven leukemia.

In this study, we focus our attention on the role of *Mll1* in *HOX* gene regulation and leukemogenesis driven by *NUP98* fusions. However, there is likely some contribution from the NSL complex components, such as MOF, to *NUP98*-fusion driven leukemia. The MOF-containing NSL complex, an evolutionary conserved complex in *Drosophila* and mammals, is important for genome-wide H4K16 acetylation and associated with transcriptional activation (Prestel et al., 2010; Raja et al., 2010; Cai et al., 2010). MOF (MYST1), a member of the MYST (Moz-Ybf2/Sas3-Sas2-Tip60) family of histone acetyltransferases (HATs), is a global regulator of H4K16 acetylation in mammalian cells (Prestel et al., 2010; Raja et al., 2010; Cai et al., 2010). Human MOF has been shown to physically associate with MLL1 in a multi-protein complex that catalyzes both histone acetylation and methylation (Dou et al., 2005). Indeed, we found enrichment of H4K16ac marks on NHA9 binding targets at promoters, suggesting the activation of these genes may in part be regulated by the HAT activity of MOF via its interaction with the NUP98 fusion. It will be interesting to further examine whether and how MOF affects the oncogenic program of *NUP98*-fusion driven leukemia. If so, targeting MOF may be used as a novel therapeutic approach.

In conclusion, our findings support an emerging model that various fusion oncoproteins hijack histone modifying complexes to drive leukemogenic transformation. We demonstrate that NUP98 fusion proteins interact with the NSL/MLL1 complexes via its common NH_3-terminus to drive its oncogenesis. The discovery of this common leukemogenic pathway for NUP98 fusion proteins, provides a rationale for the search of potential common therapeutic approaches in the treatment of leukemia patients carrying various *NUP98* rearrangements. The role of *Mll1* in *NUP98* fusion AML as established here, suggests that inhibition of the function of MLL1 or its interaction with menin, as recently proposed by others (Borkin et al., 2015), may be an effective treatment for patients with *NUP98* fusion leukemia. Further studies will determine whether modulation of MOF HAT activity or interruption of the association between NUP98 fusions and the NSL/MLL1 complexes with small molecules would represent a novel approach in treating poor prognosis pediatric AMLs with *NUP98* fusions.

EXPERIMENTAL PROCEDURES

Mice

The generation of the *Mll1* conditional knockout mouse has been described previously (Jude et al., 2007). *Mll1*$^{f/f}$ mice were crossed to *ER*^{T2}*-cre* mice to generate *ER*^{T2}*-cre; Mll1*$^{f/f}$ mice; and *ER*^{T2}*-cre* was maintained as a heterozygous allele. Genotyping strategies were described previously (Jude et al., 2007). Wild type C57BL/6 mice were purchased from Taconic, Hudson, NY. All animal experiments described in this study were approved by and adhered to the guidelines of the Memorial Sloan-Kettering Cancer Center Animal Care and Use Committee.

Plasmids and constructs

NUP98-HOXA9 and full-length *NUP98* cDNAs with NH_3-terminal HA tags in an MSCV-IRES-GFP vector were provided by Dr. Nabeel R. Yaseen (Ghannam et al., 2004); *NUP98-HOXD13* cDNA by Dr. Peter Aplan, *NUP98-PHF23* and *NUP98-JARID1A* in MSCV-IRES-puro by Dr. David Allis (Wang et al., 2009); and *NUP98-TOP1* in MSCV-IRES-GFP and *Meis1a* in MSCV-IRES-YFP by Dr. Keith Humphries (Gurevich et al., 2004; Pineault et al., 2003). NH_3-terminal HA-tagged *NUP98-HOXD13* and HA-tagged *N-NUP98* (1-469 amino acids of the NH_3-terminal NUP98) were constructed by PCR, checked by sequencing, and subcloned into the XhoI and EcoRI site of MSCV-IRES-GFP. NH_3-terminal Flag-tagged WT *NUP98* and *NUP98-HOXD13* were amplified by PCR and subcloned into the XhoI and EcoRI site of MSCV-IRES-GFP. C-terminal Flag-Avi-tagged *NUP98-HOXA9, NUP98-HOXD13*, *NUP98-TOP1* and *N-NUP98* were constructed by PCR and subcloned into the HpaI site of the MSCV-IRES-puro plasmid. The MSCV-*Hoxa9-Meis1*-IRES-hygromycin, MSCV-*Hoxa9*-IRES-puro, MSCV-*BirA*-YFP, MSCV-*MLL-AF9*-IRES-GFP and *NUP98-NSD1* plasmid have been previously described (Bernt et al., 2011; Deshpande et al., 2014). The *Hoxb6* plasmid was purchased from GE Dharmacon (CO, clone ID: 4223365) and subcloned into the HpaI site of an MSCV-IRES-miCD2 plasmid. The *pCL-Eco* plasmid was used for retroviral packaging. The COOH-terminal Flag-Avi-tagged NHA9 mutants NHA9-GLFG-1 del (deletion of the first GLFG domain, 2-156 residues), NHA9-GLEBS del (deletion of the GLEBS domain, 157-213 residues), NHA9-GLFG-2 del (deletion of the second GLFG domain, 214-469 residues) and NHA9-(GLFG-1+2) del (deletion of both GLFG domains), were generated using the Q5® Site-Directed Mutagenesis Kit (New England BioLabs, Ipswich, MA). The mutant constructs were verified by sequencing.

Cell culture

293T cells were cultured in DMEM, supplemented with heat inactivated 10% fetal bovine serum and 50 U/mL penicillin/streptomycin (all Thermo Fisher Scientific, Waltham, MA). *In vitro* transformed *NUP98-HOXA9, NUP98-HOXD13, NUP98-JARID1A, NUP98-TOP1, MLL-AF9* or *Hoxa9/Meis1* mouse LSKs were cultured in IMDM, supplemented with heat inactivated 10% fetal bovine serum, 50 U/mL penicillin/streptomycin (all Thermo Fisher Scientific, Waltham,

MA) and murine IL3 (10 ng/mL), IL6 (10 ng/mL) and SCF (20 ng/mL)(all PeproTech, Rocky Hill, NJ). Methylcellulose M3234 (Stemcell Technologies, Vancouver, BC, Canada).

Isolation of murine LSKs for *in vitro* transformation

WT, *Mll1$^{f/f}$ ER^{T2}-Cre*, *Mll1$^{f/+}$ ER^{T2}-Cre* and *Mll1$^{f/f}$* mice were sacrificed, and BM cell suspensions were prepared by crushing bones in a mortar after removal of muscle and connective tissues. Lineage depletion was performed by labeling BM cells with purified, biotinylated monoclonal antibodies to CD3e, CD11b (MAC1), CD45R (B220), Ly6G (GR1) and TER119 (Biotin mouse lineage panel, BD, San Jose, CA). Lin$^+$ cells were in majority removed by magnetic bead depletion with streptavidin conjugated MicroBeads over an LD column (both Miltenyi Biotech, San Diego, CA). LSKs were then obtained by staining lineage depleted (Lin$^-$) cells with Streptavidin APC/Cy7, (Biolegend, San Diego, CA), CD117 (cKIT) APC and Ly6A/E (SCA1) PE/Cy7 (both eBioscience, San Diego, CA), and sorting the LSK population.

Data Analysis and Statistical Methods

Microsoft Excel and GraphPad Prism software were used for statistical analysis. Statistical significance between 2 groups was determined by unpaired 2-tailed Student's t-test. The Kaplan-Meier method was used to plot survival curves for murine leukemic transplant data, and the log-rank test was used to evaluate statistical differences. The hypergeometric test was performed in R to calculate the statistical significance of overlapped targets. A p-value less than 0.05 was considered significant.

RNA-seq raw reads were aligned to NCBI37/mm9 and normalized using STAR. Differential expression data were obtained using the DEseq algorithm. These analyses were done through the platform from Basepair (New York City, NY). DEseq output tables are attached as supplemental tables. Gene set enrichment analyses (GSEAs) were performed using the Broad Institute web platform by pre-ranking the RNA-seq list based on log2 fold change. The *NUP98-NSD1* and *AML1-ETO* pediatric AML gene expression data were obtained from the GEO GSE17855 dataset (Hollink et al., 2011). The *NUP98-HOXA9* and *AML1-ETO* human cord blood gene expression data were obtained from the GEO GSE57194 dataset (Abdul-Nabi et al., 2010).

The ChIP-seq analysis was performed using pipelines on Basepair software (http://www.basepair.io). The fastq files were trimmed to remove adapter and low quality sequences using trim_galore and then aligned to the UCSC genome assembly mm9 using Bowtie (version 2.1.0) (Langmead et al., 2010). Duplicate reads were removed using Picard MarkDuplicates. To detect peaks, the software MACS (version 1.4) (Zhang et al., 2008) was applied using default parameters unless otherwise stated. For NUP98-HOXA9, NUP98-HOXD13, H3K4me3 and H4K16ac peak detection, the p-value cutoff was set to 10^{-5}, for MLL1 peak calling the p-value cutoff was set to 10^{-3}. Peaks were annotated to genomic features (Promoter, Gene body, Intergenic) using custom scripts at Basepair, based on the UCSC database for mm9. The integrative analysis of histone modification levels and gene expression was performed using iCanPlot (http://www.icanplot.org) (Sinha et al., 2010).

ACCESSION NUMBERS

RNA-seq and ChIP-seq data have been deposited at the NCBI Gene Expression Omnibus (http://www.ncbi.nlm.nih.gov.ezp-prod1.hul.harvard.edu/geo/) with accession codes GSE75997 (Expression changes after loss of *Mll1* in murine NHA9 transformed cells), GSE76001 (NUP98-HOXA9, NUP98-HOXD13, MLL1, H3K4me3 and H4K16ac ChIP-seq data), GSE83221 (MLL1 ChIP-seq data with Hsieh lab antibody MO435, NUP98-TOP1 and N-NUP98 ChIP-seq data).

ACKNOWLEDGMENTS

We acknowledge Alan Chramiec, Matthew Witkin and Li Yang for assistance with the preparation of ChIP-seq libraries, and Ke Xu for assistance with the confocal microscopy. This work was supported by NIH grants PO1 CA66996, R01 CA140575, the leukemia and lymphoma society and Gabrielle's Angel Research Foundation (S.A.A.); DoD Bone Marrow Failure Postdoctoral Fellowship Award (W81XWH-12-1-0568) (H.X.); and a CURE Childhood Cancer Research Grant (D.G.V.).

AUTHORSHIP CONTRIBUTIONS

H.X., D.G.V., and S.A.A. conceived the study and designed the experiments; H.X., D.G.V. and M.E.E. performed experiments; C.C., S.H.C. and G.L.B. gave experimental and conceptual guidance; H.X. and D.G.V. performed data analysis; A.S., R.P.K. and W.H. assisted with RNA-seq and ChIP-seq data analysis; J.J.H. generated and provided the MLL1 ChIP antibody; P.E. generated the conditional *Mll1* knockout mouse model; H.X., D.G.V. and S.A.A. wrote the manuscript.

DISCLOSURE OF CONFLICTS OF INTEREST

S.A.A. is a consultant for Epizyme Inc. and Imago Biosciences. Other authors declare no conflict of interest.

REFERENCES

Abdul-Nabi, A. M., Yassin, E. R., Varghese, N., Deshmukh, H., and Yaseen, N. R. (2010). In vitro transformation of primary human CD34+ cells by AML fusion oncogenes: early gene expression profiling reveals possible drug target in AML. PloS One. 5, e12464.

Artinger, E.L., Mishra, B. P., Zaffuto, K.M., Li, B.E., Chung, E.K., Moore, A.W., Chen, Y., Cheng, C., Ernst, P. (2013). An MLL-dependent network sustains hematopoiesis. . Proc Natl Acad Sci U S A. 110, 12000-12005.

Ayton, P. M., and Cleary, M. L. (2003). Transformation of myeloid progenitors by MLL oncoproteins is dependent on Hoxa7 and Hoxa9. Genes Dev. 17, 2298-2307.

Bernt, K. M., Zhu, N., Sinha, A. U., Vempati, S., Faber, J., Krivtsov, A. V., Feng, Z., Punt, N., Daigle, A., Bullinger, L., et al. (2011). MLL-rearranged leukemia is dependent on aberrant H3K79 methylation by DOT1L. Cancer Cell. 20, 66-78.

Bijl, J., Thompson, A., Ramirez-Solis, R., Krosl, J., Grier, D. G., Lawrence, H. J., and Sauvageau, G. (2006). Analysis of HSC activity and compensatory Hox gene expression profile in Hoxb cluster mutant fetal liver cells. Blood. 108, 116-122.

Bisio V, Pigazzi M, Manara E, Masetti R, Togni M, Astolfi A, Mecucci C, Zappavigna V, Salsi V, Merli P, Rizzari C, Fagioli F, Locatelli F and Basso G. NUP98 Fusion Proteins Are Recurrent Aberrancies in Childhood Acute Myeloid Leukemia: A Report from the AIEOP AML-2001-02 Study Group. 56th ASH annual meeting, San Francisco, December 6-9, 2014.

Borkin, D., He, S., Miao, H., Kempinska, K., Pollock, J., Chase, J., Purohit, T., Malik, B., Zhao, T., Wang, J., et al. (2015). Pharmacologic inhibition of the Menin-MLL interaction blocks progression of MLL leukemia in vivo. Cancer Cell. 27, 589-602.

Cai, Y., Jin, J., Swanson, S. K., Cole, M. D., Choi, S. H., Florens, L., Washburn, M. P., Conaway, J. W., and Conaway, R. C. (2010). Subunit composition and substrate specificity of a MOF-containing histone acetyltransferase distinct from the male-specific lethal (MSL) complex. J Biol Chem. 285, 4268-4272.

Cao F, T. E., Karatas H, Xu J, Li L, Lee S, Liu L, Chen Y, Ouillette P, Zhu J, Hess JL, Atadja P, Lei M, Qin ZS, Malek S, Wang S, Dou Y. (2014). Targeting MLL1 H3K4 methyltransferase activity in mixed-lineage leukemia. Mol Cell. 53, 247-261.

Capelson, M., Liang, Y., Schulte, R., Mair, W., Wagner, U., and Hetzer, M. W. (2010). Chromatin-bound nuclear pore components regulate gene expression in higher eukaryotes. Cell. 140, 372-383.

Chou, W,C,, Chen, C.Y., Hou, H.A., Lin, L.I., Tang, J.L., Yao, M., Tsay, W., Ko, B.S., Wu, S.J., Huang, S.Y., Hsu, S.C., Chen, Y.C., Huang, Y.N., Tseng, M.H., Huang, C.F., Tien, H.F (2009). Acute myeloid leukemia bearing t(7;11)(p15;p15) is a distinct cytogenetic entity with poor outcome and a distinct mutation profile: comparative analysis of 493 adult patients. Leukemia. 23: 1303-1310.

Chung, K. Y., Morrone, G., Schuringa, J. J., Plasilova, M., Shieh, J. H., Zhang, Y., Zhou, P., and Moore, M. A. (2006). Enforced expression of NUP98-HOXA9 in human CD34(+) cells enhances stem cell proliferation. Cancer Res. 66, 11781-11791.

D'Angelo M.A., Hetzer, M. W. (2008). Structure, dynamics and function of nuclear pore complexes. Trends Cell Biol 18, 456–466.

de Rooij, J.D., Hollink. I., Arentsen-Peters ST, van Galen JF, Berna Beverloo, H., Baruchel, A., Trka J, Reinhardt, D., Sonneveld, E., Zimmermann, M., Alonzo, T.A., Pieters, R., Meshinchi, S., van den Heuvel-Eibrink, M.M., Zwaan, C.M. (2013). NUP98/JARID1A is a novel recurrent abnormality in pediatric acute megakaryoblastic leukemia with a distinct HOX gene expression pattern. Leukemia. 27, 2280-2288.

Deshpande, A. J., Deshpande, A., Sinha, A. U., Chen, L., Chang, J., Cihan, A., Fazio, M., Chen, C. W., Zhu, N., Koche, R., et al. (2014). AF10 regulates progressive H3K79 methylation and HOX gene expression in diverse AML subtypes. Cancer Cell. 26, 896-908.

Dou, Y., Milne, T. A., Tackett, A. J., Smith, E. R., Fukuda, A., Wysocka, J., Allis, C. D., Chait, B. T., Hess, J. L., and Roeder, R. G. (2005). Physical association and coordinate function of the H3 K4 methyltransferase MLL1 and the H4 K16 acetyltransferase MOF. Cell. 121, 873-885.

Enninga J, L. D., Blobel G, Fontoura BM. (2002). Role of nucleoporin induction in releasing an mRNA nuclear export block. Science. 295, 1523-1525.

Ernst, P., Mabon, M., Davidson, A. J., Zon, L. I., and Korsmeyer, S. J. (2004). An Mll-dependent Hox program drives hematopoietic progenitor expansion. Curr Biol. 14, 2063-2069.

Fontoura, B.M., Blobel, G., Matunis, M.J. (1999). A conserved biogenesis pathway for nucleoporins: proteolytic processing of a 186-kilodalton precursor generates Nup98 and the novel nucleoporin, Nup96. J Cell Biol. 144, 1097-1112.

Ghannam, G., Takeda, A., Camarata, T., Moore, M. A., Viale, A., and Yaseen, N. R. (2004). The oncogene Nup98-HOXA9 induces gene transcription in myeloid cells. J Biol Chem. 279, 866-875.

Gough, S. M., Lee, F., Yang, F., Walker, R. L., Zhu, Y. J., Pineda, M., Onozawa, M., Chung, Y. J., Bilke, S., Wagner, E. K., et al. (2014). NUP98-PHF23 is a chromatin-modifying oncoprotein that causes a wide array of leukemias sensitive to inhibition of PHD histone reader function. Cancer Discov. 4, 564-577.

Gough, S.M., Slape, C.I., Aplan, P.D. (2011). NUP98 gene fusions and hematopoietic malignancies: common themes and new biologic insights. Blood. 118, 6247-6257.

Griffis, E. R., Altan, N., Lippincott-Schwartz, J., and Powers, M. A. (2002). Nup98 is a mobile nucleoporin with transcription-dependent dynamics. Mol Biol Cell. 13, 1282-1297.

Gurevich RM, A. P., Humphries RK. (2004). NUP98-topoisomerase I acute myeloid leukemia-associated fusion gene has potent leukemogenic activities independent of an engineered catalytic site mutation. Blood. 104, 1127-36.

Hollink, I. H., van den Heuvel-Eibrink, M. M., Arentsen-Peters, S. T., Pratcorona, M., Abbas, S., Kuipers, J. E., van Galen, J. F., Beverloo, H. B., Sonneveld, E., Kaspers, G. J., et al. (2011). NUP98/NSD1 characterizes a novel poor prognostic group in acute myeloid leukemia with a distinct HOX gene expression pattern. Blood. 118, 3645-3656.

Hsieh, J.J., Cheng, E.H., Korsmeyer, S.J. (2003). Taspase1: a threonine aspartase required for cleavage of MLL and proper HOX gene expression. Cell. 115, 293–303.

Huang, Y., Sitwala, K., Bronstein, J., Sanders, D., Dandekar, M., Collins, C., Robertson, G., MacDonald, J., Cezard, T., Bilenky, M., Thiessen, N., Zhao, Y., Zeng, T., Hirst, M,. Hero, A., Jones, S., Hess, J.L. (2012). Identification and characterization of Hoxa9 binding sites in hematopoietic cells. Blood. 119, 388-398.

Iwamoto, M., Asakawa, H., Ohtsuki, C., Osakada, H., Koujin, T., Hiraoka, Y., and Haraguchi, T. (2013).

Monoclonal antibodies recognize gly-leu-phe-gly repeat of nucleoporin nup98 of tetrahymena, yeasts, and humans. Monoclon Antib Immunodiagn Immunother. 32, 81-90.

Hess, JL. (2004). MLL: a histone methyltransferase disrupted in leukemia. Trends Mol Med 10: 500–507.

Jude, C. D., Climer, L., Xu, D., Artinger, E., Fisher, J. K., and Ernst, P. (2007). Unique and independent roles for MLL in adult hematopoietic stem cells and progenitors. Cell Stem Cell. 1, 324-337.

Kalverda, B., Pickersgill, H., Shloma, V. V., and Fornerod, M. (2010). Nucleoporins directly stimulate expression of developmental and cell-cycle genes inside the nucleoplasm. Cell. 140, 360-371.

Krivtsov, A. V., Feng, Z., Lemieux, M. E., Faber, J., Vempati, S., Sinha, A. U., Xia, X., Jesneck, J., Bracken, A. P., Silverman, L. B., et al. (2008). H3K79 methylation profiles define murine and human MLL-AF4 leukemias. Cancer Cell. 14, 355-368.

Kroon, E., Thorsteinsdottir, U., Mayotte, N., Nakamura, T., Sauvageau, G. (2001). NUP98-HOXA9 expression in hemopoietic stem cells induces chronic and acute myeloid leukemias in mice. . EMBO J 20, 350-361.

Kumar, A. R., Li, Q., Hudson, W. A., Chen, W., Sam, T., Yao, Q., Lund, E. A., Wu, B., Kowal, B. J., and Kersey, J. H. (2009). A role for MEIS1 in MLL-fusion gene leukemia. Blood. 113, 1756-1758.

Langmead, B. (2010). Aligning short sequencing reads with Bowtie. Current protocols in bioinformatics / editoral board, Andreas D Baxevanis [et al] Chapter 11, Unit 11 17.

Liu H, W. T., Cashen A, Piwnica-Worms DR, Kunkle L, Vij R, Pham CG, DiPersio J, Cheng EH, Hsieh JJ. (2014). Proteasome inhibitors evoke latent tumor suppression programs in pro-B MLL leukemias through MLL-AF4. Cancer Cell. 25, 530-542.

Martin, ME, Milne, T.A., Bloyer, S., Galoian, K., Shen, W., Gibbs, D., Brock, H.W., Slany, R., Hess, J.L. (2003). Dimerization of MLL fusion proteins immortalizes hematopoietic cells. Cancer Cell. 4, 197-207.

Milne, TA, Briggs, S.D., Brock, H,W,, Martin, M.E., Gibbs, D., Allis, C.D., Hess, J.L. (2002). MLL targets SET domain methyltransferase activity to Hox gene promoters. Mol Cell. 10, 1107–1117.

Milne, T. A., Dou, Y., Martin, M. E., Brock, H. W., Roeder, R. G., and Hess, J. L. (2005). MLL associates specifically with a subset of transcriptionally active target genes. Proc Natl Acad Sci U S A. 102, 14765-14770.

Milne, T. A., Kim, J., Wang, G. G., Stadler, S. C., Basrur, V., Whitcomb, S. J., Wang, Z., Ruthenburg, A. J., Elenitoba-Johnson, K. S., Roeder, R. G., and Allis, C. D. (2010). Multiple interactions recruit MLL1 and MLL1 fusion proteins to the HOXA9 locus in leukemogenesis. Mol Cell. 38, 853-863.

Mishra, B. P., Zaffuto, K. M., Artinger, E. L., Org, T., Mikkola, H. K., Cheng, C., Djabali, M., and Ernst, P. (2014). The histone methyltransferase activity of MLL1 is dispensable for hematopoiesis and leukemogenesis. Cell Rep 7, 1239-1247.

Oka M, M. S., Yamada K, Sangel P, Hirata S, Maehara K, Kawakami K, Tachibana T, Ohkawa Y, Kimura H, Yoneda Y. (2016). Chromatin-prebound Crm1 recruits Nup98-HoxA9 fusion to induce aberrant expression of Hox cluster genes. Elife 5.

Palmqvist, L., Pineault, N., Wasslavik, C., and Humphries, R. K. (2007). Candidate genes for expansion and transformation of hematopoietic stem cells by NUP98-HOX fusion genes. PloS One. 2, e768.

Pascual-Garcia, P., Jeong, J., and Capelson, M. (2014). Nucleoporin Nup98 associates with Trx/MLL

and NSL histone-modifying complexes and regulates Hox gene expression. Cell Rep. 9, 433-442.

Pineault, N., Buske, C., Feuring-Buske, M., Abramovich, C., Rosten, P., Hogge, D. E., Aplan, P. D., and Humphries, R. K. (2003). Induction of acute myeloid leukemia in mice by the human leukemia-specific fusion gene NUP98-HOXD13 in concert with Meis1. Blood. 101, 4529-4538.

Powers MA, Forbes, D.J., Dahlberg, J.E., Lund, E. (1997). The vertebrate GLFG nucleoporin, Nup98, is an essential component of multiple RNA export pathways. J Cell Biol. 136, 241-250.

Prestel, M., Feller, C., Straub, T., Mitlohner, H., and Becker, P. B. (2010). The activation potential of MOF is constrained for dosage compensation. Mol Cell. 38, 815-826.

Radu A., Blobel, G., Moore, M.S. (1995). Identification of a protein complex that is required for nuclear protein import and mediates docking of importsubstrate to distinct nucleoporins. Proc Natl Acad Sci U S A. 92, 1769-1773.

Raja, S. J., Charapitsa, I., Conrad, T., Vaquerizas, J. M., Gebhardt, P., Holz, H., Kadlec, J., Fraterman, S., Luscombe, N. M., and Akhtar, A. (2010). The nonspecific lethal complex is a transcriptional regulator in Drosophila. Mol Cell. 38, 827-841.

Sauvageau, G., Thorsteinsdottir, U., Eaves, C.J., Lawrence, H.J., Largman, C., Lansdorp, P.M., Humphries, R.K. (1995). Overexpression of HOXB4 in hematopoietic cells causes the selective expansion of more primitive populations in vitro and in vivo. Genes Dev. 9, 1753-1765.

Saw J, C. D., Hussey DJ, Dobrovic A, Aplan PD, Slape CI. (2013). The fusion partner specifies the oncogenic potential of NUP98 fusion proteins. Leuk Res. 37, 1668-73.

Shiba, N., Ichikawa, H., Taki, T., Park, M.J., Jo, A., Mitani, S., Kobayashi, T., Shimada, A., Sotomatsu, M., Arakawa, H., Adachi, S., Tawa, A., Horibe, K., Tsuchida, M., Hanada, R.,Tsukimoto, I., Hayashi, Y. (2013). NUP98-NSD1 gene fusion and its related gene expression signature are strongly associated with a poor prognosis in pediatric acute myeloid leukemia. Genes Chromosomes Cancer. 52, 683-693.

Sinha, A. U., and Armstrong, S. A. (2012). iCanPlot: visual exploration of high-throughput omics data using interactive Canvas plotting. PloS One. 7, e31690.

Slape, C., Hartung, H., Lin, Y. W., Bies, J., Wolff, L., and Aplan, P. D. (2007). Retroviral insertional mutagenesis identifies genes that collaborate with NUP98-HOXD13 during leukemic transformation. Cancer Res. 67, 5148-5155.

Takeda, A., Goolsby, C., and Yaseen, N. R. (2006). NUP98-HOXA9 induces long-term proliferation and blocks differentiation of primary human CD34+ hematopoietic cells. Cancer Res. 66, 6628-6637.

Thiel, A. T., Blessington, P., Zou, T., Feather, D., Wu, X., Yan, J., Zhang, H., Liu, Z., Ernst, P., Koretzky, G. A., and Hua, X. (2010). MLL-AF9-induced leukemogenesis requires coexpression of the wild type Mll allele. Cancer Cell 17, 148-159.

Tran, E. J., and Wente, S. R. (2006). Dynamic nuclear pore complexes: life on the edge. Cell. 125, 1041-1053.

Wang, G.G., Cai, L., Pasillas, M.P., Kamps, M.P. (2007). NUP98-NSD1 links H3K36 methylation to Hox-A gene activation and leukaemogenesis. Nat Cell Biol. 9, 804-812.

Wang, G. G., Song, J., Wang, Z., Dormann, H. L., Casadio, F., Li, H., Luo, J. L., Patel, D. J., and Allis, C. D. (2009). Haematopoietic malignancies caused by dysregulation of a chromatin-binding PHD finger. Nature. 459, 847-851.

Xu, S., Powers, M.A. (2013) In vivo analysis of human nucleoporin repeat domain interactions. Mol Biol Cell. 24,1222-31.

Yu, BD, Hess, J.L, Horning, S.E., Brown, G.A., Korsmeyer, S.J. (1995). Altered Hox expression and segmental identity in Mll-mutant mice. Nature. 378, 505–508.

Zhang, Y., Liu, T., Meyer, C. A., Eeckhoute, J., Johnson, D. S., Bernstein, B. E., Nusbaum, C., Myers, R. M., Brown, M., Li, W., and Liu, X. S. (2008). Model-based analysis of ChIP-seq (MACS). Genome Biol. 9, R137.

SUPPLEMENTAL DATA

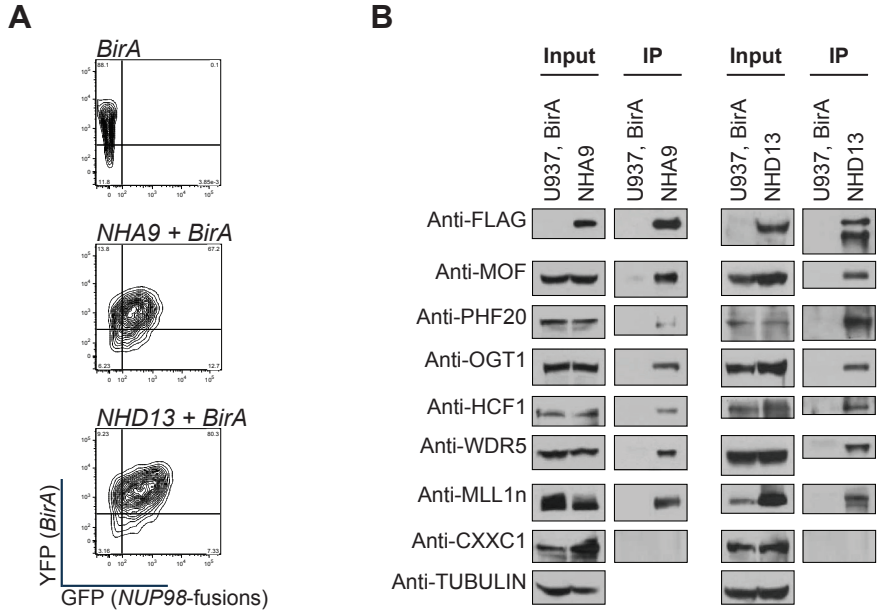

Figure S1, related to Figure 2. NHA9 and NHD13 interact with MLL1 and the NSL histone-modifying complex in U937 cells

(A) U937 cells were retrovirally transduced with an MSCV-IRES-*BirA*-YFP retrovirus, and YFP$^+$ cells were sorted by FACS, 48 hours post-transduction (top plot). These sorted cells were then transduced with Flag-Avi-tagged *NHA9* or *NHD13* in an MSCV-IRES-GFP vector and GFP$^+$YFP$^+$ cells were sorted (middle and lower plot).

(B) Whole cell lysates were prepared from U937 cells with stable expression of the Flag-Avi-tagged NHA9 or NHD13 and BirA biotin ligase and subjected to IP using streptavidin magnetic beads. Cell lysates (Input) and proteins eluted from the streptavidin beads (IP) were separated by SDS–PAGE and analyzed by Western blotting with anti-Flag, anti-MOF, anti-PHF20, anti-OGT1, anti-HCF1, anti-WDR5, anti-MLL1n, anti-CXXC1 and anti-beta Tubulin antibodies.

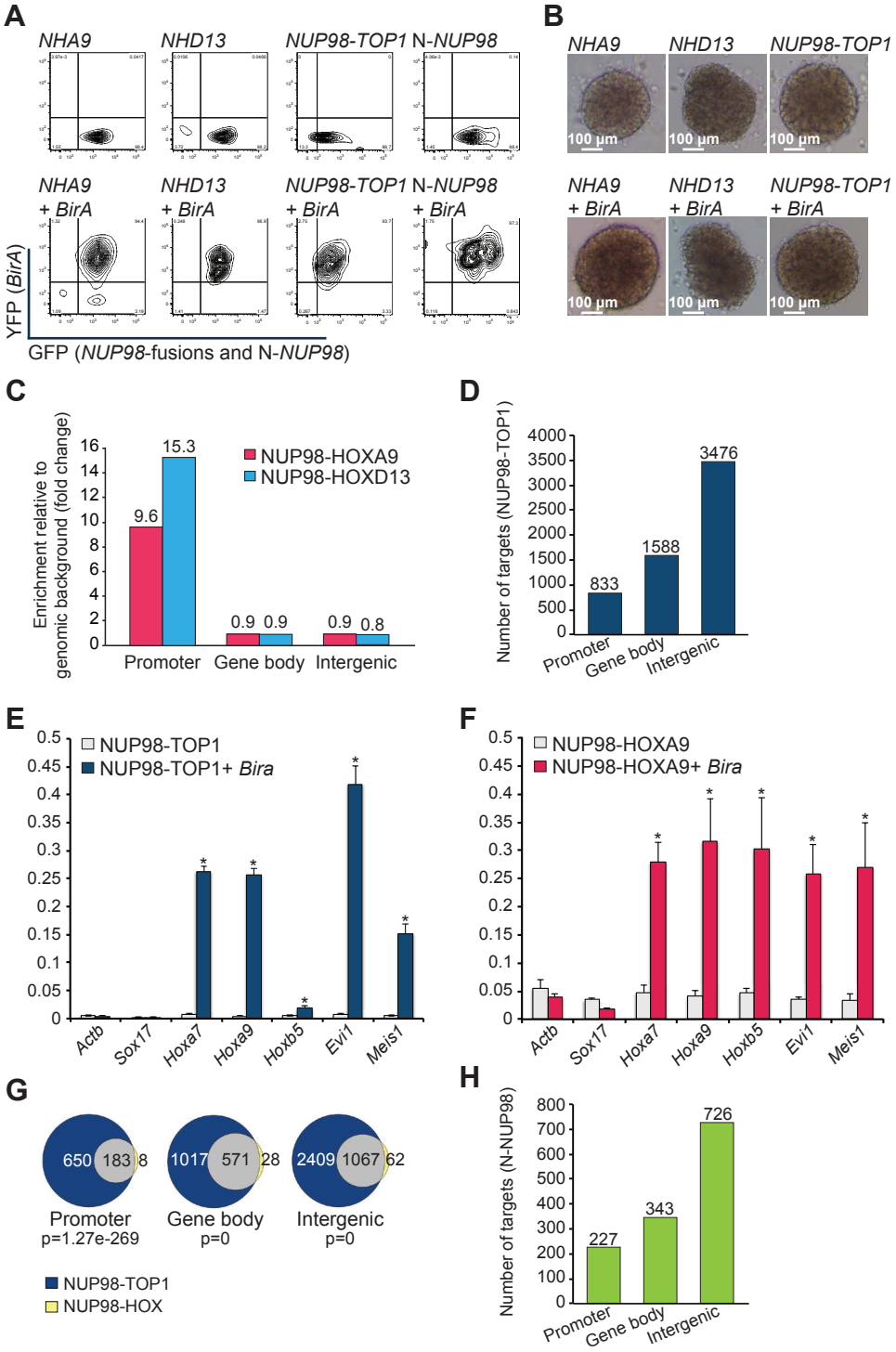
A
NHA9
NHD13
NUP98-TOP1
N-NUP98
NHA9 + BirA
NHD13 + BirA
NUP98-TOP1 + BirA
N-NUP98 + BirA
YFP (BirA)
GFP (NUP98-fusions and N-NUP98)
B
NHA9
NHD13
NUP98-TOP1
NHA9 + BirA
NHD13 + BirA
NUP98-TOP1 + BirA
100 µm
C
Enrichment relative to genomic background (fold change)
NUP98-HOXA9
NUP98-HOXD13
9.6
15.3
0.9 0.9
0.9 0.8
Promoter
Gene body
Intergenic
D
Number of targets (NUP98-TOP1)
833
1588
3476
Promoter
Gene body
Intergenic
E
NUP98-TOP1
NUP98-TOP1+ Bira
Actb
Sox17
Hoxa7
Hoxa9
Hoxb5
Evi1
Meis1
F
NUP98-HOXA9
NUP98-HOXA9+ Bira
Actb
Sox17
Hoxa7
Hoxa9
Hoxb5
Evi1
Meis1
G
650 183 8
1017 571 28
2409 1067 62
Promoter
p=1.27e-269
Gene body
p=0
Intergenic
p=0
NUP98-TOP1
NUP98-HOX
H
Number of targets (N-NUP98)
227
343
726
Promoter
Gene body
Intergenic

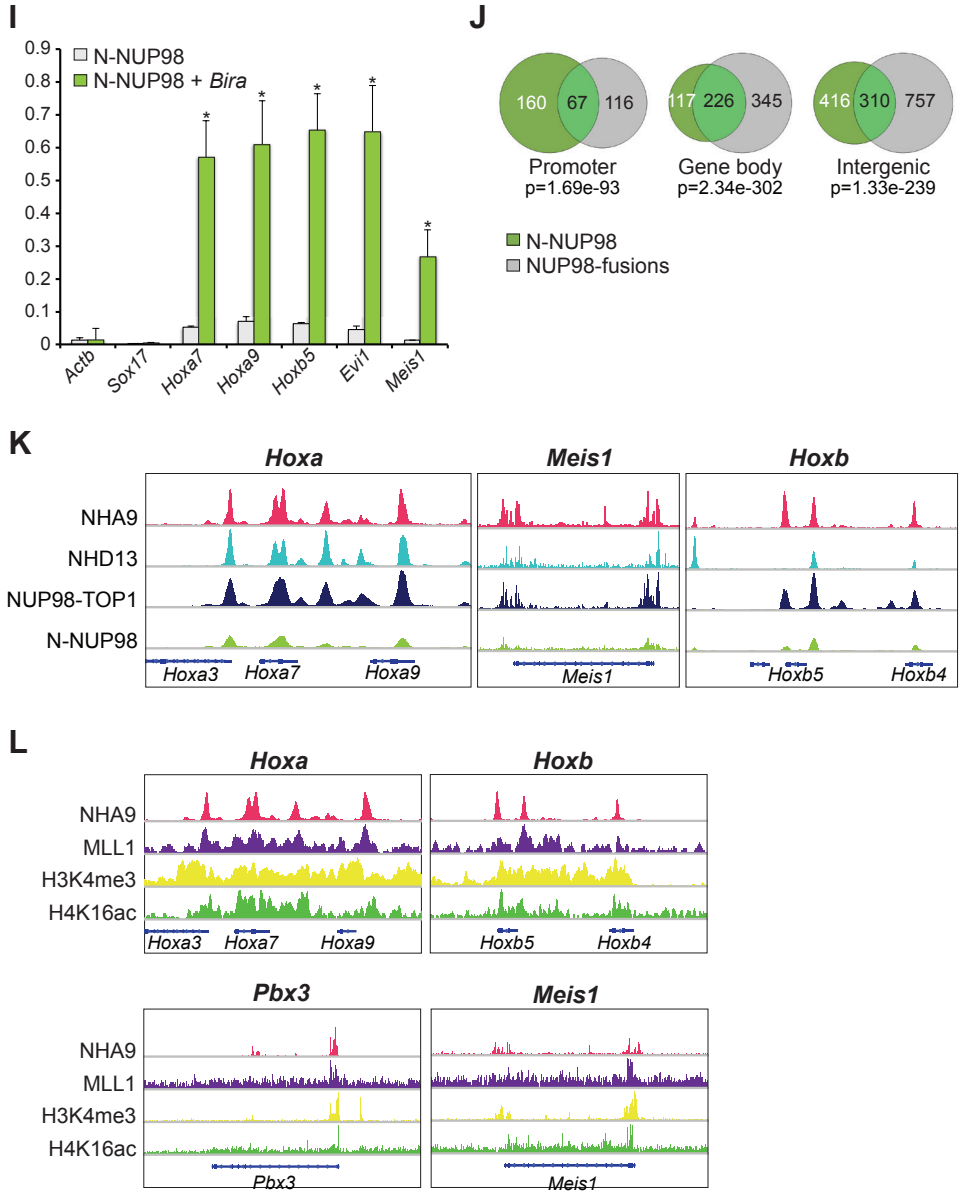

Figure S2, related to Figure 3 and 4. NHA9, NHD13, NUP98-TOP1, N-NUP98 and MLL1 ChIP and ChIP-seq

(A) Purified mouse BM LSKs were retrovirally transduced with Flag-Avi-tagged *NHA9*, *NHD13*, *NUP98-TOP1* or N-*NUP98* in an MSCV-IRES-GFP vector, and GFP⁺ cells were sorted by FACS, 48 hours post transduction. FACS sorting strategy is shown in the top plots. The sorted cells were then transduced with an MSCV-IRES-YFP retrovirus and GFP⁺YFP⁺ cells were sorted (lower two plots).

(B) Representative images of colonies formed at day 7 of CFU assay of *NHA9*, *NHD13* and *NUP98-TOP1* immortalized mouse LSKs with or without *BirA* expression.

(C) The percentage of promoters, gene bodies, and intergenic sites bound by the fusion proteins was compared to the background distribution for all such sites, based on genome annotations compiled from RefSeq for mm9.
(D) Biotin-mediated chromatin affinity purification coupled with high throughput sequencing experiments (ChIP-seq) were performed using *NUP98-TOP1* Flag-Avi-tagged immortalized mouse BM LSKs. Bar graph indicates the number of *NUP98-TOP1*-bound targets at promoter, gene body or intergenic regions.
(E, F, I) ChIP-seq experiments were performed using mouse BM cells by enforced expression of *NHA9*, *NUP98-TOP1* or N-*NUP98* through retroviral transduction of LSKs with vectors carrying Flag-Avi-tagged *NHA9*, *NUP98-TOP1* or N-*NUP98*, and *BirA* ligase. Enrichment of the indicated NUP98 fusion at specific gene loci by RT-qPCR is shown (n=3 independent experiments).
(G) The Venn diagrams illustrate overlap in NUP98-TOP1 targets and common NUP98-HOX fusion targets with a p-value calculated using the hypergeometric test.
(H) ChIP-seq experiment using N-*NUP98* Flag-Avi-tagged immortalized mouse BM LSKs. Bar graph indicates the number of N-NUP98-bound targets at promoter, gene body or intergenic regions.
(J) The Venn diagrams illustrate overlap in N-NUP98 targets and common NUP98 fusion targets with a p-value calculated using the hypergeometric test.
(K) Genome browser tracks representing the shared binding sites of NHA9 , NHD13 , NUP98-TOP1 and N-NUP98 at *Hoxa* loci (left), *Hoxb* loci (middle) and the *Meis1* locus (right).
(L) Genome browser tracks of genomic regions showing colocalization of NHA9, MLL1, H3K4me3 and H4K16ac at four representative MLL1 targets; *Hoxa* genes (left), *Hoxb* genes (middle left), *Pbx3* (middle right) and *Meis1* (right). An anti-N terminus MLL antibody (MO435) was used to perform this ChIP-seq experiment.
* $p < 0.05$. Error bars represent SE of mean.

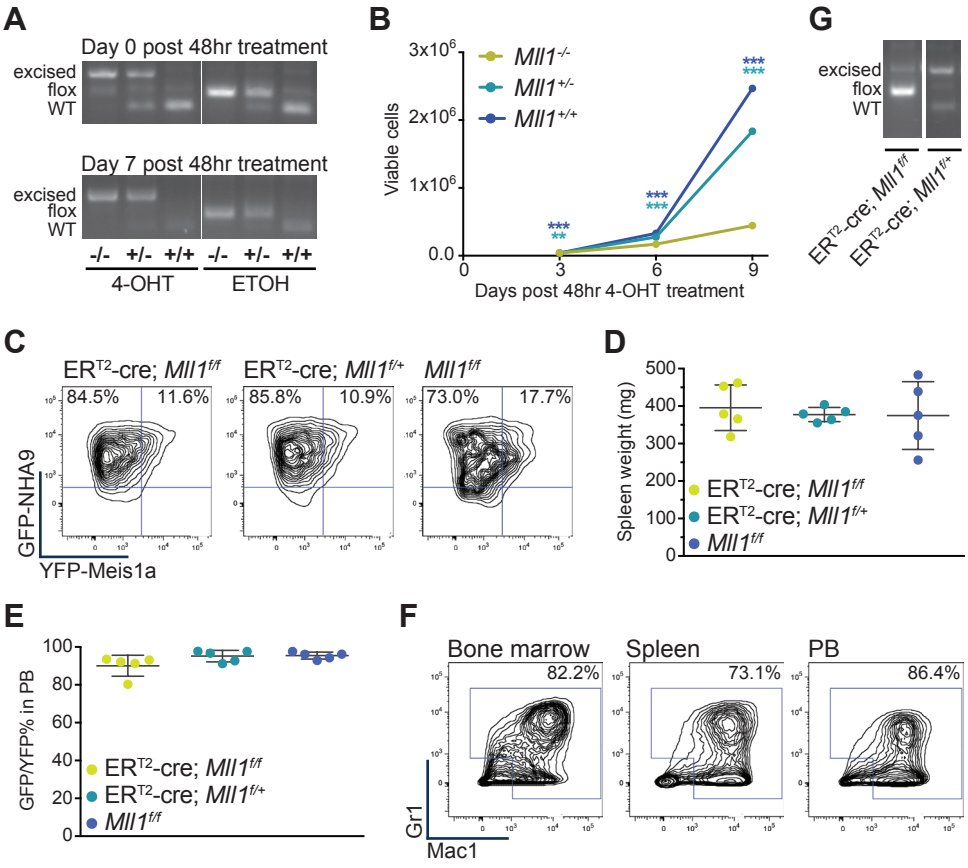

Figure S3, related to Figure 5. *Mll1* loss in a murine *NHA9* driven leukemia model leads to differentiation, decrease in tumor load and prolonged survival

(A) *NHA9 in vitro* transformed *ER^{T2}-cre;Mll1$^{f/f}$*, *ER^{T2}-cre;Mll1$^{f/+}$* or wild type (*Mll1$^{+/+}$*) LSKs were plated in methylcellulose after 48 hours of 4-OHT treatment. PCR analysis illustrates *Mll1* excision throughout the duration of the 7-day colony forming experiment. Representative gel images are shown.

(B) *NHA9 in vitro* transformed *ER^{T2}-cre;Mll1$^{f/f}$*, *ER^{T2}-cre;Mll1$^{f/+}$* or *Mll1$^{+/+}$* LSKs were plated in liquid culture after 48 hours of 4-OHT treatment. Cells were replated and harvested every 3 days. The graph illustrates total number of viable cells over time, extrapolated from the number of cells plated and the number of cells in culture at replating. Cell growth between day 0 and day 3 has been excluded from the calculation, since unspecific death due to *Cre* expression and 4-OHT treatment skews the data. Asterisks represent the p-value of a t-test comparing *Mll1$^{-/-}$* to either *Mll1$^{+/+}$* (dark blue) or *Mll1$^{+/-}$* (turquoise). Data are representative of three individual experiments.

(C) Flow cytometry plots illustrate the sort strategy for *ER^{T2}-cre;Mll1$^{f/f}$*, *ER^{T2}-cre;Mll1$^{f/+}$* or *Mll1$^{f/f}$* LSKs retrovirally transduced with GFP-*NUP98-HOXA9* and YFP-*Meis1a*. Double positive (GFP^{+}YFP^{+}) cells were sorted and used for *in vivo* experiments.

(D) The spleen weight of AML mice at time of death. A dot represents a single mouse.

(E) The percentage of GFP^{+}YFP^{+} cells in PB of primary mice transplanted with *ER^{T2}-cre;Mll1$^{f/f}$*, *ER^{T2}-cre;Mll1$^{f/+}$* or *Mll1$^{f/f}$ NHA9-Meis1a* cells at time of death. A dot represents a single mouse.

(F) Representative flow cytometry plots illustrate the expression of myeloid markers (Mac-1 and Gr-1) on GFP^{+}YFP^{+} mouse BM, spleen and PB cells at time mice succumbed to AML.

(G) PCR analysis illustrates *Mll1* excision in murine BM at time of death. Representative images shown.

** $p < 0.01$, *** $p < 0.001$. Error bars represent SD of mean.

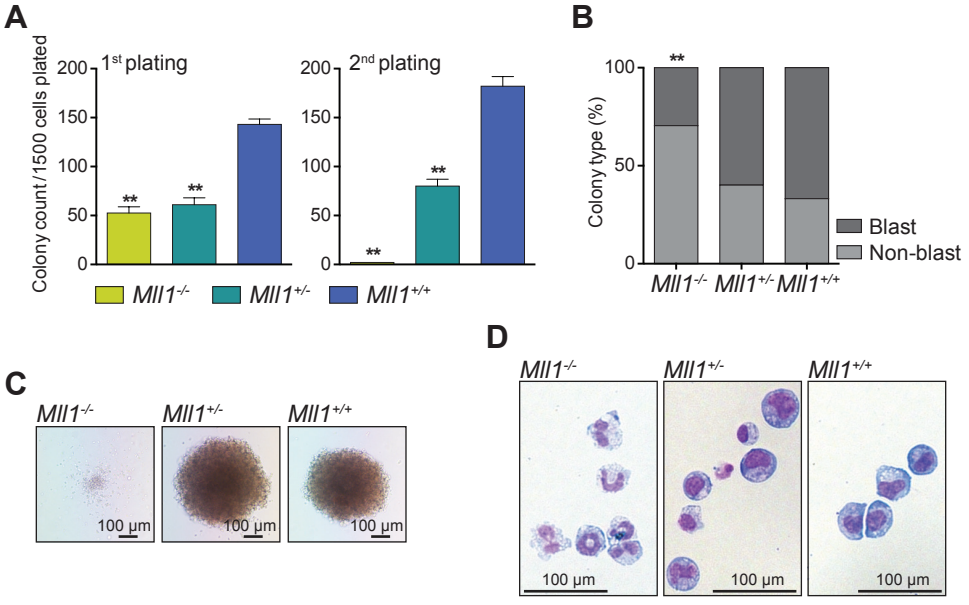

NUP98-HOXD13

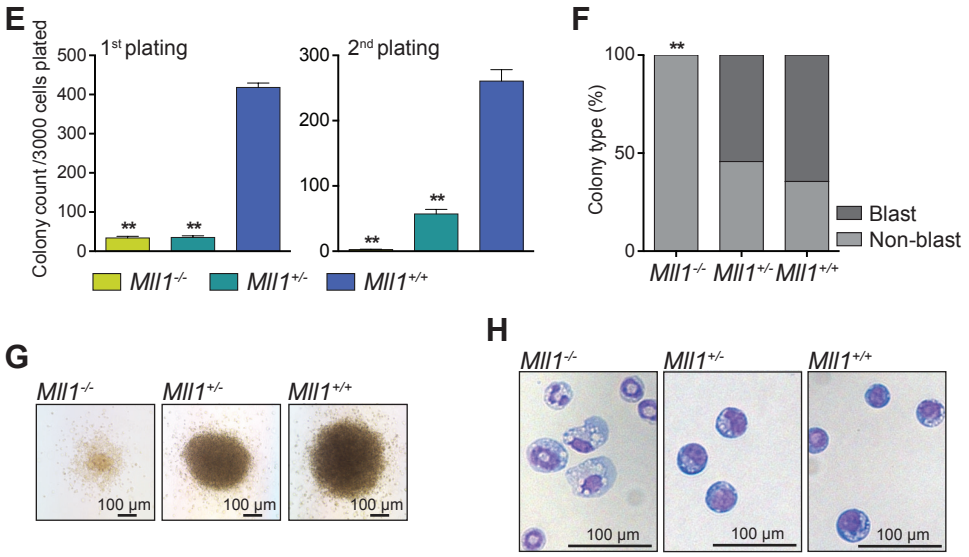

NUP98-JARID1A

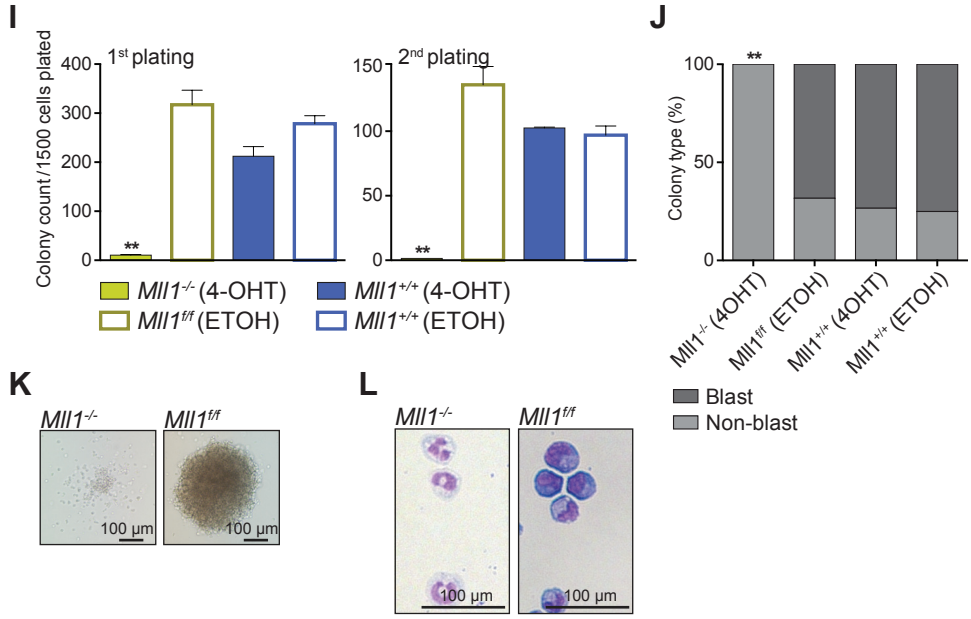

NUP98-TOP1

Figure S4, related to Figure 5. *Mll1* loss leads to differentiation, impaired colony formation and downregulation of target genes in various *NUP98*-fusion driven leukemia models

(A) Day 7 of the 1st plating (left) and 2nd plating (right) of a CFU assay of *NHD13 in vitro* transformed *ER^{T2}-cre;Mll1$^{f/f}$, ER^{T2}-cre;Mll1$^{f/+}$* or wild type (*Mll1$^{+/+}$*) LSKs, plated after 48 hours of tamoxifen (4-OHT) treatment. Bar graphs display mean number of colonies per 35mm dish. 1500 cells were plated per dish. Data are representative of two individual experiments.

(B) Shown is the mean percentage of blast versus non-blast colonies relative to all colonies counted per dish, per sample, after the 1st plating.

(C) Representative images of colonies formed at day 7 of the 1st plating.

(D) Representative images of Wright-Giemsa–stained cytospin preparations of cells harvested at day 7 of the 1st plating.

(E) Day 7 of the 1st plating (left) and 2nd plating (right) of a CFU assay of *NUP98-JARID1A in vitro* transformed *ER^{T2}-cre;Mll1$^{f/f}$, ER^{T2}-cre;Mll1$^{f/+}$* or *Mll1$^{+/+}$* LSKs, plated after 48 hours of 4-OHT treatment. Bar graphs display mean number of colonies per 35mm dish. 3000 cells were plated per dish. Data are representative of two individual experiments.

(F) Shown is the mean percentage of blast versus non-blast colonies relative to all colonies counted per dish, per sample, after the 1st plating.

(G) Representative images of colonies formed at day 7 of the 1st plating.

(H) Representative images of Wright-Giemsa–stained cytospin preparations of cells harvested at day 7 of the 1st plating.

(I) Day 7 of the 1st plating (left) and 2nd plating (right) of a CFU assay of *NUP98-TOP1 in vitro* transformed *ER^{T2}-cre;Mll1$^{f/f}$ or Mll1$^{+/+}$* LSKs, plated after 48 hours of 4-OHT or vehicle control (ETOH) treatment. Bar graphs display mean number of colonies per 35mm dish. 1500 cells were plated per dish. Data are representative of two individual experiments.

(J) Shown is the mean percentage of blast versus non-blast colonies relative to all colonies counted per dish, per sample, after the 1st plating.

(K) Representative images of colonies formed at day 7 of the 1st plating.

(L) Representative images of Wright-Giemsa–stained cytospin preparations of cells harvested at day 7 of the 1st plating.

** $p < 0.01$. Error bars represent SD of mean.

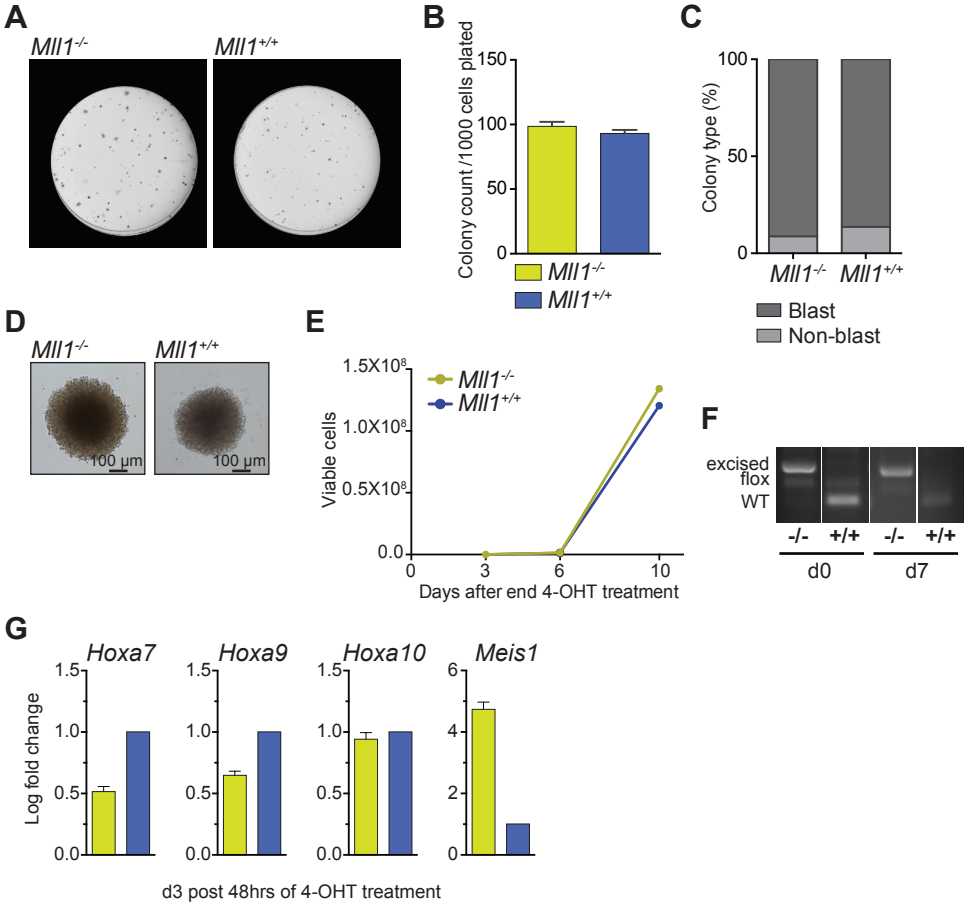

MLL-AF9

Figure S5, related to Figure 5. Deletion of *Mll1* in *MLL-AF9* or *Hoxa9/Meis1* transformed LSKs does not affect proliferation, colony forming potential or *in vivo* leukemogenesis

(A) Day 7 of CFU assay of *MLL-AF9 in vitro* transformed ER^{T2}*-cre;Mll1*$^{f/f}$ or wild type (*Mll1*$^{+/+}$) LSKs plated after 48 hours of tamoxifen (4-OHT) treatment. Representative petri dishes are shown.

(B) Bar graph indicates mean number of colonies per 35mm dish after 7 days. 1000 cells were plated per dish. Data are representative of two individual experiments.

(C) Shown is the mean percentage of blast versus non-blast colonies relative to all colonies counted per dish, per cell type.

(D) Colonies at day 7 of CFU assay. Representative images are shown.

(E) *MLL-AF9 in vitro* transformed ER^{T2}*-cre;Mll1*$^{f/f}$ or *Mll1*$^{+/+}$ LSKs were plated in liquid culture after 48 hours of 4-OHT treatment. Cells were replated and harvested every 3 to 4 days. The graph illustrates total number of viable cells over time, extrapolated from the number of cells plated and the number of cells in culture at replating. Cell growth between day 0 and 3 has been excluded from the calculation, since unspecific death due to 4-OHT treatment skews the data. Data are representative of two individual experiments.

(F) PCR analysis illustrates *Mll1* excision throughout the duration of a 7-day colony forming experiment. Representative gel images are shown.

(G) Bar graphs illustrate relative expression levels (RT-qPCR) as mean log fold change compared to 4-OHT treated *Mll1*$^{+/+}$ cells.

Error bars represent SD of mean.

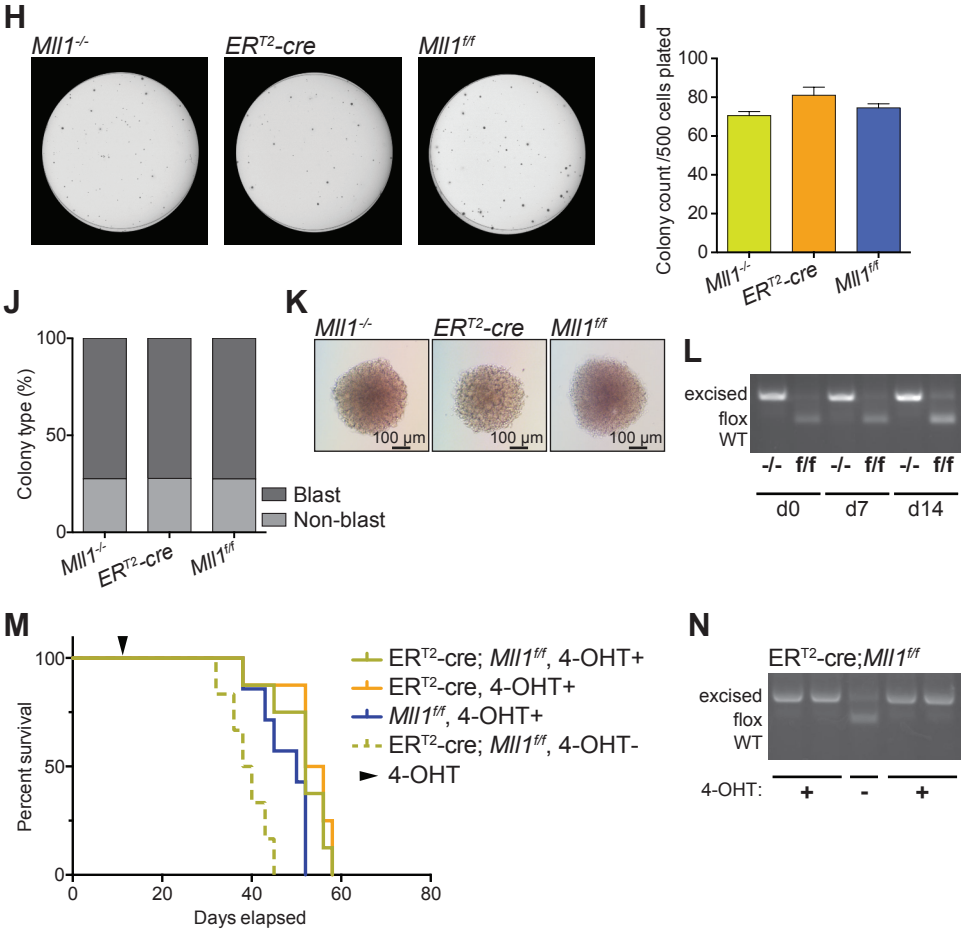

HOXA9/MEIS1

Figure S5, continued

(H) Day 7 of CFU assay of *Hoxa9/Meis1 in vitro* transformed *ER^{T2}-cre;Mll1$^{f/f}$*, *ER^{T2}-cre* or *Mll1$^{f/f}$* LSKs plated after 48 hours of 4-OHT treatment. Representative petri dishes are shown.

(I) Bar graph indicates mean number of colonies per 35mm dish after 7 days. 500 cells were plated per dish. Data are representative of two individual experiments.

(J) Shown is the mean percentage of blast versus non-blast colonies relative to all colonies counted per dish, per cell type.

(K) Colonies at day 7 of CFU assay. Representative images are shown.

(L) PCR analysis illustrates *Mll1* excision throughout the duration of the colony forming experiment. Representative gel images are shown.

(M) *ER^{T2}-cre;Mll1$^{f/f}$*, *ER^{T2}-cre* or *Mll1$^{f/f}$* LSKs were retrovirally transduced with Hygro-*Hoxa9/Meis1*, selected and injected into lethally irradiated C57Bl/6 mice (n=6 per group). Mice were treated with 4-OHT at day 11 post transplant to excise *Mll1*. The survival curve is shown. Data are representative of two individual experiments.

(N) PCR analysis illustrates *Mll1* excision in murine BM at time of death. Representative gel images are shown.

Error bars represent SD of mean.

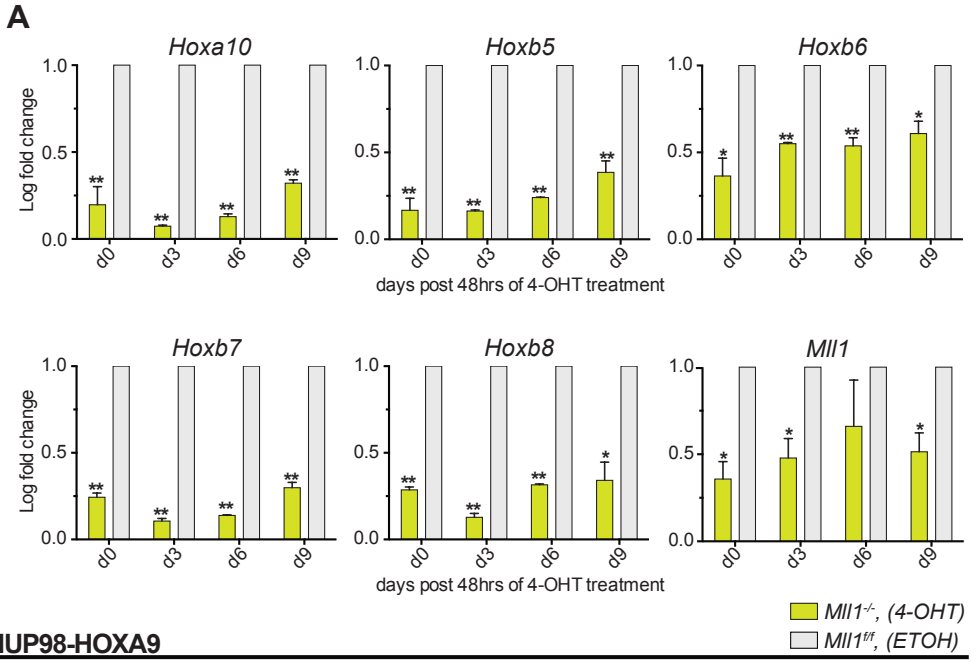

NUP98-HOXA9

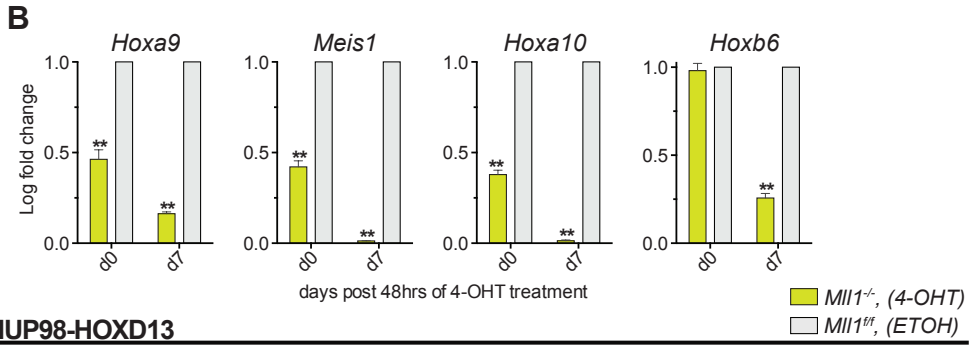

NUP98-HOXD13

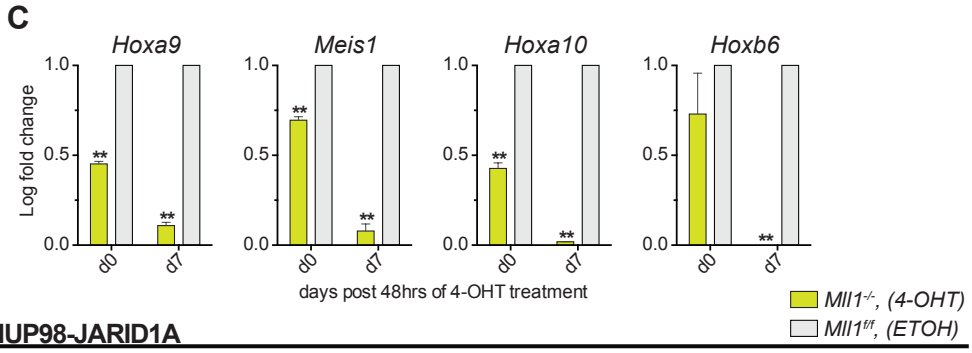

NUP98-JARID1A

Figure S6, related to Figure 6. *Mll1* regulates *Hoxa* and *Hoxb* expression in *NHA9* transformed murine LSKs

(A) *NHA9 in vitro* transformed *ER^{T2}-cre;Mll1$^{f/f}$* LSKs were plated in liquid culture following 48 hours of tamoxifen (4-OHT) or vehicle (ETOH) treatment. Cells were replated and harvested every 3 days. Bar graphs illustrate relative expression levels (RT-qPCR) as mean log fold change compared to vehicle control treated cells. The x-axis indicates cells harvested at various time-points post treatment. Data are representative of three individual experiments.

(B) *NHD13 in vitro* transformed *ER^{T2}-cre;Mll1$^{f/f}$* LSKs were plated in methylcellulose following 48 hours of 4-OHT or vehicle treatment. Cells were replated and harvested after 7 days. Bar graphs illustrate relative expression levels (RT-qPCR) as mean log fold change compared to vehicle control treated cells. The x-axis indicates cells harvested at various time-points post treatment.

(C) Bar graphs illustrate relative expression levels as mean log fold change compared to vehicle control treated *NUP98-JARID1A* transformed cells.

* $p < 0.05$, ** $p < 0.01$. Error bars represent SD of mean.

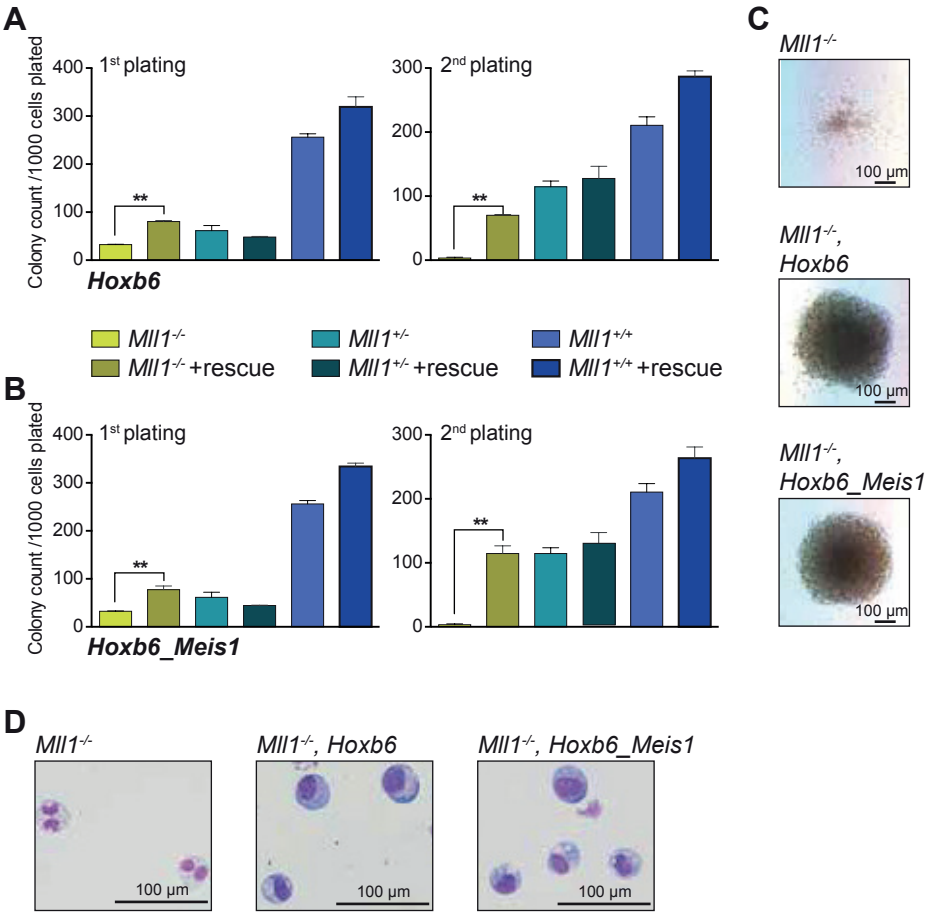

Figure S7, related to Figure 7. *Hoxb6* overexpression rescues *NHA9* transformed cells from *Mll1* dependence

(A) Day 7 of the 1st plating (left) and 2nd plating (right) of a CFU assay with *NHA9 in vitro* transformed *ER^{T2}-cre;Mll1$^{f/f}$*, *ER^{T2}-cre;Mll1$^{f/+}$* or wild type (*Mll1$^{+/+}$*) LSKs, plated after 48 hours of tamoxifen (4-OHT) treatment. Samples stating "+rescue" were transduced with *Hoxb6* and sorted prior to excision. Bar graphs display mean number of colonies per 35mm dish. 1000 cells were plated per dish. Data are representative of two individual experiments.

(B) Samples stating "+rescue" were transduced with *Hoxb6* and *Meis1* and sorted prior to excision. Bar graphs display mean number of colonies per 35mm dish at day 7 of the 1st plating (left) and 2nd plating (right) of a CFU assay. 1000 cells were plated per dish. Data are representative of two individual experiments.

(C) Representative images of colonies formed at day 7 of the 1st plating.

(D) Representative images of Wright-Giemsa–stained cytospin preparations of cells harvested at day 7 of the 1st plating.

** $p < 0.01$. Error bars represent SD of mean.

SUPPLEMENTAL EXPERIMENTAL PROCEDURES

Indirect immunofluorescence

293T cells were seeded in 12-well plates and subsequently transfected with the HA-tagged *NUP98*, *NUP98-HOXA9*, and *N-NUP98* MSCV-IRES-GFP vectors. After 24 hours, cells were washed with PBS, fixed with 4% paraformaldehyde, and permeabilized with PBS–0.2% Triton X-100 for 5 minutes at room temperature. Fixed cells were blocked with 2% bovine serum albumin (Sigma, St. Louis, MO) in PBS at room temperature for 1 hour, then incubated with either anti-HA antibody (HA.11, Covance, Dedham, MA) and anti-NUP214 antibody (Abcam, Cambridge, MA) or anti-Flag M2 antibody (F1804, Sigma, St. Louis, MO) and anti-NUP214 antibody (Abcam, Cambridge, MA) overnight at 4°C, followed by a 50-minute incubation with Alexa Fluor 568-conjugated donkey anti-mouse secondary antibody and Alexa Fluor 488-conjugated goat anti-rabbit secondary antibody. Coverslips were then mounted with ProLong Diamond Antifade Mountant with DAPI mounting medium (P36962, Thermo Fisher Scientific, Waltham, MA), and images were captured using a laser confocal microscope (Leica TCS SP5-II, Leica Microsystems CMS GmbH, Mannheim, Germany).

Co-immunoprecipitation (Co-IP) and Western blotting

To generate cell lines with stable expression of BirA and NUP98 fusions, 293T or U937 cells were infected with *BirA* IRES-YFP virus, and sorted for YFP positive cells 48 hours after infection. YFP positive 293T or U937 cells were then transfected with C-terminal Flag-Avi-tagged *NUP98-HOXA9*, *NUP98-HOXD13,* or *N-NUP98* MSCV-puro vectors and selected in liquid culture with puromycin (Sigma, St. Louis, MO) 2.5 ug/mL for 7 days. Single YFP^+ cells were sorted into 96 well plates (one YFP^+ cell/well), and maintained in culture with 2.5 ug/mL puromycin for 2 weeks. The cells with high expression of the NUP98 fusions, as identified by Western, were used for IP experiments.

293T cells with stable expression of NUP98 fusions or 293T cells 48 hours post transient transfection with *NUP98* and *NUP98* fusion vectors were lysed in 1X cell lysis buffer (20 mM Tris-HCl (pH 7.5), 150 mM NaCl, 1 mM Na_2EDTA, 1 mM EGTA, 1% Triton, 2.5 mM sodium pyrophosphate, 1 mM β-glycerophosphate, 1 mM Na_3VO_4, 1 µg/ml leupeptin) (#9803, Cell Signaling, Danvers, MA). Dynabeads M-280 Streptavidin (11205D, Thermo Fisher Scientific, Waltham, MA) or anti-Flag M2 Affinity Gel (A2220, Sigma-Aldrich, St. Louis, MO) were added into the lysates and samples were incubated overnight at 4°C. Next, protein complexes were washed 5 times with 1 mL lysis buffer. After the final wash, 2X SDS sample was added, and the beads were heated to 100°C for 5 minutes and analyzed by SDS-PAGE.

Western blotting was done following standard procedures using a 4-12% Bis-Tris Gel (Nupage, Invitrogen, Carlsbad, CA, USA) and transferred onto PVDF membranes. For assessment of HA-tagged or Flag-tagged proteins by Western blot, the anti-HA antibody (HA.11, Covance, Dedham, MA) or anti-Flag M2 antibody (F1804, Sigma, St. Louis, MO) was used. For detecting NSL/MLL1 complex components the following antibodies were used: anti-PHF20 (ab157192), anti-HCF1 (ab137618), anti-WDR5 (ab178410), anti-beta

Tubulin (TUBB) (ab6046) and anti-CXXC1 (ab56035) from Abcam (Cambridge, MA); anti-MOF (A300-993A) and anti-MLL1n (A300-086A) from Bethyl Labs (Montgomery, TX); anti-OGT1(MBS274885) from MyBioSource (San Diego, CA); and anti-EZH2 antibody (07-689) from EMD Millipore (Billerica, MA). The sheep anti-mouse IgG (NA931V) or the anti-rabbit IgG (NA934V) ECL horseradish peroxidase linked whole antibody from GE healthcare (Little Chalfont Buckinghamshire, UK) was used as the secondary antibody.

***In vitro* experiments with murine *NUP98* fusion, *MLL-AF9* or *Hoxa9/Meis1* cells**

For studying the impact of *Mll1* deletion on LSKs transformed by *NUP98* fusions, *Hoxa9/Meis1* or *MLL-AF9*, LSKs were retrovirally transduced with MSCV-*NUP98-HOXA9*-IRES-GFP, MSCV-*NUP98-HOXD13*-IRES-GFP, MSCV-*NUP98-TOP1*-IRES-GFP, MSCV-*NUP98-JARID1A*-IRES-puro, MSCV-*Hoxa9-Meis1*-IRES-hygro or MSCV-*MLL-AF9*-IRES-GFP, sorted for GFP or selected with hygromycin (Calbiochem, San Diego, CA) or puromycin (Sigma, St. Louis, MO), and grown out for several weeks to obtain highly proliferative transformed cultures. Subsequently, cells were treated with 300nM tamoxifen (4-OHT, Sigma-Aldrich, Carlsbad, CA) for 48 hours and then either plated in methylcellulose for colony-forming assays or in supplemented IMDM for liquid culture. Colonies were scored every 7 days using the Eclipse TS100 inverted microscope (Nikon, Tokyo, Japan). Since almost all colonies were either compact and hypercellular (blast-like) or small and diffuse (consistent with differentiation), colonies were classified into these two categories. Cells from pooled colony aggregates were then assessed for *Mll1* excision, used for cytospins, and replated to test replating capacity. For liquid proliferation assays, cells were plated in triplicate in a 96-well flat bottom non-treated cell culture plate (Falcon, Corning Life Sciences, Corning, NY). Cells were counted every 3 or 4 days on a FACS CANTOII (BD) with DAPI viability stain (Thermo Fisher Scientific, Waltham, MA). Cells were then harvested for gene expression assays and replated up and till 15 days after 4-OHT treatments.

For the *Hoxa9, Hoxb6* and *Meis1* rescue experiments, *NUP98-HOXA9 in vitro* transformed cells were infected with retrovirus containing MSCV-*Hoxa9-Meis1*-IRES-hygromycin, MSCV-*Hoxa9*-IRES-miCD2, MSCV-*Hoxb6*-IRES-miCD2 and/or MSCV-*Meis1*-IRES-YFP. Cells were selected in liquid culture with hygromycin (Calbiochem, San Diego, CA) 50ug/mL for 10 days or sorted for hCD2 positivity. Effects of *Mll1* excision were assessed as described above.

***In vivo* experiments**

For primary NHA9 AML experiments, *Mll1*$^{f/f}$ *ER*^{T2}*-cre*, *Mll1*$^{f/+}$ *ER*^{T2}*-cre*, *ER*^{T2}*-cre* and *Mll1*$^{f/f}$ mouse LSKs were harvested and infected with MSCV-*NUP98-HOXA9*-IRES-GFP. After 2 weeks of cell culture, cells were infected with MSCV-*Meis1a*-IRES-YFP and sorted for GFP/YFP double positive cells after 4 days. In case of the *Hoxa9/Meis1 in vivo* rescue experiment, cells were also infected with MSCV-*Hoxa9*-IRES-miCD2 and sorted. Cells were cultured for a total of 3-4 weeks before injection of 1,250,000-2,300,000 GFP^{+}YFP^{+} cells with 200,000 helper cells into lethally irradiated (2 x 500 cGy), 6-8 week old C57BL/6 female recipients. Mice

were euthanized at time of clinical symptoms of disease, coincided by leukocytosis. At time of death, bone marrow, spleen and peripheral blood were assessed for GFP and various immunophenotypic markers by flow cytometry on a FACS CANTOII (BD, San Jose, CA). Cell surface marks used were: CD117 APC/Cy7 (cKIT), Ly-6G PE (GR1), CD3e pacific blue (all Biolegend, San Diego, CA), CD45R PE/Cy7 (B220), Ly6A/E PE/Cy7 (SCA1), CD11b APC (MAC1) (all eBioscience, San Diego, CA). For primary *Mll1* excision experiments, mice were treated by oral gavage with 1 dose of 8mg 4-OHT (Toronto Research Chemicals, Toronto, Canada) dissolved in corn oil (Sigma-Aldrich, Carlsbad, CA).

For secondary transplant experiments, viable frozen bone marrow cells from primary leukemic, untreated mice were thawed and 10,000 cells injected into sub-lethally irradiated (1 x 500 cGy) 7-week-old C57BL/6 female recipients. Mice were treated by oral gavage with 1 dose of 8mg 4-OHT dissolved in corn oil, 7 days post transplant.

For primary *Hoxa9/Meis1* AML experiments, *Mll1$^{f/f}$ ER^{T2}-cre*, *ER^{T2}-cre* and *Mll1$^{f/f}$* mouse Lin^{-}/cKIT^{+} BM cells were harvested, infected with MSCV-*Hoxa9-Meis1*-IRES-hygro and selected with hygromycine as described. After 2 weeks of culture, 2,000,000 cells were injected into sub-lethally irradiated (1 x 600 cGy), 7-week-old C57BL/6 female recipients. Mice were treated by oral gavage with 1 dose of 8mg 4-OHT dissolved in corn oil, 15 days post transplant.

Cytospins and microscopic imaging

Cytospins were generated by spinning 50,000-100,000 cells onto glass slides (500 rpm for 10 minutes) using the Shandon Cytospin 4 cytofuge (Thermo Fisher Scientific, Waltham, MA). Colony-forming assay dishes were imaged with the Gelcount (Oxford Optronix, Oxfordshire, UK). Pictures of individual colonies were taken using the Nikon Eclipse TE2000-E and pictures of Wright-Giemsa stained cytospin preparations were made using the Nikon Eclipse E800 microscope (both Nikon, Tokyo, Japan).

RNA extraction, real-time PCR and RNA sequencing

Trizol (Invitrogen, Carlsbad, CA) was used to extract RNA from viable cells. After this step, inventoried taqman gene expression assays (Invitrogen, Carlsbad, CA) were used for real-time quantitative PCR. Assays used were: *Meis1* (Mm00487664_m1), *Hoxb5* (Mm00439368_m1), *Hoxb6* (Mm00433970_m1), *Hoxb7* (Mm00650702_m1), *Hoxb8* (Mm00439368_m1) and *Hoxa10* (Mm00433966_m1). For *Hoxa9*, SYBR Green primers were designed in the 5'-end of the gene to avoid picking up *HOXA9* expression from the *NUP98-HOXA9* fusion. Primers were 5'-TGGCATTAAACCTGAACCGC-3' and 5'-GGACAAAGTGTGAGTGTCAAGC-3'. For *Mll1*, a custom-made taqman assay was used as described by Jude et al. (Jude et al., 2007). PCR master mixes were used (SYBR Green and Taqman, both Applied Biosystems, Grand Island, NY) and real-time PCR was performed on the ViiA 6 Real-Time PCR System (Applied Biosystems, Grand Island, NY). Further assay details can be provided on request.

RNA for RNA sequencing was QCed on the Agilent Bioanalyzer 2100 platform (Agilent, Santa Clara, CA) and Poly-A tail selection was performed. Sequencing was done using the

Illumina Next-Gen Sequencing HiSeq platform (Illumina, San Diego, CA) with 30-45 million 50bp, paired-end reads.

Chromatin immunoprecipitation (ChIP-qPCR and ChIP-seq)

For ChIP of NUP98-HOXA9, NUP98-HOXD13, NUP98-TOP1 and N-NUP98, C-terminal Flag-Avi-tagged *NUP98-HOXA9, NUP98-HOXD13, NUP98-TOP1* or *N-NUP98* were cloned into the MSCV-IRES-GFP retroviral vector. Ecotropic retrovirus was produced as described above. Retroviruses containing *BirA* were produced similarly using an MSCV-based vector with an YFP selection cassette. WT BM LSKs were isolated and co-transduced with both retroviruses as described above. After transduction for 2 to 4 days, GFP^+YFP^+ cells were sorted and maintained in liquid culture.

ChIP was performed similarly as described (Krivtsov et al., 2008). Briefly, cells were fixed in PBS 1% formalin (v/v) with gentle rotation for 10 minutes at room temperature. Fixation was stopped by the addition of glycine (125 mM final concentration). Fixed cells were washed twice in ice-cold PBS, resuspended in SDS lysis buffer (1% SDS, 10mM EDTA, 50 mM Tris-HCl, pH 8.1). Chromatin was sheared by sonication to about 100-500bp fragments using bioruptor (diagenode, Denville, NJ) and diluted ten fold with dilution buffer (0.01% SDS, 1.1% Triton-X100, 1.2 mM EDTA, 16.7 mM Tris-HCl, pH 8.1,167 mM NaCl). Antibodies against specific histone modifications, MLL1n (A300-086A, Bethyl Labs, Montgomery, TX) or Dynabeads M-280 Streptavidin (11205D, Thermo Fisher Scientific, Waltham, MA) were used to precipitate DNA fragments associated with modified histones, MLL1 or biotinylated NUP98 fusions (NUP98-HOXA9 or NUP98-HOXD13) respectively. Precipitates were washed sequentially with ice cold low salt wash (0.1% SDS, 1% Triton-X-100, 2mM EDTA, 20mM Tris-HCl, pH8.1, 150mM NaCl), high salt wash (0.1% SDS, 1% Triton-X-100, 2mM EDTA, 20mM Tris-HCl, pH 8.1, 500mM NaCl), LiCl wash (0.25M LiCl, 1% IGEPAL CA-630, 1% deoxycholic acid, 1mM EDTA, 10mM Tris-HCl, pH 8.1) and TE wash (1mM EDTA, 10mM Tris-HCl, pH 8.1) and eluted in elution buffer (1% SDS, 0.1 M NaHCO3). For biotinylated NHA9, NHD13, NUP98-TOP1 and N-NUP98 ChIP, a 2% SDS wash was conducted in addition to the washes described above and all washes were carried out at room temperature. All buffers except for the elution buffer were supplemented with protease inhibitor (Complete mini protease inhibitor cocktail tablets, Roche, Indianapolis, IN). Eluted DNA fragments were analyzed by quantitative PCR using promoter specific primers as listed. The anti-N terminus MLL antibody (MO435) , generated by a synthetic peptide of MLL amino acids 752–949 as immunogen in Dr. James J. Hsieh lab as described previously (Liu et al., 2014), was used to perform an additional ChIP-seq experiment.

ChIP for H3K4me3 (ab8580, Abcam, Cambridge, MA) and H4K16ac (39167, Active Motif, Carlsbad, CA) in murine *NUP98-HOXA9* transformed cells was performed as described above. For ChIP sequencing, ChIP DNA libraries were made following Illumina ChIP-seq library preparation kit and subjected to Solexa sequencing.

Primers for ChIP-RT-q-PCR

Hoxa7 FW	5'-CTCTTCTGTTTCCCATCCTGGT-3'
Hoxa7 RV	5'-GGCAATATCCGGGATCCACT-3'
Hoxa9 FW	5'-GGAATAGGAGGAAAAAACAGAAGAGG-3'
Hoxa9 RV	5'-TGTATGAACCGCTCTGGTATCCTT-3'
Hoxa10 FW	5'-CCTTTTTGGTCGACTCGCTC-3'
Hoxa10 RV	5'-CAACACCAGCCTCGCCTCT-3'
Meis1 FW	5'-TCACCACGTTGACAACCTCG-3'
Meis1 RV	5'-GCTTTCTGCCACTCCAGCTG-3'
Hoxb5 FW	5'- CTCATTCCACCTGCAAACCT-3'
Hoxb5 RV	5'- CTTTCCACCAAGACCCAGAA-3'
Evi1 FW	5'-CTCACACCCCTGAAAGCAAT-3'
Evi1 RV	5'-CTGAGCACAAGGGTGTGTGT-3'
Sox17 FW	5'-GAGAGGTTGCACCAGAGAGG-3'
Sox17 RV	5'-GCGGCCGGTACTTGTAGTT-3'
Actin FW	5'-GGGAACCAGACGCTACGATC-3'
Actin RV	5'-TTGGACAAAGACCCAGAGGC-3'

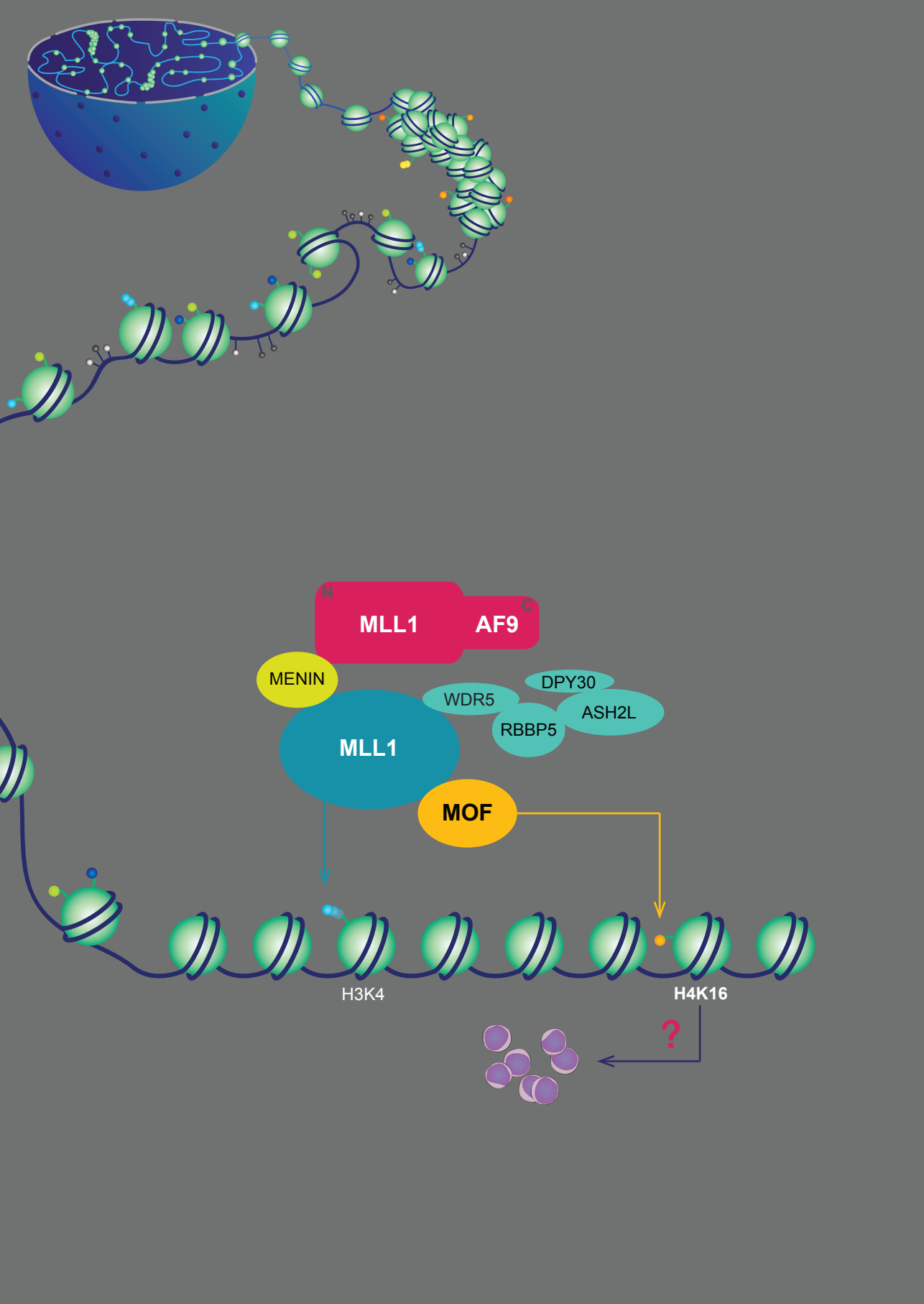
N
MLL1
AF9
C
MENIN
WDR5
DPY30
ASH2L
RBBP5
MLL1
MOF
H3K4
H4K16
?

4

HISTONE ACETYLTRANSFERASE ACTIVITY OF MOF IS REQUIRED FOR *MLL-AF9* LEUKEMOGENESIS

Daria G. Valerio, Haiming Xu, Chun-Wei Chen, Takayuki Hoshii, Meghan E. Eisold, Christopher Delaney, Monica Cusan, Aniruddha J. Deshpande, Chun-Hao Huang, Amaia Lujambio, George Zheng, Tej K. Pandita, Scott W. Lowe, Scott A. Armstrong

Cancer Research, under review

ABSTRACT

Given the recent interest in targeting chromatin-based mechanisms in acute myeloid leukemia, we conducted a chromatin regulator-focused RNAi screen to identify novel druggable targets in *MLL*-rearranged leukemia. In this screen we found hairpins targeting the *Mof* gene to be among the most potent suppressors of cell growth. MOF is an H4K16 acetyltransferase and member of the MYST family of histone acetyltransferases (HATs). Using a conditional *Mof* knockout model, we studied the role of MOF in *MLL-AF9* leukemogenesis and found that *Mof* inactivation led to reduced tumor burden and prolonged survival in an *MLL-AF9* mouse model. RNA sequencing of *Mof*-deficient cells showed significant downregulation of genes within DNA damage repair pathways, and *Mof*-deficient *MLL-AF9* cells indeed contained significantly more yH2AX foci. In addition, we found a loss of global H4K16 acetylation (H4K16ac) upon *Mof* deletion. We performed rescue experiments using MOF mutants that lack HAT activity and found that MOF enzymatic activity is indispensable for *MLL-AF9* leukemia maintenance. Finally, MG149, a MYST protein HAT inhibitor, had a strong anti-proliferative effect on murine, as well as human *MLL-AF9* leukemia cell lines. These results indicate that MOF HAT activity is required for *MLL-AF9* leukemia maintenance with loss of MOF HAT activity leading to elevated DNA damage. Based on our findings, we believe that small molecule inhibition of MOF HAT activity may prove to be a novel approach for the treatment of patients with *MLL*-rearranged leukemia.

INTRODUCTION

Chromosomal rearrangements at 11q23 are associated with the development of acute leukemia and led to the discovery of the *Mixed-Lineage Leukemia 1* (*MLL1*) gene.[1,2] *MLL* translocations are found in about 10% of all patients with acute leukemia and are generally associated with an unfavorable prognosis.[3] *MLL* translocations are more frequently present in infant and pediatric patients with the highest frequency (80%) in infant acute lymphoblastic leukemia (ALL).[4,5]

It is evident that chromatin modifications, including DNA methylation and histone modifications, enforce oncogenic gene expression programs and substantially contribute to the initiation and maintenance of leukemia cells.[6,7] Epigenomic studies utilizing *in vivo* and *in vitro* models of *MLL*-rearranged leukemia have revealed that direct targets of MLL1 fusion proteins such as *HOXA* cluster genes are associated with aberrantly high levels of histone 3 lysine 79 dimethylation (H3K79me2).[8,9] DOT1L was found to be the key regulator of H3K79me2 and *MLL*-rearranged cells were shown to be highly dependent on *Dot1l* for leukemia initiation and maintenance.[10-13] This discovery led to the development of small molecule inhibitors targeting DOT1L, one of which is currently undergoing early phase trials.[14,15] Similarly, *MLL*-rearranged leukemia maintenance was shown to be critically dependent upon expression of *Bromodomain Containing 4* (*Brd4*).[16,17] BRD4 is a well-known member of the bromodomain family, a family of epigenetic ''readers'', important for recognizing posttranslational chromatin modifications and recruiting downstream effector proteins to specific loci to activate gene expression programs.[18] Multiple bromodomain inhibitors are currently under investigation in early phase clinical trials.[18]

Findings such as these indicate the importance of chromatin regulation in leukemia. In order to identify novel druggable epigenetic targets in *MLL*-rearranged leukemia, we conducted a chromatin regulator-focused RNAi screen in murine *MLL-AF9* leukemia cells and found hairpins targeting (K)Lysine Acetyltransferase 8 (*Kat8*, also known as *Mof*) and the previously identified target *Brd4*[16], to be the most potent suppressors of cell growth. MOF is a histone 4 lysine 16 (H4K16) acetyltransferase and member of the MYST family of lysine acetyltransferases. The MYST family is named for its founding members MOZ, YBF2, SAS2 and TIP60, proteins that all contain a MYST region with a canonical acetyl coenzyme A (CoA) binding site and C2HC-type zinc finger motif.[19] MOF is one of the best-characterized MYST-family proteins and was shown to be crucial for murine embryogenesis. MOF functions as a cell-type dependent regulator of chromatin state and controls various cellular processes such as T-cell differentiation[20], DNA damage response[21-25], cell cycle progression[21,26] and embryonic stem cell self-renewal and pluripotency[27].

The role of MOF in tumorigenesis seems complex. Studies in breast carcinoma[28], medulloblastoma[28] and ovarian cancer[29] suggest that tumor progression is associated with downregulation of *MOF* and H4K16 acetylation (H4K16ac). On the other hand, studies in lung[30,31] and oral[32] carcinoma have associated high expression of *MOF* with carcinogenesis and suppression of *MOF* with cancer cell death. This suggests that MOF may regulate

tumorigenesis in a cell- and tissue- dependent manner.

While MOF's enzymatic activity is druggable by small molecules[33] and our RNAi screen suggests a crucial role for MOF in *MLL-AF9* leukemogenesis, we studied the role of *Mof* in detail using a conditional murine *Mof* knockout system[34]. Our current findings indicate a strong dependency of *MLL-AF9* leukemic cells on *Mof*. Gene expression and immunofluorescence data suggest that the importance of MOF in *MLL-AF9* leukemogenesis may be through DNA damage repair. *Mof* knockout in *MLL-AF9* transformed cells led to loss of global H4K16ac and in line with this finding, rescue experiments with histone acetyltransferase (HAT) domain mutated MOF illustrated that the HAT activity of MOF is indispensable for *MLL-AF9* leukemia maintenance. Finally, experiments with the selective MYST protein HAT inhibitor MG149, showed a strong anti-proliferative effect on murine as well as human *MLL-AF9* leukemia cell lines. MOF HAT activity may be a good target for novel small molecule inhibitor development to improve the treatement of patients with *MLL*-rearranged leukemia.

RESULTS

Chromatin regulator focused RNAi screen in *MLL-AF9* leukemia identifies *Mof* as a key regulator

To identify novel druggable targets within epigenetic pathways required for *MLL-AF9* (*MA9*) leukemia maintenance, we conducted a customized, chromatin regulator focused RNAi screen in murine, *MA9* leukemia cells (Figure 1A). An shRNA library containing 2,252 shRNAs targeting 468 known chromatin regulators was constructed in TRMPV-Neo and transduced as one pool into Tet-on-competent, monoclonal mouse *MA9* leukemic cells. After Neomycin (G418) selection, shRNA expression was induced by Doxycycline treatment. shRNA expressing cells were then sorted and changes in shRNA library representation after 12 days of culture were assessed by high-throughput sequencing (HiSeq) of shRNA guide strands as previously described.[16,35] Using the scoring criterion of more than 256-fold depletion in each of two independent replicates, 20 shRNAs targeting 18 genes were strongly depleted (Figure 1B). Only two out of these 18 had two independent shRNAs that showed strong depletion, namely *Mof* and the previously identified target *Brd4*[16] (Figure 1B, S1A, S1B). This RNAi screen strongly suggests that the acetyltransferase MOF is crucial for *MA9* leukemic cell growth.

Mof loss in a murine *MLL-AF9* leukemia model leads to impaired colony-forming capacity, a phenotype rescued by exogenous full-length *Mof*

To study the role of MOF in *MA9* leukemogenesis and validate the results of our RNAi screen we used a well-described conditional *Mof* knockout (KO) mouse in a C57Bl/6 background.[34] For the initial *in vitro* experiments, $Mof^{f/f}$, $Mof^{f/+}$ and wild type ($Mof^{+/+}$) adult mice were euthanized and Lin^-, $SCA1^+$, $cKIT^+$ cells (LSKs) were harvested from the bone marrow (BM) (Figure 2A). These fresh LSKs were infected with *MA9* in an MSCV-Migr1 retroviral vector

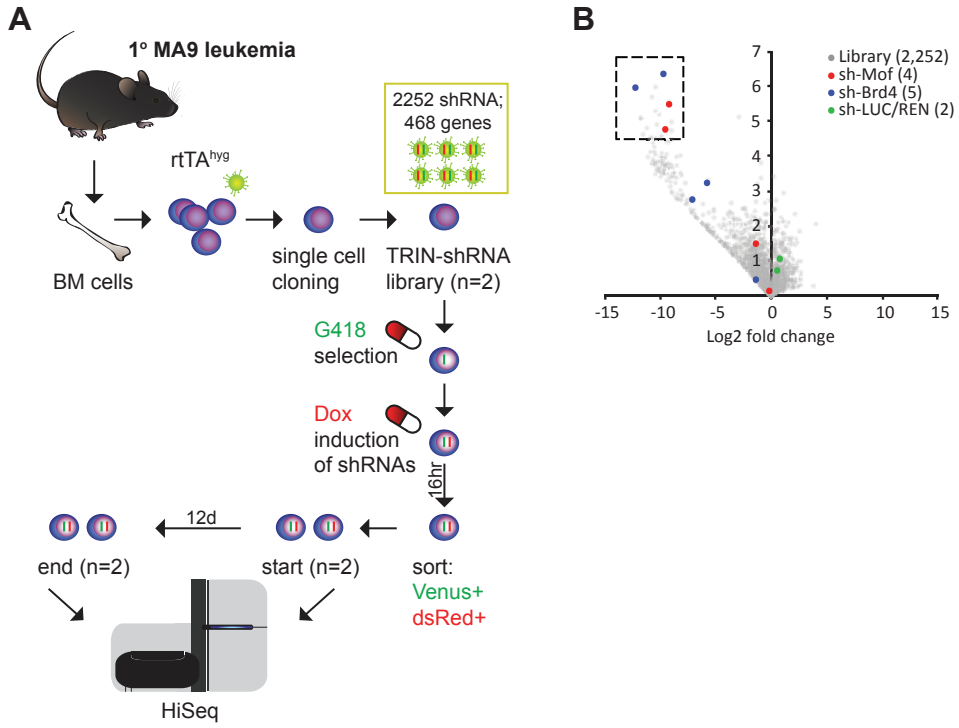

Figure 1. Chromatin regulator focused RNAi screen in *MLL-AF9* leukemia identifies *Mof* as a key regulator

(A) Schematic outline of chromatin regulator focused shRNA library screen coupled with high-throughput sequencing (HiSeq) in murine bone marrow (BM) *MA9* monoclonal leukemia cells. Dox: Doxycycline. (B) Volcano plot depicting the changes in representation (x-axis) and significance (y-axis) of each shRNA construct in the screen before versus 12 days after hairpin-induced knockdown. One dot represents the mean for two independent experiments. The dotted area contains the 20 most significantly depleted hairpins in the screen (more than 256-fold depletion, significance (defined as $-\log_{10}$ of the p-value) ≥ 4.5). Total library (gray; 2,252 shRNAs, 468 genes), shMof (red; four shRNAs) and shBRD4 (blue; five shRNAs) are highlighted as the only two genes with two hits.

containing the GFP selection marker. Following a few days of liquid culture, cells were sorted for GFP positivity. These stable *MA9* transformed cells grow indefinitely and were capable of forming dense, round colonies (blast colonies, data not shown).

For *in vitro* excision of *Mof, MA9* cells were infected with an MSCV-dTomato retrovirus containing *Cre*. 48 hours after infection, *Cre* positive $Mof^{f/f}$, $Mof^{f/+}$ and $Mof^{+/+}$ cells were sorted, counted and immediately plated in myeloid cytokine supplemented methylcellulose for colony-forming unit (CFU) assays. Homozygous *Mof* loss significantly reduced colony-

forming capacity of *MA9* cells (Figure 2B and C). No difference in colony morphology was observed (Figure 2D). Heterozygous loss of *Mof* (*Mof*$^{f/+}$) also led to a reduction of total colony number (Figure 2C), albeit less dramatic compared to full *Mof* deletion, suggesting a potential gene dosage effect of *Mof* on the clonogenic capacity and cell growth of *MA9* cells. However, *Mof* excision PCR data consistently illustrated that although at time of plating, all cells in *Mof*$^{f/f}$ and *Mof*$^{f/+}$ were completely excised (Figure 2E), all *Mof*$^{f/f}$ colonies that had formed at day 7 of the CFU assay were in fact unexcised, whereas the floxed-allele in the *Mof*$^{f/+}$ colonies remained fully excised (Figure 2E). These PCR data indicate strong selective pressure against homozygous, but not heterozygous *Mof* loss in an *MA9* leukemic setting.

To assess specificity of the observed phenotype, a *Mof* full-length rescue experiment was performed. *Mof*$^{f/f}$, *Mof*$^{f/+}$ and *Mof*$^{+/+}$ *MA9* cells were transduced with either an MSCV-miCD2 retrovirus containing full-length, human influenza hemagglutinin (HA)-tagged *Mof* or the empty vector (Figure 2A). hCD2 positive cells were sorted and subsequent Western blot analysis for the HA-tagged MOF indicated that exogenous *Mof* was expressed (Figure S2A). These cells were then transduced with *Cre* and *Cre* positive cells were used for CFU assays as before. Figure 2F shows full rescue of the phenotype observed in *Mof*$^{f/f}$, *miCD2* cells by exogenous expression of full length *Mof* (*Mof*$^{f/f}$, *miCD2-Mof*). *Mof* excision PCR analysis confirms this rescue. While *Mof*$^{f/f}$, *miCD2* cells are fully unexcised 9 days post *Cre* infection, *Mof*$^{f/f}$, *miCD2-Mof* cells remain largely excised (Figure 2G). Taken together, these findings demonstrate that *Mof* is required for the colony-forming capacity of *MA9* leukemic cells.

Mof loss leads to reduced tumor burden and prolonged survival in an *in vivo MLL-AF9* leukemia model

Mof dependency in *MA9* leukemia was further assessed using an *in vivo* secondary, murine leukemia model. *Mx1-cre; Mof*$^{f/f}$ and *Mx1-cre* mouse BM LSKs were transduced with GFP-tagged *MA9* and 48 hours after infection, GFP^{+} cells were sorted and injected into sub-lethally irradiated (600 cGy) C57Bl/6 mice. These mice developed acute myeloid leukemia (AML) within 4-8 weeks post transplant (data not shown). Leukemic mice were sacrificed and BM cells obtained. 45,000 GFP^{+} primary leukemic *Mx1-cre; Mof*$^{f/f}$ or *Mx1-cre* BM cells were then injected into sub-lethally irradiated C57Bl/6 mice (Figure 3A). At day 13 post transplant, mice were bled to check engraftment (pre pIpC, Figure 3B). That same day, half of the mice per group (n = 10 for *Mx1-cre*, n = 20 for *Mx1-cre; Mof*$^{f/f}$) were injected with poly(I:C) (pIpC) to induce *Cre* expression. pIpC treated mice received a total of three dosages, one every other day and were bled again, 7 days after the last dose. The white blood cell (WBC) count (Figure 3C) and GFP% in peripheral blood (PB) (Figure 3B) illustrate the lethality of *Mof* loss to *MA9* leukemic cells. Seven days after pIpC treatment *Mx1-cre; Mof*$^{f/f}$, pIpC+ mice had a mean WBC count of 3 K/uL versus 112 K/uL (*Mx1-cre; Mof*$^{f/f}$, pIpC-) and 104 K/uL (*Mx1-cre,* pIpC+), and a significantly lower GFP% of 38% versus 92% (*Mx1-cre; Mof*$^{f/f}$, pIpC-) and 95% (*Mx1-cre,* pIpC+). Several mice within the *Mx1-cre; Mof*$^{f/f}$, pIpC+ group had an actual reduction of GFP% in the PB after receiving pIpC injections (Figure 3D) indicating a reduction of tumor burden upon *Mof* loss.

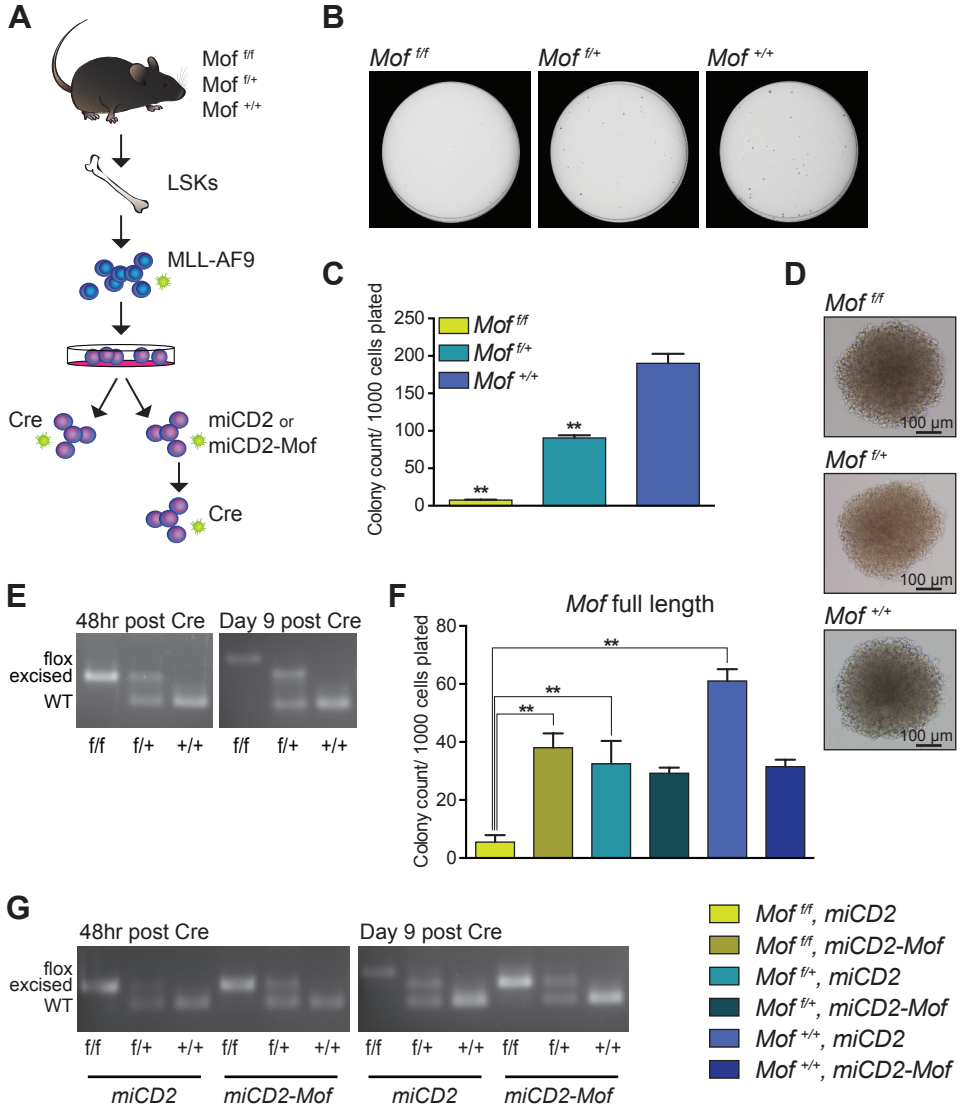

Figure 2. *Mof* loss in murine *MLL-AF9* leukemia model leads to impaired colony-forming capacity, a phenotype rescued by exogenous full-length *Mof*

(A) Schematic for *in vitro Mof* knockout and full-length *Mof* rescue experiments.

(B) Day 7 of methylcellulose colony-forming assay of *MA9 in vitro* transformed *Mof*$^{f/f}$, *Mof*$^{f/+}$ or wild type (*Mof*$^{+/+}$) LSKs plated immediately upon sorting *Cre* positive cells. Representative petri dishes are shown.

(C) Bar graph indicating mean number of colonies per 35mm dish after 7 days. 1000 cells were plated per dish. Data are representative of four individual experiments.

(D) Colonies at day 7 of CFU assay. Representative images are shown.

(E) PCR analysis illustrating excision at indicated time points of the 7-day colony-forming experiment. Representative gel images are shown.
(F) Day 7 of CFU assay of *MA9 in vitro* transformed *Mof*$^{f/f}$, *Mof*$^{f/+}$ or *Mof*$^{+/+}$ LSKs that were infected with full-length *Mof* (*miCD2-Mof*) or empty vector control (*miCD2*) and selected by sorting hCD2 positive cells. Bar graph indicates mean number of colonies per 35mm dish after 7 days. 3000 cells were plated per dish. Data are representative of three individual experiments.
(G) PCR analysis illustrates excision throughout the duration of the 7-day colony-forming experiment. Representative gel images are shown.
** $p < 0.01$. Error bars represent SD of mean.

All mice eventually succumbed to AML. At time of death, mice had elevated WBC counts (data not shown) and splenomegaly (Figure S3A). FACS analysis showed more than 90% GFP$^+$ cells in BM (Figure S3B), spleen and PB (data not shown). The majority of GFP$^+$ cells in BM, spleen and PB expressed myeloid cell markers MAC1, GR1 and cKIT, indicating a myeloid leukemic phenotype (Figure S3C and D). Animals in all three control groups died with a median survival of 22 (*Mx1-cre,* pIpC+), or 24 days (*Mx1-cre; Mof*$^{f/f}$ and *Mx1-cre,* pIpC-). *Mx1-cre; Mof*$^{f/f}$, pIpC+ mice lived significantly longer with a median survival of 31 days ($p < 0.0001$; Figure 3E). At time of death, GFP$^+$ BM cells of *Mx1-cre; Mof*$^{f/f}$, pIpC+ mice showed incomplete excision (Figure S3E), illustrating that *Mof*-deficient *MA9* cells have a strong disadvantage of forming leukemia *in vivo*. When we ended the experiment (day 60), the last living mouse in the *Mx1-cre; Mof*$^{f/f}$, pIpC+ cohort did not have any GFP$^+$ cells in the PB or BM. Together these *in vivo* data demonstrate that *Mof* is important for maintenance of *MA9* driven AML.

Homozygous *Mof* loss in *MLL-AF9* transformed mouse LSKs leads to cell death and DNA damage

Our CFU assay data show a strong dependence for *Mof* in *MA9* cells. To study the potential underlying mechanism, we performed *in vitro* excision of *Mof* in *MA9* transformed murine LSKs as described above. While the strong dependency caused a rapid loss of *Mof* excision (Figure 2E and G), we first had to define the latest time point after *Cre* infection at which *MA9* cells are still fully excised. PCR analysis indicated complete *Mof* excision up to 72 hours after *Cre* infection (Figure 4A). We next performed RNA sequencing (RNA-seq) on *Mof*$^{f/f}$ and *Mof*$^{+/+}$ *MA9* cells, harvested 72 hours after *Cre* infection. Gene ontology (GO) analysis comparing *MA9* cells with homozygous *Mof* loss to the wild type control, showed a significant enrichment of cell division and DNA damage repair pathways in genes that are downregulated in *MA9 Mof* KO cells. To verify this finding, we stained *MA9* transformed LSKs at 48 or 72 hours after *Cre* infection with an immunofluorescent-labeled yH2AX antibody. Confocal microscopy revealed significantly more yH2AX foci per cell nucleus in *Mof*-deficient

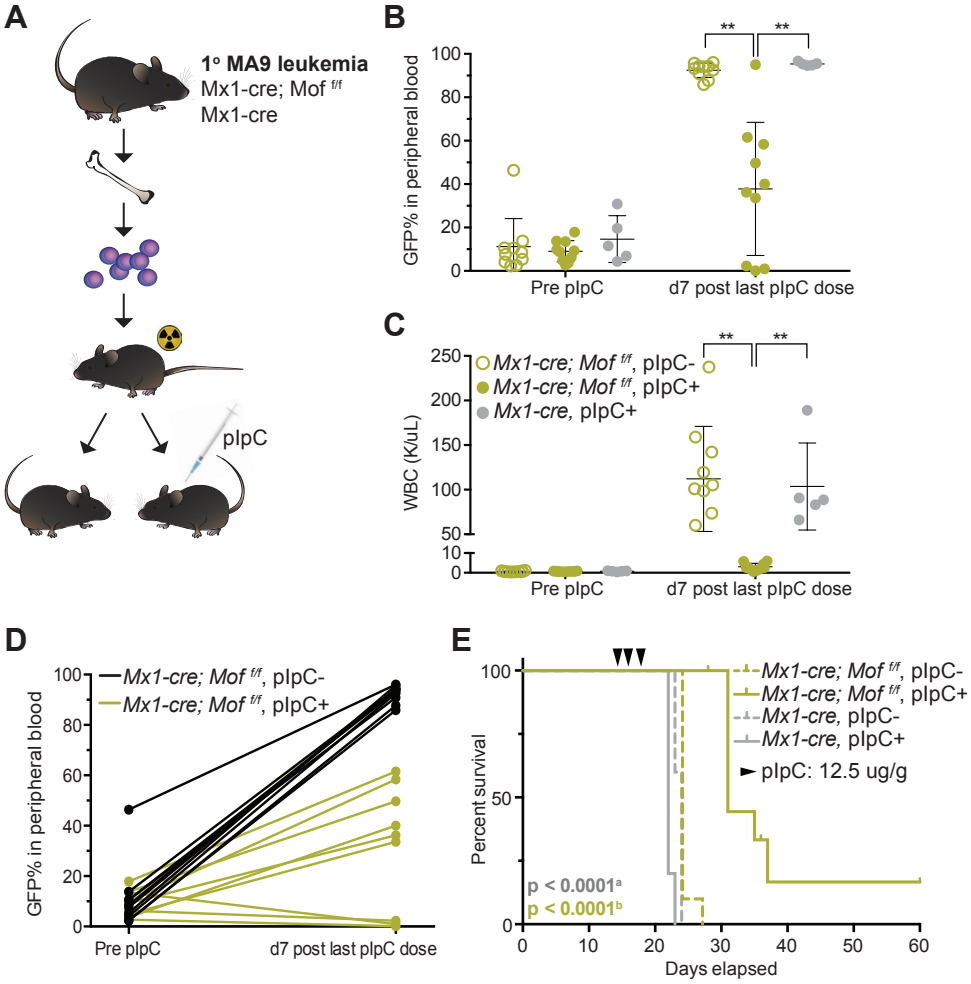

Figure 3. *Mof* loss leads to reduced tumor burden and prolonged survival in an *in vivo MLL-AF9* leukemia model

(A) Schematic for *in vivo Mof* excision experiment. Primary, GFP-tagged *MA9* leukemia BM cells in an *Mx1-cre; Mof*$^{f/f}$ or *Mx1-cre* background were injected into sub-lethally irradiated C57Bl/6 mice (n=10 for Mx1-cre and n=20 for *Mx1-cre; Mof*$^{f/f}$). Half of the mice per group were treated with poly(I:C) pIpC at day 15 post transplant to induce *Mof* excision.

(B) GFP% of live cells in peripheral blood of mice before and after pIpC treatment. A dot represents a single mouse in the experiment.

(C) White blood cell (WBC) counts before and after pIpC treatment.

(D) GFP% of live cells in peripheral blood of mice before and after pIpC treatment. A line connects the two values for a single mouse in the experiment.

(E) Survival curve of mice in secondary leukemia experiment. Data are representative of two individual experiments. Arrows indicate pIpC treatment.

a. Log-rank test p-value comparing survival of pIpC treated *Mx1-cre; Moff/f* mice to either of the *Mx1-cre* control groups.

b. Log-rank test p-value comparing survival of *Mx1-cre; Moff/f* mice treated with pIpC to the untreated group.

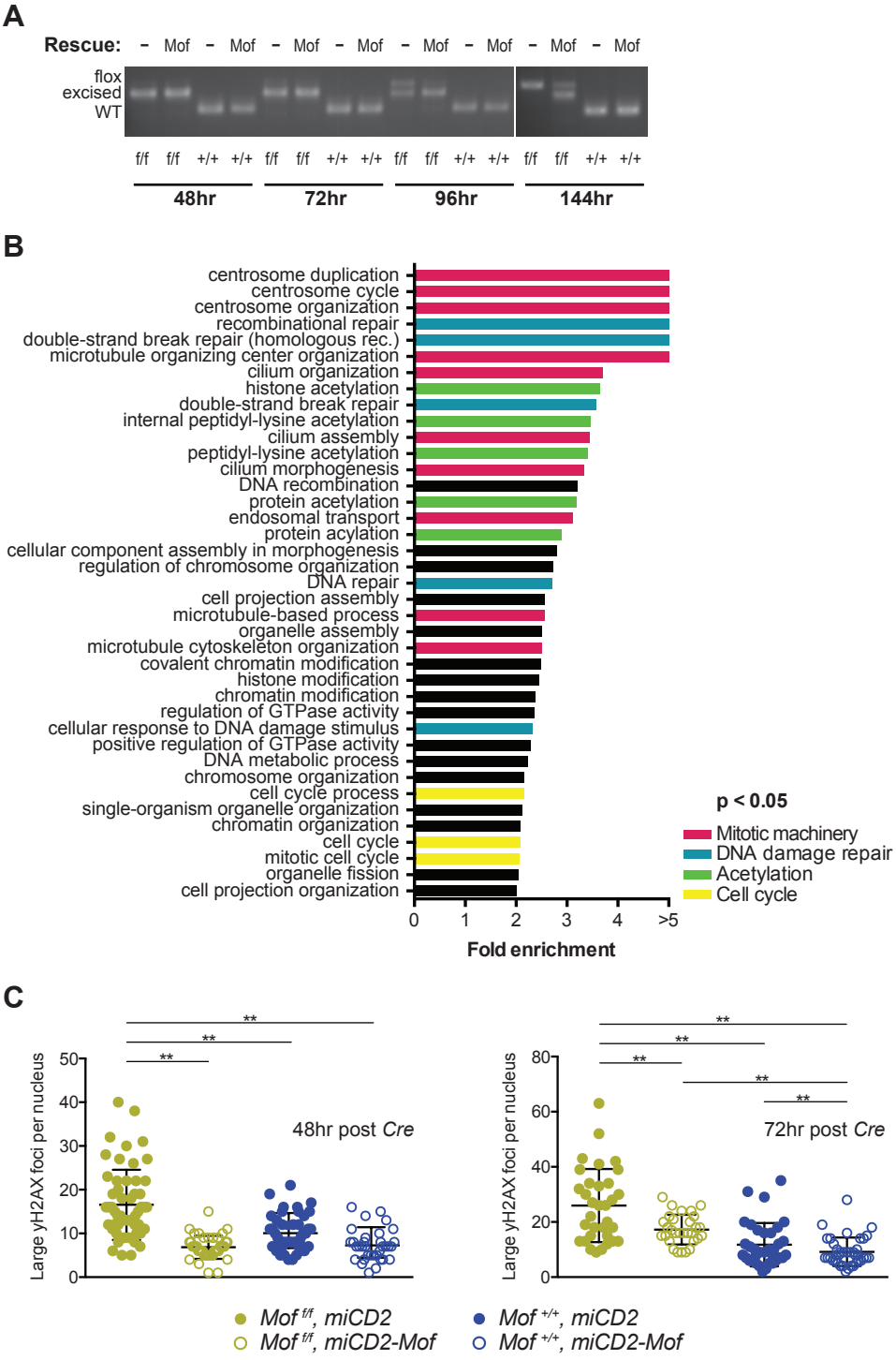
A
Rescue: - Mof - Mof - Mof - Mof - Mof - Mof - Mof - Mof
flox
excised
WT
f/f f/f +/+ +/+ f/f f/f +/+ +/+ f/f f/f +/+ +/+ f/f f/f +/+ +/+
48hr
72hr
96hr
144hr
B
centrosome duplication
centrosome cycle
centrosome organization
recombinational repair
double-strand break repair (homologous rec.)
microtubule organizing center organization
cilium organization
histone acetylation
double-strand break repair
internal peptidyl-lysine acetylation
cilium assembly
peptidyl-lysine acetylation
cilium morphogenesis
DNA recombination
protein acetylation
endosomal transport
protein acylation
cellular component assembly in morphogenesis
regulation of chromosome organization
DNA repair
cell projection assembly
microtubule-based process
organelle assembly
microtubule cytoskeleton organization
covalent chromatin modification
histone modification
chromatin modification
regulation of GTPase activity
cellular response to DNA damage stimulus
positive regulation of GTPase activity
DNA metabolic process
chromosome organization
cell cycle process
single-organism organelle organization
chromatin organization
cell cycle
mitotic cell cycle
organelle fission
cell projection organization
0 1 2 3 4 >5
Fold enrichment
p < 0.05
Mitotic machinery
DNA damage repair
Acetylation
Cell cycle
C
Large γH2AX foci per nucleus
48hr post Cre
72hr post Cre
Mof f/f, miCD2
Mof f/f, miCD2-Mof
Mof +/+, miCD2
Mof +/+, miCD2-Mof

Figure 4. Homozygous *Mof* loss in *MLL-AF9* transformed mouse LSKs leads to cell death and DNA damage

(A) *MA9 in vitro* transformed *Mof*$^{f/f}$ or *Mof*$^{+/+}$ LSKs were infected with full-length *Mof* or empty vector control (*miCD2*) and selected by sorting hCD2 positive cells. Cells were then plated in liquid culture immediately upon sorting dTomato positive cells, 48 hours after infection with dTomato-*Cre*. PCR analysis illustrates excision at 48, 72, 96 and 144 hours post *Cre* infection.

(B) Gene ontology analysis with a differential expression analysis list of significantly ($p < 0.05$) downregulated genes comparing *Mof*$^{f/f}$ cells to *Mof*$^{+/+}$ cells at 72 hours post *Cre* infection.

(C) Number of large yH2AX foci per cell nucleus at 48 or 72 hours post *Cre* infection. A dot represents a single cell.

** $p < 0.01$. Error bars represent SD of mean.

MA9 cells compared to controls ($p < 0.01$; Figure 4C), indicative of more DNA damage. This increase in DNA damage was largely rescued by overexpression of full-length *Mof* (Figure 4C). These experiments demonstrate that there is evidence of cell death and DNA damage in *MA9* cells upon *Mof* loss.

Mof histone acetyltransferase activity is required for colony formation of *MLL-AF9* transformed mouse LSKs

MOF has been identified as the major H4K16 acetyltransferase in humans, mice and *Drosophila*.[26,34,37-39] MOF contains a HAT domain with a CoA binding site that was found to be crucial for its acetyltransferase activity.[19,37] While MOF possesses acetyltransferase activity on various histones and nucleosomes, depletion of MOF in HeLa cells was shown to lead to a dramatic decrease in H4K16ac whereas other acetylation sites appeared to be unaffected.[26]

Since our data indicate a strong *Mof* dependence in *MA9* leukemic cells, we set out to establish whether this dependence is through MOF HAT activity. When assessing changes in global H4K16ac upon *Mof* loss in *MA9* cells, we found a significant decrease of H4K16ac (Figure 5A), a decrease that was averted by expression of exogenous *Mof* (*Mof*$^{f/f}$*, miCD2-Mof*). Next, we designed two HA-tagged, HAT inactivated *Mof* retroviral constructs (Figure 5B) in which either the CoA binding site was deleted (*Mof-CoAdel*) or a HAT inactivating point mutation (G327E) was introduced (*Mof-G327E*). The HAT inactivating point mutation in the MOF CoA binding domain was first described in *Drosophila*[37] and later used in a human *MOF* construct where it was also found to diminish H4K16ac[40]. Alignment of *Drosophila*, murine and human MOF illustrates that the point mutation involves replacement of glycine by glutamic acid on position 327 (G327E) in murine, as well as human MOF. The constructs were packaged in an miCD2-MSCV retroviral vector with the hCD2 selection marker (*miCD2-Mof-CoAdel* and *miCD2-Mof-G327E*).

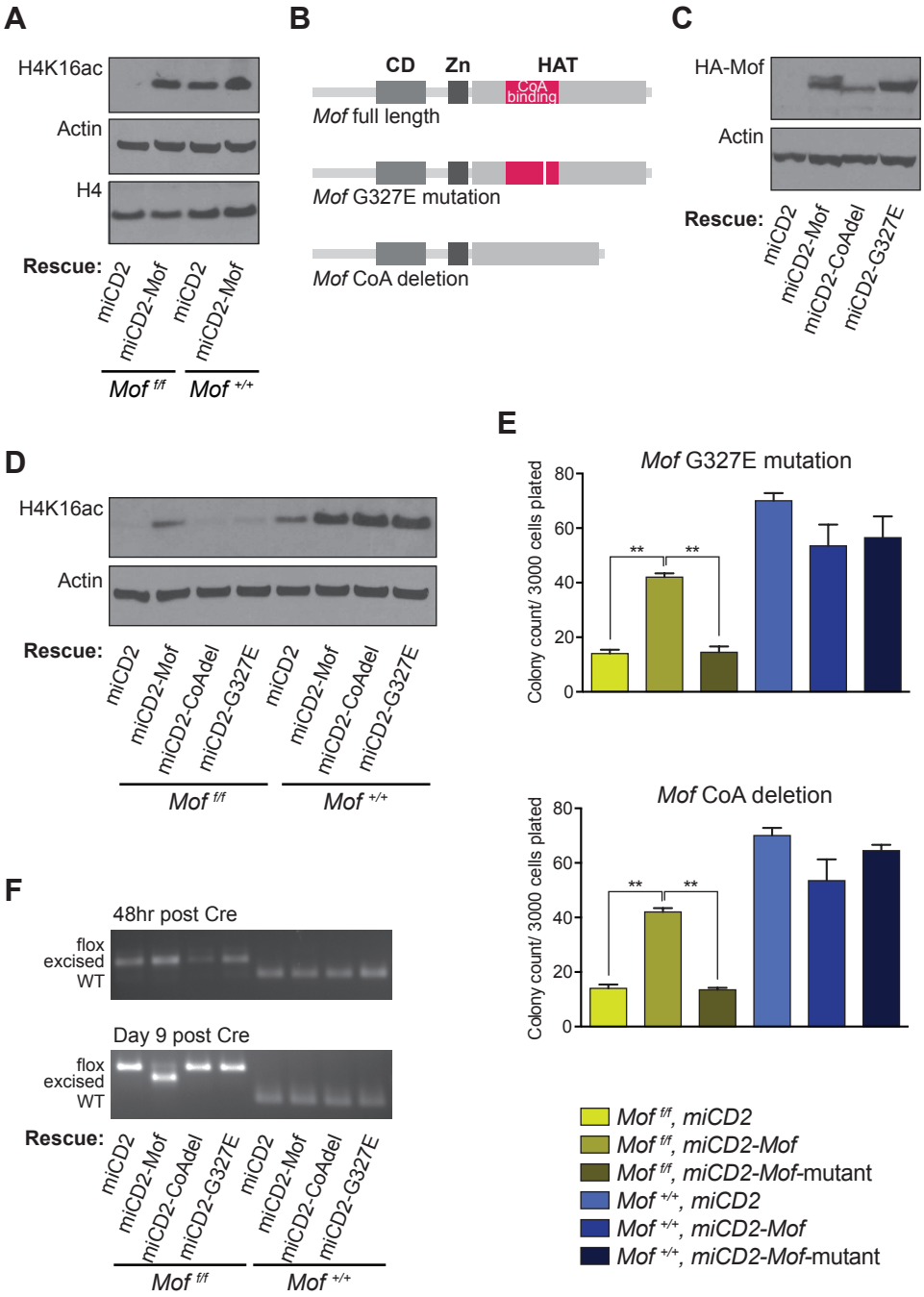
A
H4K16ac
Actin
H4
Rescue:
miCD2
miCD2-Mof
miCD2
miCD2-Mof
Mof f/f
Mof +/+
B
CD
Zn
HAT
CoA binding
Mof full length
Mof G327E mutation
Mof CoA deletion
C
HA-Mof
Actin
Rescue:
miCD2
miCD2-Mof
miCD2-CoAdel
miCD2-G327E
D
H4K16ac
Actin
Rescue:
miCD2
miCD2-Mof
miCD2-CoAdel
miCD2-G327E
miCD2
miCD2-Mof
miCD2-CoAdel
miCD2-G327E
Mof f/f
Mof +/+
E
Mof G327E mutation
Colony count/ 3000 cells plated
0
20
40
60
80
**
**
Mof CoA deletion
Colony count/ 3000 cells plated
0
20
40
60
80
**
**
Mof f/f, miCD2
Mof f/f, miCD2-Mof
Mof f/f, miCD2-Mof-mutant
Mof +/+, miCD2
Mof +/+, miCD2-Mof
Mof +/+, miCD2-Mof-mutant
F
48hr post Cre
flox
excised
WT
Day 9 post Cre
flox
excised
WT
Rescue:
miCD2
miCD2-Mof
miCD2-CoAdel
miCD2-G327E
miCD2
miCD2-Mof
miCD2-CoAdel
miCD2-G327E
Mof f/f
Mof +/+

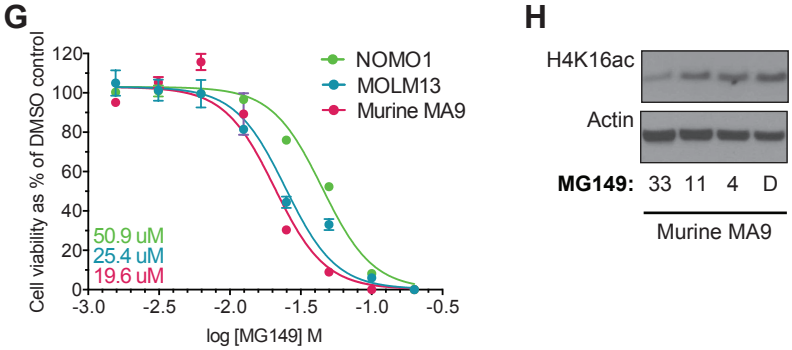

Figure 5. *Mof* histone acetyltransferase activity is required for colony formation of *MLL-AF9* transformed mouse LSKs

(A) *MA9 in vitro* transformed *Mof*$^{f/f}$ or *Mof*$^{+/+}$ LSKs were infected with full-length *Mof* or empty vector control (*miCD2*) and selected by sorting hCD2 positive cells. Cells were then infected with dTomato-*Cre*, 48 hours later sorted and another 24 hours later harvested. Western blot was performed on whole protein lysates.

(B) Schematic illustrating full length *Mof* and two *Mof* mutants with either a G327E point mutation or a CoA binding-site deletion.

(C) *MA9 in vitro* transformed *Mof*$^{f/f}$ or *Mof*$^{+/+}$ LSKs were infected with HA-tagged full-length *Mof*, CoA deleted *Mof* (CoAdel), *Mof* with a G327E mutation or empty vector control, and selected by sorting hCD2 positive cells. Western blot for HA confirms presence of these exogenous constructs.

(D) Cells were infected with dTomato-*Cre* and 48 hours later sorted and harvested. Western blot illustrates global H4K16ac and Actin in protein lysates.

(E) Day 7 of CFU assay. Cells were plated immediately upon sorting dTomato positive cells, 48 hours after infection with dTomato-*Cre*. Bar graph indicates mean number of colonies per 35mm dish after 7 days. Data are representative of three individual experiments.

(F) PCR analysis illustrating excision throughout the duration of the 7-day colony-forming experiment. Representative gel images are shown.

(G) MOLM13, NOMO1 and murine polyclonal *MA9* cells were plated in liquid culture and treated with various concentrations of MG149. Plotted is the IC50 curve for cell viability as a percentage of the vehicle (DMSO) control at day 3 of treatment. Numbers indicate the IC50 per cell type (by color).

(H) Western blot showing global H4K16ac and Actin in murine *MA9* cells after 3 days of MG149 treatment at various concentrations.

** $p < 0.01$. Error bars represent SD of mean.

We infected unexcised *Mof*$^{f/f}$ and *Mof*$^{+/+}$ *MA9* cells with either *miCD2-Mof, miCD2-CoAdel, miCD2-G327E* or *miCD2* and sorted hCD2 positive cells. Western blot analysis for HA-tagged MOF indicated that exogenous *Mof* was expressed at similar levels in *miCD2-Mof* and *miCD2-G327E,* though *Mof* expression seemed a little lower with the *miCD2-CoAdel*

construct (Figure 5C). Upon *in vitro Mof* KO by transduction with retroviral *Cre*, Western blot analysis confirmed that exogenous full-length *Mof* was capable of restoring H4K16ac levels, while both HAT domain mutant *Mof* constructs were not (Figure 5D). When using these *Cre* transduced *MA9* cells for a CFU assay, full-length *Mof* indeed rescued colony formation of *Mof*$^{f/f}$ cells while exogenous, HAT-deficient *Mof* could not (Figure 5E). *Mof* excision PCR analysis reaffirms these findings where *Mof*$^{f/f}$ *miCD2, miCD2-CoAdel* and *miCD2-G327E* cells have fully lost excision at day 9 post *Cre* infection, but *miCD2-Mof* cells are still largely excised (Figure 5F). In summary, we found a loss of global H4K16ac upon *Mof* KO and in line with this finding of H4K16ac loss, rescue experiments with HAT domain mutated MOF illustrated that the HAT activity of MOF is indispensable for *MA9* colony-forming capacity.

Our finding that MOF HAT activity is required for *MA9* leukemia suggests that targeting MOF HAT activity could provide us with a new approach in treating *MA9* leukemia patients. In 2011 a selective small molecule inhibitor of MYST protein HAT activity, MG149, was designed.[33] While this small molecule is not particularly potent, we decided to use this inhibitor to test its effect on cell viability in the human *MA9* AML cell lines NOMO1 and MOLM13 and in murine, polyclonal *MA9* primary leukemia cells. A dose response curve showed a strong anti-proliferative effect on all three *MA9* cells with an IC50 of 19.6 uM (murine *MA9*), 25.4 uM (MOLM13) and 50.9 uM (NOMO1). In addition, MG149 inhibition induced global H4K16ac loss in murine *MA9* cells (Figure 5H). These results suggest that MG149 effectively targets MOF HAT activity with an anti-proliferative effect on human as well as murine *MA9* leukemia cells.

DISCUSSION

To identify novel druggable targets in *MLL*-rearranged leukemia, we performed an RNAi screen focused on chromatin regulators. This resulted in the identification of *Mof* as one of the most potent suppressors of cell growth in murine *MA9* leukemia. We found that homozygous *Mof* loss led to a significant decrease in colony-forming ability, reduced tumor burden and prolonged survival in mice. RNA-seq of *Mof*-deficient *MA9* cells showed significant downregulation of genes associated with DNA damage repair pathways, and upon validation by immunofluorescence we indeed found a significant increase of γH2AX foci in *Mof*-deficient *MA9* cells. In addition, we uncovered a loss of global H4K16ac upon *Mof* KO. Rescue experiments with HAT domain mutated MOF illustrated that MOF HAT activity is indispensable for *MA9* leukemia maintenance. This new insight could be utilized in the development of a small molecule inhibitor for the treatment of leukemia patients carrying an *MLL* translocation.

Gene expression analysis in *Mof*-deficient *MA9* cells indicated that MOF loss does not lead to clear downregulation of MA9 target genes such as *Meis1* and *Hoxa* cluster genes. Our RNA-seq data suggested that MOF loss leads to impairment of more general biological processes required for cellular integrity (Figure 4B). This finding implies that MOF

may not only be required for *MA9* leukemogenesis and not even only for *MLL*-rearranged leukemia, but for a broad range of acute leukemias. We identified DNA damage repair as a possible mechanism of cell death in *Mof*-deficient leukemia cells (Figure 4C). *Mof*-null murine embryonic fibroblasts (MEFs) were previously shown to be deficient in DNA damage repair after ionizing radiation.[23] In wild type MEFs, radiation induced DNA damage led to an increase of global H4K16ac[23], suggesting that a MOF-induced increase of H4K16ac may be essential for an appropriate DNA damage response. Unacetylated H4K16 is required to achieve the maximum tendency of *in vitro* nucleosome arrays to fold into secondary or tertiary chromatin structures.[41] In contrast, 30% H4K16 acetylation alleviates compaction of the chromatin fiber.[42] Therefore it may be that the MOF-loss induced global H4K16ac depletion influences the DNA damage response and/or chromatin integrity by increasing chromatin compaction.

GO analysis on our RNA-seq data suggested that loss of *Mof* in *MA9* leukemic cells may not only lead to DNA damage, but also general chromosomal instability (Figure 4B). This could contribute to the rapid cell death we observed in *Mof*-deficient *MA9* cells. Genetic and biochemical data underscore the importance of unacetylated acidic histone tails in gene silencing.[43] Interestingly, the yeast ortholog of *MOF*, *SAS2*, was previously shown to lead to telomeric silencing[44] and it is well established that telomeric dysfunction can lead to chromosomal instability[45]. Future experiments will be required to assess how *Mof*-loss induced H4K16ac depletion may contribute to chromosomal instability in *Mof*-deficient *MA9* cells, and whether telomeric silencing is involved.

MOF was shown to functionally and physically interact with the histone methyltransferase MLL1. The interaction between MOF and MLL1 is important for the chromatin regulatory function of both enzymes.[46] In normal hematopoiesis, *Mll1* is essential for development and maintenance of both embryonic and adult progenitors and hematopoietic stem cells (HSCs).[47] In addition, it has been suggested that wild type MLL1 may play a role in *MLL*-rearranged leukemogenesis.[48] However, in both normal and malignant hematopoiesis, MLL1s H3K4 methyltransferase activity is dispensable.[49] Given the identified *MA9* leukemia dependence on the enzymatic activity of MOF (Figure 5E), it may be that, in the setting of *MLL*-rearranged leukemia, it is in fact the HAT activity of MOF that is required for leukemogenesis, and MLL1 merely functions as a scaffolding protein, recruiting MOF to targets of the oncogenic fusion.

Over the last decade, many advances have been made in the field of cancer epigenomics. Our vastly expanding knowledge on the role of chromatin regulation in cancer has led to the development of various drug compounds that target the cancer epigenome, several of which are currently in clinical trials.[6,50] Here we have established that MOF HAT activity is required *for MA9* leukemia maintenance and loss of MOF HAT activity leads to elevated DNA damage. In addition, we have successfully inhibited cell growth of human and murine *MA9* leukemia cells by using a first generation small molecule MYST protein HAT inhibitor. Based on our findings, we believe that inhibiting MOF HAT activity by small molecules may prove to be an effective, novel approach for the treatment of patients with *MLL*-rearranged and perhaps other leukemias.

EXPERIMENTAL PROCEDURES

RNAi screen

A customized shRNA library (TRMPV-Neo system) focused on mouse chromatin-regulating genes, together with control shRNAs, was designed as previously described.[16,35] After sequence verification the virus library containing 2,252 shRNAs targeting 468 genes (four to six shRNAs per gene), was pooled. The virus pool was transduced into monoclonal mouse *MA9* leukemic cells (two replicates), stably expressing rtTA3 (Tet-on system), at a viral titer that on average causes a single viral transduction per cell and at which each shRNA is represented in at least 2,000 cells. The infected cells were selected for two days in 1 mg/mL Neomycin (G418 sulfate, Corning, NY) and subsequently shRNA expression was induced by adding 1 ug/mL Doxycycline (Sigma-Aldrich, St. Louis, MO). The shRNA-expressing cells (dsRed and Venus double positive) were sorted (T0) using a FACS ARIA (BD, San Jose, CA), and cultured for 12 days (T12).[36] The integrated shRNA sequences in T0 and T12 cell samples were assessed by HiSeq using the Illumina Next-Gen Sequencing HiSeq platform (Illumina, San Diego, CA), as previously described.[16,35]

Mice

The generation of *Mof* conditional knockout mouse in a C57Bl/6 background has been described.[34] To generate *Mx1-cre; Mof$^{f/f}$* mice, *Mof$^{f/f}$* mice were crossed to *Mx1-cre* mice and *Cre* was maintained as a heterozygous allele. Genotyping strategies were previously described.[34] Wild type C57Bl/6 mice were purchased from Taconic, Hudson, NY. All animal experiments in this study were approved by, and adhered to guidelines of the Memorial Sloan-Kettering Cancer Center Animal Care and Use Committee.

Isolation of murine LSKs for *in vitro MLL-AF9* transformation

Mx1-cre; *Mof$^{f/f}$*, *Mof$^{f/f}$, Mof$^{f/+}$, Mx1-cre* and wild type (*Mof$^{+/+}$*) adult mice were sacrificed and femurs, tibias, fibulas, pelvis and spine were extracted. Single cell suspensions were prepared by crushing bones in a mortar after removal of muscle and connective tissues.

Lineage depletion was performed by labeling BM cells with purified, biotinylated monoclonal antibodies to CD3e, CD11b (MAC1), CD45R (B220), Ly-6G (GR1) and TER119 (Biotin mouse lineage panel, BD, San Jose, CA). Lineage positive (Lin$^+$) cells were in majority removed by magnetic bead depletion with streptavidin conjugated MicroBeads over an LD column (both Miltenyi Biotech, San Diego, CA). Lin$^-$, SCA1$^+$, cKIT$^+$ cells (LSK) were then obtained by staining lineage depleted cells with Streptavidin APC/Cy7, (Biolegend, San Diego, CA), CD117 (cKIT) APC and Ly-6A/E (SCA1) PE/Cy7 (both eBioscience, San Diego, CA), and sorting the LSK population.

Fresh LSKs were infected with MSCV-*MLL-AF9*-IRES-GFP retrovirus and GFP positive cells sorted on a FACS ARIA cell sorter 48 hours post infection. Cells were then immediately used for transplantation or grown out for several weeks to obtain highly proliferative transformed cultures for *in vitro* assays.

In vitro colony-forming assays

To study the impact of *Mof* deletion on the colony-forming capacity of *Mof*-deficient *MA9* cells, *Mof*$^{f/f}$, *Mof*$^{f/+}$ or *Mof*$^{+/+}$ *MA9 in vitro* transformed LSKs were transduced with MSCV-*Cre*-IRES-dTomato. After 48 hours, cells were sorted for dTomato positivity, counted and plated in methylcellulose M3234 (Stemcell Technologies, Vancouver, BC, Canada), supplemented with murine IL3 (10 ng/mL), IL6 (10 ng/mL) and SCF (20 ng/mL) in 35mm culture dishes. Colonies were scored after 7 days, using the Eclipse TS100 inverted microscope (Nikon, Tokyo, Japan). Since almost all colonies were either compact and hypercellular (blast-like) or small and diffuse (consistent with differentiation), colonies were classified into these two categories. Cells from pooled colony aggregates were then counted and assessed for *Mof* excision by PCR.

For *Mof* rescue experiments, *MA9 in vitro* transformed LSKs were infected with retrovirus containing *miCD2*, *miCD2-Mof*, *miCD2-Mof-CoAdel* or *miCD2-Mof-G327E*. After 48 hours of liquid culture, cells were sorted for hCD2 positivity and expanded to test exogenous *Mof* expression by Western blot. Subsequently, *Mof* was excised by transduction with *Cre* and CFU assays were performed as described above.

Transplant experiments

For secondary transplant experiments, viable frozen BM cells from primary *MA9* leukemic mice in an *Mx1-cre; Mof*$^{f/f}$ or *Mx1-cre* background were thawed and injected into sub-lethally irradiated (600cGy) 6-8 week-old C57Bl/6 female recipients (45,000 GFP$^+$ cells per mouse). At day 13 post transplant, mice were injected with poly(I:C) (pIpC, Invivogen, San Diego, USA) to induce *Cre* expression. pIpC treated mice received a total of three intraperitoneal pIpC injections, each dose 12.5 ug per gram of mouse weight, one every other day. Mice were euthanized at time of clinical symptoms of disease, coincided by leukocytosis.

RNA extraction and RNA sequencing

Trizol (Invitrogen, Carlsbad, CA) was used to extract RNA from viable cells. RNA was QCed on the Agilent Bioanalyzer 2100 platform (Agilent, Santa Clara, CA) and Poly-A tail selection was performed. Sequencing (RNA-seq) was done using the Illumina Next-Gen Sequencing HiSeq platform (Illumina, San Diego, CA) with 30-45 million 50bp, paired-end reads.

Data Analysis and Statistical Methods

GraphPad Prism software was used for statistical analysis. Statistical significance between 2 groups was determined by unpaired 2-tailed Student's t-test. The Kaplan-Meier method was applied to plot survival curves for murine leukemic transplant data, and the log-rank test to determine statistical significance.

RNA-seq raw reads were aligned to NCBI37/mm9 and normalized using STAR. Differential expression data were obtained using the DEseq algorithm. These analyses were done through the Basepair platform (New York City, NY). Raw data were deposited in GEO (GSE80671). GO analyses were performed using the PANTHER gene analysis tool.

ACKNOWLEDGMENTS

We would like to thank C.M. Woolthuis for critically reading the manuscript and Z. Feng for administrative assistance. This work was supported by a CURE Childhood Cancer Research Grant (D.G.V.); NIH grants PO1 CA66996 and R01 CA140575 (S.A.A.); the Leukemia and Lymphoma Society (S.A.A.); Gabrielle's Angel Research Foundation (S.A.A.); and an NIH Memorial Sloan Kettering Cancer Center Support Grant (P30 CA008748).

AUTHORSHIP CONTRIBUTIONS

D.G.V. and S.A.A. conceived the study and designed the experiments; D.G.V., H.X., T.H., M.E.E. and C.D. performed experiments; C.C., C.H., A.L. and S.W.L. designed and analyzed the RNAi screen; D.G.V. performed all other data analysis; H.X., C.C., M.C. and A.J.D. gave conceptual advice; G.Z. provided MG149 compound; T.K.P. generated the conditional *Mof* knockout mouse model; D.G.V. and S.A.A. wrote the manuscript.

DISCLOSURE OF CONFLICTS OF INTEREST

S.A.A. is a consultant for Epizyme Inc. and Imago Biosciences. Other authors declare no conflict of interest.

REFERENCES

1. Djabali M, Selleri L, Parry P, Bower M, Young BD, Evans GA. A trithorax-like gene is interrupted by chromosome 11q23 translocations in acute leukaemias. *Nat Genet.* 1992;2(2):113-118.
2. Tkachuk DC, Kohler S, Cleary ML. Involvement of a homolog of Drosophila trithorax by 11q23 chromosomal translocations in acute leukemias. *Cell.* 1992;71(4):691-700.
3. Muntean AG, Hess JL. The pathogenesis of mixed-lineage leukemia. *Annu Rev Pathol.* 2012;7:283-301.
4. Greaves MF. Infant leukaemia biology, aetiology and treatment. *Leukemia.* 1996;10(2):372-377.
5. Meyer C, Hofmann J, Burmeister T, et al. The MLL recombinome of acute leukemias in 2013. *Leukemia.* 2013;27(11):2165-2176.
6. Brien Gerard L, Valerio Daria G, Armstrong Scott A. Exploiting the Epigenome to Control Cancer-Promoting Gene-Expression Programs. *Cancer Cell.* 2016;29(4):464-476.
7. Chi P, Allis CD, Wang GG. Covalent histone modifications-miswritten, misinterpreted and mis-erased in human cancers. *Nat Rev Cancer.* 2010;10(7):457-469.
8. Guenther MG, Lawton LN, Rozovskaia T, et al. Aberrant chromatin at genes encoding stem cell regulators in human mixed-lineage leukemia. *Genes Dev.* 2008;22(24):3403-3408.
9. Krivtsov AV, Feng Z, Lemieux ME, et al. H3K79 methylation profiles define murine and human MLL-AF4 leukemias. *Cancer Cell.* 2008;14(5):355-368.
10. Bernt KM, Zhu N, Sinha AU, et al. MLL-rearranged leukemia is dependent on aberrant H3K79 methylation by DOT1L. *Cancer Cell.* 2011;20(1):66-78.
11. Deshpande AJ, Deshpande A, Sinha AU, et al. AF10 regulates progressive H3K79 methylation and HOX gene expression in diverse AML subtypes. *Cancer Cell.* 2014;26(6):896-908.
12. Chang MJ, Wu H, Achille NJ, et al. Histone H3 lysine 79 methyltransferase Dot1 is required for immortalization by MLL oncogenes. *Cancer Res.* 2010;70(24):10234-10242.
13. Jo SY, Granowicz EM, Maillard I, Thomas D, Hess JL. Requirement for Dot1l in murine postnatal hematopoiesis and leukemogenesis by MLL translocation. *Blood.* 2011;117(18):4759-4768.
14. Daigle SR, Olhava EJ, Therkelsen CA, et al. Potent inhibition of DOT1L as treatment of MLL-fusion leukemia. *Blood.* 2013;122(6):1017-1025.
15. Daigle SR, Olhava EJ, Therkelsen CA, et al. Selective killing of mixed lineage leukemia cells by a potent small-molecule DOT1L inhibitor. *Cancer Cell.* 2011;20(1):53-65.
16. Zuber J, Shi J, Wang E, et al. RNAi screen identifies Brd4 as a therapeutic target in acute myeloid leukaemia. *Nature.* 2011;478(7370):524-528.
17. Dawson MA, Prinjha RK, Dittmann A, et al. Inhibition of BET recruitment to chromatin as an effective treatment for MLL-fusion leukaemia. *Nature.* 2011;478(7370):529-533.
18. Filippakopoulos P, Knapp S. Targeting bromodomains: epigenetic readers of lysine acetylation. *Nat Rev Drug Discov.* 2014;13(5):337-356.
19. Yang XJ, Ullah M. MOZ and MORF, two large MYSTic HATs in normal and cancer stem cells. *Oncogene.* 2007;26(37):5408-5419.
20. Gupta A, Hunt CR, Pandita RK, et al. T-cell-specific deletion of Mof blocks their differentiation and results in genomic instability in mice. *Mutagenesis.* 2013;28(3):263-270.
21. Gupta A, Hunt CR, Hegde ML, et al. MOF phosphorylation by ATM regulates 53BP1-mediated double-strand break repair pathway choice. *Cell Reports.* 2014;8(1):177-189.
22. Gupta A, Sharma GG, Young CS, et al. Involvement of human MOF in ATM function. *Mol Cell Biol.* 2005;25(12):5292-5305.
23. Li X, Corsa CA, Pan PW, et al. MOF and H4 K16 acetylation play important roles in DNA damage repair by modulating recruitment of DNA damage repair protein Mdc1. *Mol Cell Biol.* 2010;30(22):5335-5347.
24. Sharma GG, So S, Gupta A, et al. MOF and histone H4 acetylation at lysine 16 are critical for DNA

damage response and double-strand break repair. *Mol Cell Biol.* 2010;30(14):3582-3595.
25. Bhadra MP, Horikoshi N, Pushpavallipvalli SN, et al. The role of MOF in the ionizing radiation response is conserved in Drosophila melanogaster. *Chromosoma.* 2012;121(1):79-90.
26. Taipale M, Rea S, Richter K, et al. hMOF histone acetyltransferase is required for histone H4 lysine 16 acetylation in mammalian cells. *Mol Cell Biol.* 2005;25(15):6798-6810.
27. Li X, Li L, Pandey R, et al. The histone acetyltransferase MOF is a key regulator of the embryonic stem cell core transcriptional network. *Cell Stem Cell.* 2012;11(2):163-178.
28. Pfister S, Rea S, Taipale M, et al. The histone acetyltransferase hMOF is frequently downregulated in primary breast carcinoma and medulloblastoma and constitutes a biomarker for clinical outcome in medulloblastoma. *International Journal of Cancer.* 2008;122(6):1207-1213.
29. Cai M, Hu Z, Liu J, et al. Expression of hMOF in different ovarian tissues and its effects on ovarian cancer prognosis. *Oncology reports.* 2015;33(2):685-692.
30. Zhang S, Liu X, Zhang Y, Cheng Y, Li Y. RNAi screening identifies KAT8 as a key molecule important for cancer cell survival. *Int J Cancer.* 2013;6(5):870-877.
31. Zhao L, Wang DL, Liu Y, Chen S, Sun FL. Histone acetyltransferase hMOF promotes S phase entry and tumorigenesis in lung cancer. *Cell Signal.* 2013;25(8):1689-1698.
32. Li Q, Sun H, Shu Y, Zou X, Zhao Y, Ge C. hMOF (human males absent on the first), an oncogenic protein of human oral tongue squamous cell carcinoma, targeting EZH2 (enhancer of zeste homolog 2). *Cell Prolif.* 2015;48(4):436-442.
33. Wu J, Wang J, Li M, Yang Y, Wang B, Zheng YG. Small molecule inhibitors of histone acetyltransferase Tip60. *Bioorg Chem.* 2011;39(1):53-58.
34. Gupta A, Guerin-Peyrou TG, Sharma GG, et al. The mammalian ortholog of Drosophila MOF that acetylates histone H4 lysine 16 is essential for embryogenesis and oncogenesis. *Mol Cell Biol.* 2008;28(1):397-409.
35. Huang CH, Lujambio A, Zuber J, et al. CDK9-mediated transcription elongation is required for MYC addiction in hepatocellular carcinoma. *Genes Dev.* 2014;28(16):1800-1814.
36. Chen CW, Koche RP, Sinha AU, et al. DOT1L inhibits SIRT1-mediated epigenetic silencing to maintain leukemic gene expression in MLL-rearranged leukemia. *Nat Med.* 2015;21(4):335-343.
37. Akhtar A, Becker PB. Activation of transcription through histone H4 acetylation by MOF, an acetyltransferase essential for dosage compensation in Drosophila. *Mol Cell.* 2000;5(2):367-375.
38. Smith ER, Cayrou C, Huang R, Lane WS, Cote J, Lucchesi JC. A human protein complex homologous to the Drosophila MSL complex is responsible for the majority of histone H4 acetylation at lysine 16. *Mol Cell Biol.* 2005;25(21):9175-9188.
39. Thomas T, Dixon MP, Kueh AJ, Voss AK. Mof (MYST1 or KAT8) is essential for progression of embryonic development past the blastocyst stage and required for normal chromatin architecture. *Mol Cell Biol.* 2008;28(16):5093-5105.
40. Zhao X, Su J, Wang F, et al. Crosstalk between NSL histone acetyltransferase and MLL/SET complexes: NSL complex functions in promoting histone H3K4 di-methylation activity by MLL/SET complexes. *PLoS Genet.* 2013;9(11):e1003940.
41. Shogren-Knaak M, Ishii H, Sun JM, Pazin MJ, Davie JR, Peterson CL. Histone H4-K16 acetylation controls chromatin structure and protein interactions. *Science.* 2006;311(5762):844-847.
42. Robinson PJ, An W, Routh A, et al. 30 nm chromatin fibre decompaction requires both H4-K16 acetylation and linker histone eviction. *J Mol Biol.* 2008;381(4):816-825.
43. Pillus LaMG. Chromatin structure and epigenetic regulation in yeast. *Chromatin Structure & Gene Expression.* Oxford: Oxford University Press; 1995:123-146.
44. Reifsnyder C, Lowell J, Clarke A, Pillus L. Yeast SAS silencing genes and human genes associated with AML and HIV-1 Tat interactions are homologous with acetyltransferases. *Nat Genet.* 1996;14(1):42-49.
45. Greenberg RA. Telomeres, crisis and cancer. *Curr Mol Med.* 2005;5(2):213-218.

46. Dou Y, Milne TA, Tackett AJ, et al. Physical association and coordinate function of the H3 K4 methyltransferase MLL1 and the H4 K16 acetyltransferase MOF. *Cell.* 2005;121(6):873-885.
47. Jude CD, Climer L, Xu D, Artinger E, Fisher JK, Ernst P. Unique and independent roles for MLL in adult hematopoietic stem cells and progenitors. *Cell Stem Cell.* 2007;1(3):324-337.
48. Thiel AT, Blessington P, Zou T, et al. MLL-AF9-induced leukemogenesis requires coexpression of the wild type Mll allele. *Cancer Cell.* 2010;17(2):148-159.
49. Mishra BP, Zaffuto KM, Artinger EL, et al. The histone methyltransferase activity of MLL1 is dispensable for hematopoiesis and leukemogenesis. *Cell Reports.* 2014;7(4):1239-1247.
50. Cai SF, Chen CW, Armstrong SA. Drugging Chromatin in Cancer: Recent Advances and Novel Approaches. *Mol Cell.* 2015;60(4):561-570.

SUPPLEMENTAL DATA

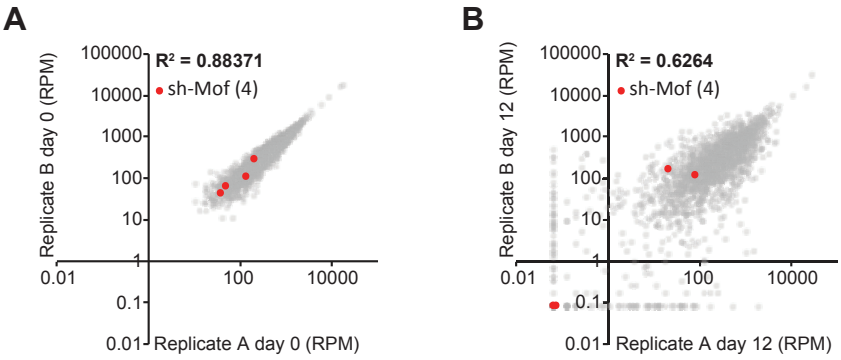

Figure S1, related to Figure 1. Chromatin regulator focused RNAi screen in *MLL-AF9* leukemia identifies *Mof* as a key regulator

(A) A chromatin regulator focused shRNA library screen was performed in murine primary *MA9* monoclonal leukemia cells. Plotted is the high throughput sequencing (HiSeq) normalized read-count (RPM) for replicate A (x-axis) versus B (y-axis) at day 0 (before activation of knockdown by doxycycline treatment). One dot represents one shRNA (total library 2,252 shRNA, 468 genes). *Mof* hairpins are highlighted in red. All hairpins with less than 600 reads were excluded from the analysis.

(B) Plotted is the Hiseq RPM for replicate A (x-axis) versus B (y-axis) at day 12 after knockdown. *Mof* hairpins are highlighted in red.

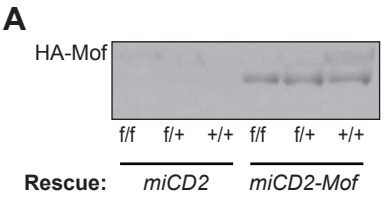

Figure S2, related to Figure 2. *Mof* loss in a murine *MLL-AF9* leukemia model leads to impaired colony-forming capacity, a phenotype rescued by exogenous full-length *Mof*
(A) *MA9 in vitro* transformed $Mof^{f/f}$, $Mof^{f/+}$ or $Mof^{+/+}$ LSKs were infected with HA-tagged full-length *Mof* or empty vector control (*miCD2*), and selected by sorting hCD2 positive cells. Western blot for HA confirmed the presence of the exogenous construct.

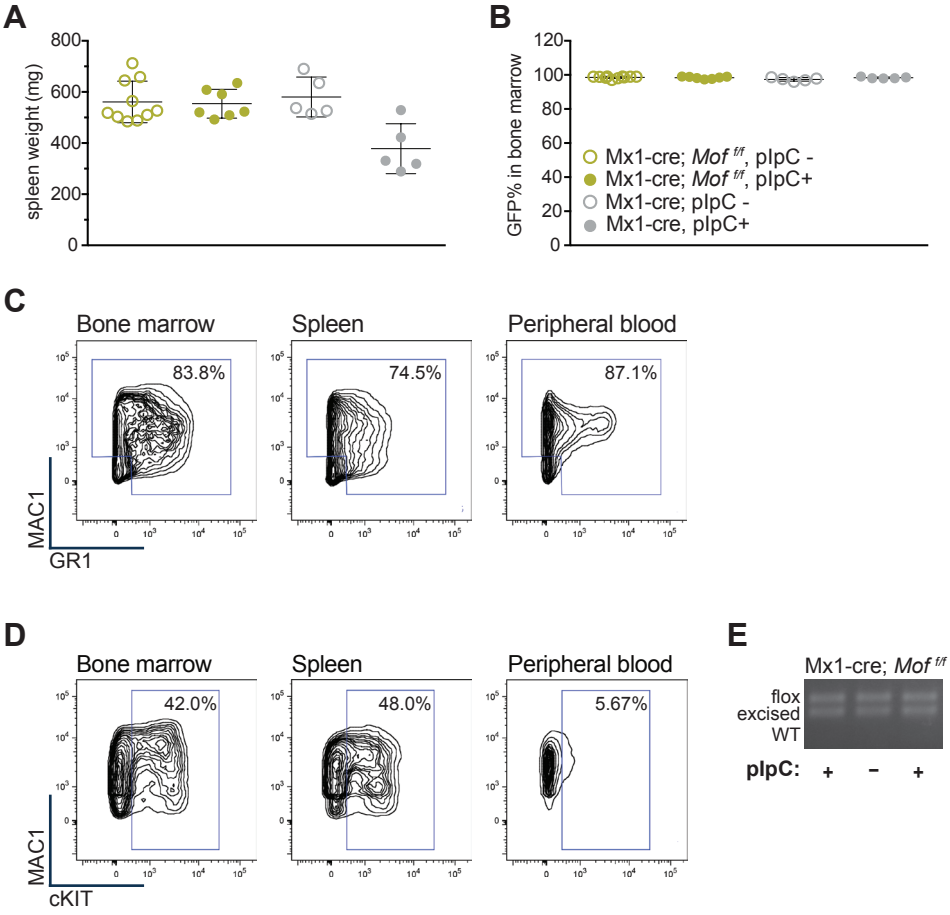

Figure S3, related to Figure 3. *Mof* loss leads to reduced tumor burden and prolonged survival in an *in vivo MLL-AF9* leukemia model

(A) Primary, GFP-tagged *MA9* leukemia BM cells in an *Mx1-cre; Mof*$^{f/f}$ or *Mx1-cre* background were injected into sub-lethally irradiated C57Bl/6 mice (n=10 for *Mx1-cre* and n=20 for *Mx1-cre; Mof* $^{f/f}$). Half of the mice per group were treated with poly-IC (pIpC) at day 15 post transplant to induce *Mof* excision. Plotted is the spleen weight of mice at time of death. A dot represents a single mouse.

(B) Graph illustrating the GFP% of live cells in bone marrow of mice at time of death.

(C) FACS plots illustrating presence of myeloid cell surface markers (MAC1 and GR1) in GFP$^+$ bone marrow, spleen and peripheral blood cells at time of death. Representative images are shown.

(D) FACS plots illustrating presence of myeloid cell surface markers (MAC1 and cKIT) in GFP$^+$ bone marrow, spleen and peripheral blood cells at time of death. Representative images are shown.

(E) PCR analysis illustrating *Mof* excision at time of death. A representative gel image is shown.

SUPPLEMENTAL EXPERIMENTAL PROCEDURES

Plasmids and constructs

NH_3-terminal HA-tagged WT *Mof* was amplified by PCR and subcloned into the HpaI site of the retroviral vector MSCV-IRES-miCD2 (MSCV-HA-*Mof*-IRES-miCD2). To generate the two *Mof* HAT domain mutants MSCV-HA-*Mof-G327E*-IRES-miCD2 and MSCV-HA-*Mof-CoAdel*-IRES-miCD2, HA-tagged *Mof-G327E* (327 glycine to glutamic acid mutation), and HA-tagged *Mof-CoAdel* (deletion of the CoA binding pocket of the MOF HAT domain, 314-333 residues) were generated using the Q5® Site-Directed Mutagenesis Kit (New England BioLabs, Ipswich, MA). The mutant and WT *Mof* constructs were verified by sequencing. The MSCV-*MLL-AF9*-IRES-GFP and MSCV-*Cre*-IRES-dTomato plasmid have been previously described.[1,2] The *pCL-Eco* plasmid was used for retroviral packaging.

Transplant experiments

For primary AML experiments, *Mx1-cre; Mof$^{f/f}$* and *Mx1-cre* mouse LSKs were harvested and infected with MSCV-*MLL-AF9*-IRES-GFP retrovirus as described. GFP$^+$ cells were sorted at 48 hours post infection and 35,000 GFP$^+$ cells injected into sub-lethally irradiated (600 cGy) 7-week-old C57Bl/6 mice. These mice developed acute myeloid leukemia (AML) within 4-8 weeks post transplant. Leukemic mice were euthanized and BM cells obtained. For secondary transplant experiments, viable frozen BM cells from primary leukemic mice were thawed and 45,000 GFP$^+$ cells injected into sub-lethally irradiated (600cGy) 6-8 week-old C57Bl/6 female recipients. At day 13 post transplant, mice were bled to check engraftment (pre pIpC). That same day, half of the mice per group were injected with pIpC (Invivogen, San Diego, USA) to induce *Cre* expression. pIpC treated mice received a total of three intraperitoneal pIpC injections, each dose 12.5 ug per gram of mouse weight, one every other day. Mice were euthanized at time of clinical symptoms of disease, coincided by leukocytosis. At time of death, bone marrow, spleen and peripheral blood were obtained. The Hemavet (Drew Scientific, Waterbury, CT) was used to obtain complete blood counts. Spleen cell suspensions were prepared by crushing the tissue through a 0.45 µm mesh filter and BM, PB and spleen cells were assessed for GFP and various immunophenotypic markers by flow cytometry on a FACS CANTOII (BD, San Jose, CA). FACS cell surface markers used were: SCA1 PE-Cy7 (eBioscience, San Diego, CA), MAC1 APC, GR1 PE, cKIT APC, cKIT PE-Cy7 and streptavidin APC-Cy7 (all Biolegend, San Diego, CA).

Western blot

Murine, *in vitro* transformed LSKs with stable expression of the *MA9* fusion and *miCD2*, *miCD2-Mof*, *miCD2-Mof-CoAdel* or *miCD2-Mof-G327E* were lysed in 1X lysis buffer (#9803, Cell Signaling, Danvers, MA). Samples were heated at 75 °C for 10 minutes, sonicated for 10 times 30 seconds and analyzed by SDS-PAGE.

Western blotting was done following standard procedures using a 10% Bis-Tris Gel (Nupage, Invitrogen, Carlsbad, CA). Proteins were transferred onto PVDF membranes

using the iBlot dry transfer system (Invitrogen, Carlsbad, CA). For assessing presence of HA-tagged MOF, H4K16ac, H4 and Actin, anti-HA antibody (HA.11, Covance, Dedham, MA), anti-H4K16ac antibody (07-329) anti-H4 antibody (07-108) and anti-Actin antibody (MAB1501R, all EMD Millipore, Billerica, MA) were used. The secondary antibodies used were either sheep anti-mouse IgG (NA931V) or anti-rabbit IgG (NA934V) ECL horseradish peroxidase linked whole antibody from GE Healthcare (Little Chalfont Buckinghamshire, UK).

Liquid cell culture

293T cells used for retroviral production were cultured in DMEM, supplemented with heat inactivated 10% fetal bovine serum (FBS) and 50 U/mL penicillin/streptomycin (all Thermo Fisher Scientific, Waltham, MA). *In vitro* transformed *MA9* mouse LSKs and *MA9* primary leukemia cells were cultured in IMDM, supplemented with heat inactivated 10% FBS, 50 U/mL penicillin/streptomycin (all Thermo Fisher Scientific, Waltham, MA) and murine IL3 (10 ng/mL), IL6 (10 ng/mL) and SCF (20 ng/mL)(all PeproTech, Rocky Hill, NJ). MOLM13 and NOMO1 cells were culture in RPMI, supplemented with heat inactivated 10% fetal bovine serum (FBS) and 50 U/mL penicillin/streptomycin (all Thermo Fisher Scientific, Waltham, MA).

yH2AX immunofluorescence staining

Cytospins were fixed using a 4% PFA/PBS mix and cells perforated with 50ug/mL Digitonin in PBS. Cells were incubated at 4 °C overnight with yH2A.X p-S139 (Abcam, Cambridge, MA) and 30 minutes at room temperature with the secondary antibody anti-rabbit Alexa488 (Molecular Probes, Thermo Fisher Scientific, Waltham, MA). Then cells were stained with DAPI and mounted using Prolong Gold Antifade Reagent (both Thermo Fisher Scientific, Waltham, MA). The number of yH2AX foci was determined using ImageJ software on representative confocal microscopy images.

MG149 treatment experiment

MG149 was dissolved in dimethyl sulfoxide (DMSO, Thermo Fisher Scientific, Waltham, MA). For MG149 treatment experiments, MOLM13, NOMO1 and murine, polyclonal primary *MA9* leukemia BM cells were plated in triplicate in a 96-well flat bottom non-treated cell culture plate (Falcon, Corning Life Sciences, Corning, NY). Cells were counted at day 3 and day 5 on a FACS CANTOII with DAPI viability stain (Thermo Fisher Scientific, Waltham, MA).

REFERENCES

1. Bernt KM, Zhu N, Sinha AU, et al. MLL-rearranged leukemia is dependent on aberrant H3K79 methylation by DOT1L. *Cancer Cell.* 2011;20(1):66-78.
2. Deshpande AJ, Deshpande A, Sinha AU, et al. AF10 regulates progressive H3K79 methylation and HOX gene expression in diverse AML subtypes. *Cancer Cell.* 2014;26(6):896-908.

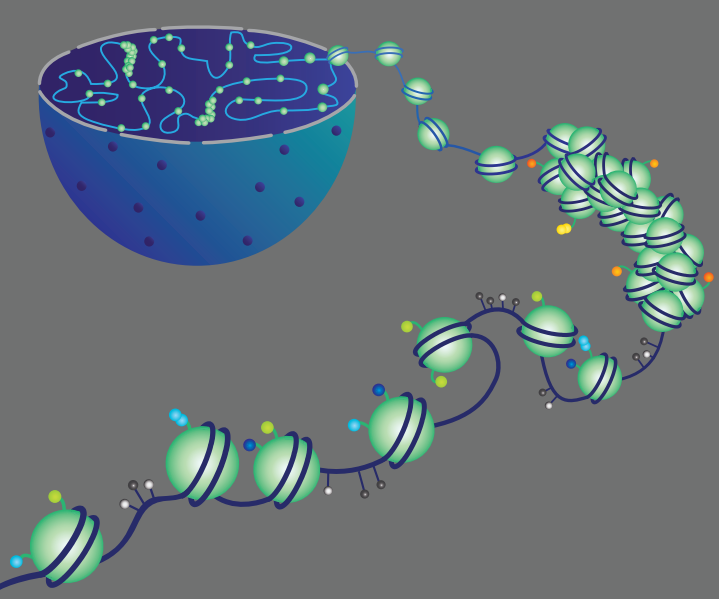

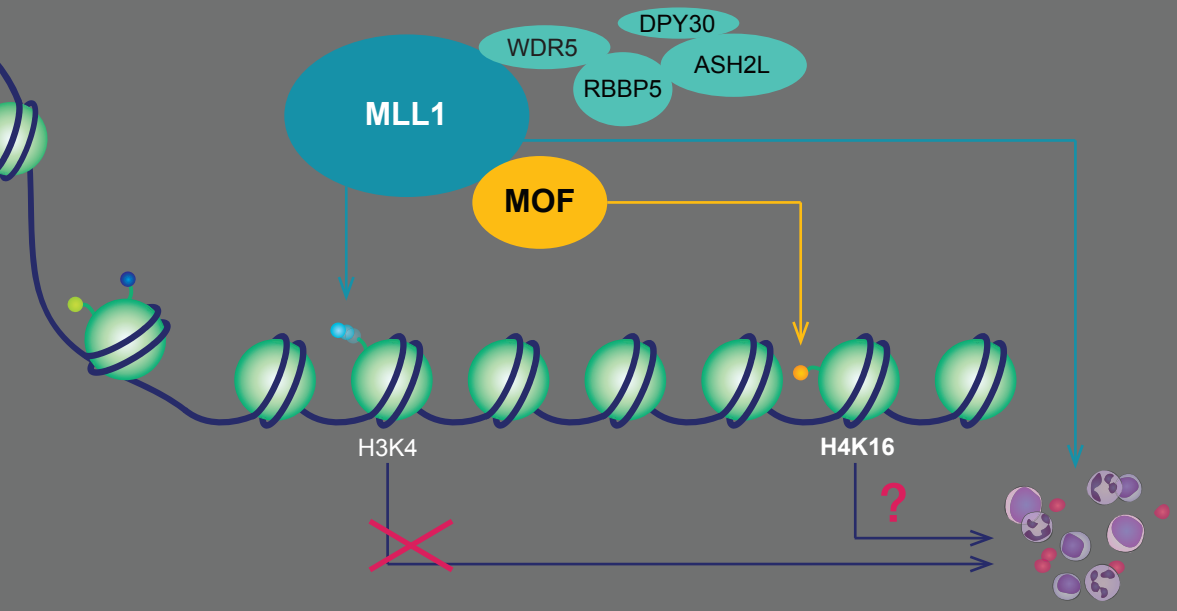
DPY30
WDR5
ASH2L
RBBP5
MLL1
MOF
H3K4
H4K16
?

5

HISTONE ACETYLTRANSFERASE ACTIVITY OF MOF IS REQUIRED FOR ADULT, BUT NOT EARLY FETAL HEMATOPOIESIS IN MICE

Daria G. Valerio & Haiming Xu, Meghan E. Eisold, Carolien M. Woolthuis, Tej K. Pandita, Scott A. Armstrong

Blood. 2016; in press

KEY POINT

MOF acetyltransferase activity is essential for adult, but not early and mid- gestational murine hematopoietic maintenance.

ABSTRACT

K(Lysine) Acetyltransferase 8 (KAT8, also known as MOF) is a histone 4 lysine 16 (H4K16) acetyltransferase and crucial for murine embryogenesis. Lysine acetyltransferases have been shown to regulate various stages of normal hematopoiesis. However, the function of *Mof* in hematopoietic stem cell (HSC) development has not yet been elucidated. We set out to study the role of MOF in general hematopoiesis by using a *Vav1-cre* induced conditional murine *Mof* knockout system, and found that MOF is critical for hematopoietic cell maintenance and HSC engraftment capacity in adult hematopoiesis. Rescue experiments with a *Mof* histone acetyltransferase domain mutant illustrated the requirement for *Mof* acetyltransferase activity in the clonogenic capacity of HSCs and progenitors. In stark contrast, fetal steady-state hematopoiesis at embryonic day 14.5 was not affected by homozygous *Mof* deletion despite dramatic loss of global H4K16ac. Hematopoietic defects start manifesting in late gestation at E17.5. The discovery that *Mof* and its H4K16 acetyltransferase activity are required for adult, but not early and mid- gestational hematopoiesis, supports the notion that multiple chromatin regulators may be crucial for hematopoiesis at varying stages of development. *Mof* is therefore a developmental-stage-specific chromatin regulator found to be essential for adult, but not early fetal hematopoiesis.

INTRODUCTION

Histone acetylation was first reported in 1964.[1] More recently, histone acetyltransferases (HATs) have been shown to acetylate various non-histone substrates, thus HATs are now categorized as lysine acetyltransferases (KATs).[2] KATs play key roles in normal and malignant hematopoiesis.[3] Acetyltransferases such as p300, CBP, MOZ GCN5 and HBO1 were shown to regulate various stages of normal blood cell development including hematopoietic stem cell (HSC) maintenance, myeloid proliferation, B-cell apoptosis and erythropoiesis.[4-8]

KATs are divided into five families according to their homology and mechanism of acetylation, among which the MYST family is the largest.[9] All members of the MYST family (named for its founding members MOZ, YBF2, SAS2 and TIP60) contain a MYST region with a canonical acetyl coenzyme A (CoA) binding site and C2HC-type zinc finger motif.[10] One of the best-characterized MYST-family proteins is K(Lysine) Acetyltransferase 8 (KAT8, also known as MOF). MOF is a histone 4 lysine 16 (H4K16) acetyltransferase[11-13] and is crucial for murine embryogenesis[13,14]. Murine embryos with homozygous, constitutional loss of *Mof* do not develop past the blastocyst stage. MOF is a cell type-dependent regulator of chromatin state and controls various essential cellular processes such as DNA damage response[15-19], cell cycle progression[15,20] and embryonic stem cell self-renewal and pluripotency[21].

MOF was shown to functionally and physically interact with the histone methyltransferase Mixed-Lineage Leukemia 1 (MLL1).[22] In hematopoiesis, *Mll1* is essential for development and maintenance of both embryonic and adult progenitors and HSCs.[23,24] However, it's methyltransferase activity was recently shown to be dispensable for HSC maintenance and functionality.[25] These findings prompt the question whether MOF and its HAT activity are required for hematopoiesis. In 2013, Gupta et al. have shown that T-cell specific deletion of *Mof* blocks differentiation and reduces T-cell numbers.[26] To assess the role of MOF in hematopoietic development and HSC maintenance and differentiation, we used a conditional murine system[14] in which the *Vav1* promoter drives early embryonic hematopoietic expression of *Cre* recombinase[27] (*Vav1-cre*; *Mof*$^{f/f}$ mice). We found that MOF is critical for hematopoiesis in newborn and adult mice. In addition, we show that MOF acetyltransferase activity is required for hematopoietic stem cell and progenitor maintenance and colony-forming capacity. However, MOF and H4K16ac seem dispensable for maintenance of the highly proliferative E14.5 fetal hematopoietic system. Together our findings illustrate that MOF-controlled chromatin regulation is a developmental-stage-specific mechanism for hematopoietic maintenance.

RESULTS

Homozygous *Mof* loss leads to lethal hematopoietic failure in mice shortly after birth

To examine the function of *Mof* in hematopoiesis, we used a conditional murine system[14] in which the *Vav1* promoter drives hematopoietic expression of *Cre* recombinase[27]. *Mof*$^{f/f}$ mice

were backcrossed to C57Bl/6 mice.[14] Mice with homozygous *Mof* loss in the hematopoietic compartment (*Vav1-cre*; *Mof$^{f/f}$*) were carried to term and born with Mendelian frequencies, but died 8 to 11 days after birth (P8-P11) whereas heterozygous *Mof* loss (*Vav1-cre*; *Mof$^{f/+}$*) did not affect survival (Figure 1A). At time of death, *Vav1-cre*; *Mof$^{f/f}$* P9 pups were smaller than both the heterozygous and wild type (*Mof$^{f/f}$*) control (Figure 1B), had a smaller spleen and thymus (Figure 1C and S1A), were pancytopenic (Figure 1D) and had low bone marrow (BM) cellularity (Figure 1E). Flow cytometry (FACS) analysis of BM and spleen indicated that the absolute number of mature myeloid, lymphoid and erythroid cells was significantly reduced in *Vav1-cre*; *Mof$^{f/f}$* P9 pups (Figure 1F, S1B and S1C). A similar pattern was found in the T-cell lineage in thymoid tissue (Figure S1D and S1E). Total number of myeloid progenitors (MPs, Lin$^-$SCA1$^-$cKIT$^+$) and Lin$^-$SCA1$^+$cKIT$^+$ (LSK) cells in *Vav1-cre*; *Mof$^{f/f}$* P9 BM were also significantly lower (Figure 1G). Within the BM compartment the relative number of mature myeloid and lymphoid cells (Figure S1F), and erythroid cells (data not shown) remained similar, while the percentage of LSKs and MPs was significantly reduced in *Vav1-cre*; *Mof$^{f/f}$* P9 pups (Figure S2A and S2B). FACS analysis indicated a reduction of cKIT$^+$ cells within the Lin$^-$ BM population of *Vav1-cre*; *Mof$^{f/f}$* pups (Figure S2A). These FACS analyses indicate that in steady state hematopoiesis, while absolute numbers of all hematopoietic populations are down, LSKs and MPs are also reduced in percentage relative to total hematopoietic cells. Together, these data show that homozygous *Mof* loss leads to lethal hematopoietic failure in mice shortly after birth, and that while cell numbers in all lineages are affected, HSC-enriched populations may suffer the greatest losses.

Vav1-cre-Mof$^{f/f}$ P9 hematopoietic bone marrow cells are functionally impaired

To test the functionality of P9 *Vav1-cre*; *Mof$^{f/f}$* BM MPs and HSCs, colony-forming capacity was tested in a colony-forming unit (CFU) assay. Figure 2A illustrates a significant but variable reduction in colony count and total number of live cells in *Vav1-cre*; *Mof$^{f/f}$* BM cells compared to *Vav1-cre*; *Mof$^{f/+}$* or *Mof$^{f/f}$* BM cells. The type of colonies generated by *Vav1-cre*; *Mof$^{f/f}$* BM cells did not differ significantly (Figure 2B). Next, we performed non-competitive transplant experiments where 633,000 *Vav1-cre*; *Mof$^{f/f}$*, *Vav1-cre*; *Mof$^{f/+}$* or *Mof$^{f/f}$* CD45.2$^+$ BM cells were

Figure 1. *Vav1-cre* induced homozygous *Mof* loss leads to lethal hematopoietic failure in pups
(A) Survival curve of *Vav1-cre-Mof$^{f/f}$* and *Vav1-cre-Mof$^{f/+}$* mice represented as days after birth (x-axis).
(B) Representative photographs of 9-day-old *Vav1-cre-Mof$^{f/f}$*, *Vav1-cre-Mof$^{f/+}$* and *Mof$^{f/f}$* pups.
(C) Representative photographs of spleen, thymus and liver of 9-day-old *Vav1-cre-Mof$^{f/f}$*, *Vav1-cre-Mof$^{f/+}$* and *Mof$^{f/f}$* pups. Colors of arrows correlate to mouse genotype (*Vav1-cre-Mof$^{f/f}$* orange, *Vav1-cre-Mof$^{f/+}$* mustard green, *Mof$^{f/f}$* blue).
(D) White blood cell (WBC) count, hemoglobin (Hb) and platelet count at time of sacrifice.

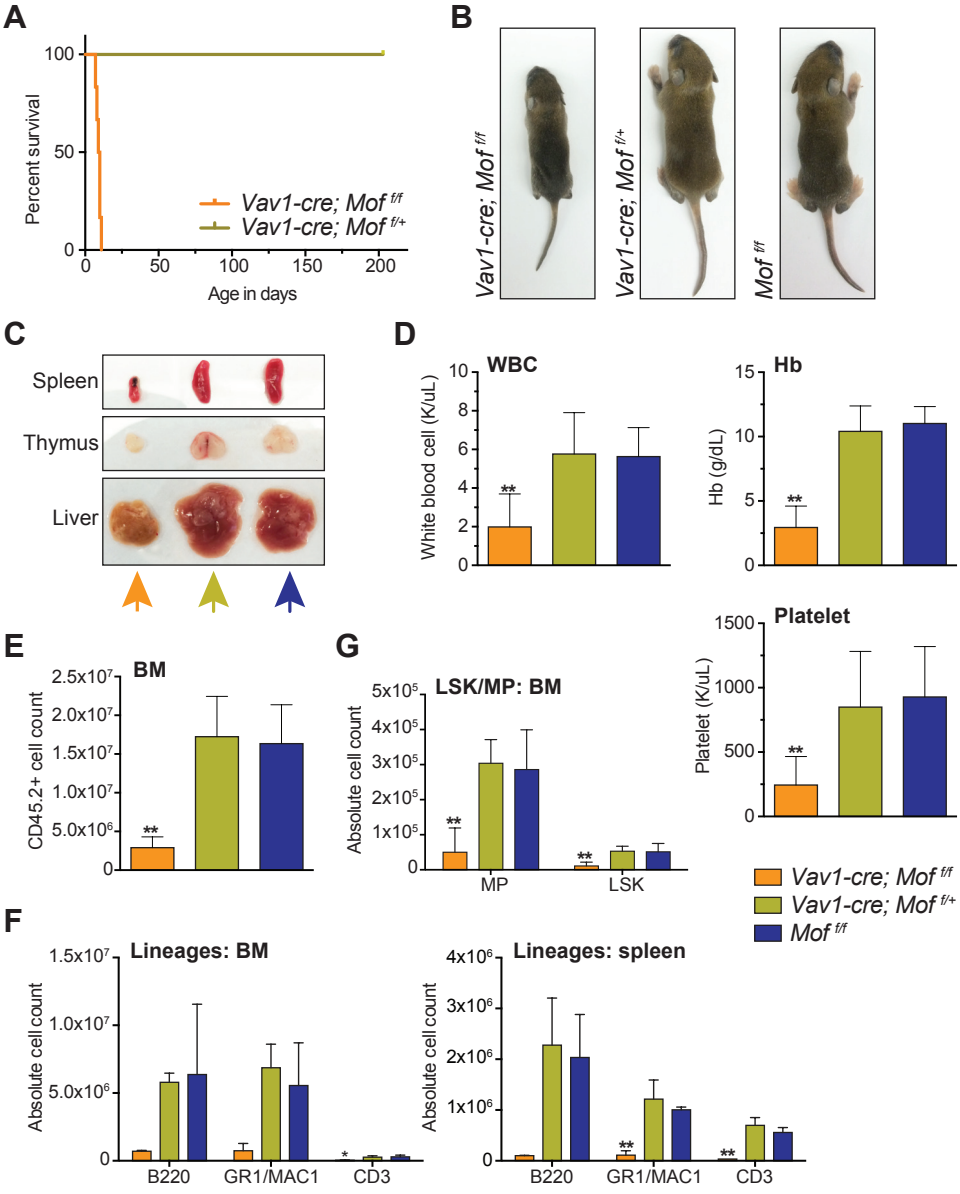

(E) Bone marrow (BM) cell count after CD45.2 selection.

(F) Bar graphs representing the total number of mature B-cells (B220$^+$), myeloid cells (GR1$^+$/MAC1$^+$), and T-cells (CD3$^+$) in BM (harvested from femurs, pelvic bones, tibias and spine) and spleen as measured by FACS.

(G) Bar graph representing the total number of myeloid progenitor (MP) and Lin$^-$SCA1$^+$cKIT$^+$ LSKs in BM as measured by FACS.

* $p < 0.05$, ** $p < 0.01$. Error bars show SD of mean. Significance compared to *Moff/f.*

injected into lethally irradiated B6.SJL (CD45.1+) mice (Figure 2C). Two out of four *Vav1-cre*; *Mof*$^{f/f}$ recipients had to be sacrificed within 12 days post transplant (Figure 2D) due to failure of donor cells to give rise to the minimally required hematopoiesis to survive lethal irradiation (data not shown). Figure 2E illustrates the low percentage of donor cells (CD45.2+) present in the recipient BM of the *Vav1-cre*; *Mof*$^{f/f}$ recipient mice that failed to engraft, compared to a properly engrafted *Vav1-cre*; *Mof*$^{f/+}$ recipient mouse (8.8% versus 96.5%). CD45.2 percentages of all surviving recipients were monitored every 4 weeks (Figure 2F) and mice were sacrificed 16 weeks post transplant, at which time BM engraftment was around 90% in all groups (data not shown). PCR analysis of *Mof* excision demonstrated incomplete excision in CD45.2+ BM cells derived from *Vav1-cre*; *Mof*$^{f/f}$ recipients whereas the floxed allele was completely excised in CD45.2+ BM cells from heterozygous recipients (Figure 2G), indicating that complete homozygous deletion of *Mof* is not compatible with engraftment. Overall these functional experiments showed a variable phenotype of hematopoietic *Vav1-cre*; *Mof*$^{f/f}$ cells. However, excision PCR data (Figure 2G) suggest that this variability is due to a high selection pressure against complete excision of *Mof*, indicating that complete homozygous excision is not compatible with functional engraftment of post-natal hematopoietic cells in a non-competitive transplant setting.

Mx1-cre induced homozygous *Mof* loss in adult mice results in dramatic hematopoietic failure

Since *Vav1-cre*; *Mof*$^{f/f}$ mice did not live past the first 2 weeks of life, we utilized the *Mx1-cre* system to assess the effect of *Mof* loss on adult hematopoiesis. In *Mx1-cre* mice, the *Mx1* promoter drives expression of *Cre* and can be induced by synthetic double-stranded RNA such as poly I:C (pIpC). In adult *Mx1-cre*; *Mof*$^{f/f}$ and *Mx1-cre*; *Mof*$^{f/+}$ mice, induction of *Cre* by pIpC injections resulted in a rapid and lethal pancytopenia in *Mx1-cre*; *Mof*$^{f/f}$ mice (data not shown). While *Mx1* is not only expressed in hematopoietic tissue, but in various organs, we used a competitive transplant model to better assess the fate of adult hematopoietic

Figure 2. *Vav1-cre-Mof*$^{f/f}$ P9 hematopoietic bone marrow cells are functionally impaired

(A) Day 10 of CFU assay of fresh, CD45.2+ *Vav1-cre-Mof*$^{f/f}$, *Vav1-cre-Mof*$^{f/+}$ and *Mof*$^{f/f}$ P9 bone marrow (BM) cells. Bar graphs indicate mean number of colonies after 10 days (left) and number of live cells (right) per plating. 20,000 cells were plated per dish. Data are representative of 3 experiments with multiple donor mice per experiment.

(B) Mean percentage of the various colony types relative to all colonies counted per dish per genotype.

(C) Schematic for transplant experiment with CD45.2+ *Vav1-cre-Mof*$^{f/f}$, *Vav1-cre-Mof*$^{f/+}$ and *Mof*$^{f/f}$ P9 BM cells. B6.SJL recipient mice were injected with BM cells shortly after lethal irradiation (2 x 5Gy). The experiment was repeated three times with multiple donor mice per genotype, per experiment.

(D) Survival curve of recipient mice. Mice were all sacrificed 16 weeks (wks) post transplant. *Vav1-cre-Mof*$^{f/f}$ n=4, *Vav1-cre-Mof*$^{f/+}$ n=8, *Mof*$^{f/f}$ n=9.

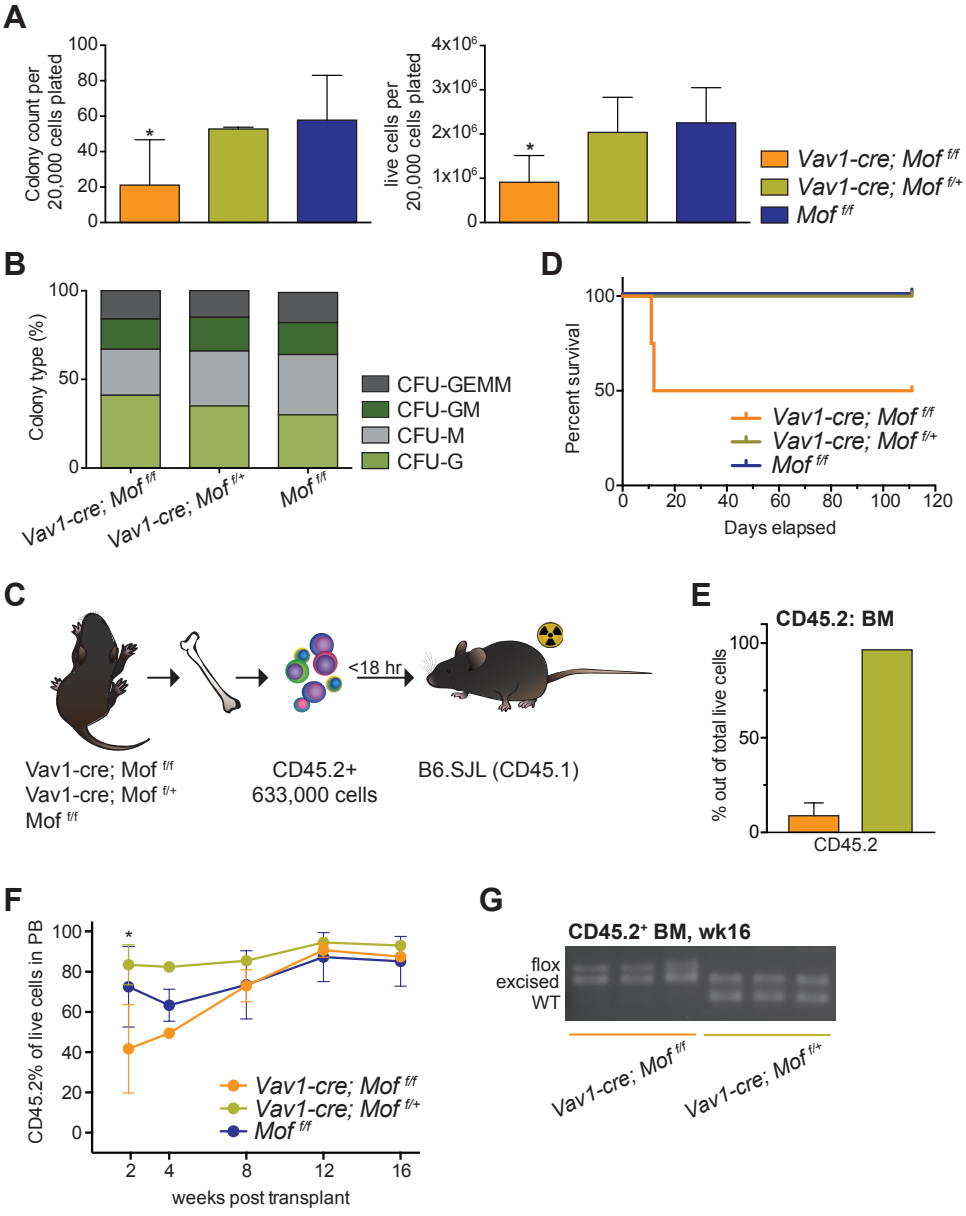

(E) Bar graph illustrating the percentage of donor cells (CD45.2+) present in recipient BM comparing the failed *Vav1-cre*; *Mof*$^{f/f}$ recipient mice to a properly engrafted *Vav1-cre*; *Mof*$^{f/+}$ recipient mouse.
(F) CD45.2% of live cells in peripheral blood (PB) over the time-course of the transplant experiments.
(G) PCR analysis illustrating *Mof* excision in CD45.2+ BM cells at time of sacrifice. A representative image is shown.
* $p < 0.05$. Error bars show SD of mean. Significance compared to *Moff/f*.

cells upon MOF loss. Whole BM cells derived from an *Mx1-cre*; *Mof*$^{f/f}$, *Mx1-cre* or *Mof*$^{f/f}$ mouse were mixed at a 1:1 ratio with whole BM cells from a wild type (WT) B6.SJL mouse and injected into lethally irradiated B6.SJL recipients (Figure 3A). After 16 weeks the mean CD45.2 percentage in the peripheral blood (PB) was 26% in *Mx1-cre*; *Mof*$^{f/f}$ recipients, 37% in *Mx1-cre* recipients and 44% in *Mof*$^{f/f}$ recipients (data not shown). Per genotype, mice were split in two even groups with a similar mean CD45.2 percentage and *Cre* expression was induced in one group each, by pIpC injections. Two weeks after the last dose, mice were euthanized and processed. Figure 3B, C and D show the CD45.2 percentage of live cells in PB, BM and spleen respectively, illustrating that homozygous *Mof* loss leads to a rapid and nearly complete loss of adult hematopoietic cells. While mature myeloid cells are relatively more depleted in *Mx1-cre*; *Mof*$^{f/f}$ pIpC+ CD45.2$^+$ BM cells than mature lymphoid cells (Figure 3E), it becomes evident from the absolute cell counts (Figure 3F) that all lineages within the CD45.2$^+$ compartment are dramatically depleted. A similar pattern was observed for the few residual CD45.2$^+$ cells that remained in PB and spleen (Figure S3A and S3B). FACS analysis for progenitors and HSCs showed a significant depletion of MPs, LSKs and LT-HSCs relative to the total number of CD45.2$^+$ cells in *Mof*-deficient BM cells (Figure 3G, S3C and S3D). Our findings indicate that *Mof* is not only required to maintain postnatal, but also adult hematopoiesis. Similar to what was found in postnatal hematopoiesis, cell numbers in all lineages are strongly affected by *Mof* loss in an adult transplant setting, but HSCs and progenitors suffer the greatest losses.

→

Figure 3. *Mx1-cre* induced homozygous *Mof* loss in adult mice results in dramatic hematopoietic failure

(A) Schematic for competitive transplant experiment with whole bone marrow (BM) cells derived from adult *Mx1-cre-Mof*$^{f/f}$, *Mx1-cre* and *Mof*$^{f/f}$ mice and BM cells from a B6.SJL mouse. B6.SJL recipient mice were injected with fresh BM cells shortly after lethal irradiation. After 16 weeks, half of the mice per genotype were injected with pIpC and 2 weeks after the 5th dose of pIpC, mice were euthanized and processed. The experiment was performed with 2 donors per genotype and 16-18 recipients per group.
(B) CD45.2% of live cells in peripheral blood (PB) of mice at time of sacrifice, post pIpC treatment. Each dot represents a single mouse in the experiment.
(C) CD45.2% of live cells in bone marrow (BM) of mice at time of sacrifice, post pIpC treatment.
(D) CD45.2% of live cells in spleen of mice at time of sacrifice, post pIpC treatment.
(E) Percentages of mature B-cells (B220$^+$), myeloid cells (GR1$^+$/MAC1$^+$), and T-cells (CD3$^+$) in live, CD45.2$^+$ BM cells as measured by FACS at time of sacrifice.
(F) The total number of CD45.2$^+$ mature B-cells, myeloid cells, and T-cells as measured by FACS at time of sacrifice.
(G) Percentages of LT-HSCs (CD150$^+$/CD48$^-$) within the live, CD45.2$^+$, LSK BM population as measured by FACS at time of sacrifice.
* p = 0.0006, ** p = 0.0001, **** p < 0.000006. Error bars show SD of mean.

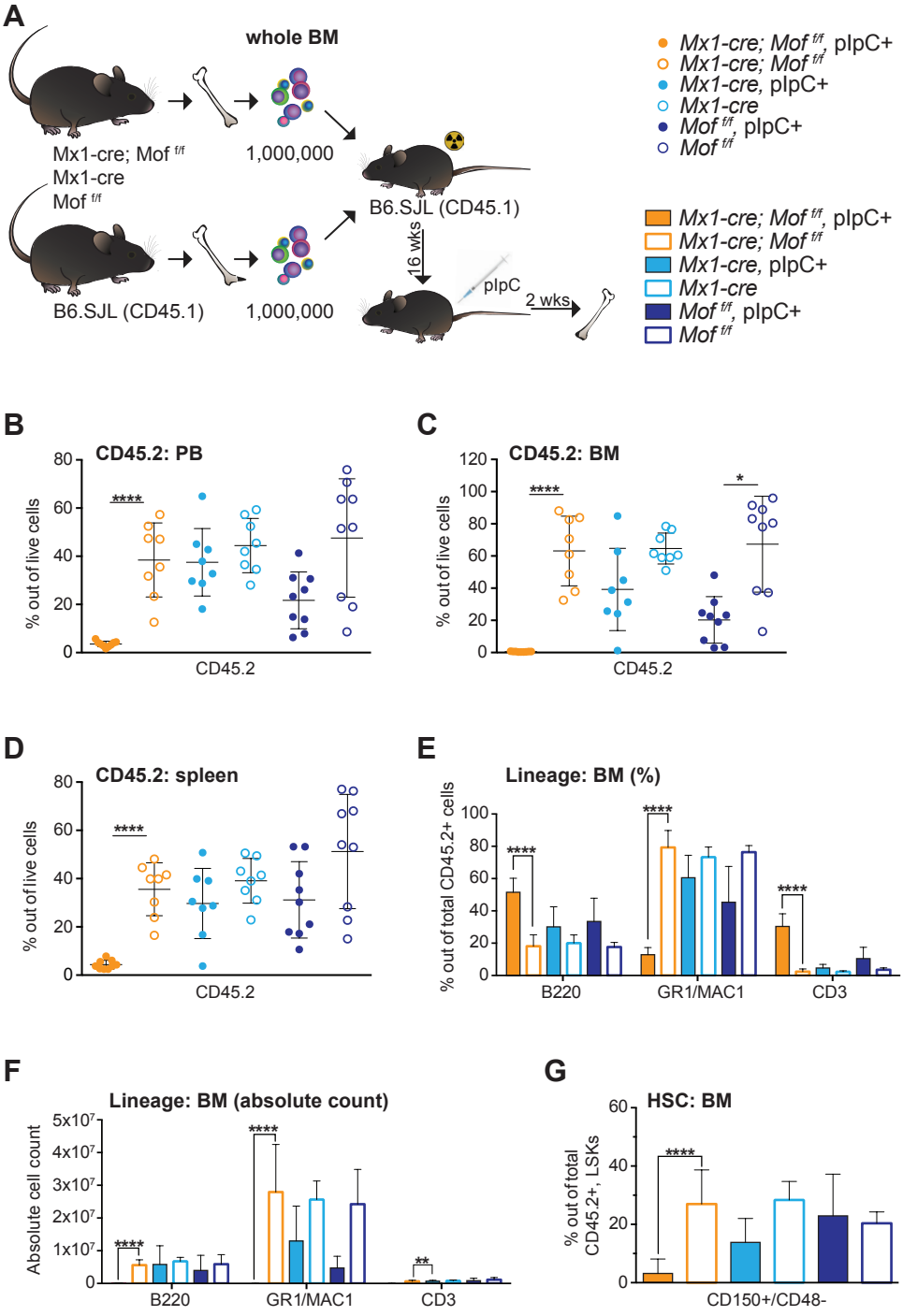
A
whole BM
Mx1-cre; Mof f/f
Mx1-cre
Mof f/f
1,000,000
B6.SJL (CD45.1)
B6.SJL (CD45.1)
1,000,000
16 wks
pIpC
2 wks
Mx1-cre; Mof f/f, pIpC+
Mx1-cre; Mof f/f
Mx1-cre, pIpC+
Mx1-cre
Mof f/f, pIpC+
Mof f/f
B
CD45.2: PB
% out of live cells
CD45.2
C
CD45.2: BM
% out of live cells
CD45.2
D
CD45.2: spleen
% out of live cells
CD45.2
E
Lineage: BM (%)
% out of total CD45.2+ cells
B220
GR1/MAC1
CD3
F
Lineage: BM (absolute count)
Absolute cell count
B220
GR1/MAC1
CD3
G
HSC: BM
% out of total CD45.2+, LSKs
CD150+/CD48-

Homozygous *Mof* loss does not affect fetal hematopoiesis at E14.5

Essentially all definitive blood cells and a significant proportion of yolk sac derived primitive blood cells express *Vav1*.[27] In the embryo, *Vav1* expression appears first in the liver, where it becomes just detectable at E9.5 and stronger at E12.5. At that stage, the liver has begun to replace the yolk sac and Aorta-Gonad-Mesonephros system as the major hematopoietic organ.[28] At E14.5, fetal hematopoiesis is at its peak in the liver after which it starts to divert to the BM. At E18 most of the hematopoietic progenitors are still located in the liver, but gradually decrease through postnatal day 14 (P14) and already at P4, the majority of hematopoietic progenitors are found in the BM compartment.[29]

Since *Vav1-cre*; *Mof*$^{f/f}$ pups were delivered to term but displayed lethal hematopoietic defects about a week after birth, we set out to study the effects of *Mof* loss on hematopoiesis in murine embryos at E14.5 when fetal liver (FL) hematopoiesis is at its peak. The appearance of *Vav1-cre*; *Mof*$^{f/f}$ embryos did not differ from their heterozygous and WT siblings (Figure 4A) and FL cellularity was consistent over all three genotypes (Figure 4B). PCR analysis on fresh, CD45.2$^+$ FL cells illustrated complete *Mof* excision of the floxed alleles in *Vav1-cre*; *Mof*$^{f/f}$ and *Vav1-cre*; *Mof*$^{f/+}$ (Figure 4C) and RT-qPCR data show substantial downregulation of *Mof* in the homozygous knockout cells (Figure S4A). Consistent with homozygous *Mof* deletion, Western blot analysis showed loss of global H4K16ac in CD45.2$^+$ *Vav1-cre*; *Mof*$^{f/f}$ FL cells (Figure 4D). Despite this significant loss of H4K16ac in *Mof*-deficient FL cells, FACS analysis showed no change in lymphoid, myeloid and erythroid lineages (Figure 4E and 4F), and also MP, LSK and HSC populations were preserved (Figure 4G). These data indicate that *Mof* and subsequent H4K16ac loss does not affect steady state fetal hematopoiesis at E14.5.

Figure 4. *Vav1-cre* induced homozygous *Mof* loss does not affect fetal hematopoiesis at E14.5

(A) Representative photographs of *Vav1-cre-Mof*$^{f/f}$, *Vav1-cre-Mof*$^{f/+}$ and *Mof*$^{f/f}$ embryos at E14.5.

(B) Total live fetal liver (FL) cell count.

(C) PCR analysis illustrating *Mof* excision in fresh CD45.2$^+$ FL cells. A representative image is shown.

(D) Western blot showing global H4K16ac, H4 and Actin in fresh CD45.2$^+$ FL cells.

(E) Percentages of mature B-cells (B220$^+$), myeloid cells (GR1$^+$), and T-cells (CD3$^+$) in live FL cells as measured by FACS.

(F) Percentages of cells at various stages of differentiation within the erythroid lineage in live FL cells as measured by FACS.

(G) Percentages of MPs and LSKs in live, Lin$^-$ FL cells, and HSCs (CD150$^+$/CD48$^-$) as a percentage of LSKs, all measured by FACS.

Error bars show SD of mean.

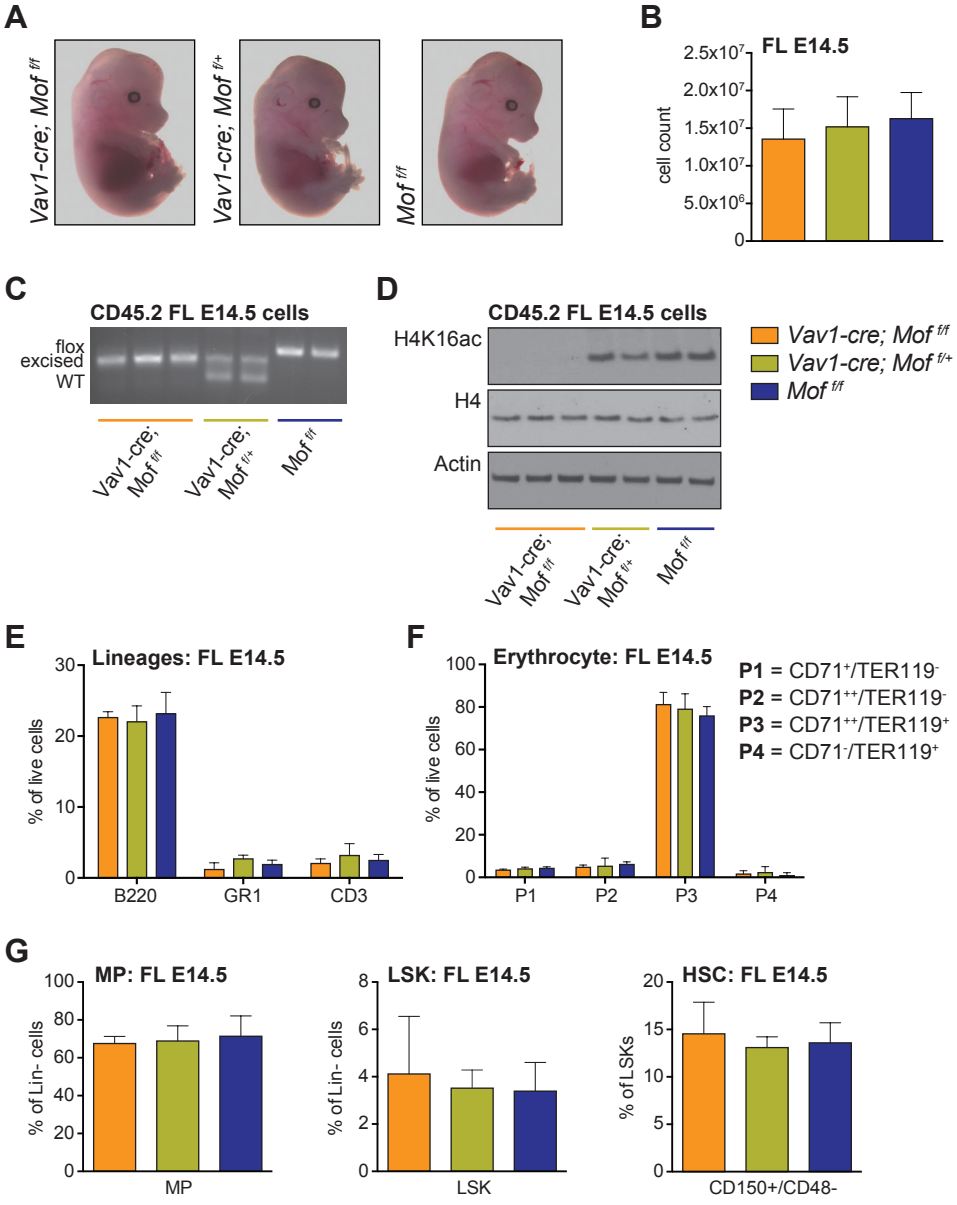

***Vav1-cre-Mof*$^{f/f}$ hematopoietic E14.5 fetal liver cells are functionally impaired**

CFU assays were performed to assess the functional capacity of E14.5 *Vav1-cre*; *Mof*$^{f/f}$ FL HSCs and myeloid progenitors. The colony-forming capacity of *Vav1-cre*; *Mof*$^{f/f}$ FL cells was greatly diminished (Figure 5A). The few colonies that formed were more mature (CFU-M

and CFU-G, Figure 5B), suggesting that HSCs or early progenitors may be affected by *Mof* loss to a greater extent than the more mature populations. Next, we performed two non-competitive transplant experiments where 2,000,000 *Vav1-cre*; *Mof*$^{f/f}$, *Vav1-cre*; *Mof*$^{f/+}$ or *Mof*$^{f/f}$ unselected FL cells were injected into lethally irradiated B6.SJL mice (Figure 5C). All six *Vav1-cre*; *Mof*$^{f/f}$ recipients had to be sacrificed within 12 days post transplant (Figure 5D) due to failure of donor cells to give rise to the minimally required hematopoiesis to survive lethal irradiation (CBC data not shown). Figure 5E shows the percentage of donor cells (CD45.2^{+}) present in the recipient PB. This shows that *Mof*-deficient E14.5 FL cells were unable to reconstitute hematopoiesis in adult mice, whereas heterozygous *Mof* loss did not affect reconstitution. These findings are suggestive of a possible homing defect of FL cells to the BM and indeed, we found *Vav1-cre*; *Mof*$^{f/f}$ cells to exhibit impaired homing capacity in a transplant setting (Figure S4B and S4C).

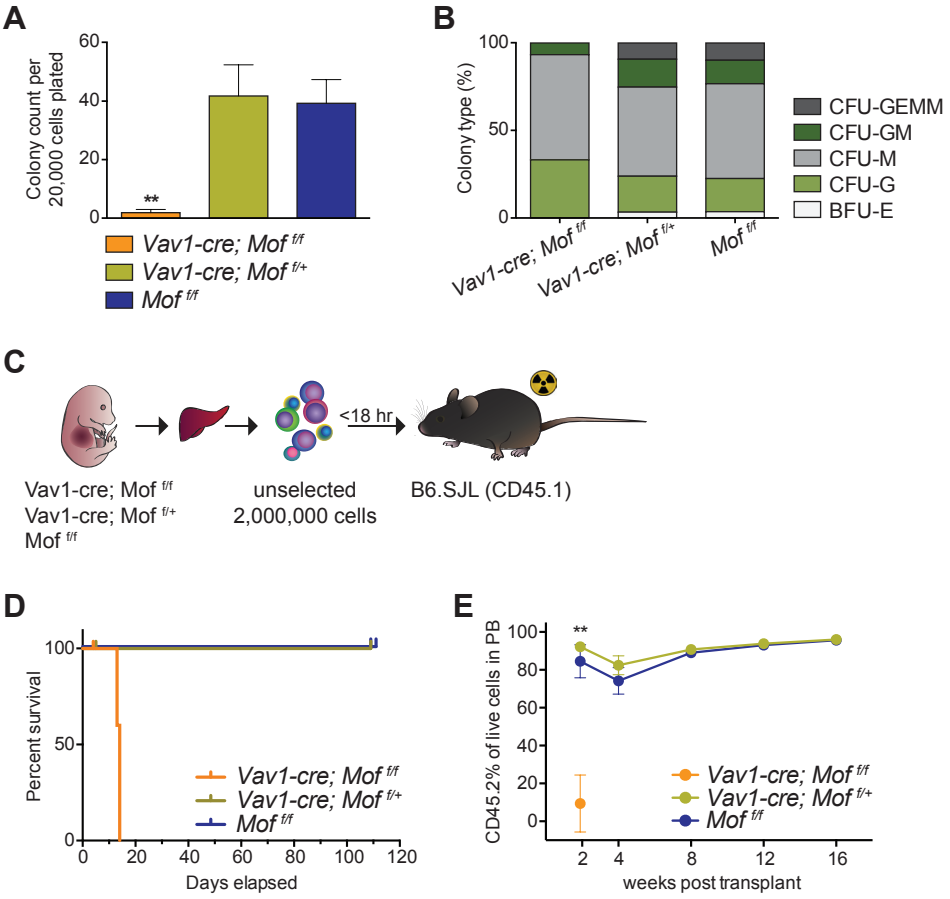

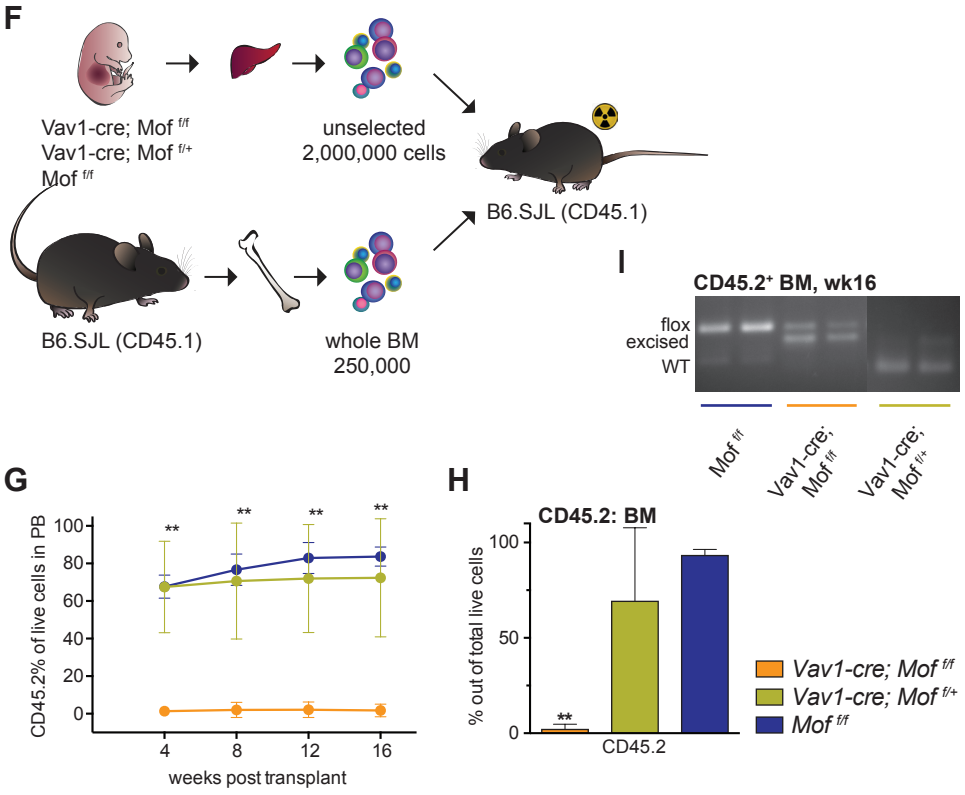

Figure 5. *Vav1-cre-Mof$^{f/f}$* hematopoietic E14.5 fetal liver cells are functionally impaired

(A) Day 10 of CFU assay of fresh fetal liver (FL) cells derived from E14.5 *Vav1-cre-Mof$^{f/f}$*, *Vav1-cre-Mof$^{f/+}$* and *Mof$^{f/f}$* embryos. Bar graph indicates mean number of colonies per dish after 10 days. 20,000 cells were plated per dish. Data are representative of 3 experiments with multiple embryos per experiment.

(B) Mean percentage of the various colony types relative to all colonies counted per dish per genotype.

(C) Schematic for transplant experiment with FL cells derived from E14.5 *Vav1-cre-Mof$^{f/f}$*, *Vav1-cre-Mof$^{f/+}$* and *Mof$^{f/f}$* embryos. B6.SJL recipient mice were injected with FL cells shortly after lethal irradiation (2 x 5Gy). The experiment was repeated 2 times with multiple donor embryos per genotype, per experiment.

(D) Survival curve of recipient mice. Mice were all sacrificed 16 weeks post transplant. *Vav1-cre-Mof$^{f/f}$* n=6, *Vav1-cre-Mof$^{f/+}$* n=6, *Mof$^{f/f}$* n=7.

(E) CD45.2% of live cells in peripheral blood (PB) over the time-course of the transplant experiments.

(F) Schematic for transplant experiment with FL cells derived from E14.5 *Vav1-cre-Mof$^{f/f}$*, *Vav1-cre-Mof$^{f/+}$* and *Mof$^{f/f}$* embryos and 250,000 whole BM helper cells. B6.SJL recipient mice were injected with cells shortly after lethal irradiation. The experiment was repeated two times with multiple donor embryos per genotype, per experiment.

(G) CD45.2% of live cells in the peripheral blood over the time-course of the transplant experiments. *Vav1-cre-Mof$^{f/f}$* n=6, *Vav1-cre-Mof$^{f/+}$* n=5, *Mof$^{f/f}$* n=5.

(H) CD45.2% of live cells in BM of recipient mice at week 16.

(I) PCR analysis illustrating *Mof* excision in CD45.2^{+} BM cells at time of sacrifice.

** $p < 0.01$. Error bars show SD of mean. Significance compared to *Moff/f*.

To determine short- and long-term engraftment potential of *Mof*-deficient E14.5 FL cells, the rapid death of recipient mice due to lethal irradiation had to be circumvented. Therefore, we repeated the FL transplants, but now co-injected 250,000 whole BM, CD45.1$^+$ WT helper cells (Figure 5F). These helper cells were capable of rescuing *Vav1-cre*; *Mof$^{f/f}$* recipient mice from lethal irradiation death. Over the entire time course of the experiment, CD45.2 percentages did not rise above 2% in the PB of *Vav1-cre*; *Mof$^{f/f}$* FL recipients while *Vav1-cre*; *Mof$^{f/+}$ and Mof$^{f/f}$* recipients demonstrated stable engraftment with CD45.2 percentages around 75% (Figure 5G). At time of sacrifice (week 16 post transplant), the mean CD45.2 percentage in BM of *Mof*-deficient FL recipients was 1.8%; significantly lower than the CD45.2 percentage in *Vav1-cre*; *Mof$^{f/+}$* (69.2%) or *Mof$^{f/f}$* (93.2%) FL recipients (Figure 5H). The few FL cells that did engraft in the *Vav1-cre*; *Mof$^{f/f}$* group were only partially excised, unlike the engrafted *Vav1-cre*; *Mof$^{f/+}$* FL cells in which the one allele was completely excised (Figure 5I). FACS analysis of the CD45.2$^+$ BM cells revealed no significant differences between the three groups with regard to the percentage of mature lymphocytes, myeloid cells (Figure S4D), LSKs and LT-HSCs (Figure S4E).

In contrast to the presumably normal hematopoiesis in *Vav1-cre*; *Mof$^{f/f}$* embryos, these experiments demonstrated significant functional impairment of *Mof*-deficient E14.5 FL cells. However, these experiments address fetal HSC functionality outside of the fetal microenvironment and therefore suggest an important role of the fetal microenvironment in maintaining normal hematopoiesis in *Vav1-cre*; *Mof$^{f/f}$* embryos.

Mof-deficient embryos start manifesting hematopoietic defects at E17.5

We wished to further narrow down the time frame in which murine hematopoiesis starts to derail due to *Mof* deficiency. Given the lack of phenotype in *Mof*-deficient E14.5 hematopoiesis, we chose to assess FL hematopoiesis at E17.5, a late gestational age, only a day or two before birth. Gross morphology of *Vav1-cre*; *Mof$^{f/f}$* embryos appeared normal (Figure 6A) and the *Mof* allele was largely excised in hematopoietic *Vav1-cre*; *Mof$^{f/f}$* FL cells (Figure 6B), consistent with a loss of global H4K16ac (Figure 6C). Total FL cell counts were comparable between all three groups (Figure 6D) and erythroid populations did not appear affected by loss of *Mof* (Figure 6E), fitting with the normal appearance of *Mof*-null embryos. However, the CD45.2$^+$ cell number was significantly decreased in E17.5 *Vav1-cre*; *Mof$^{f/f}$* livers (Figure 6F). FACS analysis of these *Mof*-deficient CD45.2$^+$ FL cells indicated that the absolute number of mature myeloid and lymphoid cells (Figure 6G), and the number of MPs, LSKs and HSCs (Figure 6H), was significantly reduced in *Vav1-cre*; *Mof$^{f/f}$* embryos. These *Mof*-deficient FL cells were also functionally impaired, whereas they formed fewer colonies than the heterozygous and WT control (Figure 6I). The type of colonies did not differ significantly (Figure 6J). Together these findings suggest that the hematopoietic defects resulting from *Mof* and subsequent H4K16ac loss start manifesting in late gestation, though at E17.5 the phenotype is still quite modest compared to the phenotype in pups and adult mice. Interestingly, at E17.5 the erythroid lineage seems intact, which could explain why *Mof*-deficient embryos are born at normal ratios.

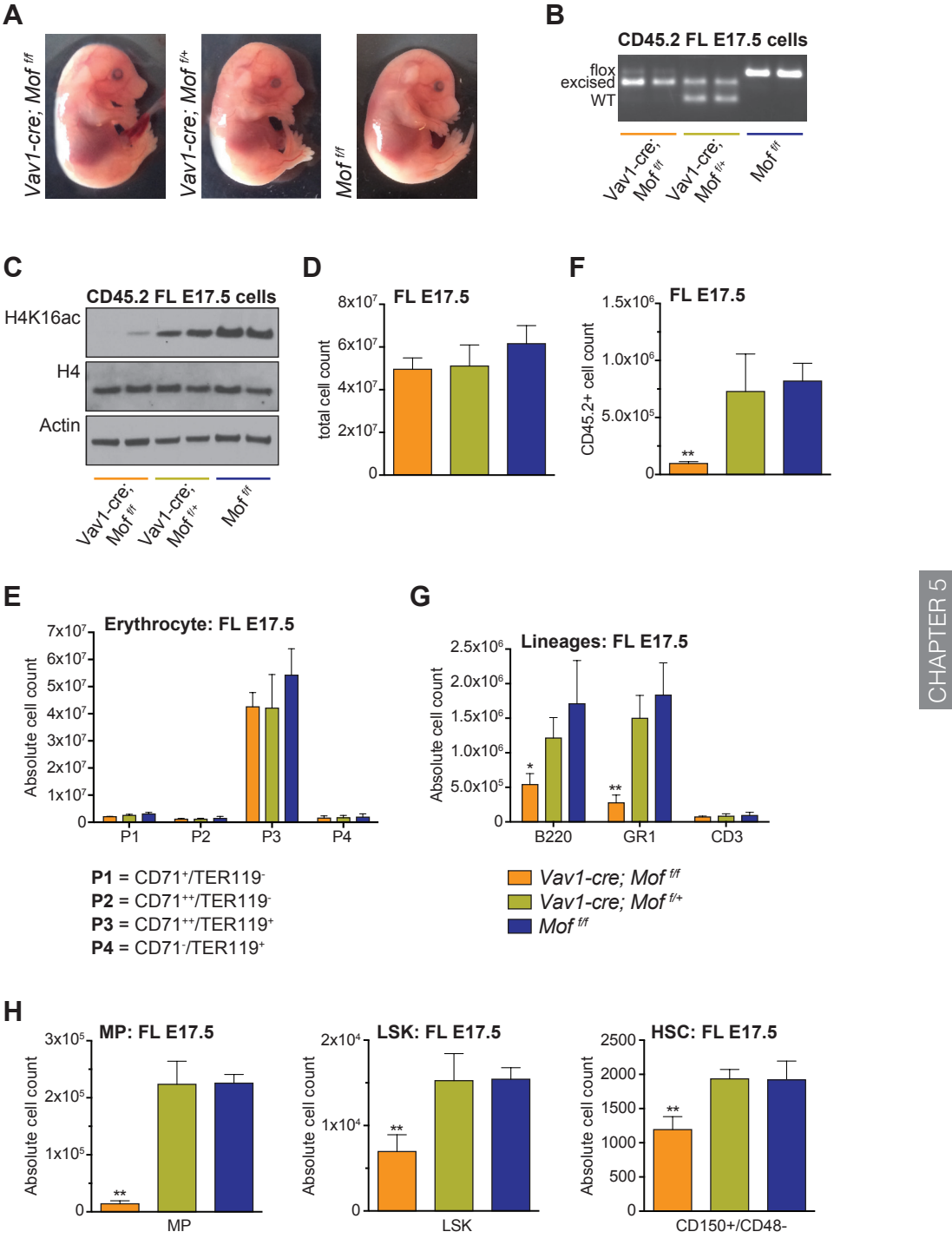
A
Vav1-cre; Mof f/f
Vav1-cre; Mof f/+
Mof f/f
B
CD45.2 FL E17.5 cells
flox
excised
WT
Vav1-cre; Mof f/f
Vav1-cre; Mof f/+
Mof f/f
C
CD45.2 FL E17.5 cells
H4K16ac
H4
Actin
Vav1-cre; Mof f/f
Vav1-cre; Mof f/+
Mof f/f
D
FL E17.5
total cell count
8x10^7
6x10^7
4x10^7
2x10^7
0
F
FL E17.5
CD45.2+ cell count
1.5x10^6
1.0x10^6
5.0x10^5
0
**
E
Erythrocyte: FL E17.5
Absolute cell count
7x10^7
6x10^7
5x10^7
4x10^7
3x10^7
2x10^7
1x10^7
0
P1
P2
P3
P4
P1 = CD71+/TER119-
P2 = CD71++/TER119-
P3 = CD71++/TER119+
P4 = CD71-/TER119+
G
Lineages: FL E17.5
Absolute cell count
2.5x10^6
2.0x10^6
1.5x10^6
1.0x10^6
5.0x10^5
0
*
**
B220
GR1
CD3
Vav1-cre; Mof f/f
Vav1-cre; Mof f/+
Mof f/f
H
MP: FL E17.5
Absolute cell count
3x10^5
2x10^5
1x10^5
0
**
MP
LSK: FL E17.5
Absolute cell count
2x10^4
1x10^4
0
**
LSK
HSC: FL E17.5
Absolute cell count
2500
2000
1500
1000
500
0
**
CD150+/CD48-

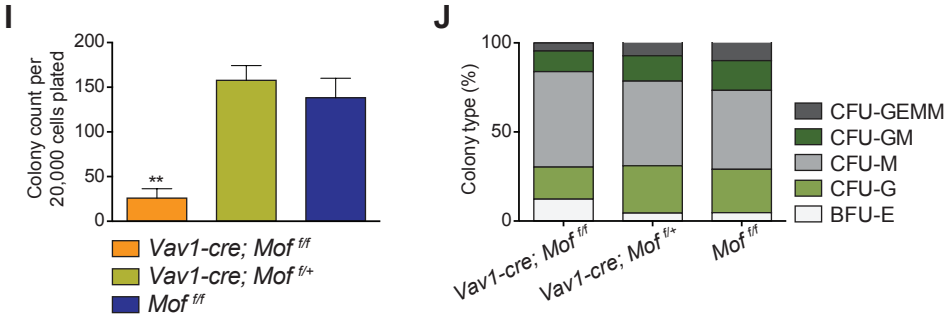

Figure 6. *Mof*-deficient embryos start manifesting hematopoietic defects at E17.5

(A) Representative photographs of *Vav1-cre-Mof$^{f/f}$*, *Vav1-cre-Mof$^{f/+}$* and *Mof$^{f/f}$* embryos at E17.5.

(B) PCR analysis illustrating *Mof* excision in fresh CD45.2$^+$ FL cells. A representative image is shown.

(C) Western blot showing global H4K16ac, H4 and Actin in fresh CD45.2$^+$ FL cells.

(D) Total live fetal liver (FL) cell count.

(E) The absolute number of cells at various stages of differentiation within the erythroid lineage in E17.5 FLs as measured by FACS.

(F) Total number of live, CD45.2+ FL cells.

(G) The absolute number of mature B-cells (B220$^+$), myeloid cells (GR1$^+$), and T-cells (CD3$^+$) in E17.5 FLs as measured by FACS.

(H) The absolute number of MPs, LSKs and HSCs (CD150$^+$/CD48$^-$) as measured by FACS.

(I) Day 10 of CFU assay of fresh FL cells derived from E17.5 *Vav1-cre-Mof$^{f/f}$*, *Vav1-cre-Mof$^{f/+}$* and *Mof$^{f/f}$* embryos. Bar graph indicates mean number of colonies per dish after 10 days. 20,000 cells were plated per dish. Each groups contains three biological replicates.

(J) Mean percentage of the various colony types relative to all colonies counted per dish per genotype.

* $p < 0.05$, ** $p < 0.01$. Error bars show SD of mean. Significance compared to *Moff/f*.

Mof histone acetyltransferase activity is required for adult hematopoietic cell survival

MOF has been identified as the major H4K16 acetyltransferase in humans, mice and *Drosophila*.[11-14,20] MOF contains a MYST family HAT domain with a CoA binding site (Figure 7A) that was shown to be crucial for its acetyltransferase activity.[10,12] While MOF possesses acetyltransferase activity on various histones and nucleosomes, depletion of MOF in HeLa cells was shown to lead to a dramatic decrease in H4K16ac, whereas other acetylation sites appeared to be unaffected.[20]

Since our data indicate a pivotal role for *Mof* in adult hematopoiesis, we set out to establish the specificity of our model for *Mof* loss and determine whether MOF HAT activity is dispensable. We designed a full-length, Human influenza hemagglutinin (HA)-tagged *Mof* and two HAT inactivated *Mof* retroviral constructs (Figure 7A) in which either the Coenzyme A (CoA) binding site was deleted (*Mof-CoAdel*) or a HAT inactivating point mutation (G327E) was introduced (*Mof-G327E*). The HAT inactivating point mutation in the MOF CoA binding domain was first described in *Drosophila*[12] and later used in a human MOF construct where

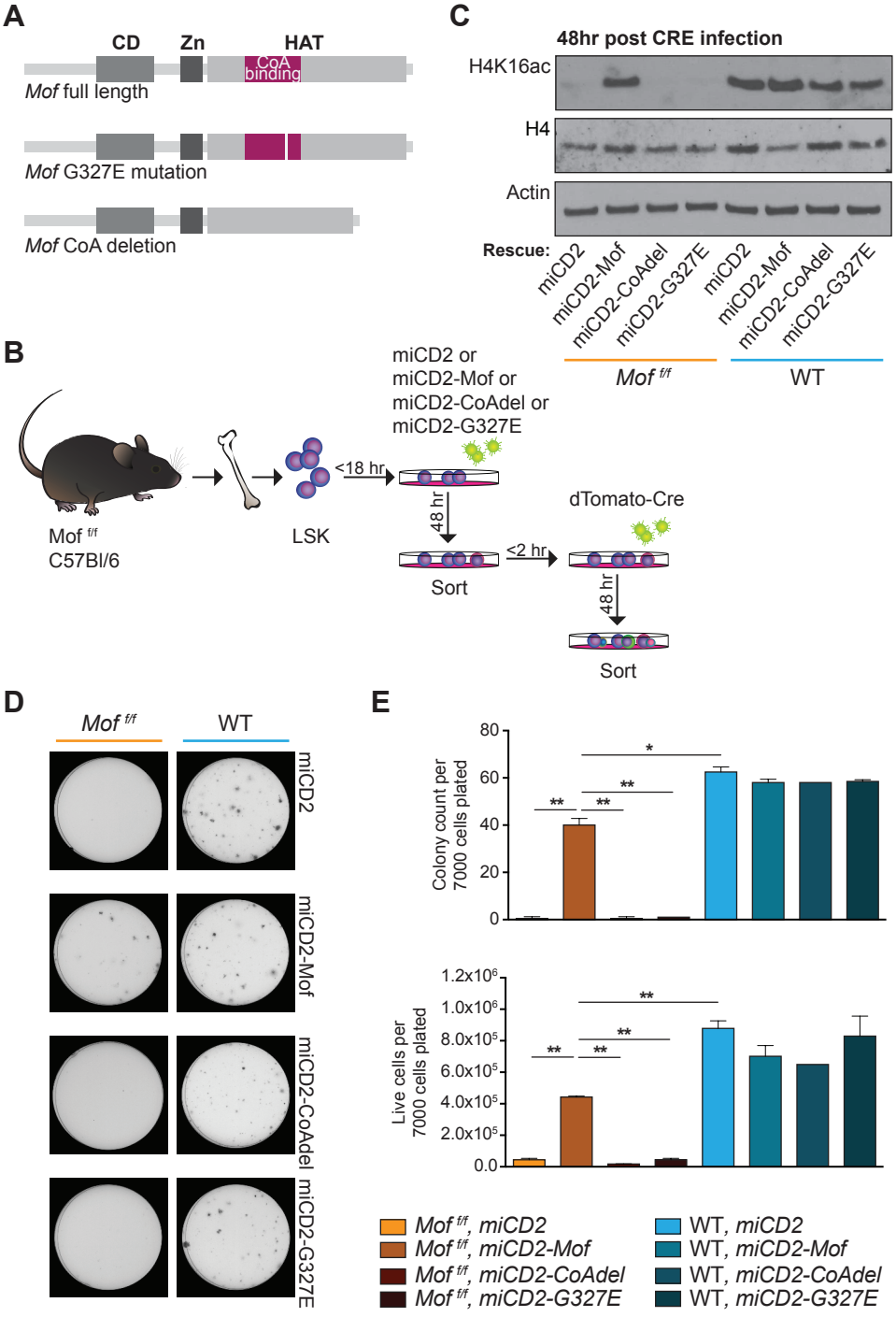
A
CD
Zn
HAT
CoA binding
Mof full length
Mof G327E mutation
Mof CoA deletion
C
48hr post CRE infection
H4K16ac
H4
Actin
Rescue:
miCD2
miCD2-Mof
miCD2-CoAdel
miCD2-G327E
miCD2
miCD2-Mof
miCD2-CoAdel
miCD2-G327E
Mof f/f
WT
B
Mof f/f
C57Bl/6
LSK
<18 hr
miCD2 or
miCD2-Mof or
miCD2-CoAdel or
miCD2-G327E
48 hr
Sort
<2 hr
dTomato-Cre
48 hr
Sort
D
Mof f/f
WT
miCD2
miCD2-Mof
miCD2-CoAdel
miCD2-G327E
E
Colony count per 7000 cells plated
80
60
40
20
0
Live cells per 7000 cells plated
1.2x10^6
1.0x10^6
8.0x10^5
6.0x10^5
4.0x10^5
2.0x10^5
0.0
Mof f/f, miCD2
Mof f/f, miCD2-Mof
Mof f/f, miCD2-CoAdel
Mof f/f, miCD2-G327E
WT, miCD2
WT, miCD2-Mof
WT, miCD2-CoAdel
WT, miCD2-G327E

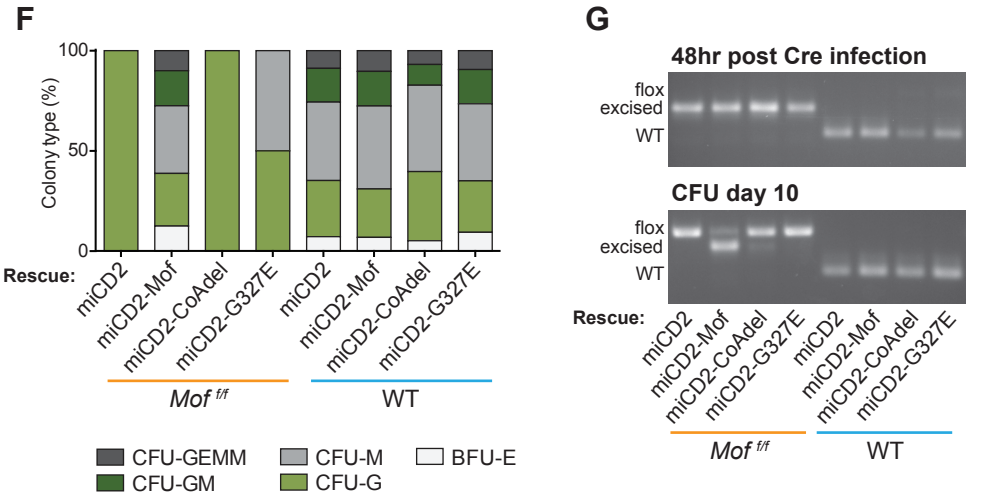

Figure 7. *Mof* histone acetyltransferase activity is required for adult hematopoietic cell survival
(A) Schematic of full-length *Mof*, CoA binding domain deleted *Mof* or G327E mutant *Mof*.
(B) Schematic for *in vitro* rescue experiment. BM LSKs derived from four *Mof*$^{f/f}$ or four WT mice were pooled by genotype and retrovirally transduced with full-length *Mof* (miCD2-Mof), a *Mof* mutant (miCD2-CoAdel or miCD2-G327E) or empty vector (miCD2) and hCD2^{+} cells were sorted after 48 hours. These cells were then infected with dTomato-Cre, sorted another 48 hour (hr) later and used for CFU assays.
(C) Western blot showing global H4K16ac, H4 and Actin in *Mof*$^{f/f}$ and wild type (WT) *miCD2*, *miCD2-Mof, miCD2-Mof-CoAdel* and *miCD2-Mof-G327E* cells at 48 hours post *Cre* transduction.
(D) Day 10 of CFU assay. 7000 cells were plated per dish. Representative petri dishes are shown.
(E) Day 10 of CFU assay. Bar graph indicates mean number of colonies per dish after 10 days (left) or mean number of live cells (right) per dish. Data are representative of two individual experiments.
(F) Mean percentage of the various colony types relative to all colonies counted per dish per genotype.
(G) PCR analysis illustrating *Mof* excision in hCD2^{+}, dTomato^{+} LSKs, 48 hours post *Cre* infection and at day 10 of the colony-forming assay. A representative image is shown.
** $p < 0.01$. Error bars show SD of mean.

it was also found to diminish H4K16ac[30]. Alignment of *Drosophila*, murine and human MOF illustrates that the point mutation involves replacement of glycine by glutamic acid on position 327 (G327E) in murine, as well as human MOF (Figure S5A). The constructs were packaged in an miCD2-MSCV retroviral vector with the hCD2 selection marker (*miCD2-Mof*, *miCD2-Mof-CoAdel* and *miCD2-Mof-G327E*). Our data on *Mof* loss in the postnatal stage indicate variability in the phenotype, most likely due to leakage of the *Cre* system and high selection pressure against excised cells (Figure 2G). We therefore set-up an *in vitro Cre* transduction experiment using adult *Mof*$^{f/f}$ or WT BM-derived LSKs. In order to assess expression of the exogenous *Mof* constructs we performed Western blot analysis for HA-tagged MOF in

transformed mouse BM LSKs. Figure S5B illustrates that exogenous *Mof* was consistently expressed by *miCD2-Mof*, *miCD2-Mof-G327E* and *miCD2-Mof-CoAdel*.

For the adult BM-derived LSK rescue experiment we transduced *Mof$^{f/f}$* or WT LSKs with *miCD2*, *miCD2-Mof*, *miCD2-Mof-G327E* or *miCD2-Mof-CoAdel*. After 48 hours, cells were sorted and then infected with dTomato-Cre. After another 48 hours of culture, dTomato positive cells were sorted, harvested for extraction of gDNA and protein and plated in methylcellulose for CFU assays (Figure 7B). Western blot analysis confirmed that exogenous full-length *Mof* was capable of restoring H4K16ac levels upon genetic *Mof* loss, while both HAT domain mutant *Mof* constructs were not (Figure 7C). CFU assays showed that exogenous expression of full-length *Mof* could indeed rescue hematopoietic *Cre* positive *Mof$^{f/f}$* cells from their detrimental fate, indicating the specificity of *Mof* loss in the observed phenotype (Figure 7D and 7E). However, HAT-deficient *Mof* was incapable of rescuing *Cre+ Mof$^{f/f}$* cells (Figure 7D and 7E). The one or two colonies that did form in *Mof*-deficient or *Mof* HAT-deficient cells were differentiated (CFU-G or CFU-M, Figure 7F). These colony-forming capacity and proliferation findings are supported by *Mof* excision PCR data where consistent and strong excision was observed in *Cre+ Mof$^{f/f}$ miCD2-Mof* cells throughout the experiment, while the few cells that did grow in the *Cre+ Mof$^{f/f}$ miCD2*, *miCD2-Mof-CoAdel* and *miCD2-Mof-G327E* setting lost *Mof* excision and were largely unexcised by day 10 of the CFU assay (Figure 7G).

Interestingly, we found that *Mof*-deficient LSKs had significantly more γH2AX foci per cell nucleus compared to the WT control ($p < 0.0001$; Figure S5C and S5D), indicative of more DNA damage. All together these data indicate that the observed phenotype of homozygous *Mof* deletion in hematopoietic adult cells is specific to the loss of *Mof*. In addition, we have demonstrated that the HAT activity of *Mof* is crucial for survival of adult hematopoietic cells and that it may be required for genomic stability or adequate DNA damage response in adult HSCs.

DISCUSSION

The discovery that *Mof* is required for adult, but not early fetal hematopoiesis sheds new light on our understanding of regulation of hematopoietic development. We demonstrate that *Mof* is critical for hematopoietic cell maintenance and reconstitution in adult hematopoiesis. Rescue experiments with *Mof* HAT domain mutants illustrated the requirement for *Mof* acetyltransferase activity in the clonogenic capacity of HSCs and progenitors. In stark contrast, fetal steady-state hematopoiesis at E14.5 did not seem to be affected by homozygous *Mof* deletion despite dramatic loss of global H4K16ac. Given that previously published work using the *Vav1-cre* system has generated defects in fetal HSCs at E14.5[31], we conclude that *Mof* plays a critical role in adult, but not early fetal HSC maintenance.

HSCs undergo discrete developmental changes throughout life, the biggest being the transition from fetal to adult hematopoiesis.[32] Early and mid- gestational hematopoiesis is characterized by rapid proliferation of undifferentiated HSCs to supply the developing

hematopoietic system.[33] In adult hematopoiesis, lifelong blood cell production depends on the delicate balance between HSC self-renewal and differentiation[34], so in contrast to fetal hematopoiesis, most adult HSCs turn quiescent[35] to ensure HSC pool maintenance. This switch sets in at E16.5 and is complete at around 3 weeks after birth.[32] As fetal HSCs markedly differ from adult HSCs with respect to cell cycle status[35], proliferative capacity[33] and differentiation potential[36], it is not surprising that they also differ in gene expression[31,37] and regulation[31,38]. While some genes[39-44] regulate HSC maintenance throughout fetal and adult life, the transcription factor *Sox17*[31] was found to be essential for fetal but not adult hematopoiesis. Similar to the observed phenotype in hematopoietic *Mof* loss, the transcriptional regulator *Bmi1* has been shown to maintain adult, but not early fetal HSCs.[38] While pluripotency and lineage differentiation depend on establishing and maintaining gene expression programs that are largely regulated by chromatin organization[45], it seems likely that multiple chromatin regulators are crucial for hematopoiesis at varying stages of development. Consistent with this notion is the finding that the chromatin regulator *Ezh2* is required for fetal but not adult hematopoiesis.[46] Our findings also support this concept that chromatin regulators are differentially involved in hematopoietic development, whereas we have shown that MOF HAT activity is a crucial regulator of post-natal and adult hematopoiesis, but not of the highly proliferative early and mid- gestational hematopoietic compartment. The fact that we can isolate fetal, phenotypically defined HSCs that are completely devoid of H4K16ac is quite remarkable and suggests a dramatic difference in chromatin structure between fetal and adult HSCs.

Further highlighting the importance of H4K16 acetylation, we have shown that the enzymatic activity of MOF is crucial for adult HSC maintenance and functionality (Figure 7E). In addition we found an increase in DNA damage in *Mof*-deficient adult HSCs (Figure S5C and S5D). Further studies will be required to test why fetal hematopoietic cells can exist despite the dramatic, MOF-loss-induced H4K16ac deficiency (Figure 4D). H4K16 acetylation was found to have a limited role in transcriptional regulation of HEK293 cells[47], as opposed to its activity in mouse embryonic stem cells[21]. While most studies on *Mof* depletion report adverse outcomes in various cell types, a recent study found that *Mof* deficiency in quiescent glomerular podocytes had no effect on kidney function in mice.[48] These findings suggest that H4K16ac requirement may indeed be cell type specific, though it remains surprising that a highly proliferative hematopoietic system such as found in an E14.5 embryo, can be maintained, despite lack of H4K16ac. This is particularly interesting, as H4K16ac is believed to be one of the most important histone modifications to maintain euchromatin in mammalian cells.[49] Previous data from murine embryonic fibroblasts (MEFs) suggest that a MOF-induced increase of H4K16ac is essential for an appropriate DNA damage response.[17] Our finding of an increase in DNA damage in *Mof*-deficient LSKs, leads us to speculate that the MOF-loss induced global H4K16ac depletion in adult HSCs potentially reduces accessibility of nucleosomes to repair proteins, by increasing chromatin compaction at the DNA damage foci, leading to gross genomic instability. Possibly other chromatin marks compensate for this lack of H4K16ac in fetal HSCs. Another possibility is that the regulation of chromatin structure

is dramatically different between fetal and adult HSCs. Future studies using quantitative mass spectrometry to define global epigenomic changes[50] could yield significant mechanistic insight into the role of altered epigenomic states throughout hematopoietic development.

The observed hematopoietic defects found in the liver of E17.5 *Mof*-deficient embryos (Figure 6), though more moderate than in pups and adults, make it unlikely that the phenotype in post-natal and adult *Mof*-null mice is solely caused by an impaired seeding capacity or engraftment of FL cells to the BM niche. Previous work has shown that distinct microenvironmental regulatory mechanisms exist between the fetal and adult HSC niche.[32,33,51,52] It is, however, conceivable that the FL microenvironment itself is also modified during fetal development in order to meet the changing needs of lineage differentiation and HSC expansion.[32] Our data suggest that earlier embryonic, *Mof*-deficient HSCs (<E15.5) are capable of proliferation and differentiation (Figure 4). However, over the next few days of gestation, intrinsic cellular requirements and microenvironmental stimuli change and it may be that *Mof*-null, H4K16ac-deficient HSCs are incapable of adapting to these changes due to significant abnormalities in chromatin structure.

As previously mentioned, MOF and MLL1 complexes interact and this interaction was shown to be important for the chromatin regulatory function of both enzymes.[22] Apart from its role in normal hematopoiesis, wild type MLL1 has been shown to play a role in *MLL*-rearranged leukemogenesis.[53,54] However, in both normal and malignant hematopoiesis, the H3K4 methyltransferase activity of MLL1 is dispensable.[25] Given the interaction of MLL1 and MOF, and the necessity of MOFs HAT activity in adult hematopoiesis, it will be interesting to determine leukemia dependence on the enzymatic activity of MOF. It may be that in the setting of *MLL*-rearranged leukemia, it is in fact the HAT activity of MOF that is required for leukemogenesis. Future experiments assessing the role of MOF HAT activity in *MLL1* fusion leukemogenesis should shed light on this hypothesis.

In conclusion, our study shows that *Mof* is a critical regulator of adult, but not early fetal hematopoiesis, thereby supporting the notion that chromatin regulation of hematopoiesis changes over time. We have identified MOF-controlled chromatin regulation as a developmental-stage-specific mechanism for adult hematopoietic maintenance.

EXPERIMENTAL PROCEDURES

Mice

The generation of *Mof* conditional knockout mouse in a C57Bl/6 (CD45.2$^+$) background has been described previously.[14] *Mof$^{f/f}$* mice were crossed to *Vav1-cre* or *Mx1-cre* mice and *Cre* was maintained as a heterozygous allele to generate *Vav1-cre; Mof$^{f/f}$* or *Mx1-cre; Mof$^{f/f}$* mice. Genotyping strategies were described previously.[14] WT B6.SJL (CD45.1$^+$) mice were purchased from Taconic, Hudson, NY. All animal experiments in this study were approved by and adhered to guidelines of the Memorial Sloan-Kettering Cancer Center Animal Care and Use Committee.

Isolation of murine hematopoietic cells

Vav1-cre; *Mof$^{f/f}$*, *Vav1-cre*; *Mof$^{f/+}$, Mof$^{f/f}$*, *Mx1-cre*; *Mof$^{f/f}$, Mx1-cre* and WT adult mice or 8-9 day-old pups were sacrificed and peripheral blood, spleen, thymus, liver and bones (femurs, tibias, fibulas, pelvis and spine) were extracted. BM cell suspensions were prepared by crushing bones after removal of muscle and connective tissue. Spleen and thymus cell suspensions were prepared by crushing the tissue through a 0.45 μm nylon mesh filter.

Vav1-cre; *Mof$^{f/f}$*, *Vav1-cre*; *Mof$^{f/+}$* and *Mof$^{f/f}$* FL cells were obtained by timed breeding of a *Vav1-cre*; *Mof$^{f/+}$*and *Mof$^{f/f}$* couple during the course of 3 days and daily checking the females for a vaginal plug. Fourteen or seventeen days after a vaginal plug was observed, pregnant females were euthanized (E14.5 or E17.5 respectively). Fetuses were extracted from the euthanized mother and kept in PBS (Thermo Fisher Scientific, Waltham, MA) for further processing. FL cell suspensions were prepared by extracting the liver from the embryo and flushing it through a 23G needle in a tube containing PBS supplemented with 2.5% fetal bovine serum (FBS, Thermo Fisher Scientific, Waltham, MA).

Transplant experiments

All transplant experiments were performed by retro-orbitally injecting freshly isolated BM or FL cells into lethally irradiated (2 x 5Gy), 6-8 week-old B6.SJL female recipient mice. Mice were euthanized at or after 16 weeks or sacrificed sooner when severely anemic. Mice were bled every 4 weeks to monitor complete blood count (CBC), CD45.2% and mature hematopoietic populations. Further details on transplant experiments can be found in the Supplemental data.

Obtaining CD45.2$^+$, Lineage depleted or LSKs

CD45.2$^+$ cells were obtained by labeling BM or FL cells with a CD45.2 APC antibody (Biolegend, San Diego, CA) and sorting positive cells on an ARIA cell sorter (BD, San Jose, CA). Lineage depletion was performed by labeling BM or FL cells with purified, biotinylated monoclonal antibodies to CD3e, CD11b (MAC1), CD45R (B220), Ly-6G (GR1) and TER119 (Biotin mouse lineage panel, BD). Lin$^+$ cells were in majority removed by magnetic bead depletion with streptavidin conjugated MicroBeads over an LD column (both Miltenyi Biotech,

San Diego, CA). If required, Lin$^-$, SCA1$^+$, cKIT$^+$ (LSK) cells were then obtained by staining lineage depleted cells with Streptavidin APC/Cy7, (Biolegend, San Diego, CA), CD117 (cKIT) APC and Ly-6A/E (SCA1) PE/Cy7 (both eBioscience, San Diego, CA), and sorting the LSK population.

***In vitro* colony-forming assays**

To study the impact of *Mof* deletion on colony-forming capacity, fresh CD45.2$^+$ sorted BM cells or whole FL cells (both 20,000 cells per dish) were plated in methylcellulose M3434 (Stemcell Technologies, Vancouver, BC, Canada) in 35mm culture dishes. Colonies were scored after 10 days, using the Eclipse TS100 inverted microscope (Nikon, Tokyo, Japan). Cells from pooled colony aggregates were then assessed for *Mof* excision.

In case of the *Mof* LSK rescue experiments, fresh LSKs from four *Mof$^{f/f}$* and four WT mice were pooled by genotype, split into four and infected with retrovirus containing *miCD2*, *miCD2-Mof*, *miCD2-Mof-CoAdel* or *miCD2-Mof-G327E*. After 48 hours of liquid culture, cells were sorted for hCD2 positivity and immediately infected with dTomato-Cre. Another 48 hours later, dTomato positive cells were sorted, counted and plated (7000 cells per dish) in M3434 methylcellulose as described.

Data Analysis and Statistical Methods

GraphPad Prism software was used for statistical analysis. Statistical significance between 2 groups was determined by unpaired 2-tailed Student's t-test. The Kaplan-Meier method was used to plot survival curves for murine leukemic transplant data.

See Supplemental Experimental Procedures for more details.

ACKNOWLEDGMENTS

We would like to acknowledge Z. Feng for administrative assistance. This work was supported by a CURE Childhood Cancer Research Grant (D.G.V.); NIH grants PO1 CA66996 and R01 CA140575 (S.A.A.); the Leukemia and Lymphoma Society (S.A.A.); Gabrielle's Angel Research Foundation (S.A.A.); a DoD Bone Marrow Failure Postdoctoral Fellowship Award (W81XWH-12-1-0568) (H.X.); NIH grants RO1 CA129537 and RO1 CA154320 (T.K.P.); and an NIH Memorial Sloan Kettering Cancer Center Support Grant (P30 CA008748).

AUTHORSHIP CONTRIBUTIONS

D.G.V., H.X. and S.A.A. conceived the study and designed experiments; D.G.V., H.X., M.E.E. and C.M.W. performed experiments; D.G.V. performed all data analysis; T.K.P. generated the conditional *Mof* knockout mouse model; D.G.V. and S.A.A. wrote the manuscript.

REFERENCES

1. Allfrey VG, Faulkner R, Mirsky AE. Acetylation and methylation of histones and their possible role in the regulation of RNA synthesis. *Proc Natl Acad Sci U S A.* 1964;51:786-794.
2. Allis CD, Berger SL, Cote J, et al. New nomenclature for chromatin-modifying enzymes. *Cell.* 2007;131(4):633-636.
3. Sun XJ, Man N, Tan Y, Nimer SD, Wang L. The Role of Histone Acetyltransferases in Normal and Malignant Hematopoiesis. *Front Oncol.* 2015;5:108.
4. Huang HT, Kathrein KL, Barton A, et al. A network of epigenetic regulators guides developmental haematopoiesis in vivo. *Nat Cell Biol.* 2013;15(12):1516-1525.
5. Perez-Campo FM, Costa G, Lie-a-Ling M, Kouskoff V, Lacaud G. The MYSTerious MOZ, a histone acetyltransferase with a key role in haematopoiesis. *Immunology.* 2013;139(2):161-165.
6. Kikuchi H, Nakayama T. GCN5 and BCR signalling collaborate to induce pre-mature B cell apoptosis through depletion of ICAD and IAP2 and activation of caspase activities. *Gene.* 2008;419(1-2):48-55.
7. Mishima Y, Miyagi S, Saraya A, et al. The Hbo1-Brd1/Brpf2 complex is responsible for global acetylation of H3K14 and required for fetal liver erythropoiesis. *Blood.* 2011;118(9):2443-2453.
8. Rebel VI, Kung AL, Tanner EA, Yang H, Bronson RT, Livingston DM. Distinct roles for CREB-binding protein and p300 in hematopoietic stem cell self-renewal. *Proc Natl Acad Sci U S A.* 2002;99(23):14789-14794.
9. Voss AK, Thomas T. MYST family histone acetyltransferases take center stage in stem cells and development. *Bioessays.* 2009;31(10):1050-1061.
10. Yang XJ, Ullah M. MOZ and MORF, two large MYSTic HATs in normal and cancer stem cells. *Oncogene.* 2007;26(37):5408-5419.
11. Smith ER, Cayrou C, Huang R, Lane WS, Cote J, Lucchesi JC. A human protein complex homologous to the Drosophila MSL complex is responsible for the majority of histone H4 acetylation at lysine 16. *Mol Cell Biol.* 2005;25(21):9175-9188.
12. Akhtar A, Becker PB. Activation of transcription through histone H4 acetylation by MOF, an acetyltransferase essential for dosage compensation in Drosophila. *Mol Cell.* 2000;5(2):367-375.
13. Thomas T, Dixon MP, Kueh AJ, Voss AK. Mof (MYST1 or KAT8) is essential for progression of embryonic development past the blastocyst stage and required for normal chromatin architecture. *Mol Cell Biol.* 2008;28(16):5093-5105.
14. Gupta A, Guerin-Peyrou TG, Sharma GG, et al. The mammalian ortholog of Drosophila MOF that acetylates histone H4 lysine 16 is essential for embryogenesis and oncogenesis. *Mol Cell Biol.* 2008;28(1):397-409.
15. Gupta A, Hunt CR, Hegde ML, et al. MOF phosphorylation by ATM regulates 53BP1-mediated double-strand break repair pathway choice. *Cell Reports.* 2014;8(1):177-189.
16. Gupta A, Sharma GG, Young CS, et al. Involvement of human MOF in ATM function. *Mol Cell Biol.* 2005;25(12):5292-5305.
17. Li X, Corsa CA, Pan PW, et al. MOF and H4 K16 acetylation play important roles in DNA damage repair by modulating recruitment of DNA damage repair protein Mdc1. *Mol Cell Biol.* 2010;30(22):5335-5347.
18. Sharma GG, So S, Gupta A, et al. MOF and histone H4 acetylation at lysine 16 are critical for DNA damage response and double-strand break repair. *Mol Cell Biol.* 2010;30(14):3582-3595.
19. Bhadra MP, Horikoshi N, Pushpavallipvalli SN, et al. The role of MOF in the ionizing radiation response is conserved in Drosophila melanogaster. *Chromosoma.* 2012;121(1):79-90.
20. Taipale M, Rea S, Richter K, et al. hMOF histone acetyltransferase is required for histone H4 lysine 16 acetylation in mammalian cells. *Mol Cell Biol.* 2005;25(15):6798-6810.
21. Li X, Li L, Pandey R, et al. The histone acetyltransferase MOF is a key regulator of the embryonic

stem cell core transcriptional network. *Cell Stem Cell.* 2012;11(2):163-178.
22. Dou Y, Milne TA, Tackett AJ, et al. Physical association and coordinate function of the H3 K4 methyltransferase MLL1 and the H4 K16 acetyltransferase MOF. *Cell.* 2005;121(6):873-885.
23. Ernst P, Fisher JK, Avery W, Wade S, Foy D, Korsmeyer SJ. Definitive hematopoiesis requires the mixed-lineage leukemia gene. *Dev Cell.* 2004;6(3):437-443.
24. Jude CD, Climer L, Xu D, Artinger E, Fisher JK, Ernst P. Unique and independent roles for MLL in adult hematopoietic stem cells and progenitors. *Cell Stem Cell.* 2007;1(3):324-337.
25. Mishra BP, Zaffuto KM, Artinger EL, et al. The histone methyltransferase activity of MLL1 is dispensable for hematopoiesis and leukemogenesis. *Cell Reports.* 2014;7(4):1239-1247.
26. Gupta A, Hunt CR, Pandita RK, et al. T-cell-specific deletion of Mof blocks their differentiation and results in genomic instability in mice. *Mutagenesis.* 2013;28(3):263-270.
27. Stadtfeld M, Graf T. Assessing the role of hematopoietic plasticity for endothelial and hepatocyte development by non-invasive lineage tracing. *Development.* 2005;132(1):203-213.
28. Dzierzak E, Medvinsky A. Mouse embryonic hematopoiesis. *Trends Genet.* 1995;11(9):359-366.
29. Wolber FM, Leonard E, Michael S, Orschell-Traycoff CM, Yoder MC, Srour EF. Roles of spleen and liver in development of the murine hematopoietic system. *Exp Hematol.* 2002;30(9):1010-1019.
30. Zhao X, Su J, Wang F, et al. Crosstalk between NSL histone acetyltransferase and MLL/SET complexes: NSL complex functions in promoting histone H3K4 di-methylation activity by MLL/SET complexes. *PLoS genetics.* 2013;9(11):e1003940.
31. Kim I, Saunders TL, Morrison SJ. Sox17 dependence distinguishes the transcriptional regulation of fetal from adult hematopoietic stem cells. *Cell.* 2007;130(3):470-483.
32. Mikkola HK, Orkin SH. The journey of developing hematopoietic stem cells. *Development.* 2006;133(19):3733-3744.
33. Lessard J, Faubert A, Sauvageau G. Genetic programs regulating HSC specification, maintenance and expansion. *Oncogene.* 2004;23(43):7199-7209.
34. Cheshier SH, Morrison SJ, Liao X, Weissman IL. In vivo proliferation and cell cycle kinetics of long-term self-renewing hematopoietic stem cells. *Proc Natl Acad Sci U S A.* 1999;96(6):3120-3125.
35. Bowie MB, McKnight KD, Kent DG, McCaffrey L, Hoodless PA, Eaves CJ. Hematopoietic stem cells proliferate until after birth and show a reversible phase-specific engraftment defect. *J Clin Invest.* 2006;116(10):2808-2816.
36. Ikuta K, Kina T, MacNeil I, et al. A developmental switch in thymic lymphocyte maturation potential occurs at the level of hematopoietic stem cells. *Cell.* 1990;62(5):863-874.
37. Ivanova NB, Dimos JT, Schaniel C, Hackney JA, Moore KA, Lemischka IR. A stem cell molecular signature. *Science.* 2002;298(5593):601-604.
38. Park IK, Qian D, Kiel M, et al. Bmi-1 is required for maintenance of adult self-renewing haematopoietic stem cells. *Nature.* 2003;423(6937):302-305.
39. Hisa T, Spence SE, Rachel RA, et al. Hematopoietic, angiogenic and eye defects in Meis1 mutant animals. *Embo J.* 2004;23(2):450-459.
40. Azcoitia V, Aracil M, Martinez AC, Torres M. The homeodomain protein Meis1 is essential for definitive hematopoiesis and vascular patterning in the mouse embryo. *Dev Biol.* 2005;280(2):307-320.
41. Kim JY, Sawada A, Tokimasa S, et al. Defective long-term repopulating ability in hematopoietic stem cells lacking the Polycomb-group gene rae28. *Eur J Haematol.* 2004;73(2):75-84.
42. Ohta H, Sawada A, Kim JY, et al. Polycomb group gene rae28 is required for sustaining activity of hematopoietic stem cells. *J Exp Med.* 2002;195(6):759-770.
43. Mucenski ML, McLain K, Kier AB, et al. A functional c-myb gene is required for normal murine fetal hepatic hematopoiesis. *Cell.* 1991;65(4):677-689.
44. Sandberg ML, Sutton SE, Pletcher MT, et al. c-Myb and p300 regulate hematopoietic stem cell proliferation and differentiation. *Dev Cell.* 2005;8(2):153-166.

45. Teitell MA, Mikkola HK. Transcriptional activators, repressors, and epigenetic modifiers controlling hematopoietic stem cell development. *Pediatr Res.* 2006;59(4 Pt 2):33r-39r.
46. Mochizuki-Kashio M, Mishima Y, Miyagi S, et al. Dependency on the polycomb gene Ezh2 distinguishes fetal from adult hematopoietic stem cells. *Blood.* 2011;118(25):6553-6561.
47. Horikoshi N, Kumar P, Sharma GG, et al. Genome-wide distribution of histone H4 Lysine 16 acetylation sites and their relationship to gene expression. *Genome Integr.* 2013;4(1):3.
48. Sheikh BN, Bechtel-Walz W, Lucci J, et al. MOF maintains transcriptional programs regulating cellular stress response. *Oncogene.* 2015.
49. Robinson PJ, An W, Routh A, et al. 30 nm chromatin fibre decompaction requires both H4-K16 acetylation and linker histone eviction. *J Mol Biol.* 2008;381(4):816-825.
50. Britton LM, Gonzales-Cope M, Zee BM, Garcia BA. Breaking the histone code with quantitative mass spectrometry. *Expert Rev Proteomics.* 2011;8(5):631-643.
51. Wilson A, Trumpp A. Bone-marrow haematopoietic-stem-cell niches. *Nat Rev Immunol.* 2006;6(2):93-106.
52. Hackney JA, Charbord P, Brunk BP, Stoeckert CJ, Lemischka IR, Moore KA. A molecular profile of a hematopoietic stem cell niche. *Proc Natl Acad Sci U S A.* 2002;99(20):13061-13066.
53. Bernt KM, Zhu N, Sinha AU, et al. MLL-rearranged leukemia is dependent on aberrant H3K79 methylation by DOT1L. *Cancer Cell.* 2011;20(1):66-78.
54. Thiel AT, Blessington P, Zou T, et al. MLL-AF9-induced leukemogenesis requires coexpression of the wild type Mll allele. *Cancer Cell.* 2010;17(2):148-159.

SUPPLEMENTAL DATA

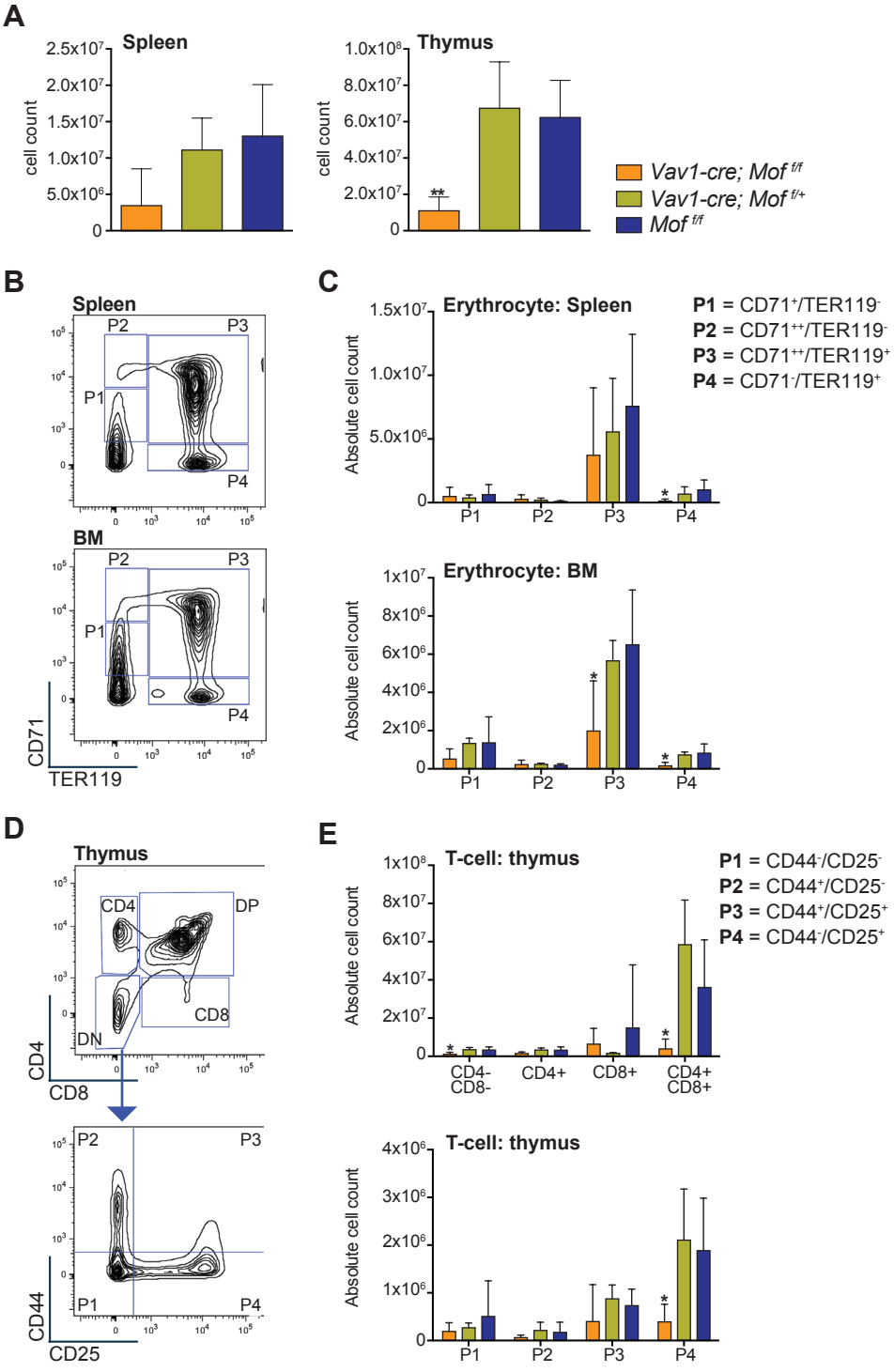
A
Spleen
cell count
2.5x10^7
2.0x10^7
1.5x10^7
1.0x10^7
5.0x10^6
0
Thymus
1.0x10^8
8.0x10^7
6.0x10^7
4.0x10^7
2.0x10^7
0
**
Vav1-cre; Mof f/f
Vav1-cre; Mof f/+
Mof f/f
B
Spleen
P1
P2
P3
P4
BM
CD71
TER119
C
Erythrocyte: Spleen
Absolute cell count
P1 = CD71+/TER119-
P2 = CD71++/TER119-
P3 = CD71++/TER119+
P4 = CD71-/TER119+
Erythrocyte: BM
D
Thymus
CD4
CD8
DP
DN
CD44
CD25
E
T-cell: thymus
P1 = CD44-/CD25-
P2 = CD44+/CD25-
P3 = CD44+/CD25+
P4 = CD44-/CD25+
CD4- CD8-
CD4+
CD8+
CD4+ CD8+

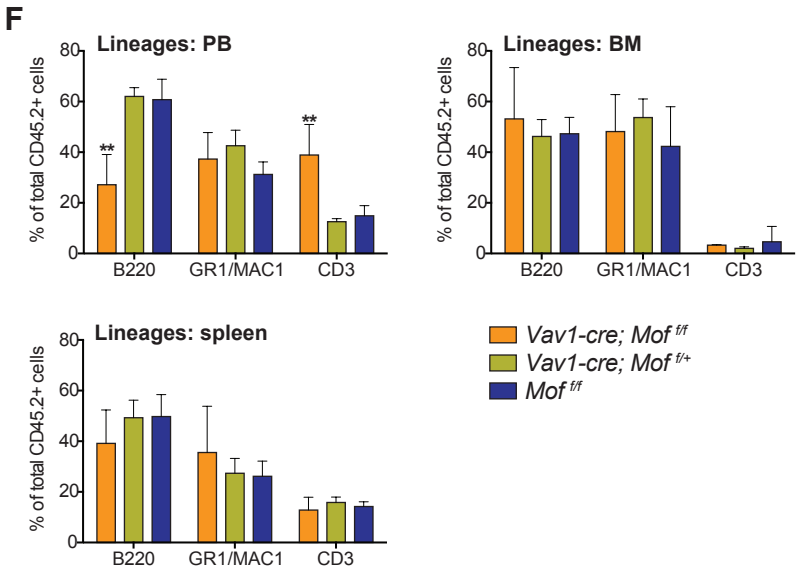

Figure S1, related to Figure 1. *Vav1-cre* induced homozygous *Mof* loss leads to lethal hematopoietic failure in mouse pups

(A) Spleen and thymus cell count of 9-day-old *Vav1-cre-Mof$^{f/f}$*, *Vav1-cre-Mof$^{f/+}$* and *Mof$^{f/f}$* pups.

(B) FACS gating strategy for measuring differentiation within the erythrocyte lineage in bone marrow (BM) and spleen. Live cells were selected prior to CD71/TER119 gating. P1 through P4 defines erythroid cell maturity where P1 consists of erythroid progenitors and P4 of mature erythrocytes. Representative images of a *Mof$^{f/f}$* mouse are shown.

(C) Total number of cells at various stages of differentiation within the erythroid lineage in BM (harvested from femurs, pelvic bones, tibias and spine) and spleen as measured by FACS.

(D) FACS gating strategy for measuring various stages of differentiation within the T-cell lineage in the thymus. Live cells were selected prior to CD4/CD8 gating. CD4$^+$ or CD8$^+$ cells are most mature and CD4$^-$/CD8$^-$ (double negative or DN) cells most immature. Within DN cells, maturity is defined by CD44 and CD25 cell surface markers where P1 is most immature and P4 most mature. Representative images of a *Mof$^{f/f}$* mouse are shown. DP = double positive.

(E) Total number of cells at various stages of differentiation within the T-cell lineage in the thymus as measured by FACS.

(F) Percentages of mature B-cells (B220$^+$), myeloid cells (GR1$^+$/MAC1$^+$), and T-cells (CD3$^+$) out of live, CD45.2$^+$ PB, BM and spleen cells as measured by FACS.

* $p < 0.05$, ** $p < 0.01$. Error bars represent SD of mean. Significance compared to *Moff/f*.

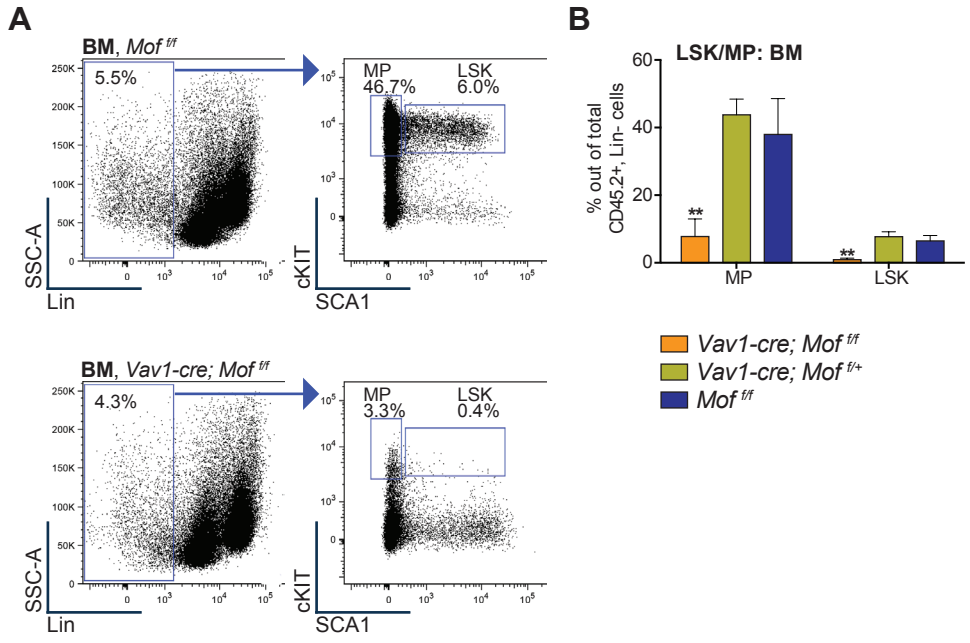

Figure S2, related to Figure 1. *Vav1-cre* induced homozygous Mof loss leads to depletion of myeloid progenitors and LSKs in mouse pups

(A) FACS gating strategy for measuring MP and LSK percentages in bone marrow (BM) derived from 9-day-old *Vav1-cre-Mof$^{f/f}$* and *Mof$^{f/f}$* pups. After CD45.2^{+} live cell selection, Lin^{-} cells are gated and the Lin^{-} population is divided into MPs and the HSC enriched LSK population by cKIT and SCA1 staining. Representative images are shown.

(B) Percentages of MP and LSK cells in Lin^{-} BM as measured by FACS.

** $p < 0.01$. Error bars represent SD of mean. Significance compared to *Moff/f*.

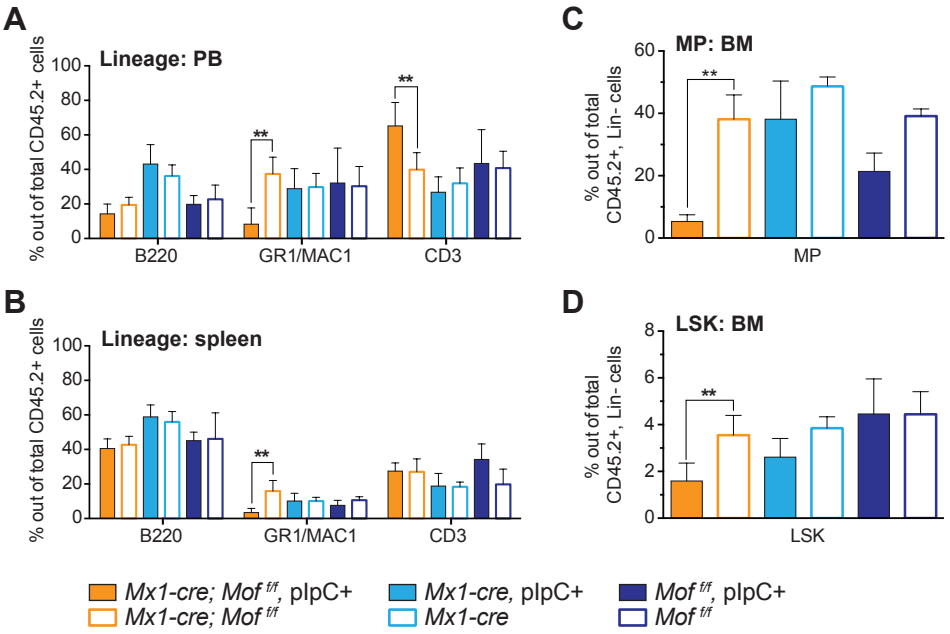

Figure S3, related to Figure 3. *Mx1-cre* induced homozygous Mof loss in adult mice results in dramatic hematopoietic failure

(A) A competitive transplant was performed with 1,000,000 whole bone marrow (BM) cells derived from adult *Mx1-cre-Mof$^{f/f}$*, *Mx1-cre* and *Mof$^{f/f}$* mice and 1,000,000 BM cells from a B6.SJL mouse. B6.SJL recipient mice were injected with the fresh BM cells shortly after lethal irradiation. After 16 weeks, half of the mice per genotype were injected with pIpC and 2 weeks after the 5th dose of pIpC, mice were euthanized and processed. Shown is the percentage of mature B-cells (B220$^+$), myeloid cells (GR1$^+$/MAC1$^+$), and T-cells (CD3$^+$) in live, CD45.2$^+$ PB cells as measured by FACS at time of sacrifice.

(B) Percentages of mature B-, myeloid and T-cells in live, CD45.2$^+$ spleen cells as measured by FACS at time of sacrifice.

(C) Percentages of MPs in live, CD45.2$^+$, Lin$^-$ BM cells as measured by FACS at time of sacrifice.

(D) Percentages of LSKs in live, CD45.2$^+$, Lin$^-$ BM cells as measured by FACS at time of sacrifice.

** $p < 0.01$. Error bars represent SD of mean.

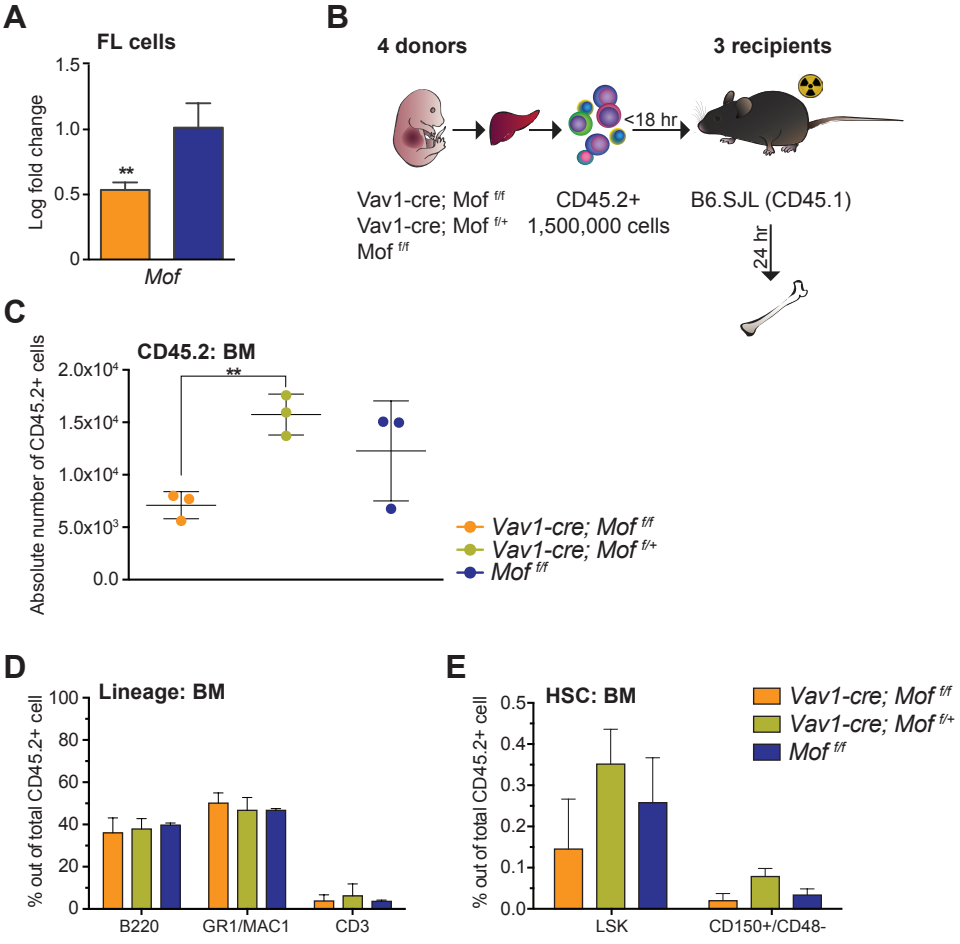

Figure S4, related to Figure 4 and 5. *Vav1-cre-Mof$^{f/f}$* hematopoietic E14.5 fetal liver cells have reduced *Mof* expression and are functionally impaired

(A) Bar graph illustrates relative expression levels (RT-qPCR) as mean log fold change in E14.5 *Vav1-cre-Mof$^{f/f}$* FL cells compared to *Mof$^{f/f}$* control cells.

(B) Schematic for homing experiment. CD45.2$^+$ FL cells derived from E14.5 *Vav1-cre-Mof$^{f/f}$*, *Vav1-cre-Mof$^{f/+}$* or *Mof$^{f/f}$* embryos (n=5 per genotype) were pooled per genotype and 1,500,000 cells injected per lethally irradiated B6.SJL recipient mouse. Mice were euthanized 24 hours after transplant to assess donor cell homing to the BM.

(C) Graph represents the absolute number of CD45.2$^+$ cells detected in the BM of recipient mice, 24 hours post transplant. Each dot represents a single recipient mouse in the experiment.

(D) Transplant experiment with 2,000,000 FL cells derived from E14.5 *Vav1-cre-Mof$^{f/f}$*, *Vav1-cre-Mof$^{f/+}$* and *Mof$^{f/f}$* embryos and 250,000 whole bone marrow (BM) helper cells. B6.SJL recipient mice were injected with cells shortly after lethal irradiation. Percentages of mature B-cells (B220$^+$), myeloid cells (GR1$^+$/MAC1$^+$), and T-cells (CD3$^+$) in live, CD45.2$^+$ BM cells are shown as measured by FACS at time of sacrifice (week 16).

(E) Percentages of LSKs and LT-HSCs (CD150$^+$/CD48$^-$) out of live, CD45.2$^+$ BM cells as measured by FACS at time of sacrifice.

** $p < 0.01$. Error bars represent SD of mean.

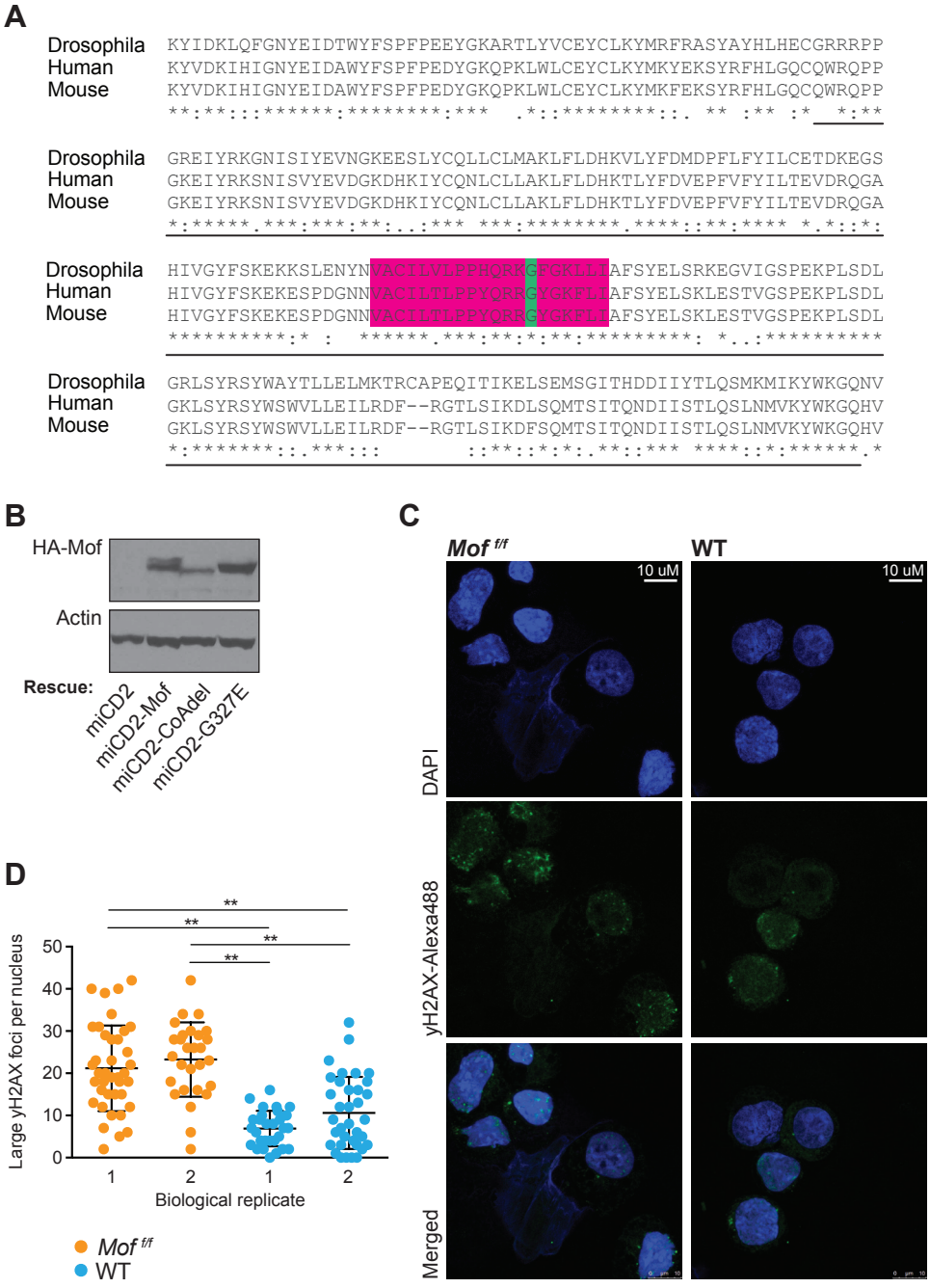
A
Drosophila
Human
Mouse
KYIDKLQFGNYEIDTWYFSPFPEEYGKARTLYVCEYCLKYMRFRASYAYHLHECGRRRPP
KYVDKIHIGNYEIDAWYFSPFPEDYGKQPKLWLCEYCLKYMKYEKSYRFHLGQCQWRQPP
KYVDKIHIGNYEIDAWYFSPFPEDYGKQPKLWLCEYCLKYMKFEKSYRFHLGQCQWRQPP
GREIYRKGNISIYEVNGKEESLYCQLLCLMAKLFLDHKVLYFDMDPFLFYILCETDKEGS
GKEIYRKSNISVYEVDGKDHKIYCQNLCLLAKLFLDHKTLYFDVEPFVFYILTEVDRQGA
GKEIYRKSNISVYEVDGKDHKIYCQNLCLLAKLFLDHKTLYFDVEPFVFYILTEVDRQGA
HIVGYFSKEKKSLENYNVACILVLPPHQRKGFGKLLLAFSYELSRKEGVIGSPEKPLSDL
HIVGYFSKEKESPDGNNVACILTLPPYQRRGYGKFLLAFSYELSKLESTVGSPEKPLSDL
HIVGYFSKEKESPDGNNVACILTLPPYQRRGYGKFLLAFSYELSKLESTVGSPEKPLSDL
GRLSYRSYWAYTLLELMKTRCAPEQITIKELSEMSGITHDDIIYTLQSMKMIKYWKGQNV
GKLSYRSYWSWVLLEILRDF--RGTLSIKDLSQMTSITQNDIISTLQSLNMVKYWKGQHV
GKLSYRSYWSWVLLEILRDF--RGTLSIKDFSQMTSITQNDIISTLQSLNMVKYWKGQHV
B
HA-Mof
Actin
Rescue:
miCD2
miCD2-Mof
miCD2-CoAdel
miCD2-G327E
C
Mof f/f
WT
10 uM
DAPI
γH2AX-Alexa488
Merged
D
Large γH2AX foci per nucleus
Biological replicate
Mof f/f
WT

Figure S5, related to Figure 7. *Mof* loss in LSKs leads to DNA damage
(A) Aligned HAT domains (underlined residues) from *Drosophila*, human and murine MOF. The Acetyl-CoA binding pocket is highlighted in purple and the position of the G327E point mutation is marked in green.
(B) While *Mof* deficient cells in pups were not fully *Mof* deficient and *Mof* deficient FL cells quickly died after putting them in culture, the functionality of these constructs had to be tested in a different murine cell type. Murine *MLL-AF9* leukemia cells in a $Mof^{f/f}$ background were infected with HA-tagged full-length *Mof* (miCD2-Mof), CoA deleted *Mof* (miCD2-CoAdel), G327E mutated *Mof* (miCD2-G327E) or empty vector control (miCD2) in an *MSCV-miCD2* retroviral vector, and selected by sorting $hCD2^+$ cells. Western blotting for HA confirms presence of these exogenous constructs.
(C) $Mof^{f/f}$ or wild type (WT) LSKs were harvested from adult mice, *in vitro* transduced with *Cre*, sorted 48 hours post *Cre* infection and fixed. DNA damage was assesed by immunofluorescence of yH2AX. Representative images are shown.
(D) Graph illustrates the number of large yH2AX foci per cell nucleus, where a dot represents a single cell. Shown are two biological replicates per genotype. There is no significant difference between biological replicates.
** $p < 0.01$. Error bars represent SD of mean.

SUPPLEMENTAL EXPERIMENTAL PROCEDURES

Plasmids and constructs

NH_3-terminal HA-tagged WT *Mof* was amplified by PCR and subcloned into the HpaI site of the retroviral vector MSCV-IRES-miCD2 (MSCV-HA-*Mof*-IRES-miCD2). To generate the two *Mof* HAT domain mutants MSCV-HA-*Mof-G327E*-IRES-miCD2 and MSCV-HA-*Mof-CoAdel*-IRES-miCD2, HA-tagged *Mof-G327E* (327 glycine to glutamic acid mutation, a point mutation in the highly conserved CoA binding pocket of the MOF HAT domain), and HA-tagged *Mof-CoAdel* (deletion of the CoA binding pocket of the MOF HAT domain, 314-333 residues) were generated using the Q5® Site-Directed Mutagenesis Kit (New England BioLabs, Ipswich, MA). The mutant and WT *Mof* constructs were verified by sequencing. The MSCV-*MLL-AF9*-IRES-GFP and MSCV-*Cre*-IRES-dTomato plasmid have been previously described.[1,2] The *pCL-Eco* plasmid was used for retroviral packaging.

Liquid cell culture

293T cells used for ecotropic retroviral production were cultured in DMEM, supplemented with heat inactivated 10% fetal bovine serum (FBS) and 50 U/mL penicillin/streptomycin (all Thermo Fisher Scientific, Waltham, MA).

In vitro transformed *MA9* mouse LSKs and fresh FL cells were cultured in IMDM, supplemented with heat inactivated 10% FBS, 50 U/mL penicillin/streptomycin (all Thermo Fisher Scientific) and murine IL3 (10 ng/mL), IL6 (10 ng/mL) and SCF (20 ng/mL)(all PeproTech, Rocky Hill, NJ).

Fresh BM LSKs or hematopoietic progenitors were cultured in Stemspan (Stemcell Technologies, Vancouver, BC, Canada), supplemented with 100ng/mL SCF, 100ng/mL TPO, 50ng/mL FLT3, 10ng/mL IL3 and 10ng/mL IL6 (all PeproTech).

Transplant experiments

Transplant experiments with P9 *Vav1-cre*; $Mof^{f/f}$, *Vav1-cre*; $Mof^{f/+}$ and $Mof^{f/f}$ BM cells were performed by isolating $CD45.2^+$ BM cells and injecting 633,000 cells per recipient. Depending on the donor cell number, 2-3 recipients per donor were used. Transplant experiments with *Vav1-cre*; $Mof^{f/f}$, *Vav1-cre*; $Mof^{f/+}$ and $Mof^{f/f}$ E14.5 FL cells were performed by injecting 2,000,000 unselected FL cells per recipient (2-3 recipients per donor). For the FL co-transplant experiments, 2,000,000 unselected FL cells and 250,000 whole BM helper cells from a B6.SJL mouse were injected per recipient. FL and P9 transplant experiments were repeated at least two times with multiple donors per genotype per experiment.

Mx1-cre; $Mof^{f/f}$, *Mx1-cre* and $Mof^{f/f}$ BM transplant experiments were conducted by isolating whole BM cells from two 20-week-old donor mice per genotype and from one B6.SJL mouse. Per recipient, 1,000,000 unselected BM cells from both the *Mx1-cre*; $Mof^{f/f}$, *Mx1-cre* or $Mof^{f/f}$ mouse and from the B6.SJL WT mouse were injected. 16 weeks post transplant, mice were split in even groups with a similar mean CD45.2 percentage after which one of the groups received five poly I:C (pIpC, Invivogen, San Diego, CA) injections every other

day (12.5 µg per gram of mouse body weight). Two weeks after the last dose, mice were euthanized and processed. We observed some depletion of CD45.2$^+$ cells in the BM of *Mof$^{f/f}$* recipients though this difference was much more dramatic in the *Mx1-cre; Mof$^{f/f}$* recipients.

Homing experiments

Homing experiments were performed by venous injection of CD45.2$^+$ E14.5 *Vav1-cre*; *Mof$^{f/f}$*, *Vav1-cre*; *Mof$^{f/+}$* or *Mof$^{f/f}$* FL cells into lethally (5 x Gy) irradiated B6.SJL recipients. Five mice were pooled per genotype and 1,500,000 cells injected per recipient mouse. Mice were euthanized exactly 24 hours after transplant and bones harvested to assess CD45.2 frequency by FACS.

FACS analysis

Mof-loss induced changes in hematopoietic populations were identified by staining cells for various surface markers and subsequent FACS analysis on a CANTO II (BD, San Jose, CA). The following FACS antibodies were used in various combinations: CD44 APC, CD25 PE, SCA1 PE-Cy7, SCA1 PerCP-Cy5.5, CD48 FITC and CD45.2 PerCP-Cy5.5 (all eBioscience, San Diego, CA), CD4 PerCP-Cy5.5, TER119 APC, B220 APC-Cy7, CD3 PB, MAC1 APC, MAC1 PerCP-Cy5.5, GR1 PE, GR1 PECy7, cKIT APC, cKIT PE-Cy7, streptavidin APC-Cy7, CD150 PE, CD45.2 APC and CD45.1 PE (all Biolegend, San Diego, CA), CD8a PB, CD71 PE and CD45.2 FITC (all BD).

Western blot

Murine, *in vitro* transformed LSKs with stable expression of the *MA9* fusion and *miCD2*, *miCD2-Mof*, *miCD2-Mof-CoAdel* or *miCD2-Mof-G327E* were lysed in 1X cell lysis buffer (#9803, Cell Signaling, Danvers, MA). Samples were heated at 75 °C for 10 minutes, sonicated for 10 times 30 seconds and analyzed by SDS-PAGE by loading a total of 2 million cells per lane. All H4K16ac and H4 Western blots were performed using either murine E14.5 or E17.5 CD45.2$^+$ FL cells or *Cre*-transduced LSKs that were lysed in an LDS lysis buffer (4X LDS sample buffer from NuPage, H_2O and 0.5M DTT, all Thermo Fisher Scientific). Samples were heated at 95 °C for 10 minutes, sonicated for 10 times 30 seconds and analyzed by SDS-PAGE by loading 100,000 cells per lane.

Western blotting was done following standard procedures using a 10% Bis-Tris Gel (Nupage, Invitrogen, Carlsbad, CA) and transferred onto PVDF membranes using the iBlot dry transfer system (Invitrogen). For assessment of HA-tagged proteins, global H4K16ac, global H4, Actin and GAPDH, anti-HA antibody (HA.11, Covance, Dedham, MA), anti-H4K16ac antibody (07-329, EMD Millipore, Billerica, MA), anti-H4 antibody (07-108, EMD Millipore, Billerica, MA), anti-Actin antibody (MAB1501R, EMD Millipore) and anti-GAPDH antibody (FL-335, Santa Cruz) were used. Secondary antibodies were either sheep anti-mouse IgG (NA931V) or anti-rabbit IgG (NA934V) ECL horseradish peroxidase linked antibody from GE Healthcare (Little Chalfont Buckinghamshire, UK).

yH2AX immunofluorescence staining

Cytospins were generated using the Shandon Cytospin 4 cytofuge (Thermo Fisher Scientific, Waltham, MA) by spinning 70,000-90,000 cells onto glass slides (500 rpm for 10 minutes). Cytospins were fixed using a 4% PFA/PBS mix and cells perforated with 50ug/mL Digitonin in PBS. Cells were incubated at 4 °C overnight with yH2A.X p-S139 (Abcam, Cambridge, MA) and 30 minutes at room temperature with the secondary anti-rabbit Alexa488 antibody (Molecular Probes, Thermo Fisher Scientific, Waltham, MA). Then cells were stained with DAPI and mounted using Prolong Gold Antifade Reagent (both Thermo Fisher Scientific, Waltham, MA). Nuclear immunofluorescence microscopy was done using a Leica SP5 upright confocal microscope (Leica, Wetzlar, Germany). The number of yH2AX foci was determined using ImageJ software on representative microscopy images.

REFERENCES

1. Bernt KM, Zhu N, Sinha AU, et al. MLL-rearranged leukemia is dependent on aberrant H3K79 methylation by DOT1L. *Cancer Cell.* 2011;20(1):66-78.
2. Deshpande AJ, Deshpande A, Sinha AU, et al. AF10 regulates progressive H3K79 methylation and HOX gene expression in diverse AML subtypes. *Cancer Cell.* 2014;26(6):896-908.

6

SUMMARY AND GENERAL DISCUSSION

In this thesis we have explored chromatin regulation in acute leukemia and normal hematopoiesis. In doing so, we have focused on the H3K4 methyltransferase MLL1 and the H4K16 acetyltransferase MOF. Here we will summarize the major findings of our experimental studies reported in Chapters 3, 4 and 5 and discuss their relevance for our understanding of the biology of leukemia as well as their potential therapeutic implications.

NUP98 FUSION PROTEINS INTERACT WITH THE NSL AND MLL1 COMPLEXES TO DRIVE LEUKEMOGENESIS

In Chapter 3 we showed that NUP98 fusion proteins encoded by *NUP98* fusion genes such as *NUP98-HOXA9*, *NUP98-HOXD13*, *NUP98-TOP1* and *NUP98-NSD1*, physically interact with MLL1 and the NSL histone modifying complexes. Using ChIP-seq, we identified significant overlap in binding targets between NUP98 fusions and MLL1 (Figure 1, top panel). Further functional assays illustrated that *Mll1* is required for the colony formation of various *NUP98*-fusion driven leukemias *in vitro* and for maintenance of *NUP98-HOXA9* (*NHA9*) leukemia *in vivo*. *Mll1* loss leads to terminal differentiation of leukemic blasts through decreased expression of genes where NUP98 fusions and MLL1 colocalize, such as *Meis1* and *Hox* cluster genes (Figure 1, bottom panel). This relation between MLL1 and NUP98 fusion target gene expression was confirmed by rescue experiments with exogenous expression of these shared target genes, which leads to rescue of the *Mll1*-loss-induced phenotype. Thus these findings indicate that MLL1 is crucial for *NUP98* fusion leukemogenesis, likely by recruiting the NUP98 fusion protein to its target gene loci.

One of the next questions is: which are the critical protein(s) that interact with the NUP98 fusion and the MLL1 and NSL complexes? Based on previous *Drosophila* data[1] it is likely that the interaction is through PHF20, which is a component of both the MLL1 and NSL complex. It is also possible that the NUP98 fusion protein interacts with the MLL1 complex through menin, similar to what has been found for the MLL-AF9 fusion protein[2], and that MOF directly binds to MLL1 as was described by Dou *et al*[3]. Knockdown experiments followed by IP of the various proteins involved, could shed light on this question.

With regard to the specific domain of interaction, our data demonstrate that MLL1 and NSL protein complexes interact with the NUP98 N-terminus, but only in case of a truncated NUP98 as found in the fusion protein; wild type NUP98 does not interact. As was previously shown in *Drosophila*[4], our findings confirm that, while wild type NUP98 is localized in the nuclear membrane as part of the nuclear pore complexes, the NUP98 N-terminus only localizes in the nucleoplasm. We found that the same nucleoplasmic localization holds true for NUP98 fusion proteins. Therefore we hypothesize that, due to this nucleoplasmic localization, MLL1 and NSL complexes can interact with the NUP98 fusion protein and that this interaction allows for the NUP98 fusion to be recruited to the DNA target loci. Based on our findings, this mechanism of oncogenicity may apply to all various *NUP98* translocations.

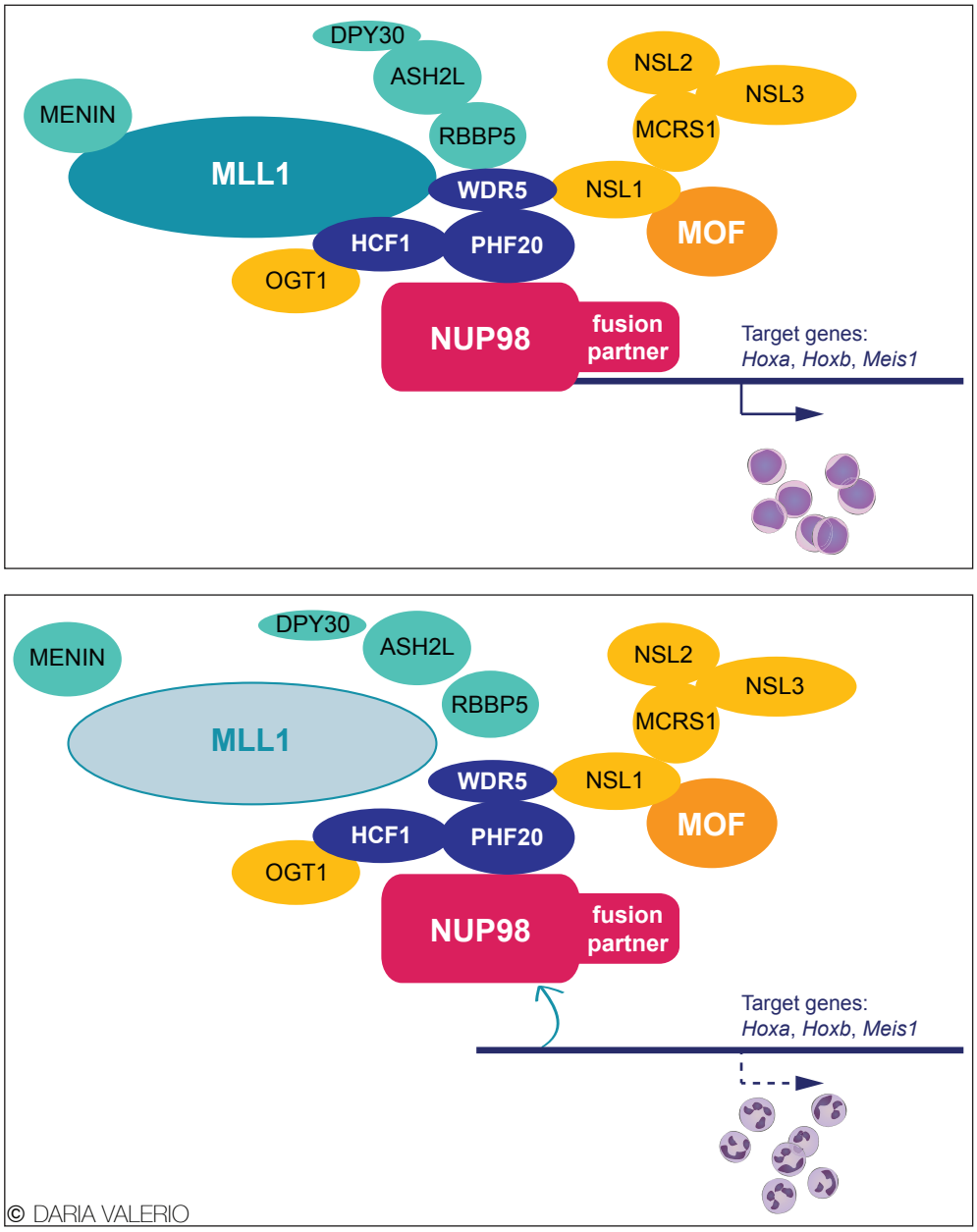

Figure 1. NUP98 fusion proteins interact with the NSL and MLL1 complexes to drive leukemogenesis
The top panel illustrates that NUP98 fusion proteins were found to physically interact with the MLL1 (turquoise colored) and NSL (yellow/orange colored) complexes. The dark blue proteins are shared between both the MLL1 and NSL complex. Based on *Drosophila* data, this interaction may be through PHF20, a protein present in both complexes. NUP98 fusion proteins bind DNA at various target genes such as *Meis1* and *Hoxa* and *b* cluster loci where they upregulate expression of these genes. The bottom panel indicates that upon MLL1 loss, expression of the target genes diminishes, possibly while NUP98 fusions are no longer able to bind the DNA loci. The decreased expression of these target genes leads to terminal differentiation of the leukemic blasts.

HISTONE ACETYLTRANSFERASE ACTIVITY OF MOF IS REQUIRED FOR *MLL-AF9* LEUKEMOGENESIS

In Chapter 4 we identified *Mof* knockdown as one of the most potent suppressors of *MLL-AF9* (*MA9*) leukemic cell growth in a chromatin regulator focused RNAi screen. Further experiments using a murine conditional *Mof* knockout (KO) model illustrated that homozygous *Mof* deletion in *MA9* leukemic cells leads to reduced tumor burden and prolonged survival in mice. RNA sequencing and immunofluorescence experiments indicate defective DNA damage repair as one of the mechanisms of cell death in *Mof*-deficient *MA9* cells. In addition, we uncovered a loss of global H4K16ac upon *Mof* KO. Rescue experiments with histone acetyltransferase (HAT) domain mutated MOF illustrated that MOF HAT activity is indispensable for *MA9* leukemia maintenance (Figure 2).

Though we have established the importance of MOF HAT activity for *MA9* leukemogenesis, we have not yet elucidated the mechanism by which H4K16ac loss leads to cell death. Based on our data and previous studies in murine embryonic fibroblasts (MEFs), impaired DNA damage and possibly chromosomal instability are involved. Li *et al.* showed that radiation induced DNA damage in wild type MEFs leads to an increase of global H4K16ac[5], suggesting that a MOF-induced increase of H4K16ac may be essential for an appropriate DNA damage response. Unacetylated H4K16 is required to achieve the maximum tendency of *in vitro* nucleosome arrays to fold into secondary or tertiary chromatin structures.[6] In contrast, 30% H4K16 acetylation alleviates compaction of the chromatin fiber.[7] Therefore it may be that global H4K16ac depletion upon loss of MOF reduces accessibility of nucleosomes to repair proteins, by increasing chromatin compaction at the DNA damage foci. Future experiments assessing chromatin accessibility in *MA9 Mof*-null cells by assay for transposase-accessible chromatin with high throughput sequencing (ATAC-seq) and micrococcal nuclease digestion assays should provide data on general chromatin compaction and may help elucidate the connection between H4K16ac and accessibility of genes involved in DNA damage repair.

HISTONE ACETYLTRANSFERASE ACTIVITY OF MOF IS REQUIRED FOR ADULT, BUT NOT EARLY FETAL HEMATOPOIESIS IN MICE

In Chapter 5 we have demonstrated that *Mof* expression is critical for hematopoietic cell maintenance and hematopoietic reconstitution in adult hematopoiesis. Rescue experiments with *Mof* HAT domain mutants illustrated the requirement for MOF acetyltransferase activity in HSC and progenitor maintenance and colony-forming capacity. In contrast, E14.5 fetal hematopoiesis did not seem affected by homozygous *Mof* deletion despite dramatic loss of global H4K16ac. Hematopoietic defects start manifesting late gestation at E17.5 (Figure 3).

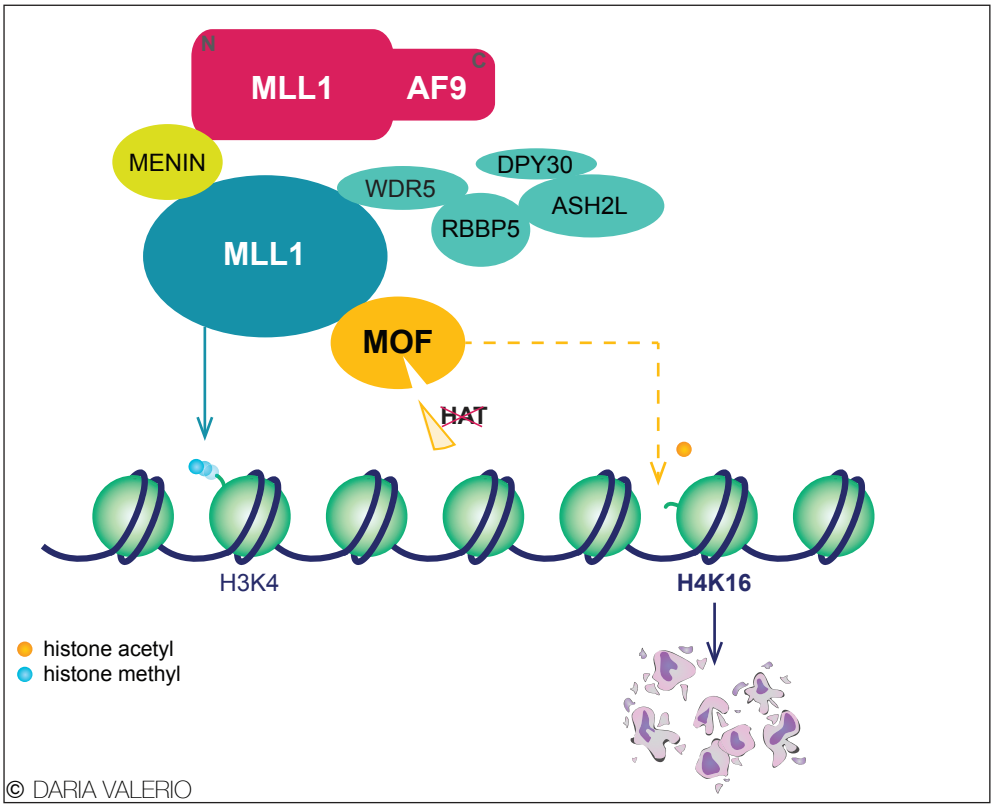

Figure 2. Histone acetyltransferase activity of MOF is required for *MLL-AF9* leukemogenesis
The physical interaction between wild type MLL1 and the MLL-AF9 fusion protein through menin has previously been established. In addition, it was shown that MOF and MLL1 not only share several proteins in their respective complexes, but also directly interact. MLL1 is an H3K4 methyltransferase, but this enzymatic function is not required for *MLL-AF9* leukemogenesis. We found that MOF and it's histone acetyltransferase (HAT) activity are required for *MLL-AF9* leukemia maintenance and that loss of MOF HAT activity leads to global loss of H4K16ac and thereby leukemic blast cell death.

It has been well established that the hematopoietic system undergoes discrete developmental changes in the transition from fetal to adult hematopoiesis. Where earlier fetal hematopoiesis demands rapid expansion of undifferentiated HSCs to supply the developing hematopoietic system[8], lifelong blood cell production in adult hematopoiesis depends on the delicate balance between HSC self-renewal and differentiation[9]. While pluripotency and lineage differentiation require the establishment and maintenance of gene expression programs that are largely regulated by chromatin organization[10], it seems likely that multiple chromatin regulators are crucial for hematopoiesis at varying stages of development. Consistent with this notion is the finding that the chromatin regulator *Ezh2* is required for fetal

but not adult hematopoiesis.[11] Our findings also support this idea of chromatin regulators being differentially involved in hematopoietic development, since we have shown that MOF HAT activity is a crucial regulator of post-natal and adult hematopoiesis, but not of the highly proliferative early and mid- gestational hematopoietic compartment.

Although many common signals may be present in both the fetal and adult HSC niche, distinct regulatory mechanisms exist to promote *de novo* generation or expansion of HSCs in the fetus, as compared to the mechanisms governing the balance of HSC differentiation and quiescence in the adult.[8] Significant progress has been made in understanding the adult hematopoietic microenvironment, but only little is known about the fetal niche. Hackney et al. have made a first step in defining key components of the fetal liver (FL) microenvironment that support HSC expansion.[12,13] By generating and comparing FL derived stromal cell lines with varying abilities to support HSC expansion, they identified multiple differentially expressed genes that play an important role in the *in vivo* FL HSC niche. It is, however, conceivable that the FL microenvironment itself is also modified during fetal development in order to meet the changing needs of lineage differentiation and HSC expansion in the embryo.[12] Our data suggest that earlier embryonic, *Mof*-deficient HSCs (<E15.5) are capable of proliferation and differentiation. However, over the next few days of gestation, intrinsic cellular requirements and microenvironmental stimuli change and it may be that *Mof*-null, H4K16ac-deficient HSCs are incapable of adapting to these changes due to significant abnormalities in chromatin structure.

Another interesting question that remains to be addressed is why E14.5 fetal hematopoietic cells can exist despite the dramatic, MOF-loss-induced H4K16ac deficiency. Most studies on *Mof* depletion report adverse outcomes in a wide array of cell types and H4K16ac has been shown to play a critical role in regulating transcription in mouse embryonic stem cells.[14] However, a recent study found that *Mof* deficiency and concurrent H4K16ac loss in quiescent glomerular podocytes had no effect on kidney function in mice.[15] These findings suggest that H4K16ac requirement may indeed be cell type or tissue specific, though it remains surprising that highly proliferative and immature fetal HSCs can function despite lack of H4K16ac. It may be that, in the earlier fetal HSC, other chromatin marks such as H3K27ac compensate for this lack of H4K16ac and thereby can maintain accessible chromatin. Future studies using quantitative mass spectrometry to define global epigenomic changes[16] could yield significant mechanistic insight into the role of altered epigenomic states throughout hematopoietic development.

ARE MOF AND MLL1 GOOD SMALL MOLECULE INHIBITOR TARGETS IN ACUTE LEUKEMIA?

In Chapter 4 we have shown that MOF HAT activity is required for *MA9* leukemogenesis and that loss inhibits leukemic cell maintenance. These findings suggest that inhibiting MOF HAT

activity with a small molecule might offer an effective approach in treating patients with *MLL*-rearranged leukemia. As a matter of fact, there already is a compound available (MG149) that effectively targets MOF HAT activity, implying that developing a more potent MOF HAT inhibitor would be technically feasible. However, our data and previous findings suggest that MOF loss rapidly kills cells, including normal adult hematopoietic cells, and, though we have identified E14.5 fetal HSCs not to be affected by MOF loss (Chapter 5), in general the effect of MOF HAT loss may not be sufficiently selective. On the other hand, this does not automatically mean that there is no therapeutic window in which a MOF HAT inhibitor

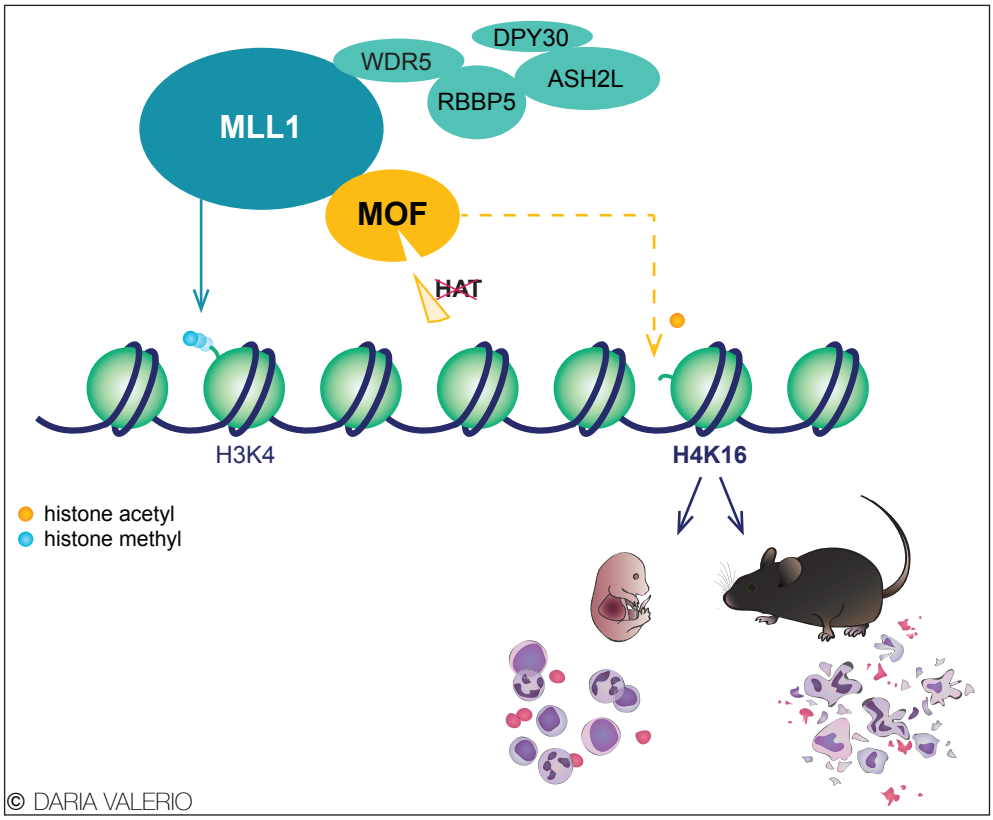

Figure 3. Histone acetyltransferase activity of MOF is required for adult, but not E14.5 fetal hematopoiesis

MOF and MLL1 physically interact. MLL1 H3K4 methyltransferase activity is not required for normal murine hematopoiesis. However, loss of MOF histone acetyltransferase (HAT) activity in murine, adult hematopoietic cells leads to global loss of H4K16ac and rapid hematopoietic cell death. The same global loss of H4K16ac is observed in fetal hematopoietic *Mof*-null cells, but despite this dramatic change, early and mid- gestational hematopoiesis does not appear to be affected.

would kill leukemic cells very effectively without too much toxicity for normal cells. Evidence suggests that cancer cells are more sensitive to inhibition of enzymatic activity of certain proteins than normal tissue, in those instances indeed allowing for a therapeutic window. Examples of epigenetic modifiers that would fall in this category are DOT1L, BRD4 and LSD1. DOT1L loss has been shown to severely impair normal hematopoiesis[17], sustained BRD4 inhibition demonstrates dramatic toxicity in most tissues[18] and LSD1 inhibition leads to severe hematopoietic toxicity[19]. However, small molecule inhibitors targeting enzymatic activity for all three of these proteins are currently in clinical trials.[20] We therefore believe it is worth further exploring MOF HAT activity as a candidate drug target in *MLL*-rearranged acute leukemia and we feel that developing potent small molecules targeting MOF activity is warranted.

In this thesis we have demonstrated that the MLL1 core complex physically interacts with oncogenic NUP98 fusion proteins and that MLL1 is required for the leukemogenic potential of *NUP98* translocations (Chapter 3). Unlike *Mof* KO, *Mll1* deficiency does not cause rapid cell death, but leads to differentiation of leukemic blasts, suggesting that, much like in *Dot1l* KO models[17], the leukemic cell resumes a more normal hematopoietic maturation program and eventually dies. However, it is as of yet unclear what part of MLL1 to target. The MLL1 SET domain has histone methyltransferase activity, methylating H3K4. We considered that it may be this histone methyltransferase activity that is required for *NUP98* fusion leukemogenesis. Yet, our unpublished data suggest that MLL1 loss in *NHA9* leukemic cells does not change global H3K4me3. In addition, we found that MLL1 SET-domain deleted hematopoietic stem- and progenitor cells are still capable of leukemic transformation upon introduction of the *NHA9* fusion (unpublished data), much like what was previously found for *MA9*[21]. These data point toward the dispensability of MLL1 histone methyltransferase activity in *NUP98* fusion leukemogenesis. We have, however, shown the colocalization of NUP98 fusion proteins and MLL1 at NUP98 fusion target loci by ChIP-seq. This finding indicates that NUP98 fusions may utilize their interaction with the MLL1 complex to be recruited to chromatin, specifically at NUP98 fusion target loci such as *Hox* cluster genes and *Meis1*. In *MLL*-rearranged leukemia, genetic deletion of *Menin* reverses aberrant *Hox* gene expression, mediated by MLL1-menin promoter-associated complexes.[22] Following the latter gene expression reversal, the differentiation arrest and oncogenic properties of *MLL1* fusion transformed leukemic blasts are abrogated. Inhibitors blocking the interaction between MLL1 and menin were shown to reverse aberrant *Hoxa9, Flt3* and *Meis1* expression and prolong survival of *MA9* leukemic mice.[23] It might be that, similar to what has been observed in *MLL*-rearranged leukemia, NUP98 fusion proteins require not only MLL1, but also the interaction between MLL1 and menin in order to bind target gene loci. This hypothesis requires further investigation, but if correct, would offer an interesting therapeutic opportunity for leukemia patients carrying a *NUP98* translocation.

REFERENCES

1. Pascual-Garcia P, Jeong J, Capelson M. Nucleoporin Nup98 associates with Trx/MLL and NSL histone-modifying complexes and regulates Hox gene expression. *Cell Rep.* 2014;9(2):433-442.
2. Thiel AT, Blessington P, Zou T, et al. MLL-AF9-induced leukemogenesis requires coexpression of the wild type Mll allele. *Cancer Cell.* 2010;17(2):148-159.
3. Dou Y, Milne TA, Tackett AJ, et al. Physical association and coordinate function of the H3 K4 methyltransferase MLL1 and the H4 K16 acetyltransferase MOF. *Cell.* 2005;121(6):873-885.
4. Kalverda B, Pickersgill H, Shloma VV, Fornerod M. Nucleoporins directly stimulate expression of developmental and cell-cycle genes inside the nucleoplasm. *Cell.* 2010;140(3):360-371.
5. Li X, Corsa CA, Pan PW, et al. MOF and H4 K16 acetylation play important roles in DNA damage repair by modulating recruitment of DNA damage repair protein Mdc1. *Mol Cell Biol.* 2010;30(22):5335-47
6. Shogren-Knaak M, Ishii H, Sun JM, Pazin MJ, Davie JR, Peterson CL. Histone H4-K16 acetylation controls chromatin structure and protein interactions. *Science.* 2006;311(5762):844-847.
7. Robinson PJ, An W, Routh A, et al. 30 nm chromatin fibre decompaction requires both H4-K16 acetylation and linker histone eviction. *J Mol Biol.* 2008;381(4):816-825.
8. Lessard J, Faubert A, Sauvageau G. Genetic programs regulating HSC specification, maintenance and expansion. *Oncogene.* 2004;23(43):7199-7209.
9. Cheshier SH, Morrison SJ, Liao X, Weissman IL. In vivo proliferation and cell cycle kinetics of long-term self-renewing hematopoietic stem cells. *Proc Natl Acad Sci U S A.* 1999;96(6):3120-3125.
10. Teitell MA, Mikkola HK. Transcriptional activators, repressors, and epigenetic modifiers controlling hematopoietic stem cell development. *Pediatr Res.* 2006;59(4 Pt 2):33r-39r.
11. Mochizuki-Kashio M, Mishima Y, Miyagi S, et al. Dependency on the polycomb gene Ezh2 distinguishes fetal from adult hematopoietic stem cells. *Blood.* 2011;118(25):6553-6561.
12. Mikkola HK, Orkin SH. The journey of developing hematopoietic stem cells. *Development.* 2006;133(19):3733-3744.
13. Hackney JA, Charbord P, Brunk BP, Stoeckert CJ, Lemischka IR, Moore KA. A molecular profile of a hematopoietic stem cell niche. *Proc Natl Acad Sci U S A.* 2002;99(20):13061-13066.
14. Li X, Li L, Pandey R, et al. The histone acetyltransferase MOF is a key regulator of the embryonic stem cell core transcriptional network. *Cell Stem Cell.* 2012;11(2):163-178.
15. Sheikh BN, Bechtel-Walz W, Lucci J, et al. MOF maintains transcriptional programs regulating cellular stress response. *Oncogene.* 2015.
16. Britton LM, Gonzales-Cope M, Zee BM, Garcia BA. Breaking the histone code with quantitative mass spectrometry. *Expert Rev Proteomics.* 2011;8(5):631-643.
17. Bernt KM, Zhu N, Sinha AU, et al. MLL-rearranged leukemia is dependent on aberrant H3K79 methylation by DOT1L. *Cancer Cell.* 2011;20(1):66-78.
18. Bolden JE, Tasdemir N, Dow LE, et al. Inducible in vivo silencing of Brd4 identifies potential toxicities of sustained BET protein inhibition. *Cell Reports.* 2014;8(6):1919-1929.
19. Sprussel A, Schulte JH, Weber S, et al. Lysine-specific demethylase 1 restricts hematopoietic progenitor proliferation and is essential for terminal differentiation. *Leukemia.*2012;26(9):2039-2051.
20. Brien Gerard L, Valerio Daria G, Armstrong Scott A. Exploiting the Epigenome to Control Cancer-Promoting Gene-Expression Programs. *Cancer Cell.* 2016;29(4):464-476.
21. Mishra BP, Zaffuto KM, Artinger EL, et al. The histone methyltransferase activity of MLL1 is dispensable for hematopoiesis and leukemogenesis. *Cell Reports.* 2014;7(4):1239-1247.
22. Yokoyama A, Somervaille TC, Smith KS, Rozenblatt-Rosen O, Meyerson M, Cleary ML. The menin tumor suppressor protein is an essential oncogenic cofactor for MLL-associated leukemogenesis. *Cell.* 2005;123(2):207-218.
23. Borkin D, He S, Miao H, et al. Pharmacologic inhibition of the Menin-MLL interaction blocks progression of MLL leukemia in vivo. *Cancer Cell.* 2015;27(4):589-602.

7

NEDERLANDSE SAMENVATTING (DUTCH SUMMARY)

BLOEDFUNCTIE EN -PRODUCTIE

Bloed bestaat uit meerdere type cellen die allen essentieel zijn voor ons bestaan. Het grootste volume van bloed wordt ingenomen door bloedplasma. In dat plasma bevinden zich rode bloedcellen (erytrocyten) die zorgen voor zuurstoftransport, witte bloedcellen (leukocyten) die dienen als afweer tegen infecties en bloedplaatjes (trombocyten) die belangrijk zijn voor de bloedstolling. Omdat de meeste bloedcellen een beperkte levensduur hebben, vindt er continu nieuwe aanmaak plaats. De productie van bloedcellen (hematopoëse) speelt zich af in het beenmerg. Aan de basis van dit systeem staan hematopoietische stamcellen. Deze stamcellen hebben de unieke eigenschap dat ze bij de celdeling zowel een nieuwe stamcel als een dochtercel kunnen produceren. De dochtercel van een stamcel noemt men een voorlopercel en deze kunnen via een stapsgewijs en complex proces uitrijpen (differentiëren) tot een van de drie verschillende soorten bloedcellen (Figuur 1 van Introductie). “Volwassen” of uitgerijpte bloedcellen komen terecht in het perifere bloed en worden dan door het hart via de circulatie rondgepompt naar de verschillende organen en weefsels om hun eerder genoemde functies uit te oefenen. In het perifere bloed zijn normaal gesproken geen hematopoietische stamcellen of voorlopercellen aanwezig.

ACUTE LEUKEMIE

Acute leukemie is bloedkanker, een ziekte waarbij onrijpe hematopoietische cellen (stamcellen of voorlopercellen) ontsporen, met een woekering (ongeremde celdeling, oftewel proliferatie) van deze cellen tot gevolg. Deze cellen (leukemische blasten) hebben tevens het vermogen tot normale differentiatie verloren. In het geval van acute leukemie ontstaat hierdoor een ophoping van leukemische blasten in het beenmerg. Zij verdringen het normale, gezonde bloedsysteem waardoor er te weinig nieuwe erytrocyten, leukocyten en trombocyten worden aangemaakt. Dit geeft klachten zoals vermoeidheid, een bleke huid, verhoogde kans op infecties en een verhoogde bloedingsneiging. Tevens lekken leukemische blasten op enig moment uit het beenmerg naar het perifere bloed, waardoor er een sterk verhoogd aantal in het perifere bloed en soms ook in andere organen te vinden kan zijn.

In algemene zin wordt in het hematopoietisch systeem onderscheid gemaakt tussen myeloïde cellen (myeloïde leukocyten, erytrocyten, trombocyten en hun voorlopercellen) en lymfoïde cellen (lymfoïde leukocyten en hun voorlopercellen). Bij acute myeloïde leukemie (AML) is sprake van afwijkingen in myeloïde voorlopercellen en bij acute lymfoïde leukemie (ALL) ontstaat de fout in lymfoïde voorlopercellen.

Hematopoietische stam- of voorlopercellen worden leukemische cellen doordat er fouten optreden in het DNA. Het DNA in onze cellen bestaat uit een zeer lange streng aan code die is opgedeeld in genen. Eén gen kan een gen-specifiek eiwit produceren. Al deze diverse eiwitten reguleren de biologische functies binnen het menselijk lichaam. Er zijn

grofweg twee soorten genetische fouten die ten grondslag kunnen liggen aan het ontstaan van leukemie doordat er geen of verkeerde eiwitten worden geproduceerd: relatief kleine fouten in de DNA-code genaamd mutaties en grotere chromosomale afwijkingen zoals translocaties waarbij een deel van het ene chromosoom wordt verwisseld met een deel van een ander chromosoom waardoor er een nieuw fusie-gen ontstaat.

Er zijn een groot aantal verschillende translocaties die leukemie kunnen veroorzaken. In dit proefschrift hebben we ons gericht op translocaties van het *MLL1*-gen en van het *NUP98*-gen. Deze translocaties, waarbij een stuk van MLL1 of NUP98 naar een ander chromosoom verhuist en daar fuseert met een stuk van een ander gen (bijvoorbeeld AF9 of HOXA9), produceren een fusie-eiwit. Deze fusie-eiwitten verstoren belangrijke functies van de hematopoietische cellen en veranderen een normale hematopoietische cel in een leukemische cel. Hoe deze fusie-eiwitten de cellen in hun groei ontregelen en daarmee leukemie veroorzaken is echter nog grotendeels onopgehelderd. Door deze ziekte-mechanismen te doorgronden kunnen er nieuwe medicijnen worden ontwikkeld die zich specifiek richten op de kankercel. Op dit moment bestaat de behandeling van patiënten met acute leukemie overwegend uit de toepassing van chemotherapie, hetgeen succesvol is bij een gedeelte van de patiënten. Een substantieel aantal patiënten reageert uiteindelijk echter onvoldoende op chemotherapie of ervaart dusdanige bijwerkingen dat zij vroeger of later komen te overlijden. Er is dan ook dringend behoefte aan nieuwe behandelingen voor deze patiëntengroep. Door kennis te vergaren over de biologie van leukemie kunnen er specifieke medicijnen ontwikkeld worden die de leukemie gerichter aanvallen op hun kwetsbare plek. Dergelijke gerichte behandeling (*targeted therapy*) zou in theorie kunnen zorgen voor een groter effect en minder bijwerkingen.

EPIGENETICA; MEER DAN DNA

De code van al het DNA in onze cellen is exact hetzelfde. Zelfs tussen mens en muis is 92% van de DNA-code gelijk. Er moeten dus mechanismen bestaan die er voor zorgen dat huidcellen, spiercellen, bloedcellen, etc. allemaal andere functies uitoefenen. Deze mechanismen scharen we onder het kopje “epigenetica”. “Epi” komt van het Griekse woord “ἐπι” wat “bovenop” betekent; dat wat zich bovenop de genetica afspeelt. Omdat er veel DNA is en dat allemaal in een zeer kleine celkern wordt opgeborgen moet het DNA slim worden opgerold. Zoals al eerder genoemd zit DNA opgerold in chromosomen. Deze chromosomen bestaan uit DNA wat rondom een eiwitcomplex gerold zit en daarmee een soort kralenkoord vormt. Dit “kralenkoord” kan strak of wat losser opgevouwen zijn en alleen als het losser gevouwen is kunnen de genen worden afgelezen en daarmee eiwitten worden geproduceerd. Zodoende worden er dus grote stukken DNA nooit of minder vaak afgelezen terwijl ander delen continu open en daarmee “aan” zijn. Dit proces wordt gereguleerd door chemische verbindingen die zich koppelen aan DNA of de eiwitten waarom het DNA zich

wikkelt (Figuur 3 van Introductie). Sommige van deze verbindingen zorgen voor gesloten en andere juist voor geopend DNA. De eiwitten die deze processen regelen en de chemische verbinding plaatsen of juist verwijderen noemen we epigenetische regulator-eiwitten.

EPIGENETISCHE DISREGULATIE IN LEUKEMIE

Epigenetische regulatie is van groot belang voor ons bestaan. Als hier fouten optreden kan dat drastische gevolgen hebben voor het functioneren van een cel. De afgelopen jaren is duidelijk geworden dat epigenetische disregulatie een belangrijke rol speelt bij het ontstaan van kanker. Veel onderzoekers hebben zich gericht op het bestuderen van epigenetische disregulatie in kankercellen, in de hoop daarmee nieuwe therapeutische aangrijpingspunten te vinden. Dat werk vordert gestaag en er zijn inmiddels diverse medicijnen op de markt of in ontwikkeling (Hoofdstuk 2). Er kan echter resistentie optreden tegen deze nieuwe medicijnen waardoor het medicijn zijn werkzaamheid verliest; uit kankercellen die resistent worden en daarmee ontsnappen aan de werking van het geneesmiddel kunnen zich weer nieuwe kankercellen ontwikkelen. De gedachte is daarom dat je meer ziekte-mechanismen tegelijk moet aanpakken om de verschillende ontsnappingsroutes te blokkeren en zodoende alle kankercellen uit te roeien. Het doel van ons onderzoek was om een deel van het epigenetische regulator-mechanisme bij acute leukemie op te helderen en daarmee een basis te leggen voor de ontwikkeling van een dergelijk nieuw medicijn.

In dit proefschrift hebben we onderzoek gedaan naar twee eiwitten die beide epigenetische regulator-eiwitten zijn: MOF en MLL1. In eerste instantie vonden we dat deze eiwitten beide binden aan het NUP98-fusie-eiwit (Hoofdstuk 3). In muismodellen bleek dat acute leukemie die aangedreven wordt door deze NUP98-translocaties niet kan bestaan zonder MLL1; de leukemische blasten die geblokkeerd zijn in hun uitrijping gaan weer differentiëren doordat de door NUP98-fusie-eiwit gedreven genexpressie programma's worden uitgezet. Binnen circa twee weken zijn alle leukemische blasten dood. Van MLL1 was reeds bekend dat het een rol speelt bij leukemie die wordt aangedreven door MLL-AF9 translocaties. Wij vroegen ons vervolgens af of ook MOF belangrijk is voor het ontstaan en het in stand houden van MLL-AF9 leukemie (Hoofdstuk 4). Wederom met behulp van muismodellen bleek dat MOF een cruciaal eiwit is voor MLL-AF9 leukemie en dat muizen geen leukemie ontwikkelen als de pre-leukemische cellen MOF verliezen. Eiwitten hebben meestal meerdere functies, maar uit ons onderzoek blijkt dat specifiek de epigenetische regulator functie van MOF essentieel is voor MLL-AF9 leukemie.

Bij het onderzoek naar de rol van bepaalde eiwitten in het ontstaan van ziekten is het ook belangrijk om te weten wat de rol van deze eiwitten is in het normale weefsel. Het was reeds bekend dat de normale hematopoëse in muizen onmogelijk is zonder MLL1. Muis-embryo's sterven vroeg in de zwangerschap doordat de vorming van hematopoietische stamcellen en voorlopercellen ontbreekt. De rol van MOF bij de normale hematopoëse was echter nog

onbekend. Wij hebben dit onderzocht door gebruik te maken van genetisch gemodificeerde muismodellen waarbij MOF al gedurende de embryonale ontwikkeling afwezig is in alle hematopoietische cellen (Hoofdstuk 5). Het blijkt dat MOF expressie essentieel is voor de aanmaak en overleving van volwassen hematopoietische cellen. Bovendien blijkt wederom de epigenetische regulator functie van MOF onmisbaar te zijn. Uit ons onderzoek blijkt echter ook dat muizen-embryo's zonder MOF expressie een normaal functionerend hematopoietisch systeem hebben, ondanks de afwezigheid van de epigenetische regulator activiteit van MOF. MOF is daarmee momenteel een van de weinige epigenetische regulator-eiwitten waarvan bekend is dat de expressie en activiteit essentieel zijn voor de volwassen hematopoëse, maar overbodig voor vroege foetale hematopoëse. Deze bevindingen benadrukken het belang van epigenetische regulatie bij de ontwikkeling van het hematopoietisch systeem in zoogdieren.

De resultaten in dit proefschrift bieden een aanzet tot het doorontwikkelen van reeds bestaande moleculen die de epigenetische activiteit van MLL1 en MOF remmen. De ontwikkeling van op deze inzichten gebaseerde medicijnen biedt perspectief voor het doelgericht behandelen van patiënten met acute leukemie.

APPENDICES

List of Abbreviations

Co-Authors and their affiliations

About the author

Curriculum Vitae
List of Publications
PhD Portfolio

Acknowledgments (Dankwoord)

LIST OF ABBREVIATIONS

4-OHT	4-Hydroxytamoxifen
AGM	Aorta-Gonad-Mesonephros
ALL	Acute Lymphoid Leukemia
AML	Acute Myeloid Leukemia
AR	Androgen Receptor
ATAC-seq	Assay for Transposase-Accessible Chromatin with high-throughput sequencing
B6.SJL	C57 black 6 mice, but hematopoietic cells express CD45.1 rather than CD45.2
BET	Bromodomain and Extra Terminal
BM	Bone Marrow
C-terminal	COOH-terminal
C57Bl/6	C57 black 6 mice with hematopoietic cells expressing CD45.2
CBC	Complete Blood Count
CFU	Colony-forming Unit
ChIP	Chromatin Immunoprecipitation
ChIP-seq	Chromatin Immunoprecipitation with high throughput sequencing
CML	Chronic Myeloid Leukemia
Co-IP	Co-Immunopreciptation
CoA	Canonical acetyl coenzyme A
CoAdel	CoA binding site deletion
Cryo-EM	Cryogenic-electron microscopy
E14.5	Embryonic age 14.5
ETOH	Ethanol
FBS	Fetal Bovine Serum
FDR	False Discovery Rate
FG	Phenylalanine, Leucine
FL	Fetal Liver
G327E	Point mutation: replacement of glycine by glutamic acid on position 327
gDNA	Genomic DNA
GLEBS	Gle2-Binding Sequence
GLFG	Glycine, Leucine, Phenylalanine, Glycine
GSEA	Gene Set Enrichment Analysis
GSI	Gamma-Secretase Inhibitors
H3K27	Histone 3, Lysine 27
H3K36	Histone 3, Lysine 36
H3K4	Histone 3, Lysine 4
H3K79	Histone 3, Lysine 79
H3K9	Histone 3, Lysine 9

H4K16	Histone 4, Lysine 16
HA	Human influenza hemagglutinin
HAT	Histone acetyltransferase
Hb	Hemoglobin
HDAC	Histone deacetylase
HMT	Histone methyltransferase
HSC	Hematopoietic Stem Cell
IC50	Half maximal inhibitory concentration
KAT	(K) Lysine acetyltransferase
KO	Knockout
Lin	Lineage (in hematopoiesis, refers to differentiated cells of all lineages)
lncRNAs	Long non-coding RNAs
LSK	Lineage-negative (Lin^-), $SCA1^+$, $cKIT^+$
LT-HSC	Long-term Hematopoietic Stem Cell
MA9	MLL-AF9
MDS	Myelodysplastic Syndrome
MEF	Murine Embryonic Fibroblast
MLL1	Mixed-Lineage Leukemia 1, also known as KMT2A
$Mll1^{-/-}$NHA9	NHA9 transformed *ERT2-cre;Mll1$^{f/f}$*
$Mll1^{+/-}$NHA9	NHA9 transformed *ERT2-cre;Mll1$^{f/+}$*
$Mll1^{+/+}$NHA9	NHA9 transformed *Mll1$^{f/f}$*
MM	Multiple Myeloma
MOF	Ortholog of *Drosophila* Males absent on the First, also known as KAT8
MP	Myeloid Progenitor
MPNST	Malignant Peripheral Nerve Sheath Tumor
MYST	Moz-Ybf2/Sas3-Sas2-Tip60
N-terminal	NH_3-terminal
NES	Normalized Enrichment Score
NHA9	NUP98-HOXA9
NHD13	NUP98-HOXD13
NLS	Nuclear Localization Signal
NMC	NUT Midline Carcinoma
NPC	Nuclear Pore Complexes
NSC	Non-Specific Lethal Complex
P9	Postnatal day 9
PB	Peripheral blood
PHD-finger	Plant Homeodomain finger
pIpC	poly(I:C)
PTM	Post-Translational Modification
qRT-PCR	Quantitative Real-Time PCR
RBD	RNA Binding Domain

RNAi	RNA interference
RNAPII	RNA Polymerase II
RNA-seq	RNA high-throughput sequencing
RTK	Receptor Tyrosine Kinase
SCLC	Small Cell Lung Cancer
SD	Stand Deviation
SET	Su(var)3-9, Enhancer of zeste, Trithorax
shRNA	short hairpin RNA
T-ALL	T-cell Acute Lymphoid Leukemia
Trx	Trithorax
WBC	White Blood Cell
WT	Wild Type

CO-AUTHORS AND THEIR AFFILIATIONS

Amaia Lujambio, PhD
Department of Oncological Sciences, Mount Sinai School of Medicine, New York, NY, USA.

Amit U. Sinha, PhD
Cancer Biology & Genetics Program, Memorial Sloan Kettering Cancer Center (MSKCC), New York, NY, USA.
Basepair, New York, NY, USA.

Aniruddha J. Deshpande, PhD
Cancer Biology & Genetics Program, MSKCC, New York, NY, USA.
Tumor Inititation and Maintenance Program, Sanford Burnham Prebys Medical Discovery Institute, La Jolla, CA, USA.

Carolien M. Woolthuis, MD, PhD
Human Oncology & Pathogenesis Program, MSKCC, New York, NY, USA.

Christopher Delaney, BS
Center for Epigenetics Research, MSKCC, New York, NY, USA.
Cancer Biology & Genetics Program, MSKCC, New York, NY, USA.

Chun-Hao Huang, PhD student
Cancer Biology & Genetics Program, MSKCC, New York, NY, USA.

Chun-Wei (David) Chen, PhD
Center for Epigenetics Research, MSKCC, New York, NY, USA.
Cancer Biology & Genetics Program, MSKCC, New York, NY, USA.

George Zheng, PhD
Pharmaceutical and Biomedical Sciences, University of Georgia, Athens, GA, USA.

Gerard L. Brien, PhD
Center for Epigenetics Research, MSKCC, New York, NY, USA.
Cancer Biology & Genetics Program, MSKCC, New York, NY, USA.

S. Haihua Chu, PhD
Center for Epigenetics Research, MSKCC, New York, NY, USA.
Cancer Biology & Genetics Program, MSKCC, New York, NY, USA.

Haiming Xu, PhD
Center for Epigenetics Research, MSKCC, New York, NY, USA.
Cancer Biology & Genetics Program, MSKCC, New York, NY, USA.

James J. Hsieh, MD, PhD
Human Oncology & Pathogenesis Program, MSKCC, New York, NY, USA.

Meghan E. Eisold, BA
Center for Epigenetics Research, MSKCC, New York, NY, USA.
Cancer Biology & Genetics Program, MSKCC, New York, NY, USA.

Monica Cusan, MD
Center for Epigenetics Research, MSKCC, New York, NY, USA.
Cancer Biology & Genetics Program, MSKCC, New York, NY, USA.

Patricia Ernst, PhD
Department of Pediatrics, University of Colorado School of Medicine, Aurora, CO, USA.

Scott A. Armstrong, MD, PhD
Center for Epigenetics Research, MSKCC, New York, NY, USA.
Cancer Biology & Genetics Program, MSKCC, New York, NY, USA.
Department of Pediatric Oncology, MSKCC, New York, NY, USA.
Department of Pediatric Oncology, Dana-Farber Cancer Institute, Boston, MA, USA.

Scott W. Lowe, PhD
Cancer Biology & Genetics Program, MSKCC, New York, NY, USA.

Takayuki Hoshii, PhD
Center for Epigenetics Research, MSKCC, New York, NY, USA.
Cancer Biology & Genetics Program, MSKCC, New York, NY, USA.

Tej K. Pandita, PhD
Department of Radiation Oncology, Houston Methodist Research Institute,
Houston, TX, USA.

Wenhuo Hu, PhD
Human Oncology & Pathogenesis Program, MSKCC, New York, NY, USA.

ABOUT THE AUTHOR: CURRICULUM VITAE

Daria Gianina Valerio was born on September 7th 1986 in La Jolla, California, USA. She attended high school at the Rijnlands Lyceum in Oegstgeest, The Netherlands, where she graduated with honors (cum-laude) in 2004. She then went to medical school at Leiden University Medical Center (LUMC) in The Netherlands. During medical school she performed a scientific internship at the department of immunology and genetics with dr. George Diaz at Mount Sinai Medical School, New York, USA. Her Dutch mentor for this project was dr. Wouter Kollen, pediatric oncologist at LUMC. Based on this scientific work, she wrote the thesis titled *"The effect of corticosteroid and β-adrenergic receptor agonist treatment on CXCR4 signaling in WHIM patients"* for which she received the LUMC Student Research Award. She performed her senior clinical rotation in 2011 at the department of pediatric oncology in the Academic Medical Center in Amsterdam and shortly after, received her medical degree cum-laude. After medical school, Daria worked as a research fellow in the laboratory of professor Michel Zwaan and dr. Marry van den Heuvel - Eibrink at the department of pediatric oncology, Erasmus Medical Center, Rotterdam, where she studied the epigenetic changes in pediatric AML and published a paper in *Haematologica* titled *"Mapping epigenetic regulatory gene mutations in cytogenetically normal pediatric acute myeloid leukemia"*. In 2013 she moved to the United States to continue her scientific education with professor Scott Armstrong at Memorial Sloan Kettering Cancer Center (MSKCC), New York. In the Armstrong lab she studied the role of various chromatin regulators in acute leukemia and normal hematopoiesis for which she received a $250,000 grant from the CURE Childhood Cancer foundation. Professor Bob Löwenberg and professor Ruud Delwel served as her Dutch mentors during her three years at MSKCC. The work Daria completed in the Armstrong lab is presented in this thesis.

ABOUT THE AUTHOR: LIST OF PUBLICATIONS

G. Brien, **D.G. Valerio**, S.A. Armstrong. Exploiting the epigenome to control cancer-promoting gene-expression programs. *Cancer Cell.* 2016;29(4):464-76

H. Xu & **D.G. Valerio**, M.E. Eisold, A. Sinha, R.P. Koche, W. Hu, C.W. Chen, S.H. Chu, G.L. Brien, J.J. Hsieh, P. Ernst, S.A. Armstrong. NUP98 fusion proteins physically interact with the NSL and MLL1 complexes to drive leukemogenesis. *Cancer Cell,* 2016, in press.

D.G. Valerio & H. Xu, M.E. Eisold, C.M. Woolthuis, T.K. Pandita, S.A. Armstrong. Histone acetyltransferase activity of MOF is required for adult, but not early fetal hematopoiesis in mice. *Blood*, 2016, in press.

D.G. Valerio, H. Xu, C.W. Chen, T. Hoshii, M.E. Eisold, C. Delaney, M. Cusan, A.J. Deshpande, C.H. Huang, A. Lujambio, G. Zheng, T.K. Pandita, S.W. Lowe, S.A. Armstrong. Histone acetyltransferase activity of MOF is required for *MLL-AF9* leukemogenesis. *Cancer Research*, under review.

D.G. Valerio, J.E. Katsman, J.H. Jansen, L.J. Verboon, V. de Haas, J. Stary, A. Baruchel, M. Zimmermann, R. Pieters, D. Reinhardt, M.M. van den Heuvel-Eibrink, C.M. Zwaan. Mapping epigenetic regulatory gene mutations in cytogenetically normal pediatric acute myeloid leukemia. *Haematologica.* 2014;99(8):e130-2.

ABOUT THE AUTHOR: PhD PORTFOLIO

Name PhD student:	Daria G. Valerio
Erasmus MC Department:	Hematology
Research School:	Molecular Medicine
PhD period:	2012-2016
Promotors:	Prof. dr. B. Löwenberg and Prof. dr. R. Delwel
Supervisor:	Prof. dr. S.A. Armstrong

PhD TRAINING

	Year	ECTS
Courses		
- Classical Methods for Data Analysis, NIHES, the Netherlands	2012	5.7
- Basic course on R, MolMed, the Netherlands	2012	1.4
- Basic and Translational Oncology, MolMed, the Netherlands	2012	1.4
- Adobe photoshop and illustrator CS5, MolMed, the Netherlands	2012	0.3
- Adobe indesign, MolMed, the Netherlands	2012	0.15
- FACS CANTO operator training, BD Biosciences, San Jose, USA	2014	2.0
Scientific symposia		
- 16th MolMed Day, Erasmus MC, Rotterdam, The Netherlands	2012	0.2
- 17th MolMed Day, Erasmus MC, Rotterdam, The Netherlands	2013	0.2
- 7th Geoffrey Beene Retreat, MSKCC, New York, USA	2014	0.5
- 8th Geoffrey Beene Retreat, MSKCC, New York, USA	2015	0.5
International conferences and presentations		
- 4th AML-BFM Research Symposium, Hannover, Germany	2012	1.0
- 6th International Symposium on MDS, EWOG-MDS, Prague, Czech Republic *(poster presentation)*	2012	1.5
- 14th Acute Leukemias biannual meeting, Münich, Germany	2013	1.0
- 56th ASH annual meeting, San Fransisco, USA	2014	1.0
- FASEB Hematologic Malignancies biannual meeting, Saxtons River, USA	2015	2.0
- 29th AACR annual meeting, New Orleans, USA *(oral presentation)*	2016	2.5
Other presentations		
- Two presentations at weekly research meeting, Department of Pediatric Oncology, Erasmus MC, Rotterdam, The Netherlands	2012-2013	1.0
- Five presentations at weekly research meeting Armstrong/Abdel-Wahab/ Kentsis Lab, MSKCC, New York, USA	2013-2016	2.0
- Presentation at weekly research meeting, Epigenetics Center, MSKCC, New York, USA	2016	1.5
Grant		
- CURE Childhood Cancer Research Grant, $249,597 over 2 years. Project titled: *"Combinatorial Targeting of Epigenetic Mechanisms in MLL-rearranged Acute Leukemia."* Principal investigator: Daria G. Valerio. Mentor, Scott A. Armstrong.	2014-2016	5.0
Teaching		
- Supervising research technician	2014-2016	5.0
- Supervising PhD rotation student, 1-month rotation	2015	2.0
- Supervising high school summer student, 2 month internship	2015	2.0

ACKNOWLEDGMENTS (DANKWOORD)

"Alone we can do so little; together we can do so much"
Helen Keller, author

I owe a huge amount of gratitude to many people who guided me through the tumultuous roads of science over the past 4 years.

Most importantly **Professor Armstrong, Scott**: when we first met at the Acute Leukemia conference in Munich, I was incredibly nervous. You told me only recently that you were intrigued by this determined, somewhat aggressive girl who was adamant about joining your lab. That you took me up in your group has been one of the best things to ever happen to me. Your mentorship is phenomenal, but even more important is the wonderful collection of people you have surrounded yourself with. A lab that is perfectly balanced, scientifically as well as with the various personalities; everyone collaborates, there is no back stabbing or competition, there is constant laughter, some tears here and there (yes, mainly mine…) and the constant string of extracurricular activities in Houston Hall or at karaoke, never disappoint. Apart from all your incredible intellect and scientific insight, your quality to pick all these people may very well be your biggest asset. Dear Scott, thank you from the bottom of my heart for having offered me the opportunity to work in your lab and guiding me to where I am today. I am already looking forward to the Armstrong Lab reunions!

Dear **Professor Löwenberg**, **Bob**, the first time you gave me career advice was right before my scientific internship in medical school. Since then, we have talked about various career choices multiple times, and each time, I come out feeling more confident about what I want and how to get there. I'm still fairly certain that your kind words were what convinced Scott to hire me and you were 100% right about him being an exceptional scientific mentor. After all of this, the realization that you were willing to be my *promotor* was a very special and emotional moment for me. You were there for the beginning and now at the end. There are no words to describe how grateful I am for all you have done. Thank you!

Dear **Professor Delwel**, **Ruud**, I couldn't wish for a better *co-promotor*! You are an amazing scientist and person, and I have loved the many talks we had about science and career choices, in Rotterdam and whenever you would visit NY. Thank you for getting the ball rolling on my thesis defense, thank you for helping me put this thesis together so quickly and thank you for the great guidance you have given me in the process. I very much look forward to the many more scientific and social interactions to come!

I would like to acknowledge **Professor Touw**, **Professor Zwaan**, **Professor de Haan**, **Professor Verrijzer** and **Dr. v.d. Heuvel-Eibrink** for being part of my thesis committee.

Thank you for your time and insight!

My scientific career began during medical school with **Dr. George Diaz** and **Professor Kurt Hirschhorn** at Mount Sinai Hospital in New York. At that time I had never held a pipet, let alone knew what a Western blot entailed. Dr. Hirschhorn, you are like a scientific grandfather to me. You introduced me to George, but during my 6 months in NY also invited me over for Sunday brunch with Mrs./Dr. Hirschhorn and even had Chris and me up to your family home at the Cape. And George, you gave me all the insight into science and pediatrics that was needed for me to get hooked. Thank you both, for your guidance!

The field of pediatric oncology stole my heart during my 5-month rotation at the AMC. All the doctors and nurses were great, clinically, as well as socially, the field is intellectually challenging and kids are the most resilient patients one could wish for. **Dr. Tytgat, Lieve**: thank you for your ongoing guidance (and friendship) throughout my research years. **Dr. Schouten** and **Dr. v.d. Wetering**: thank you for making my rotation an excellent one and for all your help and advice with regard to the residency process. And dear **Femke** and **Rutger**, you are both amazing doctors, but more than that, I have grown particularly fond of the two of you and feel lucky to call you my friends. I am excited about moving back to the Netherlands for our ongoing dinner dates, but also excited about working together again!

Dear **Professor Pieters**, **Professor Zwaan** and **Dr. v.d. Heuvel-Eibrink**, thank you so much for giving me the opportunity to work in your lab and introducing me to oncological science! And thank you for all your help in publishing my very first paper. Marry and Michel, we have had some ups and downs, but I look back at my time with you with great fondness and I am really happy that you were both willing to be on my thesis committee!

I would also like to thank **Monique**, **Jules**, **Ronald**, all the graduate students, post-docs and technicians part of the **pediatric oncology lab at Erasmus MC**. In particular, I need to thank the **AML lab** for being loving colleagues until the end.

Jasmijn, **Jenny** and **Ingrid**: in that short period of time the four of us had so much fun together and the bond that was formed, still remains. Ingrid, it was pretty special having you as my US “neighbor” and you and Jasmijn hanging out with me in NY. Jenny, thanks for all your kindness and R skills. And last but not least Jasmijn, I wish I could just type that weird teethy smiley face here for you because that says it all. Loud & Louder Productions ® forever!

During these science years I have had multiple very important mentors. The one person I absolutely have to mention in that context is **Haiming**. Haiming, the reality is that without you this thesis would not have existed. I am eternally grateful for all that you taught me (which is basically every technique used in this thesis…) and for all the scientific guidance you have provided. I know I have driven you to madness at more than one occasion, but in the end,

I really feel we were a team, and a pretty successful one at that. You are an exceptional educator with creative scientific ideas and insight and I know you'll go on to do great things. Of course I wish you a very successful scientific career, but more importantly I wish you and your family a very happy life together.

Meghan, as the third person in our team you were absolutely indispensable! Your mouse skills are unprecedented and without you, Haiming and I would still be genotyping and bleeding those hundreds of mice as we speak. Thank you for all your help in the lab, for introducing me to Madewell, for laughing at my stupid jokes, for laughing at my silly dances, for listening to Beyoncé with me, for crying during my "farewell Meghan" speech and for putting up with my demanding and somewhat anal personality. You are a champ and will go on to be a great MD!

On to my German sibling: **Michael**. When I came to the Armstrong lab for my interview I immediately liked you; you said such kind things about my meager talk and had the best smile. We had a pretty tumultuous friendship with regular lunch table disagreements and some loud arguments, but in the end also cared for each other quite a lot. I enjoyed discussing science with you, having dinner with you, Selina and Chris, dancing and running around with Filippa, meeting Casimir, dancing the night away at various occasions and last but not least singing "*Oops I did it Again*" in a sleazy karaoke bar in front of Scott and Ross (and our lab, though they had previously been exposed to your Britney Spears performances in the tissue culture room). It seems clear: you were an essential part of my life in NY. Thanks for being such a good friend!

Dear **Sheng** (a.k.a. Bruce), from the first moment we met, I knew you were one of the good guys! I have loved joking around with you, laughing a lot, daily hugs, talking about life, science and careers, drinking Billecart-Salmon, many wonderful dinners, and shenanigans in New Orleans (Lipstixxxxx…). But the absolute highlight was our Vermont trip to FASEB, with our luscious red van Sasha, swimming with or without lifejacket, rainy tennis and lots of lobster. Sheng, you are a wonderful, intelligent, funny and loving guy and I want to thank you for being not only my colleague, but a very good friend. Next time we meet will be biking in Amsterdam with your family!

Richard and **Maurizio**: our threesome was only short lived but nonetheless unforgettable. Maurizio, you are insane, but that goes pretty well with my own crazy. It was wonderful to have you as a colleague and friend those first months in the lab. I can still picture you explaining me genetically engineered murine models in the lunch space at Zuckerman. And Richard, the hours we spent talking about life (and some science) are way too many to count. You and I are a perfect ying and yang; as you put it so kindly: "Why Daria is always smiling? She is high on life itself. It's disgusting." But we both know you have a brilliant mind and a very good heart. Chase only those things you really want and keep surrounding yourself with

people who inspire and challenge you. Then everything will work out, I'm certain of it. And one last request: please don't dissect my brain! To both of you: thanks for your friendship, it means a lot and we will see each other again!

Dear **Gerry**, **Ger** thank you for teaching me the basics of Adobe Illustrator. Thanks to you, this has turned into my favorite new toy. Thanks for letting me write the *Cancer Cell* Perspective with you. Thanks for teaching me some Irish. Thanks for helping me out with cloning. Thanks for being my ally in the super-mega-enhancer diss. Thanks for letting me bounce ideas off you. Thanks for making sure I was rarely alone in the lab, even at the oddest hours. You'll go on to do great things as THE superstar scientist back in Ireland!

Dear **David**, thank you for your important scientific input, sharing your shRNA screen data, the crazy high fives in the hallway and your general happiness. As one of the brightest young scientists I have ever met, your thoughts and insight on the role of MOF in leukemia have been very helpful.

Dear **Janna**, wow did I miss you once you left the lab to continue your very promising career in medicine at NYU. It was never the same without your laughter, charm and cuddles. You know how to get people together, make them feel at ease and drive any sort of social event. Thank you for introducing me to a whole new party scene. Thank you and Jim for the numerous get-togethers where interesting people are never lacking. But most importantly, thank you for being a good friend!

Dear **Zhaohui**, thank you for being the always caring and well organized lab mom. I will miss you greatly!

Dear **Taka**, thank you for sharing your impressive scientific ideas, experimental skills, unusual Japanese treats and friendship. You are unique and amazing!

Dear **Sara**, thank you so much for your kindness, your help with the many pediatric oncology questions, your excellent sense of humor and your friendship!

Dear **Hannah**, our time together was short but sweet! Good luck in Boston and please come and visit Amsterdam for some licorice and *vla*.

Dear **Xi**, thank you for your positivity and happiness.

Dear **Haihua**, thank you for your excellent sense of humor and your scientific prowess.

Dear **Monica**, thank you for sharing all your knowledge on mouse experiments and for sharing your very witty impressions.

Dear **Ani**, **Anagha** and **Nan**, thank you for your scientific guidance, patience and kindness in my first months in the lab.

Chris, Evelyn, Jenny, Jonathan and **Rowena**: thanks for your important contribution to the lab, scientifically as well as socially. And lots of luck in your future careers!

Andrei and crew, thanks for your ChIP-seq assistance.
Dear **Kristina** and **Jessica**, thank you for all your administrative help and life-in-NYC chats. It was a pleasure getting to know the both of you!

Armstrong Lab: it has been one heck of a ride and I have loved nearly every minute of it! You guys turned the lab and MSK into a home and it was with great sadness that I left. A very special group of people who I have grown to care for deeply! As Michael put it nicely: we have family all over the world now.

Dear **Elodie** and **Gaelle**, our time with Sasha was pretty sweet! I wish both of you a lot of success and happiness and hope we meet again in Europe.

Dear **Direna** and **Javier**, you two are amazingly warm and loving and I've really enjoyed our dinners, drinks, talks and bike rides together. We'll come and visit soon or see you guys back in Spain!

Dear **Mike** (Ortiz), I feel lucky to have gotten to know you a little at AACR. Thank you so much for all you pediatric oncology advice and don't forget to visit us!

Dear **Marc**, it was only a few months, but we definitely lived it up! The peas in my head are still recovering on a saline drip.

Dear **Rob**, thanks for keeping me sane during 80-hour work weeks. Squash with you was the ultimate remedy for exhaustion, aggression, frustration, laziness and everything in between.

To our surrogate Thanksgiving family: **our drunk uncle, Maurizio, Rowena, Anton, Amandine, Carolien, Michael, Elke, Emiel, Javier, Direna, Haihua, Monica, Taka and Gerry;** the two Thanksgiving dinners we had together were among the absolute social highlights of my NY years. It may sound counterintuitive, but please do come fly out to the Netherlands for more of this turkey madness in the years to come.

Dear **Carolien**, the day we met must not have been the greatest day for you, since interviews are fairly nerve racking. Not having you join our lab was definitely our loss. Luckily you were only a few bays away, which allowed for a working relationship, but most importantly a good friendship to form. Thank you so much for basically proof reading this entire thesis! I know

your NY years have not been the easiest, but getting to know you was one of the highlights for me and FASEB wouldn't have been the same without you as my roomy. You are a creative scientist, an excellent scientific writer and most of all a loving and trustworthy person. I feel lucky to call you my friend and know we will continue to see much more of each other in the years to come.

Elke: in less than a year I have come to think of you as a pretty close friend. Sure, this is also because you, **Emiel**, Chris and I had the whole "*leefgroep*" thing going on; celebrating Thanksgiving, Christmas, New Years Eve, Easter, birthdays, etc. But that's not all there is. You are exceptionally cool (as in "oh my god, she's so cool!"), but warm and loving at the same time. We had some epic party nights together, but also so many meaningful heart-to-hearts. I trust your opinion, can laugh with you and cry with you. Although our upcoming time in Amsterdam will have significantly fewer Uber SUVs, Brooklyn warehouse parties and shared Christmas mornings, I am certain that our friendship will remain. Oh and before I forget: you are an amazingly intelligent, likeable, enthusiastic and beautiful person and you rock!!

Dear **Claire**, we have been friends for 26 years. From our diapers (well, almost…) to Sven's diapers, a pretty incredible journey! We've been together for all the important moments: graduating high school, graduating college, me marrying Chris, you marrying **Sander**, and the birth of your beautiful son. You were there for me when I needed you the most. Thank you for always giving me a sense of home, wherever we are.

Floor, to me you are the sister I've never had. A full 27 years of *"lief en leed"*. It still shocks me to think that we have lived so far apart for three years, yet somehow the space-time continuum did not rupture. Though you and **Wouter** have spend over 4 weeks with us in NY and we made sure to see each other every weekend I spent in the Netherlands, I am thrilled that we'll be residing in the same country once again. Because although our friendship is not affected by the physical distance, the world is so much better with you around, or rather next to me. Next to me on our bikes as 4-year old toddlers, next to me at the hockey field, next to me at the general practitioners office when my cheek got punctured by a stick (it was the surgeon in you), next to me during class (well, some of them), next to me when I married Chris, and now next to me during my thesis defense. In these years I have come to realize that I will always count the days, even hours until I can see you again, and I will always be deliriously happy when I do.

Dear **Anneke, Herman, Wieke, Ivo, Johannes, Maaike, Marijn, Jurre, Maas** and **Minke**: one could wish for no beter inlaws. I feel so fortunate to have gained all of you in the package deal with Chris! All your love and support throughout the years means a lot. This much extra family is a gift. En liefste **Sara**: ik zou zo heel graag willen dat je nog bij ons was. Ik geloof niet in *"The cure for cancer"* maar ik geloof wel in heel hard werken om zoveel mogelijk

kinderen met kanker helemaal beter te maken. Ik vind het erg verdrietig dat ons dat bij jou niet is gelukt.

To the **extended Eriks** and **Valerio family**: thank you for your ongoing support and love. I feel so lucky to have all of you in my life! And **Ellen**: always front row during the moments that matter. You are a wonderful person and an amazing aunt!

Enzo and **Vito**, all I'll say is this: Best Brothers Ever. I love you guys to death!

To my most wonderful parents, **mom** and **dad**: thank you for having been so extremely supportive throughout my life. Thank you for teaching me and my brothers to set goals, aim for the stars and believe in ourselves. Thank you for teaching us: no guts, no glory. Thank you for teaching us never to settle for mediocre, to do what you love, be with whom you love, work with passion and full dedication, have lots of fun on the way there and finally, but importantly, to love others deeply. I could not have done this without you!

And last but not least my amazingly patient, loving, supportive, funny and dedicated husband. The road to this thesis was long and at times dreadful, for me and you both. But not once did you complain about the long nights and weekends in the lab or my absentmindedness. You and I have had a couple of exceptional years in New York together. Thank you so much for taking this leap of faith with me! It has made me realize even more, how well we complement each other and how deeply I love you. **Chris**, I have said it before, but will say it again: we don't have a home, you are my home. Always.

No guts, No glory